DENDRITIC LIGANDS FOR HYDROFORMYLATION AND HYDROCARBONYLATION REACTIONS.

A thesis presented by

Loïc Ropartz

to the

University of St. Andrews

in application for

THE DEGREE OF DOCTOR OF PHILOSOPHY

St. Andrews August 2001

Declaration.

(i) I, Loïc Ropartz, hereby certify that this thesis, which is approximately 59,000 words in length, has been written by me, that it is the record of work carried out by me and that it has not been submitted in any previous application for a higher degree.

Date 10/09/2001 Signature of candidate

(ii) I was admitted as a research student in September 1998, and as a candidate for the degree of Doctor of Philosophy in September 1999; the higher study for which this is a record was carried out in the University of St Andrews between 1998 and 2001.

Date 10/09/2001 Signature of candidate

(iii) I hereby certify that the candidate has fulfilled the conditions of the Resolution and Regulations appropriate for the degree of Doctor of Philosophy in the University of St Andrews and that the candidate is qualified to submit this thesis in application for that degree.

Date 10/09/2001 Signature of supervisor

In submitting this thesis to the University of St Andrews I understand that I am giving permission for it to be made available for use in accordance with the regulations of the University Library for the time being in force, subject to any copyright vested in the work not being affected thereby. I also understand that the title and abstract will be published, and that a copy of the work may be made and supplied to any *bona fide* library or research worker.

Date 10/09/2001 Signature of candidate ..

Acknowledgements.

In completing this thesis, I am very much indebted to many people for their help and encouragement.

First of all, I thank Professor David Cole-Hamilton for his invaluable help and enthusiasm all along the development of this project. Thanks are also due to Professor Russell Morris for helpful discussions and to the University of St. Andrews for giving me the opportunity (funding) to carry out my project.

Several people have provided technical and practical assistance during the course of this project. I would like particularly to thank for their grateful help and advice Douglas Foster (CATS), Peter Pogorzelec (lab), Melanja Smith (NMR), Catherine Botting (MALDI-TOF), Katherine Haxton (Molecular modelling) and Alex Slawin (Crystallography).

Thanks also to all the people I met in the laboratory during these years for their help and friendship: Murielle, David, Webby, Ann, Dan, Dave (all of them!), Andrea&Matt, Guy, Martin, Gregor, Ayyub, Scott, Ruth, Nick, Stewart, Paul, Barry, etc.

Last but not least, I would like to thank my family and all my friends (Yoyopop, Andrea Teti, Fred, Claire, the Spanish and French armadas, and all the others) for encouraging and helping me all along the years.

Abstract.

Dendrimers are well-defined macromolecules radiating from a central core with a specific number of arms. They are potentially multi site ligands/catalysts since simple chemistry allows the grafting of numerous reactive/non-reactive species to their periphery. The requirement of a recovery system of the metal species in catalysis is nowadays essential for the development of an industrial process. The size and physical properties of the dendrimers allow the recovery of these compounds by ultrafiltration techniques and thus make them suitable for this task. It was therefore interesting to develop such dendritic ligands and to assess them in catalytic reactions. In addition, the controlled spatial orientation of the metal binding sites may give enhanced stability for complex formation and reduced catalyst leaching.

The synthesis of dendrimers (1^{st} and 2^{nd} generation, up to 72 arms) with chloro endgroups, as well as vinyl, allyl and hydroxy substituents is discussed in this thesis. The functionalisation of these dendrimers by phosphine or phosphite species was then carried out. Alkylphosphine (e.g. methyl, ethyl, cyclohexyl, etc.), arylphosphine (phenyl, 3,5-$C_6H_3(CF_3)_2$) and phosphite (biphenoxy) dendrimers with up to 72 arms were prepared. Radical addition of HPR_2 onto the vinyl or allyl endgroups and nucleophilic substitution of the chloride of the chlorosilane type dendrimers were the two type of reactions used to introduce the phosphine compounds. The phosphite-containing dendrimer was synthesised from a hydroxy dendritic compound.

The structure pattern of the dendrimers was also varied, since different numbers of endgroups, lengths and chemical compositions of the arms were used.

Hydroformylation and hydrocarbonylation reactions of alkenes (prop-2-en-1ol, hex-1-ene, oct-1-ene, non-1-ene) were carried out using rhodium ($[Rh(acac)(CO)_2]$, $[Rh_2(OCMe_2)_4]$) as metal-based catalyst precursor under pressure of H_2/CO. Aldehydes (hydroformylation) and alcohols (hydrocarbonylation) were produced under these conditions with high activity and good selectivity to the desired linear products. Higher selectivity to the linear aldehyde (l:b = 14:1) compared to the parent molecules was found using a specific dendritic structure with diphenylphosphine groups on the periphery of the dendrimer. This increased

selectivity showed that a 'dendritic effect' occurred. NMR and HP IR studies were carried out to determine the mode of coordination of the dendritic complexes.

Abbreviations.

This list contains some abbreviations which may be used in this thesis without definition.

AcacH	pentane-2,4-dione
Ar	Aryl.
b	Branched
BDPP	(2S,4S)-bis(diphenylphosphino)pentane.
BINAP	2,2'-Bis(diphenylphosphino)-1,1'-binaphthyl.
BISBI	*trans*-2,2'-Bis[(diphenylphosphino)methyl]-1,1-biphenyl.
^{t}Bu	*tert*-Butyl.
CATS	Catalyst Evaluation And Optimisation Service
CHIRAPHOS	(2R,3R)-bis(diphenylphosphino)butane.
CIR	Cylindrical internal reflectance.
Cy	Cyclohexyl
DBPphos	1,8-bis(diphenylphosphino) dibenzofuran.
DIOP	(-)-2,3-O-Isopropylidene-2,3-dihydroxy-1,4-bis(diphenyl-phosphino)butane.
Dppb	Bis(diphenylphosphino)butane.
Dppe	1,2-bis(diphenylphosphino)benzene
Dppf	1,1'-Bis(diphenylphosphino)ferrocene
Dppm	Bis(diphenylphosphino)methane.
Dppp	Bis(diphenylphosphino)propane.
ea	Equatorial axial.
ee	Equatorial equatorial.
Et	Ethyl
Hex	Hexyl
HP IR	High pressure Infra-red
IR	Infra-red

l	Linear.
NMR	Nuclear magnetic resonance
Me	Methyl
MS	Mass Spectrometry
Ph	phenyl
POSS	Polyhedral oligosilsesquioxane
ppm	Parts per million.
TBP	trigonal bipyramidal
THF	tetrahydrofuran
TPP	Triphenylphosphine.
Tppts	Tri(meta-sulfonyl)triphenylphosphine.
Xantphos	9,9-dimethyl-4,6-bis(diphenylphosphino) xanthene.

TABLE OF CONTENTS.

Chapter One: A brief review of dendrimers and silsesquioxanes.

1 A BRIEF REVIEW OF DENDRIMERS AND SILSESQUIOXANES.

1.1 DENDRIMERS.

1.1.1 THE CHEMISTRY OF DENDRIMERS.

Dendrimers, also known as arborols, fractal polymers or cascade molecules, are macromolecules with a three-dimensional structure in which well-defined branches radiate from a central core, becoming more branched and dense as they extend out to the periphery (Figure 1.1).[1] They are characterised by presence of a large number of functional groups on the surface and by their faculty to act as guest host.

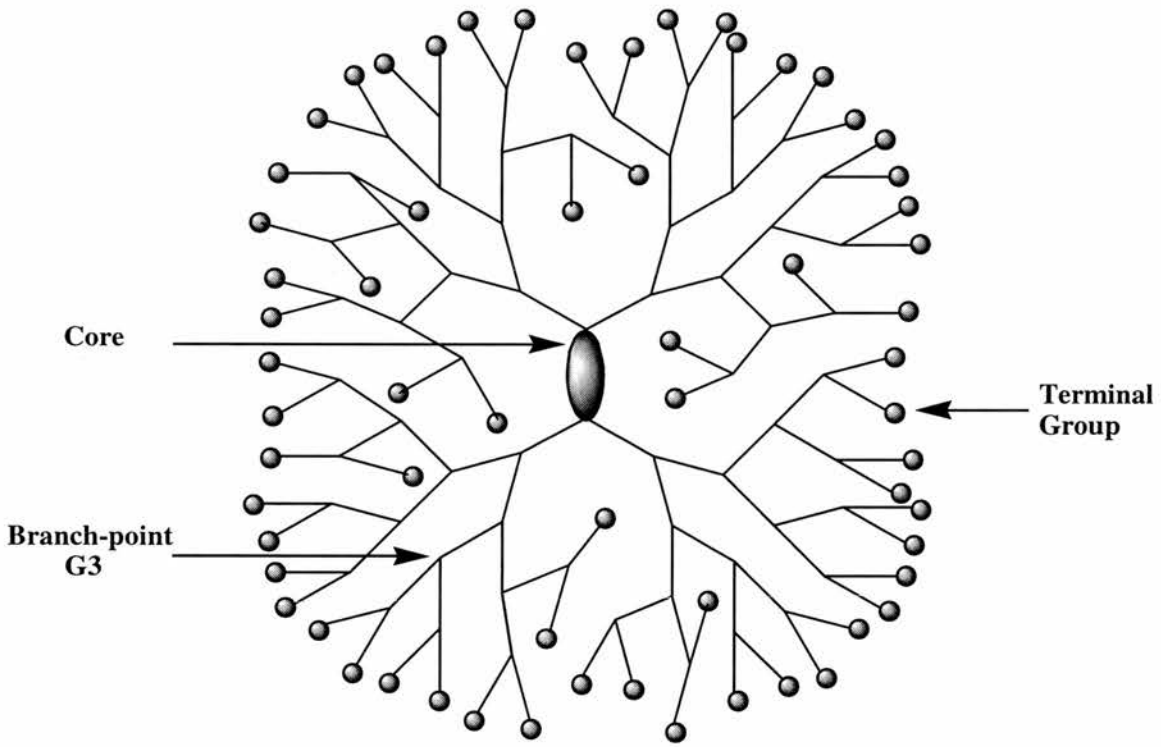

Figure 1.1: Schematic diagram of a dendritic macromolecule.

During the past two decades, undoubtedly due to their unprecedented architecture, dendrimers have become the fastest growing areas of polymer science. Since the first successful synthesis of a cascade molecules by Vögtle and co-workers in 1978,[2] and subsequent synthesis/ characterisation by Newkome[3] and Tomalia[4, 5] this class of polymers has received considerable interest.[1, 6-21] The number of publications

and patents, which was barely a dozen or so in the 1980s reached over 2500 by the end of 1999.[22] Indeed, highly pure polyamidoamine (PANAM) (Figure 1.2) and poly (propyleneimine) dendrimers are now commercially available. In the early days much of the work focused on new materials and their molecular architecture as well as design and synthesis of regular networks of branched systems. Gradually the interest in the field of chemistry has shifted to research on their properties and potential applications. The historical interest in well-defined macromolecules originates in their relevance in biochemistry and more generally in nature. A related area of study is the generation of micelles, liposomes, vesicles and oligomers. There are many potential uses of these entities in such diverse areas as drug delivery agents, synthetic cells, micelle mimics, and nanoscale reactors.[23] The well-defined architecture challenges the creativity of the chemists of all branches from inorganic and organic chemistry, polymer and material chemistry, as well as analytical chemistry, biology, medicine, pharmacology, agrochemistry, environmental chemistry and chemical engineering.

Dendrimers are generally prepared using two approaches, a divergent and a convergent method. The divergent route, first used by Tomalia[4] and Newkome[3], corresponds to successive addition of dendrimer layers (generations (Gn) or dendrons) to a core or later generation. The building of the dendrimer where the arms of the dendrimer are synthesised first and subsequently attached together at a focal point to produce the final molecule is called the convergent method.[24] A major drawback with dendrimer synthesis, especially the divergent one, is that it often requires many repetitive steps and purification in order to build the dendrimer outwards leading often to low yield preparations. However both methods have their strengths and their weakness. Indeed, the number of defects in the molecule potentially increases with the successive dendritic layers as the number of bond formation rises. In addition, a steric hindrance problem then appears which leads to partial synthesis of the outer layer terminal units. Tomalia described this limitation of the divergent synthesis by 'stardust effects'.[25] Several methods to reduce the number of synthetic steps and to obtain the desired dendrimer in high yields have been demonstrated but alternative synthetic methods are still needed.[15]

The globular architecture of these molecules leads to properties such as low intrinsic viscosity, high solubility and miscibility, and high reactivity (from the presence of many chain ends). However, it is important to keep in mind that many of the branches are in reality back-folded. The shape of the molecule is induced by the steric factors inherent in the dendritic segments. The steric crowding itself is strongly dependent on the exact structure of the dendrons. Indeed the structural properties of the arms and branching points, as well as the size (or generation number Gn) of the dendrons and the interactions between dendrons, end-groups and surrounding medium modify the spacial geometry of the molecule.[26] For higher generation dendrimers, solubility characteristics depend predominantly on the properties of their surface groups.

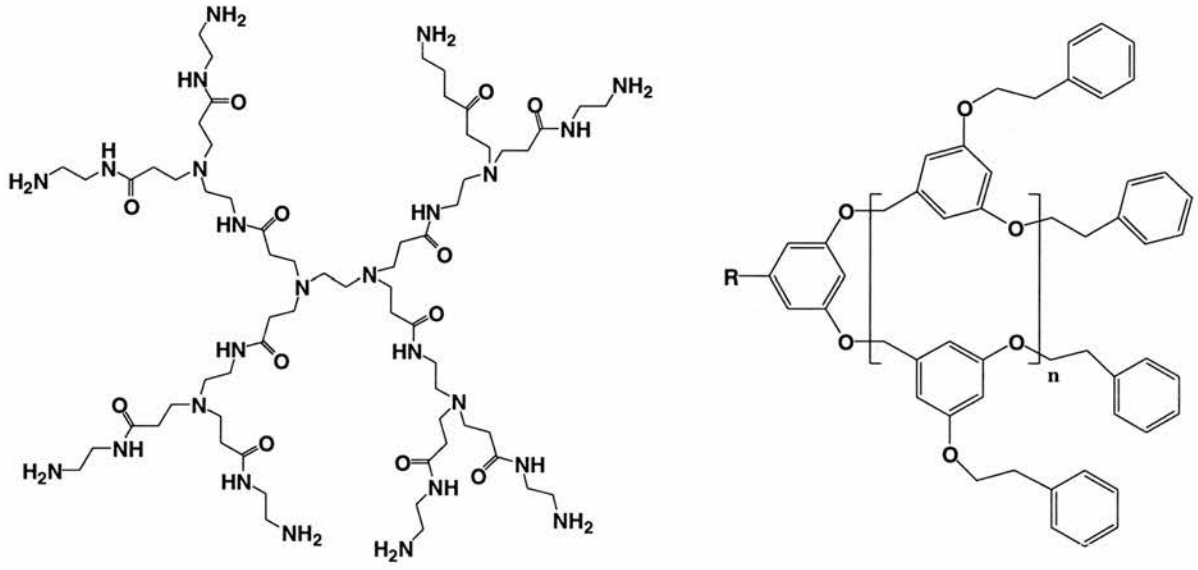

Figure 1.2 A first generation (G1) PANAM (left) and Gn generation polyether Fréchet type dendron (right).

To date, over 50 different dendrimer families with a different end group modifications have been described. Polyamidoamine (PANAM), poly (propyl imine), polyethers, polyesters, polyphenylenes, polysilanes, phosphorus dendrimers are among the most common. In addition to these covalently linked dendrimers, various types of coordinated dendritic molecules (metallodendrimers) have also been reported.[12, 14-17, 19-21, 26, 27] Potential uses and applications of metallodendrimers range from liquid crystals

and layers, as well as electroactive dendrimers and electroluminescence devices, sensors, conductive and ionic conductive polymers, to solar energy conversion and photochemical molecular devices. However, one of the most important and exciting uses of dendrimers is expected to be in the field of catalysis. Since the mid-nineties a growing number of publications has been reported on radical polymerisation,[28] Lewis acid catalysis[29] and more generally on catalysis using transition metals (C-C coupling, hydrogenation, etc.).

1.1.2 DENDRIMERS AS METAL COMPLEX CATALYSTS.

A crucial feature for the industrial development of a catalytic process is the separation of catalysts from the reaction mixture. Most of the industrial applications seen nowadays have been compelled to an efficient strategy of catalyst recovery. Moreover in fine chemical synthesis the recovery of engineered ligands can be even more costly. Therefore there is great scope for the development of new materials that combine the advantages and minimise the disadvantages associated with heterogeneous and homogeneous catalysts.[7, 30-32]. The ability to recover dendrimers using ultra- or nanofiltration nanofiltration techniques and hence facilitate the separation of the catalyst systems from the reaction mixture has thus appealed to the imagination of several research groups.

Two general strategies have been considered to tackle this promising area of catalysis. By the placement of the catalytic active site at a particular, isolated position, i.e. the core, one can imagine that it may result in beneficial interactions between the substrate and the catalyst. In the other hand, the end-groups of the dendrimer can be used to introduce many catalytic sites on the molecule, possibly resulting in anomalous and favourable, or not, catalytic behaviour.

1.1.2.1 Catalysis in the core.

Dendritic catalysts with an active central core, i.e. mimicking enzymes, are a key point of the application of dendrimers. The size of a dendrimer is roughly comparable to that of many enzymes and, just like enzymes, dendrimers are able to create a

microenvironment around a reactive site.[26] Indeed, manganese porphyrins carrying oxidatively poly(phenylester)dendrons (Figure 1.3) were reported by Moore and co-workers and were found to catalyse the shape-selective epoxidation of alkenes (iodobenzene as co-oxidant).[33, 34] Comparison studies between the growing generation dendrimer based-catalyst and the simple porphyrin model showed that the second-generation dendritic molecule was up to four times more selective towards less-hindered terminal bonds. Due to the efficient shielding of the macromolecule, the dendritic catalysts possessed excellent oxidative stability.

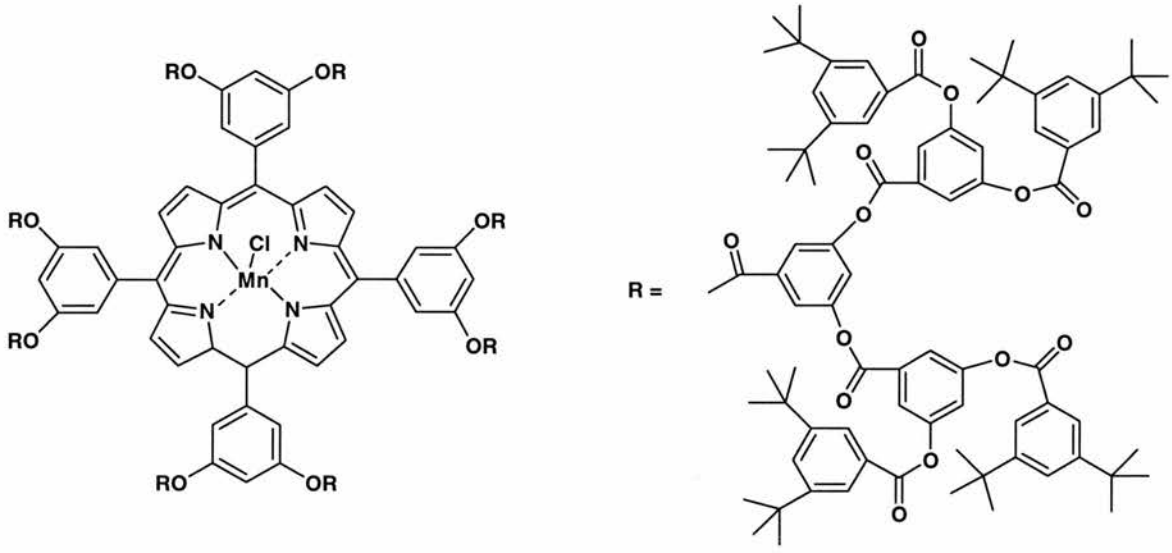

Figure 1.3 Manganese porphyrins dendrimer.

Many other studies[26] relating to the mimicry of natural oxidation catalysts or oxygen carriers have emphasised the shielding effect of higher generation dendrimers affording longer lifetimes. An example of this effect is the cobalt phthalocyanine molecule, which showed enhanced stability by the encapsulation in the dendritic structure (Figure 1.4). Moreover, the second generation cobalt-containing dendrimer catalysed thiol oxidation in 2-mercaptoethanol in presence of dioxygen with a comparable activity to that of the smaller molecules (20 % less active than G1).[35]

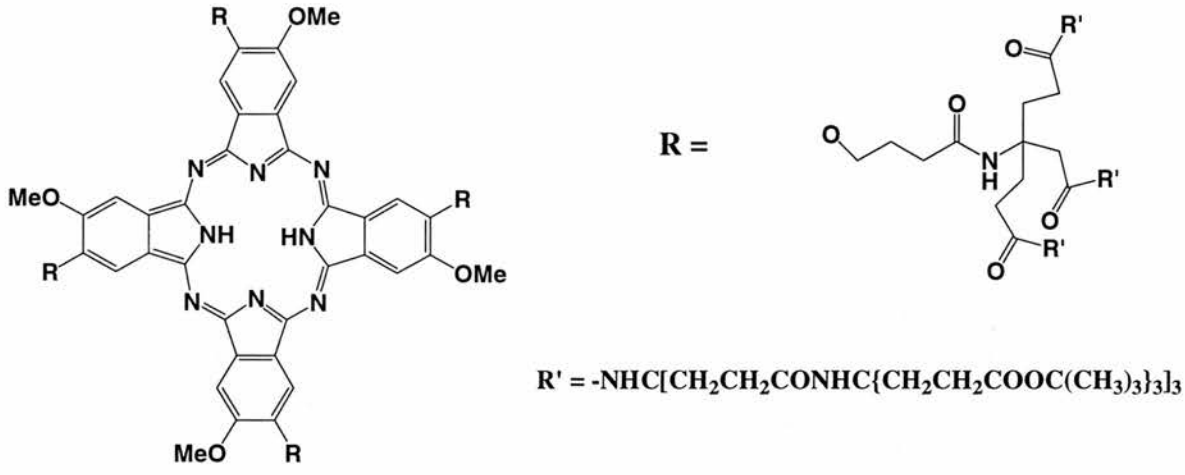

Figure 1.4 Dendritic phthacyanines used in thiol oxidation of 2-mercaptoethanol.

Chow and Mak, who prepared dendritic bis (oxazoline) copper complexes (Figure 1.5) catalysing Diels-Alder reactions,[36, 37] and van Leeuwen, who reported palladium-catalysed allylation reactions using diphosphine ligand incorporated in a carbosilane dendrimer (Figure 1.6),[38] found similar results.

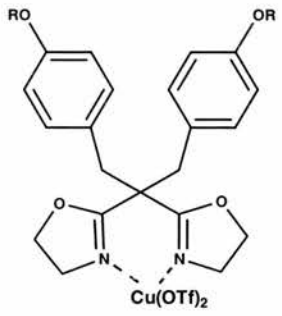

Figure 1.5 Dendritic bis (oxazoline) copper complexes (R = polyaryl dendron in Figure 1.2).

For the Diels- Alder addition, the rate reaction of the catalyst dropped when changing from the second to the third generation. Slightly higher selectivity was found for smaller dienophiles when using G3. Allylic alkylation of 3-phenylallyl acetate with diethyl 2-sodio-methylmalonate catalysed by dendritic palladium complexes (Figure 1.7) led to the same conclusion; increasing the generation number of the dendritic catalyst resulted in a rate decrease. However in this case a slight change of regioselectivity occurred leading to an increase in the amount of cis product from 12 to 21 % when passing from G1 to G3.

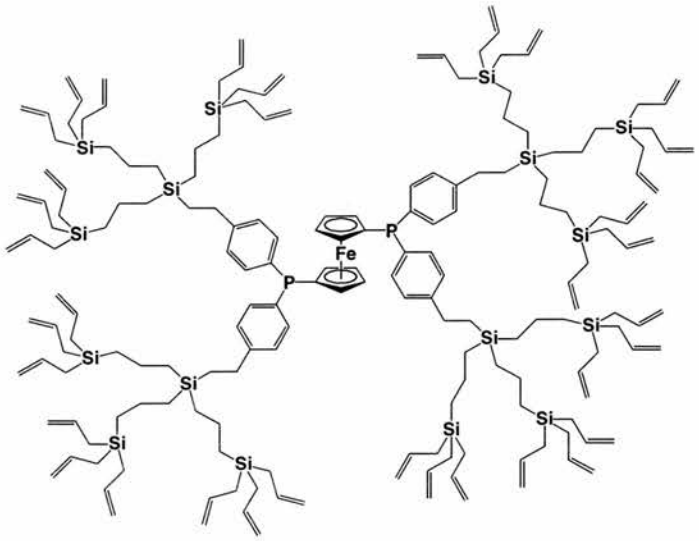

Figure 1.6 Diphenylphosphine ferrocene dendritic ligand.

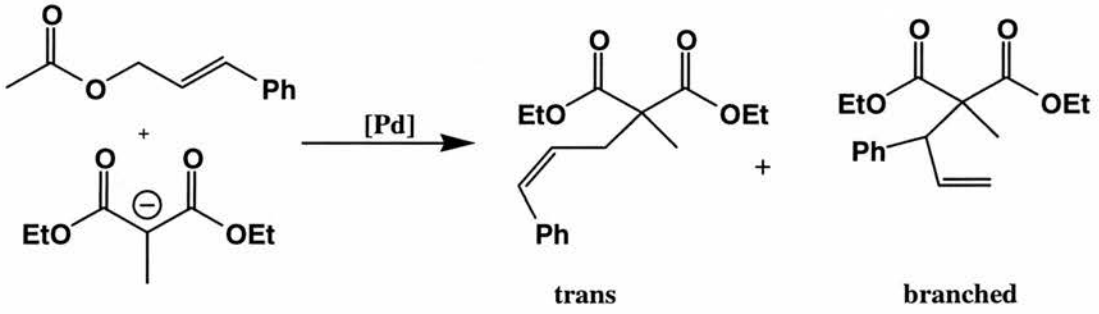

Figure 1.7 Allylic alkylation of 3-phenylallyl acetate with diethyl 2-sodio-methylmalonate catalysed by dendritic palladium complexes.

Brunner first introduced the incorporation of optically active groups in the dendritic building blocks for enantioselective catalysis purpose.[39, 40] Termed as "dendrizymes", this new class of expanded phosphine ligands (PP) was designed to induce an asymmetric metal centre through the chiral dendrimer backbone (Figure 1.7). Hydrogenation of acetamidocinnamic acid to N-acetylphenylalanine by [Rh(cod)PP] PF_6 type complex was used as the model reaction. However, enantioselectivities were usually found to be rather low. Interestingly, the rate of the reaction was dependent on the ligand; rate acceleration or retardation was found using respectively a 1,3,5 or 1,2,5-branched ligand.

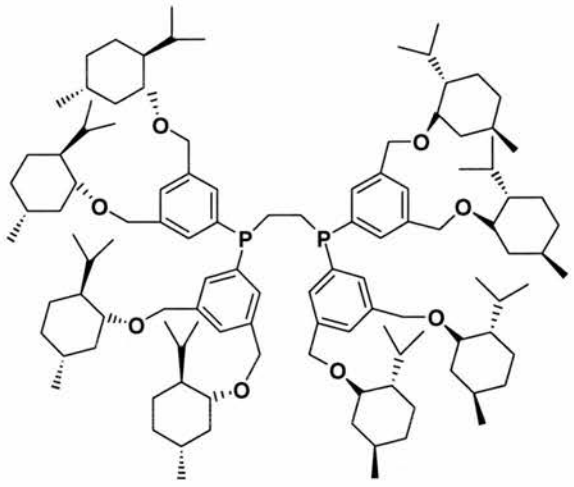

Figure 1.8 An example of Brunner's dendrizyme ligands.

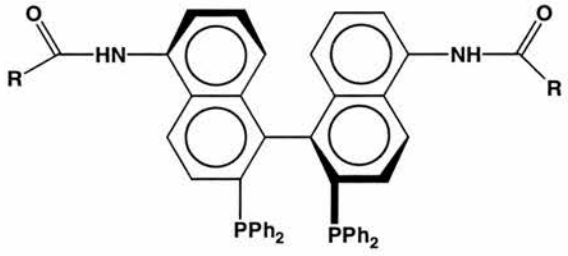

Figure 1.9 Dendritic BINAP-based ligand (R =. polyether Fréchet type dendron).

Fan and co-workers synthesised a series of dendritic polyether BINAP-based ligands (Figure 1.9) and their ruthenium complexes.[41] The core here contained the chiral information. Thus the steric bulk of the dendritic wedges could possibly enhance the chiral effect and force the substrate into an enantioselective pocket containing the catalyst. Asymmetric hydrogenation of 2-[p-(2-methylpropyl) phenyl] acrylic acid to ibuprofen was used as the model reaction ([Ru] = 0.8 mol %) (Figure 1.10). Better stereoselectivity was found for all the dendritic catalysts compared to the parent BINAP (ee up to 92.6 % instead of 89.9 %). Unlike other dendritic catalysts, the rate of the reaction increased using higher generation dendrimers. The authors suggested that the steric bulk of the dendritic wedges, which affects the dihedral angle of the two naphthalene rings in the Ru (BINAP) complex, was responsible for this size effect. Recycling of the dendritic complex was performed three times by precipitation/ filtration of the catalyst without loss of activity and selectivity.

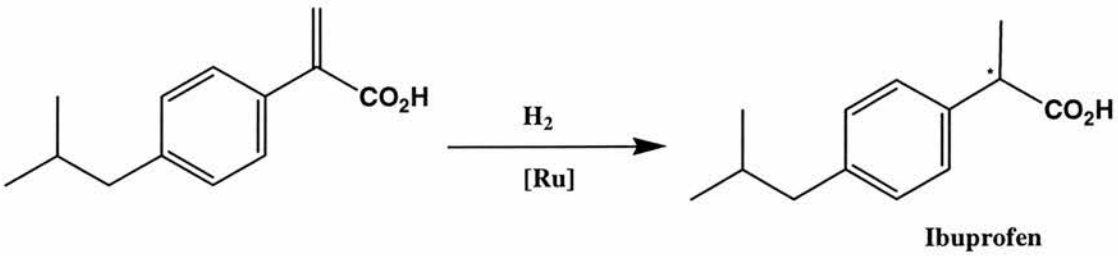

Figure 1.10 Asymmetric hydrogenation of 2-[p-(2-methylpropyl) phenyl] acrylic acid to ibuprofen.

Bolm, Pu and Seebach reported respectively the synthesis of chiral dendrimeric pyridyl alcohols,[42] titanium binaphthyl-based phenylacetylene dendrimer[43] and polyether dendritic Ti-TADDOLates (Figure 1.11),[44, 45] and their application in the asymmetric addition of diethyl zinc to benzaldehyde. Similarly, Yoshida and co-workers reported titanium-mediated allylation of benzaldehyde using a binaphthol core as ligand with a Fréchet type dendrimer.[46] Various generations of these dendritic catalysts were tested and no significant loss of activity or enantioselectivity was observed as the generation number was increased.

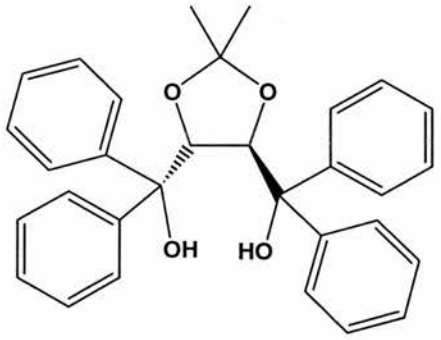

Figure 1.11 TALDDOL compound:(R,R)-α, α,α', α'-tetraaryl-1,3-dioxolane-4,5-dimethanol.

Recently van Koten and co-workers synthesised Fréchet type polyether dendritic wedges of the zeroth to third generations functionalised at their focal points with the nickel based complex [NiCl(NCN)] (Figure 1.12).[47] These 'pincer ligands' were successfully applied for the Kharasch addition of CCl_4 to methyl methacrylate (Figure 1.13). In contrast with the earlier observations on periphery functionalised dendrimers (see section 1.2) leading to loss of activity, the system showed similar rates and turnover numbers to those of the isolated complex. Complete immersion in the substrate solution

of a membrane-capped vial containing the dendrimers (G3) showed excellent retention of the active species during the catalytic reaction. However, the rate of the reaction was considerably reduced due to the poor diffusion of the substrate through the small membrane area (5 % of the vial). Although slow leaching occurred ($t_{1/2}$ > 60 days), the time scale of the reaction(48 h) allowed a possible reuse of the system.

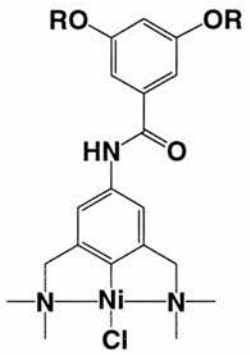

Figure 1.12 Dendritic[NiCl(NCN)] type complex (R = polyether).

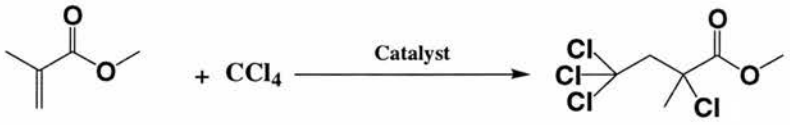

Figure 1.13 Kharasch addition of CCl_4 to methyl methacrylate catalysed by Ni-based catalyst.

Finally, a third generation phosphorus-containing dendrimer (see Figure1.32) bearing one ruthenium metallic centre [$RuH_2(PPh_3)_4$] located at the core was used for Michael addition of diethyl ethylidenemalonate to ethyl cyanoacetate.[48] The dendritic catalyst showed a better activity and could be recycled several times without loss of activity. However, no change in the diastereoselectivity was obtained.

It is clear that introducing chirality to the core or dendrons of a dendritic molecule catalyst is not sufficient to induce stereoselectivity. In addition, the dendritic structure may lead to a decrease of the catalyst activity due to mass transport limitation. However, these problems can be overcome and importantly, recycling of these dendritic system is possible without loss of activity/ selectivity.

1.1.2.2 Catalysis on the periphery.

Although excellent examples of metal free catalysis with dendrimers has been reported in the literature, [28, 49-52] we will emphasise, in this section, on catalysis with metals, and more specifically with transition metals. The first carbosilane based dendrimer system, which was designed to exploit the promising catalytic possibilities, was published in 1994 by van Koten, van Leeuwen and co-workers.[30] The ends of the branches of a carbosilane dendrimer consisted of a nickel-based catalyst (Figure 1.14). These dendrimers showed regiospecific catalytic activity for the Kharasch addition of polyhaloalkanes to carbon-carbon double bonds (Figure 1.13).

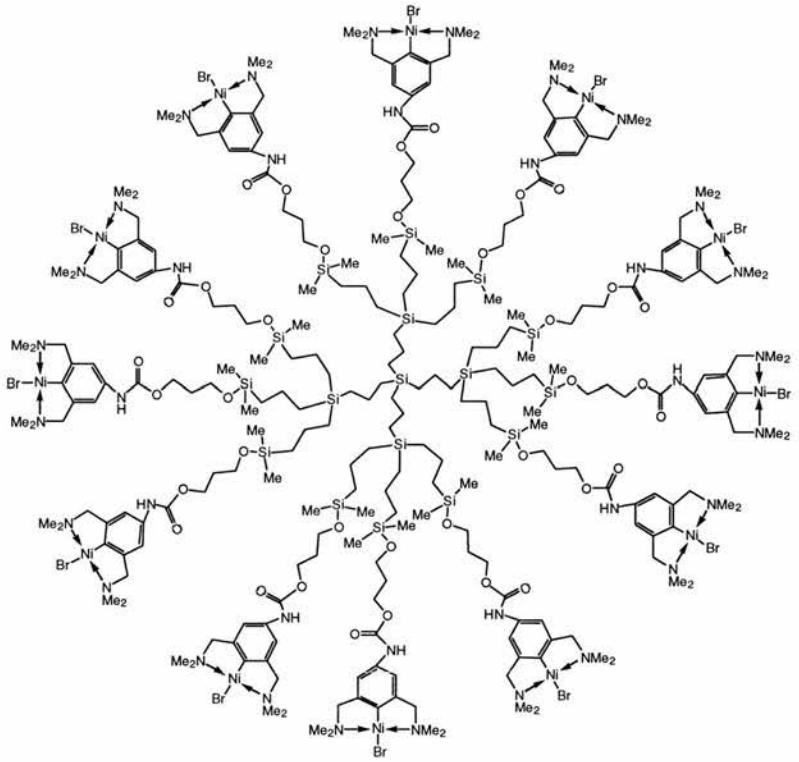

Figure 1.14: Schematic structure of the first generation polysilane dendrimer functionalised with catalytic active diamino arylnickel (II) complexes on the periphery.

The catalytic activity of these zero and first generation dendrimers, as shown by kinetic data, was 20 and 30 % respectively less than was observed with the monomeric compound.[30] Nickel 'pincer' metallodendrimers based on amino acid moieties, via urea functionality, were also described. Comparable activity to their carbosilane relatives was

found. Modifying the chain length using different carbamate[53] or silane[54-56] spacers or varying the number of arms with a Ni centre in a same generation (Figure 1.15), they showed that the increase of steric crowding at the periphery (e.g. through successive generation) led to lower activity and even partial inhibition.

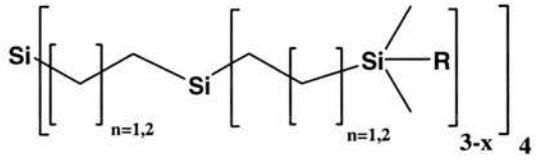

Figure 1.15 Second generation carbosilane dendrimer with R groups.

It was demonstrated that this "dendritic effect" was caused by the proximity of the nickel centres. The termination of radical intermediates (via coupling and formation of inactive Ni^{III} sites) or electron transfer processes within the dendrimer itself (formation of 'mixed valence' dendrimers) were suggested as the inhibitor factors. Despite the low activities and interaction of the substrate with the membrane, it was also demonstrated that ultrafiltration membrane reactors could be used.

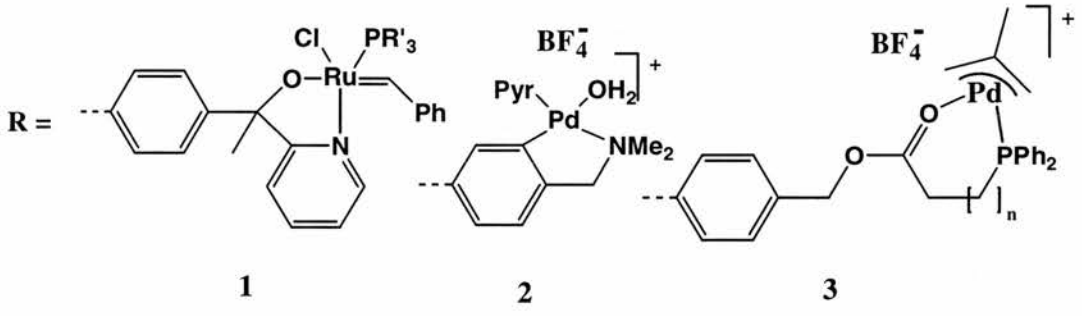

Figure 1.16 Functional groups R on carbosilane dendrimer (Figure 1.15).

Ring closure metathesis reaction of diethyl diallyl malonate (Figure 1.17) was performed using ruthenium carbosilane based dendrimers (Figure 1.16, **1**).[57] The metallodendrimer afforded similar reactivity to that of its parent catalyst (1 % mol $[C_6H_5CH{=}RuCl_2(PR'_2)_2]$ (R'= ^{i}Pr, c-Hex)). However, when using a catalyst solution separated from the substrate by a membrane, the catalytic reaction was unsuccessful probably due to decomposition of the catalyst on the membrane.

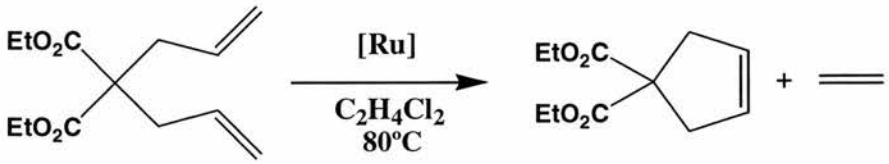

*Figure 1.17 Ring closure metathesis reaction of diethyl diallyl malonate catalyse by the dendritic catalyst **1**.*

Different generations of cyclometalated carbosilane dendrimers (**2**) were also synthesised (up to 12 end groups) using a C-H bond activation procedure. The dendrimers were used as catalysts for aldol condensation between benzaldehyde and methyl isocyanoacetate (yielding oxazolines) (1 mol % Pd) as shown in Figure 1.18.

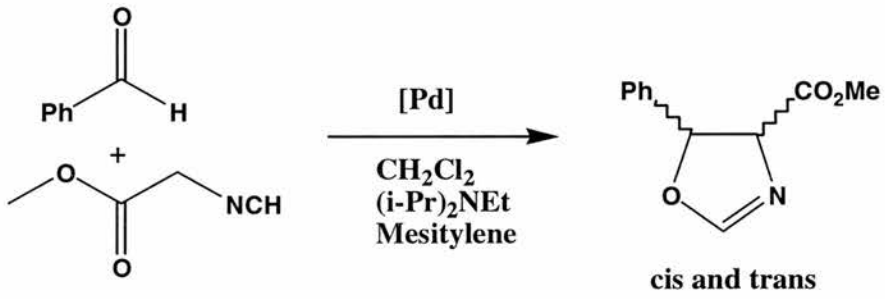

*Figure 1.18 Aldol condensation between benzaldehyde and methyl isocyanoacetate catalysed by dendritic catalyst **2**.*

These Pd(II) metallodendrimers showed the same relationship between structure and catalytic properties than most of other dendrimers, i.e. the more rigid/crowded they were (e.g. higher generation, C2 linker instead of C3 (Figure1.15)), the lower was the reaction rate. A slight selectivity change in the trans/cis ratio of the oxazoline product was also noticed due to steric effects. Palladium-containing carbosilane dendrimers with hemilabile P, O ligands (**3**) were reported as catalysts for the hydrovinylation reaction of styrene (Figure 1.19).[58, 59] The zeroth and first generation metallodendrimers were synthesised by complexation of palladium based complexes ([3-C_4H_7)Pd(cod)]]BF_4, [(allyl)PdI]$_2$/ $AgSbF_6$) with carbosilanes bearing ω-diphenyl-phosphanylcarboxylic acid ester end groups.

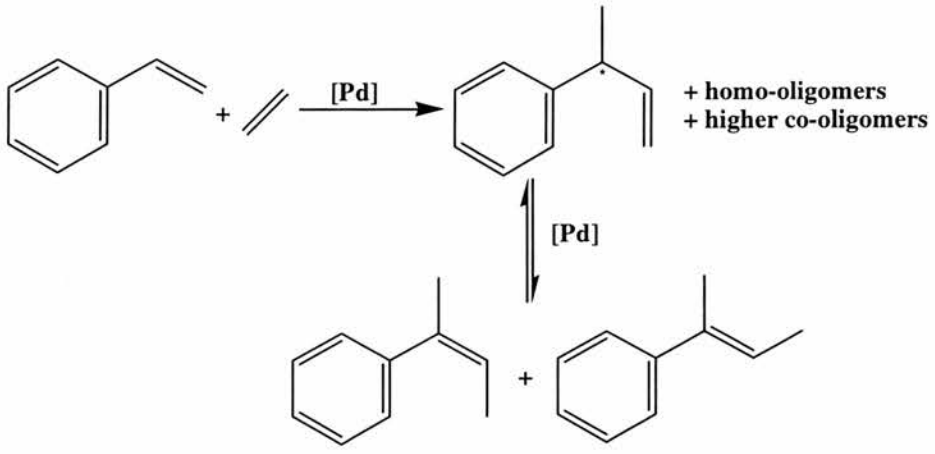

Figure 1.19 Hydrovinylation reaction of styrene and side reactions catalysed by dendritic catalyst ***3.***

The catalytic reaction was carried out in a batch reactor and continuously in a pressure membrane reactor using a nanofiltration membrane. Despite a better selectivity to 3-phenylbut-1-ene (**A**) using the continuous process, the results were relatively disappointing in all cases. The unimolecular catalysts showed higher activity, while the increase steric crowding at the dendrimer surface, as cited before, led to lower reaction rate. Deactivation of the catalytic species and leaching of the metal through the membrane gave poor conversion. Although the steric hindrance might be partly responsible for the low reactivity, the authors suggested that the close proximity of a large number of palladium centres could enhance the deactivation process (formation of black palladium).

Seebach *et al* also reported their dendrimer-bound titanium-TADDOLates this time with Lewis acid catalytic groups dispersed on the periphery.[60] Enantioselective nucleophilic alkyl addition to aldehydes or the Diels- Alder reaction were chosen as test reactions. The results obtained showed lower reactivity (than for the parent molecule) but unchanged selectivities.

DuBois and co-workers prepared palladium complexes of several small organophosphine dendrimers (Figure 1.20), which exhibited catalytic activity (similar to analogous monomeric catalysts) for the electrochemical reduction of CO_2 to CO.[61, 62] Two approaches were used to synthesise such dendrimers. The first one was a sequential addition of diethyl vinylphosphonate to primary phosphines and subsequent reduction

with lithium aluminium hydride to give compounds **4** with 15 phosphines. The second route was an addition of bis[(diethyl)phosphinoethyl]phosphine to tetravinylsilane to give compound **5** with 12 phosphorus atoms. Complexation of these dendrimers with $[Pd(MeCN)_4][BF_4]_2$ afforded the active metallodendrimers.

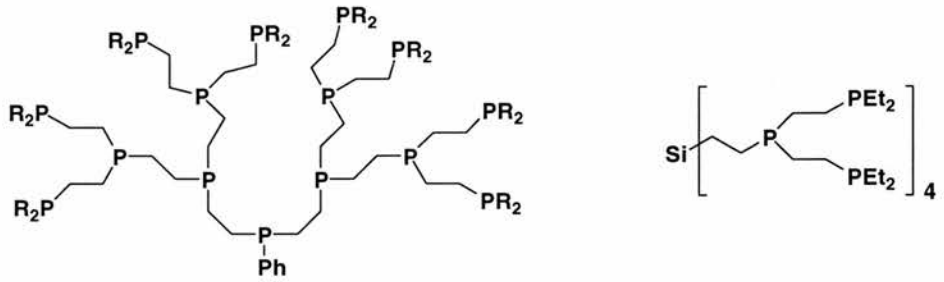

Figure 1.20 DuBois and co-workers organophosphine type dendrimers.

Reetz *et al* reported the catalytic activity of dendritic diphosphane metal complexes[63]. The 16 to 32 amine end groups of 1,4-diaminobutane-based polyamino dendrimer (DAB-dendr-$(NH_2)_{16}$) were functionalised by double phosphinomethylation by PPh_2CH_2OH (Figure 1.21). The complete or partial loading giving rise to dendrimers with metals such as Pd, Ir and Rh on the periphery was accomplished by the reaction of the phosphine-containing dendrimers with $[PdCl_2(PhCN)_2]$ or allylpalladium chloride, $[Ir(cod)_2BF_4]$ and $[Rh(cod)_2BF_4]$. The catalytic activities of palladium and rhodium complexes were tested by using respectively the Heck reaction and the hydroformylation of oct-1-ene. The Heck coupling of styrene with bromobenzene yielded stilbene (89 %) and 1,1-diphenylethylene (11 %) with good yield and selectivity. The catalyst was re-used (recovered by precipitation) to give a similar catalytic activity. Leaching of palladium was not observed. Whereas the parent Pd-complex underwent partial decomposition to give elemental palladium, the dendritic catalyst showed less precipitation of Pd under the same conditions. The stability of the catalyst led to an increase in TON for the dendritic catalyst (TON = 50 instead of 16 for the model catalyst). The authors suggested that this enhanced stability showed a higher thermal stability for the dendritic complexes. Hydroformylation of oct-1-ene by rhodium

containing-dendrimer (0.05 mol % Rh) gave quantitative formation of aldehydes (branched/ linear ratio 60:40) similar to the parent compounds.

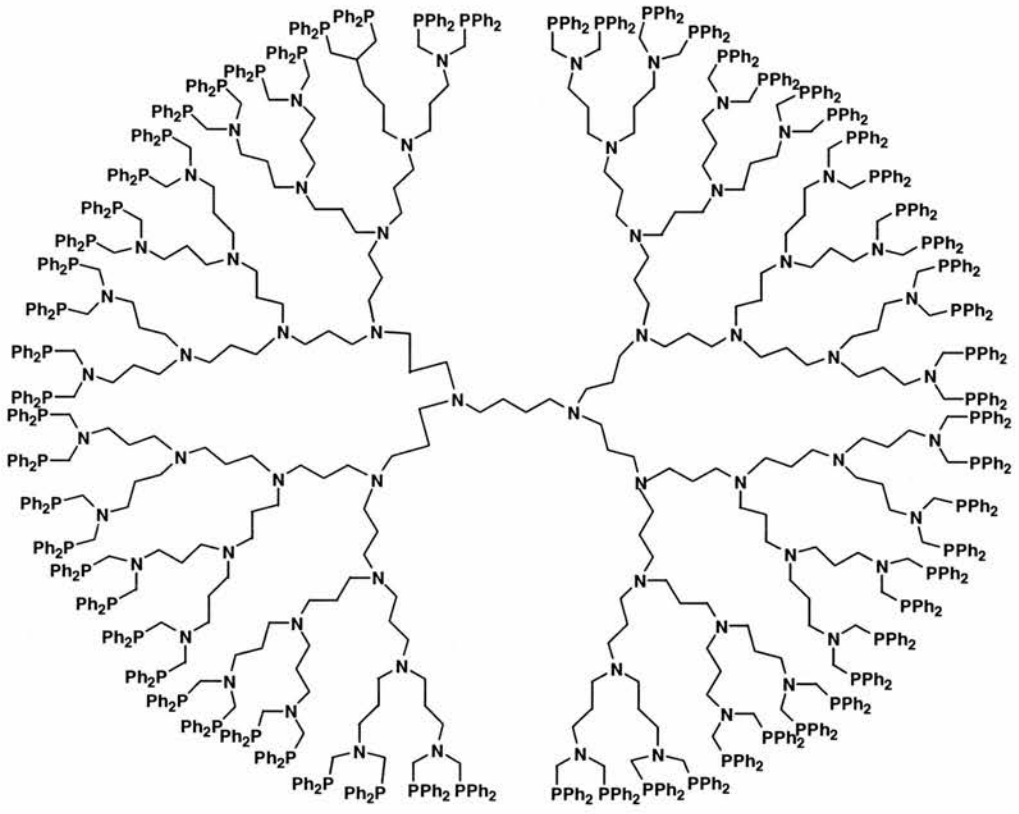

Figure 1.21: G4 DAB-dend-[N(CH$_2$PPh$_2$)$_2$]$_{32}$ type dendrimer.

They also described the retention of this DAB-dendr-[N(CH$_2$PPh$_2$)$_2$]$_{32}$ bearing palladium(II) phosphine complex by ultra or nanofiltration membranes.[64] Catalytic allylic substitution reaction involving allyl compounds and morpholine (Figure1.22), as well as re-use of the catalyst were performed. Recovery of such parent catalysts is known to be difficult. Nevertheless, with the continuously operating membrane reactor, the retention rates were found to be higher than 99.9 % resulting in a six-fold increase in the TON. Using allylpalladium chloride and palladium dendrimer, 100 % conversion (decreasing to 80 % after 100 residence times) and 95 % regioselectivity were acquired. Leaching of only 0.07 to 0.14 % of palladium per residence time was found.

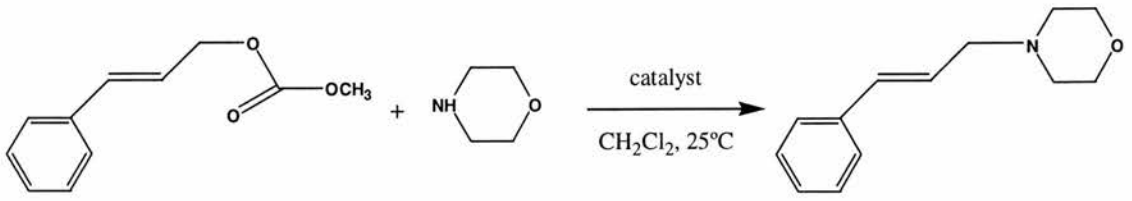

Figure 1.22 Palladium complexes catalysing allylic substitution in the synthesis of N-[3-phenyl-2-propenyl]-morpholine.

Recently the same authors also showed that cross-linked scandium-containing diaminopropyl-type dendrimers were effective Lewis Acids for heterogeneous catalysis e.g. of Diels- Alder reactions and aldol additions. [29]

The dendritic complex [{DAB-dendr-$(N(CH_2PPh_2)_2)_{16}$}$(PdCl_2)_{16}$] gave as well selective hydrogenation of conjugated dienes to monoenes.[65] Under atmospheric pressure of H_2, the dendritic complex showed higher catalytic activity than its monomer parent. This increased reactivity was shown to result from the dendritic structure containing many amino moieties (presence of bases accelerated the reaction). Interestingly, the best activity was obtained in polar solvent where the catalyst was insoluble. Recycling of the dendrimer in this heterogeneous condition was demonstrated without loss of activity. Moreover, it was found that the molecular size of dienes did not affect the hydrogenation rate.

Using diphenylphosphine functionalised carbosilane dendrimers, van Leeuwen and co-workers reported catalytic carbon-carbon coupling.[66] Nucleophilic substitution of the chlorosilane of the carbosilane by lithium diphenylphosphinomethyl-TMEDA led to the desired phosphine ligands.

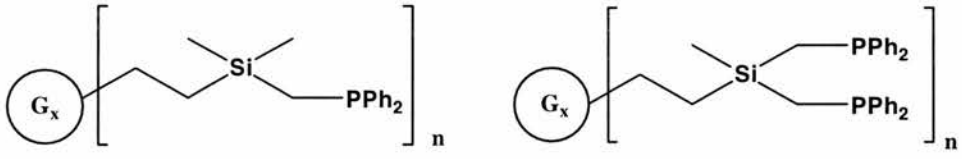

x = 0, n = 4
x = 1, n = 12
x = 2, n = 16

x = 0, n = 4
x = 1, n = 12
x = 2, n = 16

Figure 1.23 Van Leeuwen and co-workers diphenylphosphine functionalised carbosilane dendrimers.

Dendrimers with 4 and 12 endgroups each containing a chelating bidentate phosphine ligand and dendrimers with monodentate phosphine with 4 to 36 groups were synthesised (Figure 1.23). Allylpalladium complexes of these dendrimers (from $[\eta^3\text{-}C_3H_7)PdCl]_2$) were used as catalysts in the allylic alkylation reaction of allyl trifluoroacetate and sodium diethyl methylmalonate (Figure 1.24). Similar high activity was found for all the dendrimers catalysts. Attempts to use the catalytic system in a continuous flow membrane reactor gave disappointing results, the catalytic activity dropping quickly to reach zero after 15 exchange volums. The observed decrease in catalyst activity was ascribed to decomposition of the palladium compound.

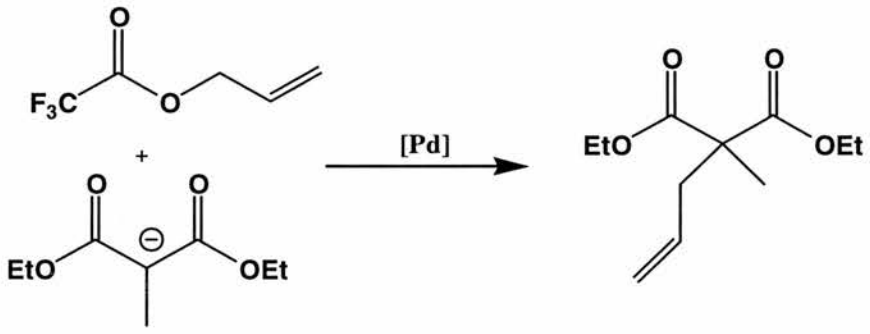

Figure 1.24 Allylic alkylation reaction of allyl trifluoroacetate and sodium diethyl methylmalonate catalysed by Pd dendritic complexes of van Leeuwen and co-workers.

Complexation with $[Rh(acac)(CO)_2]$ led under CO/H_2 pressure (20 bar) to hydroformylation of 1-octene (Figure 1.25).[67] Although the different dendrimers (i.e. successive generations, monodentate or bidentate endgroups (Figure 1.23)) and the model molecule showed identical branched/ linear selectivity (b:l) for aldehydes (b:l = 1:2.5), the reaction rates were very dependent on the structure of the phosphine ligands. All molecules with bidentate end groups (model compound and dendrimers) gave slower kinetics than their monodentate counterparts, the parent compound being three times faster than the dendrimers. However, the length of the chain between the branching point and successive generation influenced only the rates of the monodentate species. The more compact was the dendrimer (low generation, C_2 linkage), the slower were the kinetics. The authors suggested that these changes were likely to be due to the size of the

P-Rh-P ring. Increase of ligand/ rhodium ratio only modified the rate of reaction (decrease), the l:b ratio keeping unchanged.

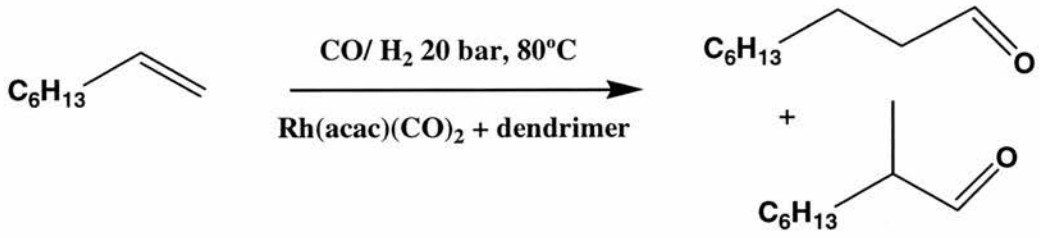

Figure 1.25 hydroformylation of 1-octene catalysed by Pd dendritic complexes of van Leeuwen and co-workers.

Another approach to the recycling of dendrimers, which has been developed by Alper *et al.* is the anchorage of phosphine-functionalised PANAM and pseudopeptide-based building block dendrimers onto respectively silica gel[68, 69] and polystyrene-based beads[70] for hydroformylation reactions. This approach allowed the recycling by microfiltration as opposed to nanofiltration techniques. The application of the diphosphonated dendrimers as ligands to rhodium complexes ($[Rh(CO)_2Cl]_2$) were shown to be excellent catalysts, i.e. highly reactive after a few cycles and regioselective for the branched aldehyde from styrene and vinyl ester systems (10-20 to 1 depending on condition and generation). Nevertheless, leaching was found to be a major problem, although higher dendritic generations and an increase in the length of the spacer chain between the N atoms afforded better activity and recyclability for the dendrimer rhodium complex. It was suggested that enhancement of reactivity was due to either well-exposed ligands on the outer-core or may have arisen from co-operative effects. In order to minimise the leaching of the metal, they targeted dendritic molecules which were designed to mimic proteins or enzymes in order to introduce ligands i.e. complexes on the inner arms (Figure 1.26).[71] This heterogenized catalytic system was selected to test the "*biomimetic-based hypothesis that ligands immersed in dendritic architectures may exhibit a prolonged reactivity by preserving the catalytic sites from the outer environment, and it may prevent leaching of the metal, etc*". These dendritic catalytic systems indeed exhibited a better response to the recycling behaviour. No reduction in

reactivity was observed with the second generation dendritic catalyst (Figure 1.26). Furthermore enhanced recycling potential, as hypothesised, was found compared to the first generation and to the results of earlier works[68, 69].

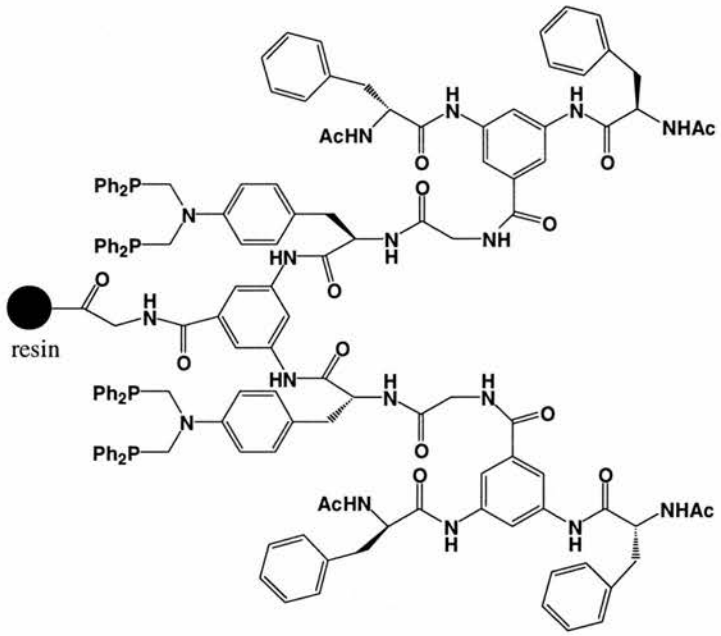

Figure 1.26 Heterogenized catalytic systems(G2) with ligands on arms.

Another interesting use of dendritic molecules for hydroformylation reaction is the combination of two-phase reaction medium with dendritic chemistry.[72] Double functionalisation of the boundaries of third generation PANAM by hydrophilic groups (1,3-propane sultone) and diphenyl phosphine [$PPh_2(CH_2OH)_2Cl$] led to water-soluble dendrimers (Figure 1.27).

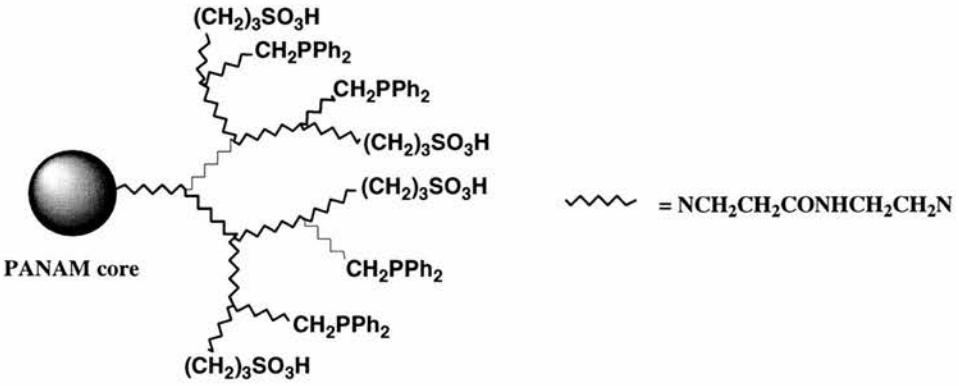

Figure 1.27 Water-soluble third generation PANAM dendrimer.

Only a monophosphination of the amino group was thought to occur leading probably to monophosphine complexes of rhodium (source $[Rh(acac)(CO)_2]$). Hydroformylation of styrene and oct-1-ene by the dendritic rhodium complexes were performed in a toluene/water biphasic medium. Small linear to branched (l:b) ratios of aldehyde (2-3 to 1) were found for oct-1-ene. Styrene hydroformylation gave better selectivities to the branched aldehyde (l:b up to 1:29). Leaching of the rhodium was found to occur; a problem that decreased with the increase of the phosphine/rhodium ratio.

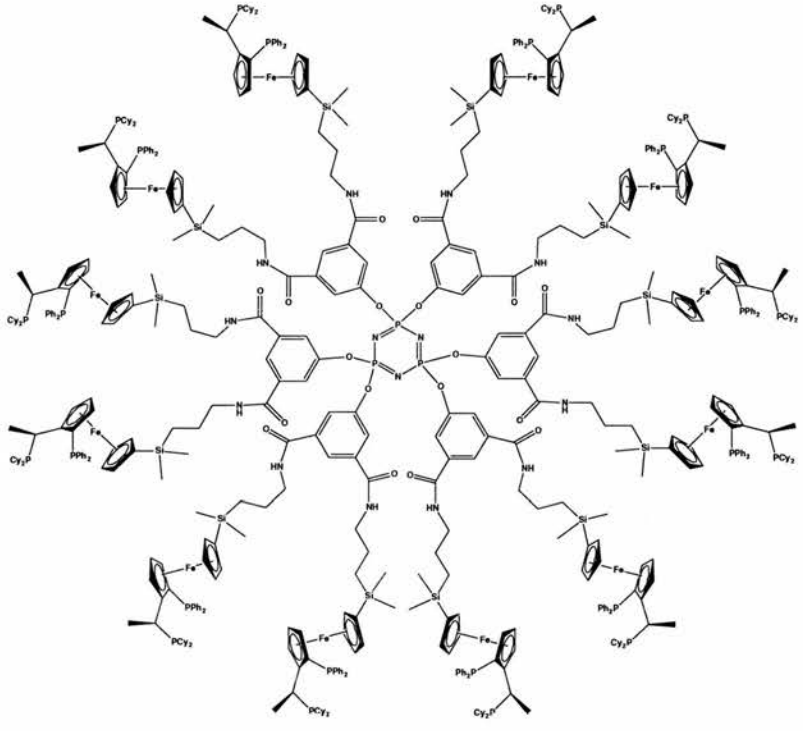

Figure 1.28 Chiral ferrocenyl ligands based on a cyclophosphazene core.

Togni *et al* synthesised dendrimers containing chiral ferrocenyl diphosphine ligands for rhodium based asymmetric catalysis. The dendritic molecules were based either on benzene 1,3,5 tricarboxylic acid and adamantane 1,3,5,7 tetracarboxylic acid cores[73] or on a cyclophosphazene core (Figure 1.28)[74] and functionalisation with Josiphos derivative (R)-(S) gave dendrimers with 6,8 or 12 and 16 ferrocenyl sites. Complexation of the different dendrimers with $[Rh(cod)_2]BF_4$ provided excellent catalysts for the hydrogenation of dimethyl itaconate in methanol (1 bar H_2, 1 % mol Rh). Only a slight decrease in selectivity (ee values of 98 % instead of 99 %) was found

but with no loss of activity. Interestingly, preliminary experiments indicated that a commercial nanofiltration membrane retained these low generation dendrimers.

Kakkar and co-workers reported a divergent synthesis of tri-branched phosphorus-containing dendrimers (Figure 1.29) and their rhodium-containing complexes.[75] Organophosphine moieties $P((CH_2)_3OH)_3$ were bound by dimethylsiloxane bridges to yield after repetitive steps dendrimers with up to 46 phosphines. Complexation with $[\mu\text{-Cl(cod)Rh}]_2$ provided efficient catalysts for alkene hydrogenation. However, a slight decrease in turnover frequencies upon growth of the complex cascade and re-use after recrystallisation was found.

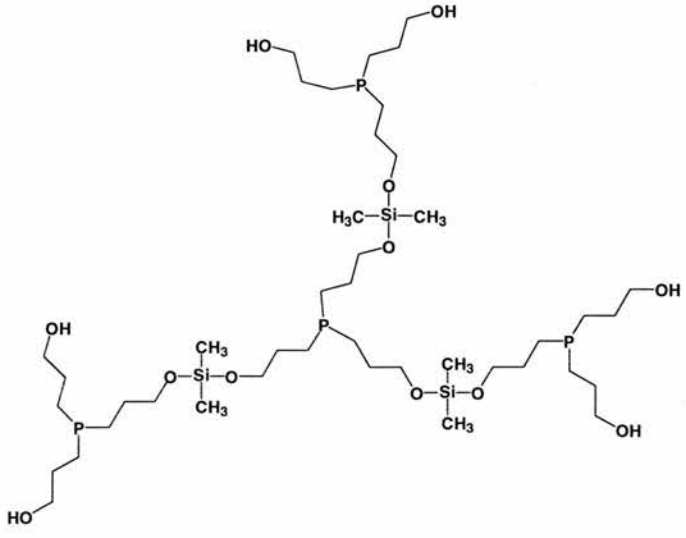

Figure 1.29 Kakkar's tribranched phosphorus containing dendrimer.

Another example of the potential of dendrimers in catalysis is the recent synthesis of copper[76] and palladium or platinum nanoclusters[77, 78]. A PANAM dendrimer was used as a synthetic template and cluster stabiliser. Dendrimer encapsulated palladium nanoparticles showed high catalytic activity for the hydrogenation of alkenes in aqueous solution or fluorous biphasic systems. Furthermore, the hydrogenation rate can be controlled, i.e. decreased, by using dendrimers with more generations (steric hindrance) and more interestingly the fluorous phase allowed the recycling up to 12 times of the dendritic molecules without leaching. Unfortunately, the rates were somewhat lower than for the polymer-supported Pd(0) catalyst.[77]

Hoveyda and co-workers reported the catalytic activity and recovery by filtration of Ru-based metathesis catalysts.[79] From a tetrapropylsilyl core they obtained a first generation dendrimer bearing four ruthenium sites (Figure 1.30). These complexes promoted catalytic ring-closing, ring-opening and intermolecular metathesis of dienes with some excellent activities. However, although the dendrimers were more readily isolable (column chromatography) and thus recyclable than their parent complexes, a higher loss of ruthenium occurred during the reaction/ recycling. The authors suggested that coiling of the relatively flexible arms of the dendrimers led to slower capture of the complex.

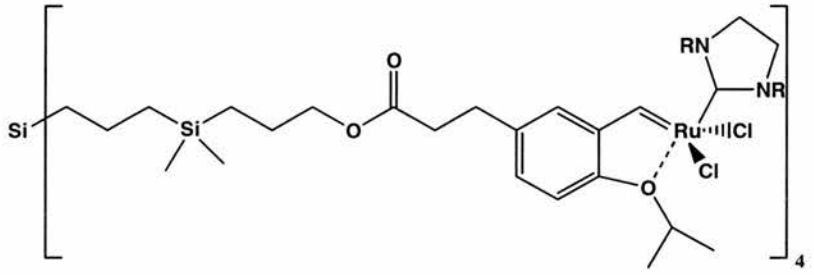

R=2,4,6-trimethylphenyl

Figure 1.30 Dendritic Ru-based metathesis catalyst.

Again in carbene chemistry, Ru-alkylidene complexes were attached by Verdonck's group to the boundary of carbosilane dendrimers (G0 and G1)(Figure 1.31).[80] The catalytic activity of the dendrimer-initiator towards ROMP catalysis of norbornene was studied. By this mean, they provided an interesting multi-arm starpolymer.

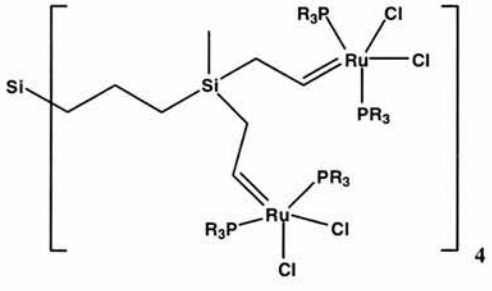

Figure 1.31 Carbosilane Ru-alkylidene complexes

Majoral , Caminade and co-workers have published some important work on phosphine-containing dendrimers.[21, 81] Metals such as palladium, platinum, rhodium, ruthenium, gold, iron, tungsten and zirconium were bound to dendritic molecules bearing ligands such as phosphine and diphosphine or internal P=N-P=S moieties. Recently they used these dendritic molecules as catalysts.[48] Third generation metallodendrimers with 24 terminal diphosphines (Figure 1.32) were found to be efficient recoverable catalysts.

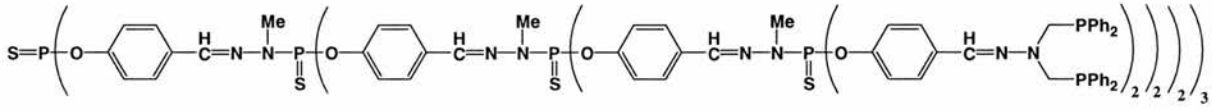

Figure 1.32 Phosphorus containing dendrimer with a phosphazene core.

The Stille coupling of methyl-2-iodobenzoate and 2-(tributylstannyl)thiophene using the palladium dendrimer complex (1 % mol Pd) (Figure 1.33) showed a better activity than the parent catalyst $[PdCl_2(PPh_3)_2]$ probably due to its improved stability (no palladium metal precipitating contrary to the monomer). Moreover the dendrimer was easily recovered by precipitation, leading to re-use up to 3 times with only a slightly decrease of activity.

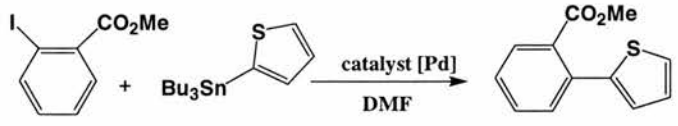

Figure 1.33 Stille coupling involving methyl-2-iodobenzoate and 2-(tributylstannyl)-thiophene.

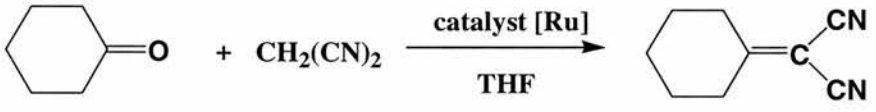

Figure 1.34 Knoevenagel condensation of malonitrile and cyclohexanone.

Similar results were acquired using the ruthenium containing dendrimer (1 % mol Ru, based catalyst $RuH_2(PPh_3)_4$) for Knoevenagel condensation of malonitrile and cyclohexanone (conversion 100 %) (Figure 1.34). Diastereoselective Michael addition of ethyl cyanoacetate and diethyl ethylidenemalonate (Figure 1.35) with the same

dendrimer led to the same conclusions, i.e. better reactivity, good recyclability, and same selectivity.

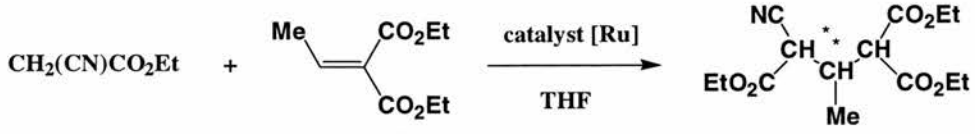

Figure 1.35 Diastereoselective Michael addition of ethyl cyanoacetate and diethyl ethylidenemalonate.

Detty *et al* reported an interesting increase of activity per catalytic group in successive dendrimer generations in the two phase-oxidation of bromide by hydrogen peroxide catalysed by phenylseleno-containing propyloxy dendrimers (Fréchet type dendrons).[82, 83] The positive bromine species were trapped by cyclohexene (Figure 1.36). Interestingly, when using the telluride compound only a statistical effect based on the number of reactive groups was obtained. The phenomenon is believed to be to due the micelle-like nature of the oxidised catalyst, structure that favoured a positive cooperativity among selenium atoms.

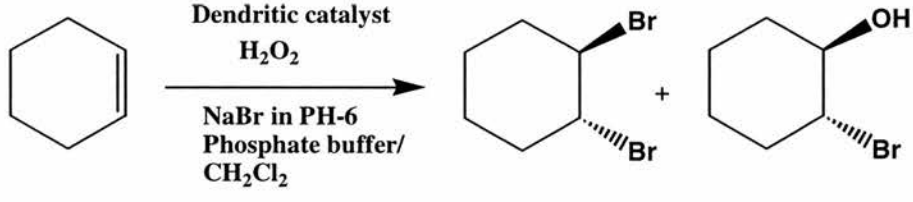

Figure 1.36 Two phase- bromination of cyclohexene by hydrogen peroxide catalysed by phenylseleno-containing propyloxy dendrimers.

Based on the hypothesis that the mechanism of asymmetric ring opening (ARO) of epoxides by metal-salen complexes (H_2salen = bis(salicycledene)ethylenediamine) involve a co-operative-bimetallic reaction, Jacobsen et al studied the reactivity of PANAM-bound [Co^{III}-(salen)] complex (up to 16 metal species) (Figure 1.37).[84] They demonstrated indeed that these catalysts exhibit significantly enhanced catalytic activity. When using a concentration of metal ([Co] = 0.025 %) which was found previously inoperant for the catalysis of vinylcyclohexane oxide, they acquired complete kinetic resolution yielding highly enantio enriched epoxide (98 % ee) at 50 % conversion.

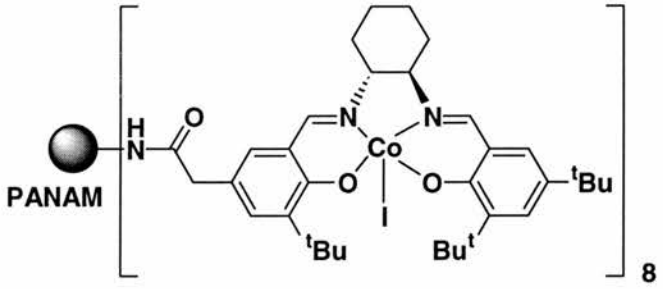

Figure 1.37 PANAM-bound [Co^{III}-(salen)] complex.

Last but not least, group four metal containing organosilicon dendrimers, and their uses as olefin polymerisation and co-polymerisation catalysts, were patented.[85]

To summarise, the dendritic structure, as shown with the active centre at the core, can modify the reactivity of the catalysts. Slow rates or worse i.e. deactivation of the catalytic species are amongst the negative contribution. However, positive effects are also widely present. Better stability and hence longer lifetime, and very importantly, better reactivity were found for these macromolecular catalysts. Moreover, ultrafiltration techniques can be successfully applied to this new class of catalysts. Therefore one can imagine that, in a close future, this promising molecules may be used in industrial processes.

1.2 SILSESQUIOXANES.

1.2.1 THE CHEMISTRY OF SILSESQUIOXANES.

The term silsesquioxane describes a class of compound that has quite a broad range. Their structures have been reported as random, ladder, cage and partial cage structures. They are three-dimensional oligomeric organo-silicon compounds with the general formula $RSiO_{3/2}$.[86, 87] The name is derived from the one and a half, or *sesqui*, stoichiometry of oxygen bound to silicon.[17]

The first commercialisation of silicones began with silsesquioxane chemistry. Resins consisting primarily of silsesquioxanes for electrical insulation at high temperature were first manufactured by the silicone industry. Today, however, polydimethylsiloxane is the predominant material used.[88] Silsesquioxane chemistry spans over half a century but interest in the area has steadily increased. There are

numerous applications for substituted silsesquioxanes, including their use as models for silica surfaces,[89, 90] Wittig reagents[91] as well as sol-gels precursors.[92] They can also be utilised as preceramic coatings that can be pyrolysed to silicon carbide,[93] nitrided glass,[94] alumino-silicates,[95, 96] silica-reinforced composites,[97] and a variety of microporous materials.[98, 99] The functionalisation by group d-transition or other metals gives metallasiloxanes,[100] which can be used as catalysts, [32, 100-103] as well as precursors for metal-containing inorganic polymers, and other materials. They have also been envisaged as single-source precursors for modified zeolites or supramolecular assemblies.

The structure that will be emphasised in this report is the polyhedral framework (cage) of formula $(RSiO_{3/2})_n$ with n = 6, 8, 10, 12... When the R group is polymerizable or graftable, the result is a novel class of compounds called **p**olyhedral **o**ligomeric **sil**sesquioxanes or POSS monomers. Although there are a variety of possible structures of polyhedral silsesquioxanes (trigonal prisms...) the compounds that are based upon a cubic structure with a general formula $Si_8O_{12}R_8$ (T_8R_8) will be discussed here. The silicon atoms are situated on each of the eight corners of the cube bridged by oxygen.[104] Each silicon is bound to a pendant group 'R' (Figure 1.38).

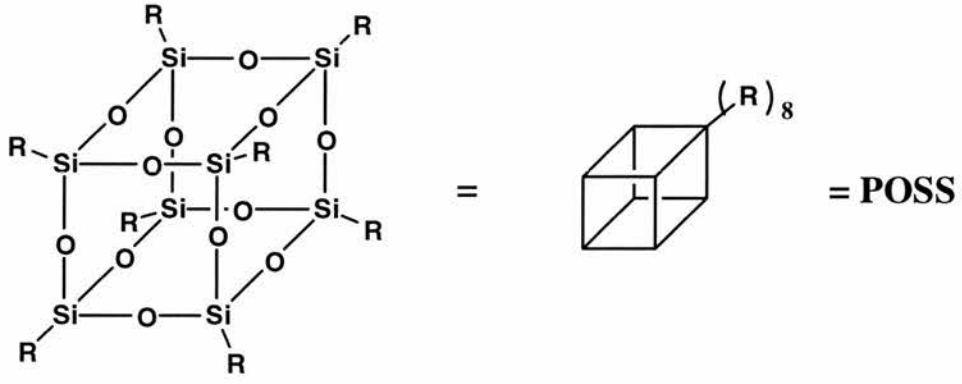

Figure 1.38: POSS molecule based on a cubic structure.

Detailed studies of other types of structures are available in the literature.[88] POSS can be obtained from the hydrolytic condensation of $RSiCl_3$ monomers and some of them are even commercially available. Which polycyclic oligomers are produced depends on many factors: solvent, reaction conditions (temperature, pH) and the nature

of the side chain R. The product(s) are often inextractable mixtures, except for those species which precipitate from the acid medium. Thus only completely condensed species with a *closo* geometry and hydrophobic alkyl groups are most often observed. Substituents on silicon (R) can include hydrogen as well as alkenyl, alkoxy, aryl functional groups etc.[105-111]

An extensive discussion of this class of compounds is beyond the scope of this report, hence a description of some aspects will be briefly covered to introduce the work done in the area. Most of the recent advances in silsesquioxane chemistry have been focussed around the POSS molecule, both the open and closed chain varieties. Not only has the impetus been on the 'R' groups bound to the silicon but also the incorporation of other elements into the framework. Extensive work has been done on the open cage (incompletely condensed) variety of the POSS molecule (Figure 1.39).

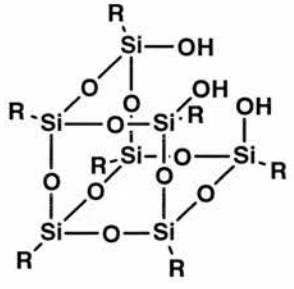

Figure 1.39 An example of a open cage POSS molecule.

As shown, one of the silicon groups is missing and hydroxide groups remain on silicon. Controlled cleavage, synthesis and reactions of the POSS molecules and framework silicones in both the open and closed cage systems have stirred interest. [109, 110, 112-116]

1.2.2 METALLOSILSESQUIOXANES.

The mono-functionalisation of a corner of the POSS has been so far the most prolific field of research. This interest emerged as an opportunity to provide insights into the chemistry of silica and silica-supported transition-metal catalysts and indeed to create new catalysts. Heterogeneous silica-supported catalysis plays an important role in the petrochemical industry and a wide range of processes such as hydrocarbon reforming and oxidation, olefin polymerisation and metathesis rely on this type of species.

However the reaction mechanism has proven difficult to model. Feher and others have published numerous works[117-119] using incompletely condensed POSS molecules. These compounds exhibit a number of features that make them suited to this task. In particular they have a sufficient degree of oligomerisation to be considered as model for silica supports. The POSS molecules possess an extensive Si—O framework and hence may have more similar electronic properties to silica and siliceous solids than simpler siloxide ligands. The rigid framework of the POSS species may allow it to dictate its coordination to a certain extent and is hence similar to a surface. It is believed that silicon atoms of a silsesquioxane framework are approximately as electron withdrawing as CF_3 groups[90]. As a consequence of their steric and electronic properties, silsesquioxane silanolate ligands increase more the Lewis acidity of the metal centres than conventional alkoxide or siloxide ligands do.

1.2.2.1 Open cage-like metallasilsesquioxanes.

Open cage structures have been used directly in catalytic systems e.g. a silsesquioxane with molybdenum incorporated in the cage (Figure 1.40) was shown rapidly to catalyse the metathesis of alkenes.[120] The catalytic polymerisation using vanadium[121], titanium[101, 122] or zirconium and hafnium complexes[123] and the catalytic epoxidation[124-127] of alkenes using titanium-containing silsesquioxane were also reported. Finally, a silica-supported vanadium-containing silsesquioxane catalyst was shown as an effective selective photo-assisted catalytic oxidation of methane to formaldehyde.[128] The POSS based catalysts were shown to exhibit similar properties to analogous non-silsesquioxane bound catalytic species.[117] Hence, the silicon framework is able to provide a useful platform upon which a catalyst is built. Not only metallasilsesquioxanes do provide realistic model compounds for silica-supported metal catalysts but they can also exhibit activities that are comparable, or even better.[100-102]

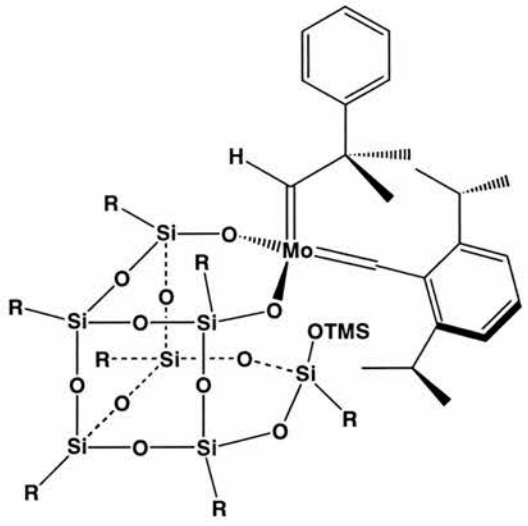

Figure 1.40 One of the four possible structures of molybdenum-containing silsesquioxane which catalyses the metathesis of alkenes.

1.2.2.2 Functionalisation of a graftable arm.

The functionalisation of the POSS by co-ordinating phosphines, or thiols is another way to provide the anchorage of a metallic centre.

Synthesis of $R_7T_8(CH_2)_3PPh_2$ compounds (R = cyclopentyl, propyl) by addition of $KPPh_2$ on the chloropropyl parent, or by reaction of the open cage $(c\text{-}C_5H_9)_7Si_7O_9(OH)_3$ with trichloro(ethyl(diphenylphosphine)silane was thus reported.[116] The ability of the phosphine compound to readily complex the tetrahedral bimetallic cluster $HFeCo_3(CO)_{12}$ (yielding $[HFeCo_3(CO)_{11}(Ph_2P(CH_2)_2T_8(c\text{-}C_5H_9)_7)]$ and $[HFeCo_3(CO)_{10}(Ph_2P(CH_2)_2T_8(c\text{-}C_5H_9)_7)_2]$) or rhodium and platinum compounds (formation of $[Rh(CO)Cl(Ph_2P(CH_2)_2T_8(C_3H_7)_7)_2]$, $[Rh(COD)Cl(Ph_2P(CH_2)_2T_8(C_3H_7)_7)]$ and $[PtCl_2.(Ph_2P(CH_2)_2T_8(C_3H_7)_7)_2]$) was shown. Maschmeyer and co-workers published earlier this year the (mono)anchorage of an active rhodium complex (Figure 1.41) for hydroformylation reaction on $[(c\text{-}C_5H_9)_7T_8(CH_2)_2PPh_2]$. Although the reactivity of the complex was tested on silica, no result on the activity/selectivity of the POSS complex was given.

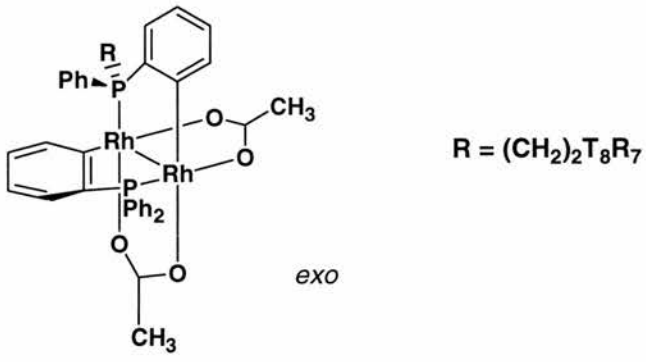

Figure 1.41 Di-rhodium complex coordinated on POSS.

The reaction between the incompletely condensed (cyclopentyl)$_7$Si$_7$O$_9$(OH)$_3$ and (3-mercaptopropyl)trimethoxysilane led to the thiol HS(CH$_2$)$_2$T$_8$(c-C$_5$H$_9$)$_7$.[129] This compound was used to quantitatively exchange the PPh$_3$ ligands in the gold cluster [(PPh$_3$)$_{12}$Au$_{55}$Cl$_6$]. Important changes in the physical and chemical behaviour of the cluster were found (stability, solubility...). In the same way HS(CH$_2$)$_2$T$_8$,(propyl)$_7$ (ssH) was used to obtain mercury and lead compounds M(ss)$_2$.[130] The Pb(ss)$_2$ was used as an intermediate to form [Au(ss)(PPh$_3$)], [Rh(ss)(CO)$_2$]$_2$, and [Rh(ss)(COD)$_2$] complexes.

Others monosubstitutions of the cube were obtained by addition of phosphoranes (R$_3$PCH$_2$) on monofunctional hydro- and chloro heptacyclohexyl POSS to give the phosphorane-substituted compounds.[91] These molecules were then used as Wittig reagents to synthesise a variety of 'monofunctionalised' cubes. The attempt to obtain octasubstitution failed.

1.2.3 POSS AS A DENDRITIC CORE

The POSS cube can be considered as a core for dendrimer growth. Indeed, the relatively inert and stable molecule provides eight functionalisable arms, the G0 generation, from which upper generations can be built. Their polyhedral structures should produce spherically symmetrical dendrimers with lower generation than other cores (e.g. tetravinyl silane). Examples of hydrosilation or substitution reactions on the POSS substituent in order to create a useful dendrimer are found in the literature (e.g. reaction of T$_8$H$_8$ with a large range of alkenes,[108-111] nucleophilic substitution of halides on the arms of the cube[131, 132] etc.). More specific chemistry was however developed by

a few research groups. Feher *et al* reported the synthesis of phosphine/ amine containing POSS. [133] The Arbuzov reaction of $T_8(p\text{-}C_6H_4CH_2I)_8$ and Ph_2POEt afforded quantitative yield of $T_8(p\text{-}C_6H_4CH_2POPh_2)_8$ which was reduced with AlH_3 to give the octa(diphenylphosphine) POSS **6** (Figure 1.42).[134] The reduction led however to incomplete conversion due to side reactions (loss of the phosphine). Addition of $[Rh(CO)_2Cl]$ to a solution of **6** resulted in the immediate formation of a gel. The gel, probably formed by cross-linking of different POSS through the phosphine rhodium species, showed no catalytic activity (hydroformylation or alkene isomerisation).

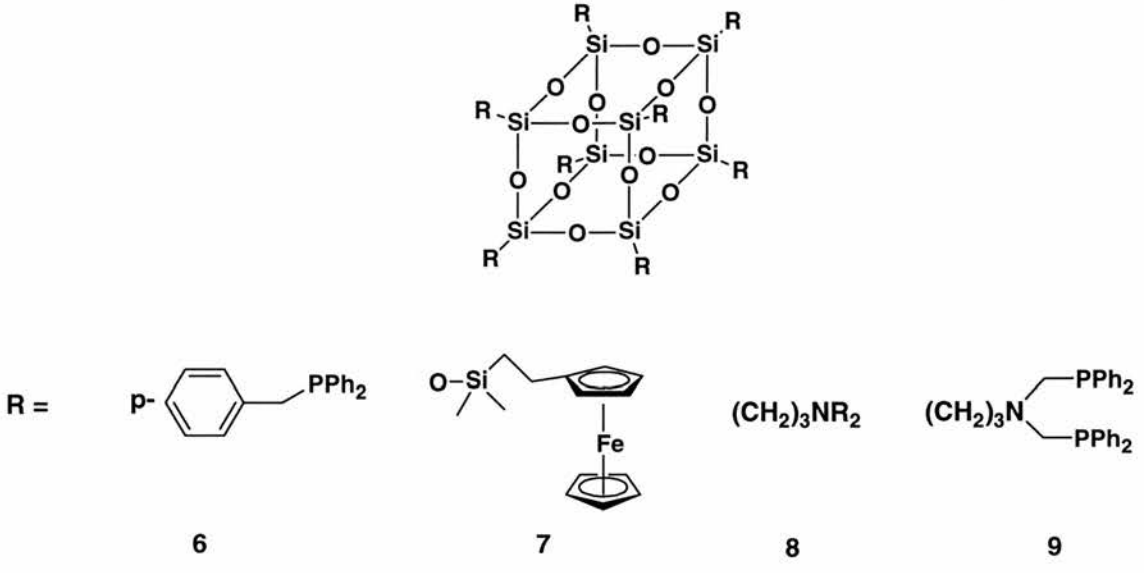

Figure 1.42 Dendritic POSS substituted by different R groups.

Lücke prepared air sensitive octa(dimethylphosphanoethyl)POSS that could easily be converted to a thio-derivative or organometallic compounds.[135] Radical addition of $HPMe_2$ to the octavinyl POSS led to the phosphorus compound that was characterised by X-ray structural analysis. Complexation with $W(CO)_5THF$, $CpMn(CO)_3$, $CpCo(CO)_2$ or $Cp^*Rh(CO)_2$ gave the octasubstituted organometallic complexes. No reactivity of these compounds was reported. In a similar way, mono-, di- or octa-thiol-containing POSS compounds complexed with metal carbonyl clusters (Ru, Os) were published by Braunstein and Marsmann.[136] The thiol moieties ($T_8[(CH_2)_3SH]_8$) were covalently bonded by oxidative addition on the metal cluster ($M_3(CO)_{10}(NCMe)_2$)

to yield for example $M_3(\mu\text{-}H)(\mu_2\text{-}SR)(CO)_{10}$ (M = Ru, Os) (R = POSS). No further chemistry was given. Another interesting synthesis is the ferrocene derivatised octasilsesquioxane.[137] Hydrosililation of vinylferrocene to the POSS gave the metallasilsesquioxane **7** (Figure 1. 42) which showed expected electrochemical properties.

More recently, a few groups have reported the use of POSS as core for higher generation dendrimers. Hong *et al* synthesised terpyridine-functionalised polyether monodendron with a POSS core and the corresponding Ru^{II} based chromophores.[138, 139] From the octa(propyldiphenylphosphine)POSS core, they prepared dendritic molecules with 8, 12 to 32 redox-active and photoactive $(bpy)_2Ru^{II}$ (tpy) groups (Figure 1.43). Feher has published the synthesis of others substituted POSS.[119] Reactions of amino pendant group **8** with electrophiles (ester, lactones,...) afforded different varieties of dendrimers such as the rather unstable γ-aminopropyl-derivatised POSS, as well as the interesting phosphine-containing dendrimer **9** $[(Ph_2PCH_2)_2N(CH_2)_3]_8Si_8O_{12}$ (yield 37 %) synthesised from reaction of PPh_2CH_2OH with the octaamino POSS. [133, 140]

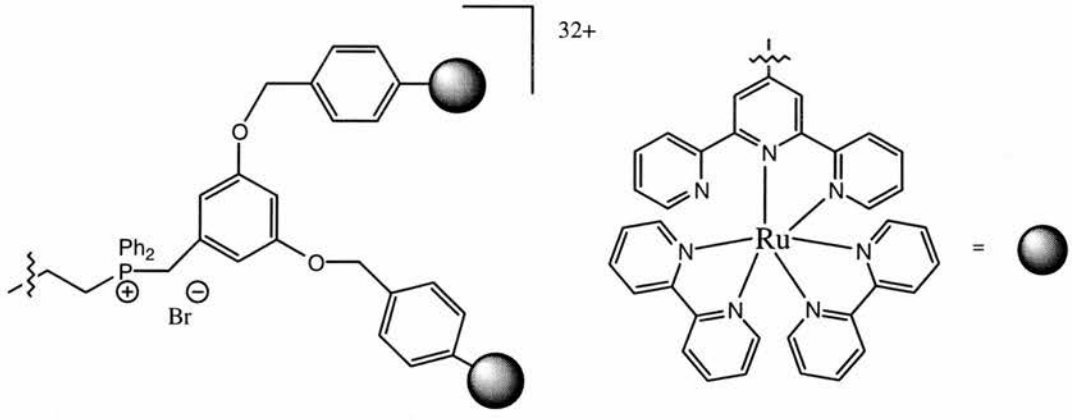

Figure 1.43 POSS core substituted by redox-active and photoactive $(bpy)_2Ru^{II}$ (tpy) groups.

Morris *et al* prepared[141] up to 72-chloride or 72-vinyl functionalised POSS by successive alkenylation- silylation reactions (Figure 1.44) (see Chapter III). They also used the smaller generation chloro compounds to synthesise silanol functionalised dendrimers (up to 16 hydroxyl groups).[142] The method of choice was found to be the reduction of the chlorosilane to Si-H using $LiAlH_4$ and subsequent catalytic hydrolysis to

Si-OH using water over palladium supported on carbon. They also characterised some octa dioxolane and aldehyde POSS that were converted to carboxylic acid and Schiff base species.[143] Applying another route to synthesise the core, conversion of the silsesquioxane-type tetramethylammonium octasilicate ($(NMe_4)_{85}Si_8O_{20}$) $69H_2O$ by addition of chlorosilanes or siloxanes, Edelmann *et al* reported successive alkenylation-silylation reactions leading to a 24 functionalised dendrimer similar to those described by Morris.[144]

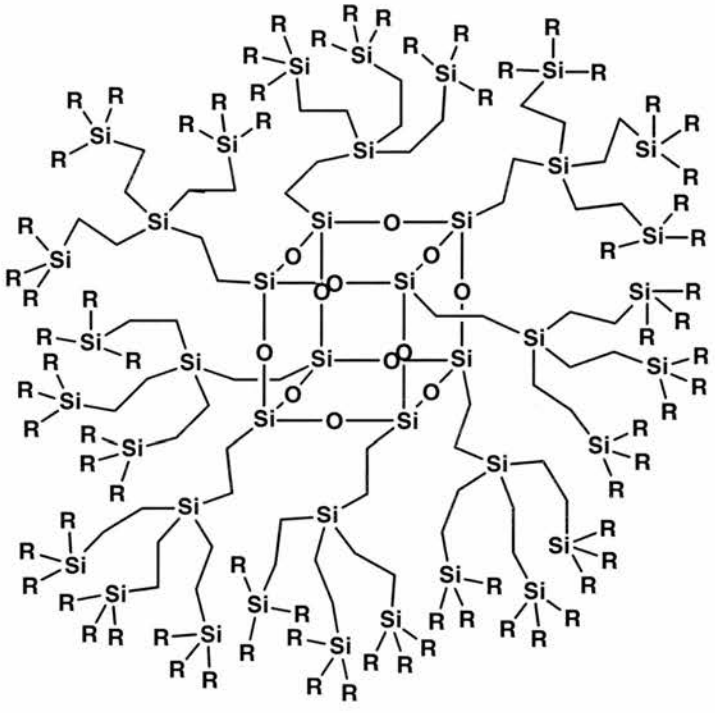

Figure 1.44 A 72-R-substituted POSS (R = Cl, Vinyl).

To conclude, the polyhedral octasilsesquioxane core has shown to be an excellent platform to build new (mono)substituted compounds or highly branched dendrimers. These new dendritic molecules are easily functionalised by simple organic or inorganic reactions. The chemistry/ properties of such macromolecules are already promising despite the few works published so far.

1.3 REFERENCES FOR CHAPTER 1.

1 N. Ardoin and D. Astruc, *Bull. Soc. Chim. Fr.*, 1995, **132**, 875.

2 E. Buhleier, W. Wehner, and F. Vögtle, *Synthesis*, 1978, 155.

3 G. R. Newkome, Z.-Q. Yao, G. R. Baker, and K. J. Gupta, *J. Org. Chem.*, 1985, **50**, 2003.

4 D. A. Tomalia, H. Baker, J. R. Dewald, M. Hall, G. Kallos, S. Martins, J. Roeck, J. Ryder, and P. Smith, *Polym. J.*, 1985, **17**, 117.

5 D. Tomalia and R. Dewald, *US Pat.*, **4 507 466**.

6 D. A. Tomalia, A. M. Naylor, and W. A. Goddard III, *Angew. Chem. Int. Ed.*, 1990, **29**, 138.

7 D. A. Tomalia and P. R. Dvornic, *Nature*, 1994, **372**, 617.

8 H.-B. Mekelburger, W. Jaworek, and F. Vögtle, *Angew. Chem. Int. Ed.*, 1992, **31**, 1571.

9 D. A. Tomalia and R. Esfand, *Chem. Ind.*, 1997, 416.

10 M. Fisher and F. Vögtle, *Angew. Chem. Int. Ed.*, 1999, **38**, 884.

11 A. Archut and F. Vögtle, *Chem. Soc. Rev.*, 1998, **27**, 233.

12 A. W. Bosman, H. M. Janssen, and E. W. Meijer, *Chem. Rev.*, 1999, **99**, 1665.

13 A. D. Schlüter and J. P. Rabe, *Angew. Chem. Int. Ed.*, 2000, **39**, 864.

14 F. Vögtle, S. Gestermann, R. Hesse, H. Schwierz, and B. Windisch, *Prog. Polym. Sci.*, 2000, **25**, 987.

15 K. Inoue, *Prog. Polym. Sci.*, 2000, **25**, 453.

16 F. J. Stoddart and T. Welton, *Polyhedron*, 1999, **18**, 3575.

17 J.-P. Marjoral and A.-M. Caminade, *Chem. Rev.*, 1999, **99**, 845.

18 G. R. Newkome, E. He, and C. N. Moorefield, *Chem. Rev.*, 1999, **99**, 1689.

19 M. A. Hearshaw and J. R. Moss, *J. Chem. Soc., Chem. Commun.*, 1999, 1.

20 I. Cuadrado, M. Morán, C. M. Casado, B. Alonso, and J. Losada, *Coord. Chem. Rev.*, 1999, **193-195**, 395.

21 A.-M. Caminade, R. Laurent, B. Chaudret, and J. P. Majoral, *Coord. Chem. Rev.*, 1998, **178-180**, 793.

22 P. R. Dvornic, A. M. de Leuze-Jallouli, M. J. Owen, and S. V. Perz, *Macromolecules*, 2000, **33**, 5366.

23 R. Dagani, *Chem. Eng. News*, 1996, 30.

24 C. J. Hawker and J. M. J. Frechet, *J. Am. Chem. Soc.*, 1990, **112**, 7638.

25 D. A. Tomalia, *Adv. Mat.*, 1994, **6**, 529.

26 S. Hecht and J. M. J. Fréchet, *Angew. Chem. Int. Ed.*, 2001, **40**, 74.

27 A. Adronov and J. M. J. Fréchet, *J. Chem. Soc., Chem. Commun.*, 2000, 1701.

28 K. Matyjaszewski, T. Shigemoto, J. M. J. Fréchet, and F. Leduc, *Macromolecules*, 1996, **29**, 4167.

29 M. Reetz and D. Giebel, *Angew. Chem. Int. Ed.*, 2000, **39**, 2498.

30 J. W. J. Knapen, A. W. van der Made, J. C. de Wilde, P. W. M. N. van Leeuwen, P. Wijkens, D. M. Grove, and G. van Koten, *Nature*, 1994, **372**, 659.

31 J. Haggin, *Chem. Eng. News*, 1995, **Feb 6**, 26.

32 L. A. van de Kuil, D. M. Grove, J. W. Zwikker, L. W. Jenneskens, W. Drenth, and G. van Koten, *Chem. Mater.*, 1994, **6**, 1675.

33 P. Bhyrappa, J. K. Young, J. S. Moore, and K. S. Suslick, *J. Am. Chem. Soc.*, 1996, **118**, 5708.

34 P. Bhyrappa, J. K. Young, J. S. Moore, and K. S. Suslick, *J. Mol. Cata. A: Chem.*, 1996, **113**, 109.

35 M. Kimura, Y. Sugihara, T. Muto, K. Hanabusa, H. Shirai, and N. Kobayashi, *Chem. Eur. J.*, 1999, **5**, 3495.

36 C. C. Mak and H.-F. Chow, *Macromolecules*, 1997, **30**, 1228.

37 H.-F. Chow and C. C. Mak, *J. Org. Chem.*, 1997, **62**, 5116.

38 G. E. Oosterom, R. J. van Haaren, J. N. H. Reek, P. C. J. Kamer, and P. W. N. M. van Leeuwen, *J. Chem. Soc., Chem. Commun.*, 1999, 1119.

39 H. Brunner, *J. Organo. Chem.*, 1995, **500**, 39.

40 H. Brunner, S. Stefaniak, and M. Zabel, *Synthesis*, 1999, 1776.

41 Q.-H. Fan, Y.-M. Chen, D.-Z. Jiang, F. Xi, and A. S. C. Chan, *J. Chem. Soc., Chem. Commun.*, 2000, 789.

42 C. Bolm, N. Derrien, and A. Seger, *Synlett*, 1996, **4**, 387.

43 Q.-S. Hu, V. Pugh, M. Sabat, and L. Pu, *J. Org. Chem.*, 1999, **64**, 7528.

44 H. Sellner and D. Seebach, *Angew. Chem. Int. Ed.*, 1999, **38**, 1918.

45 P. B. Rheiner and D. Seebach, *Chem. Eur. J.*, 1999, **5**, 3221.

46 S. Yamago, M. Furukawa, A. Azuma, and J.-I. Yoshida, *Tetrahedron Lett.*, 1998, **39**, 3783.

47 M. Albrecht, N. J. Hovestad, J. Boersma, and G. van Koten, *Chem. Eur. J.*, 2001, **7**, 1289.

48 V. Maraval, R. Laurent, A.-M. Caminade, and J.-P. Majoral, *Organometallics*, 2000, **19**, 4025.

49 I. Morao and F. P. Cossío, *Tetrahedron Lett.*, 1997, **38**, 6461.

50 M. E. Piotti, F. Rivera, R. Bond, C. J. Hawker, and J. M. J. Fréchet, *J. Am. Chem. Soc*, 1999, **121**, 9471.

51 A. Schmitzer, E. Prez, I. Rico-Lattes, and A. Lattes, *Tetrahedron Letters*, 1999, **40**, 2947.

52 C. Bolm, N. Derrien, and A. Seger, *J. Chem. Soc., Chem. Commun.*, 1999, 2087.

53 R. A. Gossage, J. T. B. H. Jastrzebski, J. van Ameijade, S. J. E. Mulders, A. J. Brouwer, R. M. J. Liskamp, and G. van Koten, *Tetrahedron Letters*, 1999, **40**, 1413.

54 G. van Koten and J. T. B. H. Jastrzebski, *J. Mol. Cata. A: Chem.*, 1999, **146**, 317.

55 A. W. Kleij, R. A. Gossage, J. T. B. H. Jastrzebski, J. Boersma, and G. van Koten, *Angew. Chem. Int. Ed.*, 2000, **39**, 176.

56 A. W. Kleij, R. J. M. Klein Gebbink, P. A. J. van den Nieuwenhuijzen, H. Kooijman, M. Lutz, A. Spek, and G. van Koten, *Organometallics*, 2001, **20**, 634.

57 P. Wijkens, J. T. B. H. Jastrzebski, P. A. van der Schaaf, R. Kolly, A. Hafner, and G. van Koten, *Org. Letters*, 2000, **2**, 1621.

58 E. B. Eggeling, N. J. Hovestad, J. T. B. H. Jastrzebski, D. Vogt, and G. van Koten, *J. Org. Chem.*, 2000, **65**, 8857.

59 N. J. Hovestad, E. B. Eggeling, H. J. Heidbüchel, J. T. B. H. Jastrzebski, U. Kragl, W. Keim, D. Vogt, and G. van Koten, *Angew. Chem. Int. Ed.*, 1999, **38**, 1655.

60 D. Seebach, R. E. Marti, and T. Hintermann, *Helv. Chim. Acta*, 1996, **79**, 1710.

61 A. Miedaner, C. J. Curtis, R. M. Barkley, and D. L. DuBois, *Inorg. Chem.*, 1994, **33**, 5482.

62 A. M. Herring, B. D. Steffey, A. Miedaner, S. A. Wander, and D. L. DuBois, *Inorg. Chem.*, 1995, **34**, 1100.

63 M. T. Reetz, G. Lohmer, and R. Schwickardi, *Angew. Chem. Int. Ed. Engl.*, 1997, **36**, 1526.

64 N. Brinkmann, G. Giebel, G. Lohmer, M. T. Reetz, and U. Kragl, *J. Catal.*, 1999, **183**, 163.

65 T. Mizugaki, M. Ooe, K. Ebitani, and K. kaneda, *J. Mol. cata. A: Chem.*, 1999, **145**, 329.

66 D. de Groot, E. Eggeling, J. C. de Wilde, H. Kooijman, R. J. van Haaren, A. W. van der Made, A. L. Spek, D. Vogt, J. N. H. Reek, P. C. J. Kamer, and P. W. N. M. van Leewen, *J. Chem. Soc., Chem. Commun.*, 1999, 1623.

67 D. de Groot, P. G. Emmerink, C. Coucke, J. N. H. Reek, P. C. J. Kamer, and P. W. N. M. van Leewen, *Inorg. Chem. Commun.*, 2000, **3**, 711.

68 S. C. Bourque, F. Maltais, W. J. Xia, O. Tardif, H. Alper, P. Arya, and L. E. Manzer, *J. Am. Chem. Soc.*, 1999, **21**, 3035.

69 S. C. Bourque and H. Alper, *J. Am. Chem. Soc.*, 2000, **122**, 956.

70 P. Arya, N. V. Rao, J. Singkhonrat, H. Alper, S. C. Bourque, and L. E. Manzer, *J. Org. Chem.*, 2000, **65**, 1881.

71 P. Arya, G. Panda, N. V. Rao, H. Alper, S. C. Bourque, and L. E. Manzer, *J. Am. Chem. Soc.*, 2001, **123**, 2889.

72 A. Gong, Q. Fan, Y. Chen, H. Liu, C. Chen, and F. Xi, *J. Molecular Cata. A: chemical*, 2000, **159**, 225.

73 C. Köllner, B. Pugin, and A. Togni, *J. Am. Chem. Soc.*, 1998, **120**, 10274.

74 R. Schneider, C. Köllner, I. Weber, and A. Togni, *J. Chem. Soc., Chem. Commun.*, 1999, 2415.

75 M. Petrucci-Samija, V. Guillemette, M. Dasgupta, and A. K. Kakkar, *J. Am. Chem. Soc.*, 1999, **121**, 1968.

76 M. Zhao, L. Sun, and R. M. Crooks, *J. Am. Chem. Soc.*, 1998, **120**, 4877.

77 V. Chechnik and R. M. Crooks, *J. Am. Chem. Soc.*, 2000, **212**, 1243.

78 M. Zhao and R. M. Crooks, *Angew. Chem. Int. Ed.*, 1999, **38**, 364.

79 S. B. Garber, J. S. Kingsbury, B. L. Gray, and A. H. Hoveyda, *J. Am. Chem. Soc.*, 2000, **122**, 8169.

80 H. Beerens, F. Verpoort, and L. Verdonck, *J. Mol. Cata. A: Chem*, 2000, **151**, 279.

81 V. Maraval, R. Laurent, B. Donnadieu, M. Mauzac, A.-M. Caminade, and J.-P. Majoral, *J. Am. Chem. Soc*, 2000, **122**, 2499.

82 C. Francavilla, F. V. Bright, and M. R. Detty, *Org. Letters.*, 1999, **1**, 1043.

83 C. Francavilla, M. D. Drake, F. V. Bright, and M. R. Detty, *J. Am. Chem. Soc.*, 2001, **123**, 57.

84 R. Breinbauer and E. R. Jacobsen, *Angew. Chem. Int. Ed.*, 2000, **39**, 3604.

85 D. Seyferth and R. Wyrwa, U. S. Patent, 5,969,073, 1999, Massachusetts Institute of Technology.

86 A. Tsuchida, c. Bolln, F. G. Sernetz, H. Frey, and R. Mulhaupt, *Macromolecules*, 1997, **30**, 2818.

87 J. Lichtenhan, *Comments Inorg. Chem.*, 1995, **17**, 115.

88 R. H. Baney, M. Itoh, A. Sakakibara, and T. Suzuki, *Chem. Rev.*, 1995, **95**, 1409.

89 F. J. Feher and T. A. Budzichowski, *Organometallics*, 1991, **10**, 812.

90 F. J. Feher and T. A. Budzichowski, *J. Organomet. Chem.*, 1989, **379**, 33.

91 F. J. Feher, K. J. Weller, and J. J. Schawb, *Organometallics*, 1995, **14**, 2009.

92 D. A. Loy and K. J. Shea, *Chem. Rev.*, 1995, **95**, 1431.

93 G. T. Burns, R. B. Taylor, Y. R. Xu, A. Zangril, and G. A. Zank, *Chem. Mater.*, 1992, **4**, 1313.

94 K. Kamiya, M. Okya, and T. Yoko, *J. Noncryst. Solids*, 1986, **83**, 208.

95 F. J. Feher and K. J. Weller, *Organometallics*, 1990, **9**, 2638.

96 F. J. Feher, K. J. Weller, and J. W. Ziller, *J. Am. Chem. Soc.*, 1992, **114**, 9686.

97 R. A. Mantz, P. F. Jones, K. P. Chaffe, J. D. Lichtenhan, J. W. Gilman, and I. M. K. Ismail, *Chem. Mater.*, 1996, **8**, 1250.

98 S. Lee, S. Makan, M. M. B. Holl, and F. R. MacFeely, *J. Am. Chem. Soc.*, 1994, **116**, 11819.

99 P. Agaskar, *J. Chem. Soc., Chem. Commun.*, 1992, 1024.

100 V. Lorenz, A. Fischer, S. Gießmann, J. W. Gilje, Y. Gun'ko, K. Jacob, and F. Edelmann, *Coord. Chem. Rev.*, 2000, **206-207**, 321.

101 J.-C. Liu, *J. Chem. Soc., Chem. Commun.*, 1996, 1109.

102 H. C. L. Abbenhuis, *Chem. Eur. J.*, 2000, **6**, 25.

103 Y.-S. Fu and S. J. Yu, *Angew. Chem. Int. Ed.*, 2001, **40**, 437.

104 M. G. Voronkov and V. L. Lavrent'yev, *Top. Curr. Chem.*, 1982, **102**, 199.

105 P. Harrison and R. Kannengieser, *J.Chem. Soc., Chem. Commun.*, 1996, 415.

106 J. Lichtenhan, N. Q. Vu, J. A. Carter, J. W. Gilman, and F. J. Feher, *Macromolecules*, 1993, **26**, 2141.

107 P. Mather, K. Chaffee, T. Haddad, and J. Lichtenhan, *Polym. Prepr. (Am. Chem. Soc. Div. Polym. Chem)*, 1996, **37**, 765.

108 C. Bolln, A. Tsuchida, H. Frey, and R. Mulhaupt, *Chem. Mater.*, 1997, **9**, 1475.

109 A. R. Bassindale and T. E. Gentle, *J. Mater. Chem*, 1993, **3**, 1319.

110 A. R. Bassindale, *J. Organomet. Chem.*, 1996, **521**, 391.

111 R. Elsäßer, G. H. Mehl, J. W. Goodby, and D. J. Photinos, *J. Chem. Soc., Chem. Commun.*, 2000, 851.

112 F. J. Feher, D. Soulivong, and G. T. Lewis, *J. Am. Chem. Soc.*, 1997, **119**, 11323.

113 F. J. Feher and S. H. Phillips, *J. Organomet. Chem.*, 1996, **521**, 401.

114 F. J. Feher, D. Soulivong, and A. G. Eklund, *J. Chem. Soc., Chem. Commun.*, 1998, 399.

115 F. J. Feher, T. A. Budzichowski, R. L. Blanski, K. J. Weller, and J. W. Ziller, *Organometallics*, 1991, **10**, 2526.

116 V. Ruffieux, G. Schmid, P. Braunstein, and J. Rose, *Chem. Eur. J.*, 1997, **3**, 900.

117 F. J. Feher and T. A. Budzichowski, *Polyhedron*, 1995, **14**, 3239.

118 F. T. Edelmann, *Angew. Chem. Int. Ed. Engl.*, 1992, **31**, 586.

119 F. J. Feher, S. H. Phillips, and J. W. Ziller, *J. Chem. Soc., Chem. Commun.*, 1997, 829.

120 F. J. Feher and T. L. Tajima, *J. Am. Chem. Soc.*, 1994, **116**, 2145.

121 F. J. Feher and R. L. Blanski, *J. Am. Chem. Soc.*, 1992, **114**, 5886.

122 R. Duchateau, H. C. L. Abbenhuis, R. A. van Santen, S. K.-H. Thiele, and M. F. H. van Tol, *Organometallics*, 1998, **17**, 5222.

123 R. Duchateau, H. C. L. Abbenhuis, R. A. van Santen, A. Meetsma, S. K.-H. Thiele, and M. F. H. van Tol, *Organometallics*, 1998, **17**, 5663.

124 S. Krijnen, H. C. L. Abbenhuis, R. W. J. M. Hanssen, J. H. C. van Hooff, and R. A. van Santen, *Angew. Chem. Int. Ed. Engl.*, 1998, **37**, 356.

125 M. Crocker, R. H. M. Herold, and A. G. Orpen, *J. Chem. Soc., Chem. Commun.*, 1997, 2411.

126 M. Crocker, R. H. M. Herold, A. G. Orpen, and M. T. A. Overgaag, *J. Chem. Soc., Dalton Trans.*, 1999, 3791.

127 T. Maschmeyer, M. C. Klunduk, C. M. Martin, D. S. Shephard, J. M. Thomas, and B. F. G. Johnson, *J. Chem. Soc., Chem. Commun.*, 1997, 1847.

128 K. Wada, M. Nakashita, A. Yamamoto, and T. Mitsudo, *J. Chem. Soc., Chem. Commun.*, 1998, 133.

129 G. Schmid, R. Pugin, J.-O. Malm, and J.-O. Bovin, *Eur. J. Inorg. Chem.*, 1998, 813.

130 B. J. Hendan and H. C. Marsmann, *Appl. Organometal. Chem.*, 1999, **13**, 287.

131 S. Lücke, K. Stoppek-Langner, B. Krebs, and M. Läge, *Z. Anorg. Allg. Chem.*, 1997, **623**, 1243.

132 U. Dittmar, B. J. Hendan, U. Flörke, and H. C. Marsmann, *J. Organomet. Chem.*, 1995, **489**, 185.

133 F. J. Feher and K. D. Wyndham, *J. Chem. Soc., Chem. Commun.*, 1998, 323.

134 F. J. Feher, J. J. Schwab, S. H. Phillips, A. Eklund, and E. Martinez, *Organometallics*, 1995, **14**, 4452.

135 S. Lücke, K. Stoppek-Langner, J. Kuchinke, and B. Krebs, *J. Organomet. Chem.*, 1999, **584**, 11.

136 P. Braunstein, J. R. Galsworthy, B. J. Hendan, and H. C. Marsmann, *J. Organomet. Chem.*, 1998, **551**, 125.

137 M. Moràn, C. M. Casado, I. Cuadrado, and J. Losada, *Organometallics*, 1993, **12**, 4327.

138 B. Hong, T. P. S. Thomas, H. J. Murfee, and M. J. Lebrun, *Inorg. Chem.*, 1997, **36**, 6146.

139 H. J. Murfee, T. P. S. Thoms, J. Greaves, and B. Hong, *Inorg. Chem.*, 2000, **39**, 5209.

140 F. J. Feher, K. D. Wyndham, D. Soulivong, and F. Nguyen, *J. Chem. Soc., Dalton Trans.*, 1999, 1491.

141 P.-A. Jaffrès and R. E. Morris, *J. Chem. Soc., Dalton Trans.*, 1998, 2767.

142 P. I. Coupar, P.-A. Jaffrès, and R. E. Morris, *J. Chem. Soc., Dalton Trans.*, 1999, 2183.

143 B. W. Manson, J. J. Morrison, P. I. Coupar, P.-A. Jaffrès, and R. E. Morris, *J. Chem. Soc., Dalton Trans.*, 2001, 1123.

144 E. Müller and F. T. Edelmann, *Main Group Metal Chemistry*, 1999, **22**, 485.

Chapter Two: Hydroformylation reaction catalysed by rhodium complexes.

2 Hydroformylation reaction catalysed by rhodium complexes.

2.1 Introduction to the hydroformylation reaction.

The hydroformylation reaction formally corresponds to an addition of formaldehyde across the double bond of an alkene catalyzed by transition metal complexes. Carbon monoxide and hydrogen are in fact the source of the formyl group yielding aldehydes. Alcohols can sometimes be the products of reaction due to subsequent hydrogenation of the aldehydes. This process is one of the most important homogeneous catalytic reactions used in industry because of the use of alcohols (produced from the aldehydes) as starting materials for plasticizers (C5-C11), surfactants (C12-C16), detergent alcohols, etc.[1]

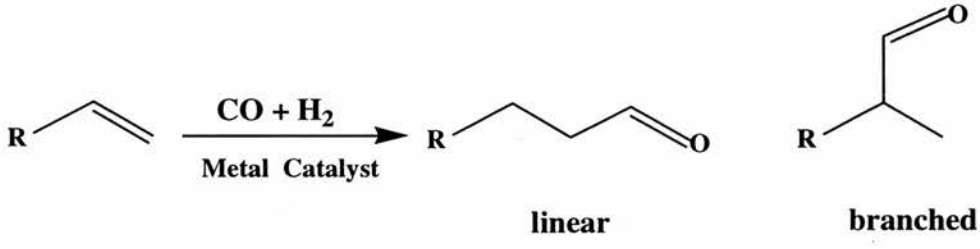

Scheme 2.1 Hydroformylation of alkene catalysed by a transition metal.

Two main products, linear or branched aldehyde, are obtained during this reaction. Consequently most of the research has focused on an increase of regioselectivity to the linear (mainly) or branched compound to avoid a difficult separation process. The main factors controlling the selectivity depend on the substrate itself, the catalytic species (ligand, metal) and the reaction conditions (solvent, temperature, pressure, etc.). For example using unmodified rhodium complexes, the regioselectivity in the hydroformylation of unsaturated vinyl substrates depends on the steric and electronic nature of the α substituent. Electron-withdrawing groups (phenyl, ester) will favor the branched isomer, while bulky groups and linear alkene compounds will give predominantly the linear compound.[1]

After the discovery by Roelen of the first 'oxo' reaction (hydroformylation reaction) in the 1930's,[2, 3] one had to wait 30 years to see the first breakthrough in rhodium-catalyzed hydroformylation.[4, 5] Although rhodium-based catalysts such as $[Rh_4(CO)_{12}]$ were found much more active and chemo-selective than the cobalt complexes as early as the end of the 1950's,[1, 6, 7] they were not really considered

before Wilkinson's work on triphenylphosphine rhodium complexes[5] due to the high hydrogen partial pressures requires to form the active hydride species.[8] The first cobalt catalysts used were unmodified metal carbonyl compounds such as $[Co_2(CO)_8]$.[9] Heck and Breslow proposed a dissociative mechanism of reaction to explain the hydroformylation process (Scheme 2.2)[10]. The catalytic conditions applied were relatively vigorous (200-400 bar and 150°C-200°C) due to the low reactivity of the cobalt catalysts and the insolubility of the complexes under low CO pressure.[11] Low and high molecular weight alkenes as well as terminal and internal ones could be converted to aldehydes. However, the vigorous conditions required, the low selectivity and the amounts of by-products (alkanes, ketones, aldol condensation products) limited the process.

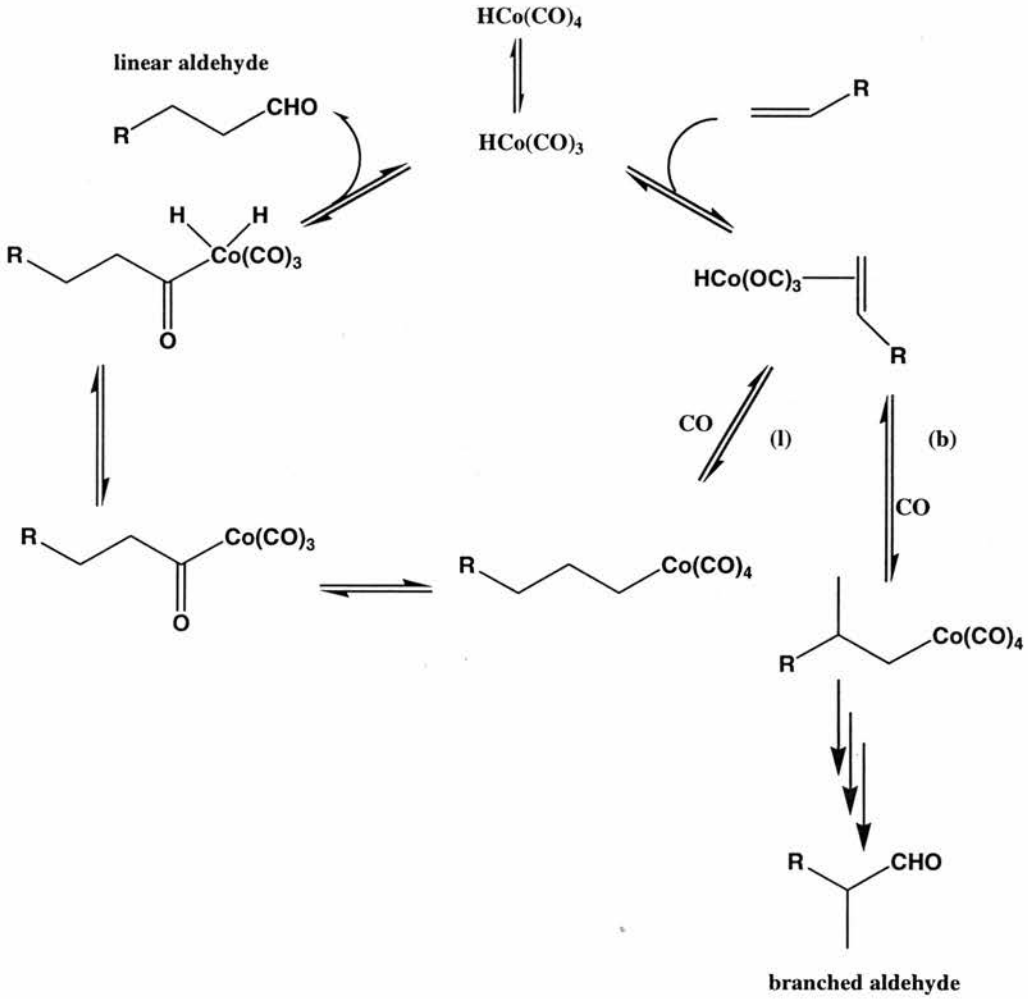

Scheme 2.2 Hydroformylation mechanism of alkene by $[HCo(CO)_4]$ proposed by Heck and Breslow.

Improved selectivity was obtained by addition of trialkylphosphine ligands.[12-14] Interestingly with these electron-donating phosphorus ligands, hydrogenation of the aldehydes to alcohols was obtained. Trialkylphosphine rhodium catalysts did not lead to the same beneficial effect (lower reactivity).[1] The synthesis, characterization and catalytic studies of rhodium-hydride complexes containing triphenylphosphine by Wilkinson's group gave birth to new catalytic systems for reactions such as hydroformylation and hydrogenation processes.[5, 15-17] They showed that these complexes afforded active and selective hydroformylation catalysts under mild conditions (20-120°C, pressure 5-50 bar). The common catalyst precursor is $[RhH(PPh_3)_3CO]$ (Scheme 2) which forms the complex $[RhH(PPh_3)_2(CO)_2]$ (**1**) under pressure of carbon monoxide and hydrogen. The active species during hydroformylation is believed to be $[RhH(PPh_3)_2CO]$ (**2**). To avoid the formation of a monophosphine complex such as $[RhH(PPh_3)(CO)_2]$ which is much less selective, a high triphenylphosphine (TPP) ratio is required. Typically the linear to branched ratio obtained during hydroformylation of linear alkenes ranges from 2.5-9:1 with a common value of 3:1. Highest ratios are reached with substituted alkenes only or with a large excess of TPP.[1]

The mechanism of reaction (Scheme 2.3) was proposed by Wilkinson and is very similar to the cobalt one.[5, 10, 17, 18] The mechanism is here simplified as many other species are in equilibrium depending on the conditions e.g. exchange of CO and TPP, β-elimination (Scheme 3), etc. The rate of β-elimination increases with the temperature and low CO pressure. This phenomena leading to isomerisation is generally blocked by an excess of phosphine ligands. Lazzaroni and co-workers showed that branched alkylrhodium intermediates (**5**) are more sensitive toward β-elimination than the linear alkyl complexes[19]. Thus it then can form isomer products or the starting material, which possibly leads to an increase of selectivity for the linear aldehyde. Poor σ-donor phosphorus ligand (e.g. phosphite or phosphine with electron-withdrawing substituents) often increase the reaction rate as a result of the more facile CO dissociation (less π back bonding) and possible faster alkene addition. Indeed, kinetic studies on phosphine-based catalysts often show that the reaction rate is first order in alkene concentration and minus first order in CO. Under 'standard' catalytic conditions (hydrogen pressure> 1 bar)[1] the reaction is first order in rhodium and zero order in hydrogen.

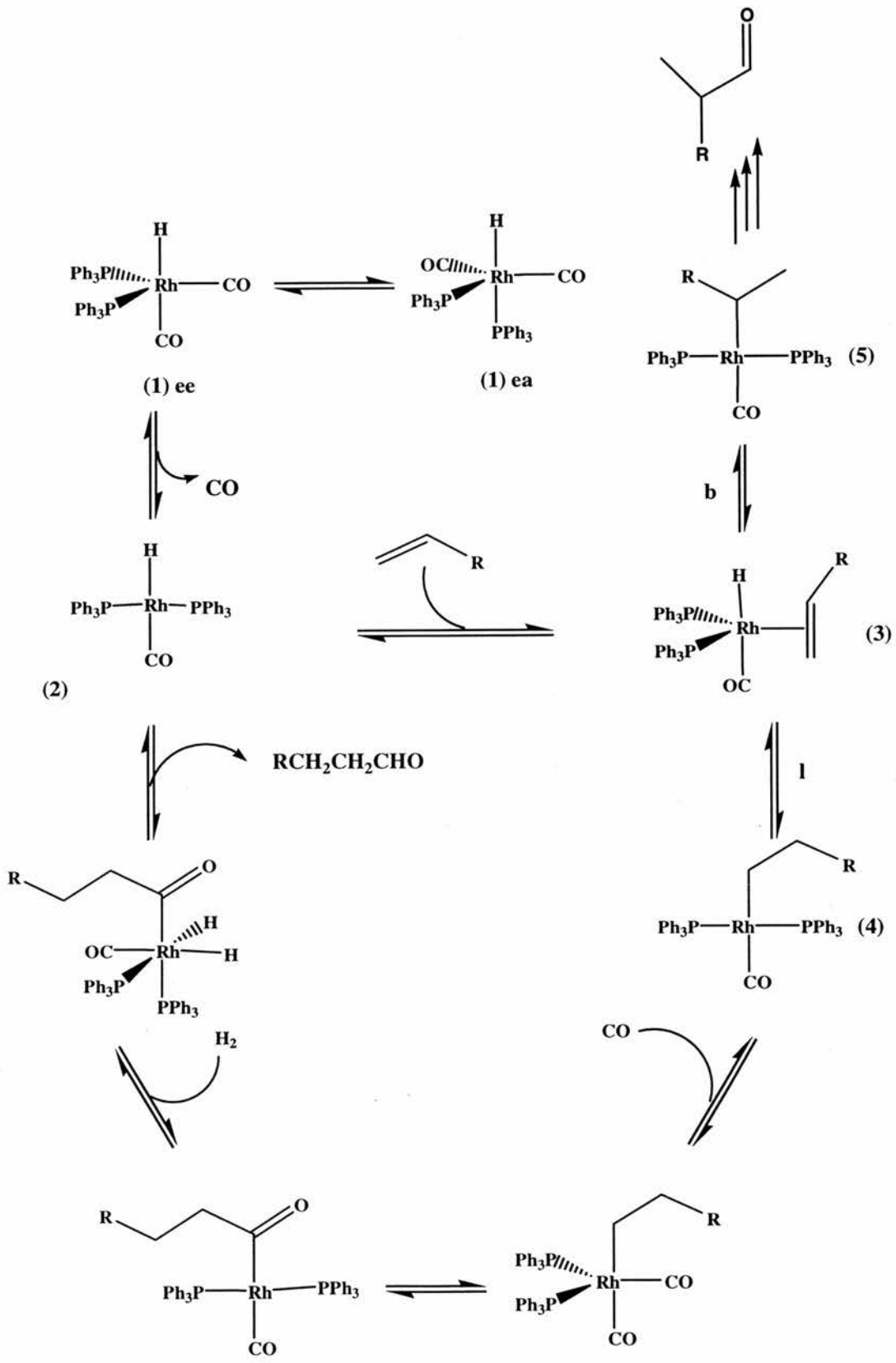

Scheme 2.3 Wilkinson's mechanism for the rhodium catalysed hydroformylation of alkenes.

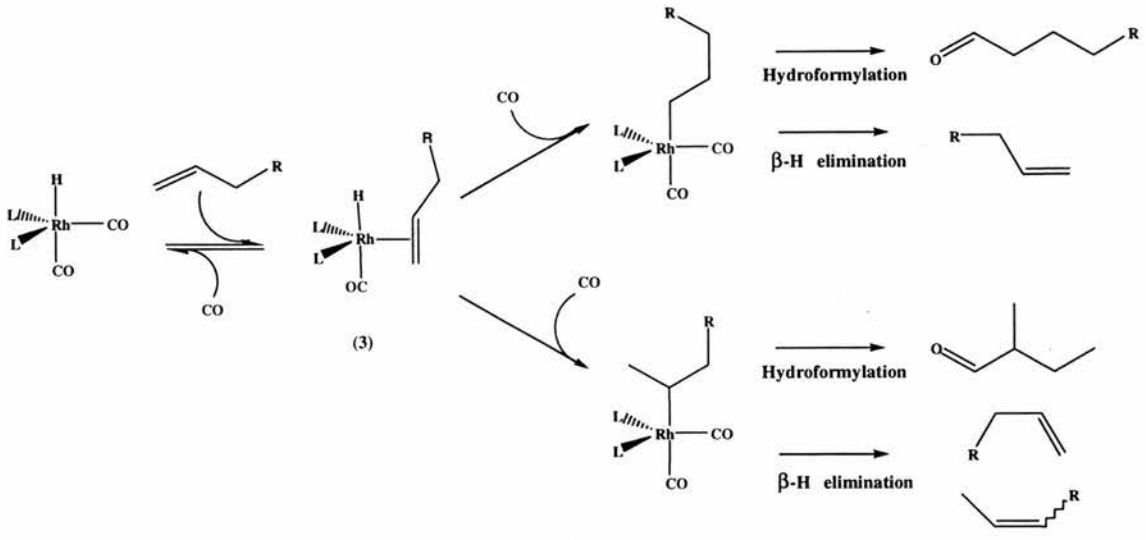

Scheme 2.4 Hydroformylation versus Isomerisation (L= ligands e.g. PPh_3).

Shortly after Wilkinson's discovery, Pruett and Smith, from Union Carbide, reported the use of phosphite ligands for rhodium catalysed hydroformylation of alkenes.[20] High rates were claimed but the instability of such ligands limited their application. Indeed, phosphite ligands were found sensitive to hydrolysis and Arbuzov type reactions (alkyl phosphite only). In 1983, Roobeek and van Leeuwen reported improve stability and high rates for internal and terminal alkene hydroformylation using bulky monophosphite ligands (Figure 2.1).[21, 22]

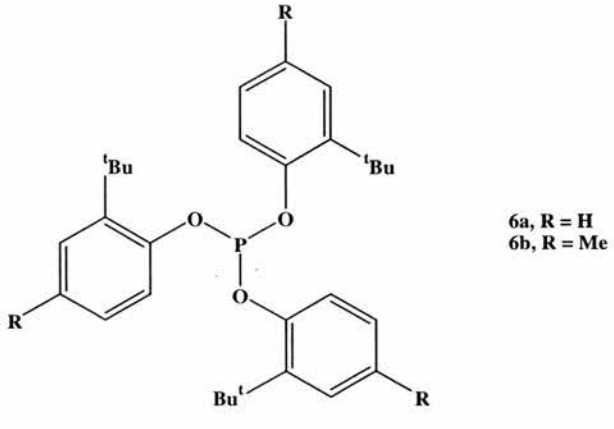

Figure 2.1 Roobeek and van Leeuwen's bulky monophosphite ligands.[21, 22]

However the selectivities to the linear aldehydes were low and the amount of isomerisation products was often high. The introduction by Bryant and co-workers of a bisphenol moiety instead of monophenol in the ligand structure gave even more stable phosphites.[23] Actually, using the bisphenol moiety not only as bulky groups

but also as ligand backbone, and so forming bidentate ligands, high selectivities to the linear aldehydes were obtained (see section 2.3).[24, 25]

Another breakthrough in the development of rhodium-based catalysts for hydroformylation is the development by Ruhrchemie/Rhône-Poulenc[26, 27] of an aqueous biphasic system using a water-soluble phosphine TPPTS: (triphenylphosphine tri-sulfonate) (Figure 2.2). This process affords an active recyclable catalyst for the hydroformylation of propene and butene.

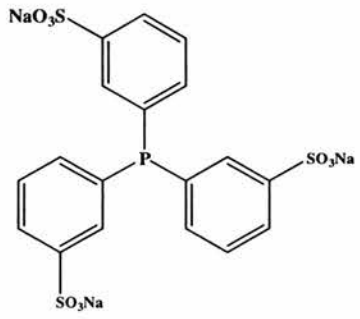

Figure 2.2 Water-soluble phosphine TPPTS: (triphenylphosphine tri-sulfonate).

The discovery that diphosphines with large bite angle (see section 2.2) can be valuable ligands to increase the regioselectivity of the reaction (see section 2.3) is the most recent improvement in this essential catalytic process.[1]

2.2 Rationalization of steric and electronic effects in catalytic reactions.

Early attempts to rationalise the effects of phosphorus ligand in catalysis mainly focused on electronic parameters. It was only in the 1970's that Tolman considered the importance of both steric and electronic parameters in such ligands.[28] He suggested that the steric bulk of the substituents on the phosphorus atom could dramatically change the properties of the transition metal complexes. An electronic parameter χ was defined as the overall effect of the electron donating and electron withdrawing (π back bonding) properties of the phosphorus ligand (Figure 2.3). Its measure (cm^{-1}) is obtained from the difference in the symmetric (A_1) carbonyl stretching frequency of the nickel complexes $[Ni(CO)_3L]$, where L is the phosphorus ligand ($\chi = 0$ for $L = PBu^t_3$). As backbonding strengthens the M-C bond but weakens the C-O bond, low C-O stretching frequencies are obtained with strong backbonding from the metal centre. A low χ value corresponds to a phosphorus ligand with strong

σ-donor and weak π- acceptor properties, and *vice versa* phosphorus ligand with weak σ-donor and strong π- acceptor properties gives a high χ value.

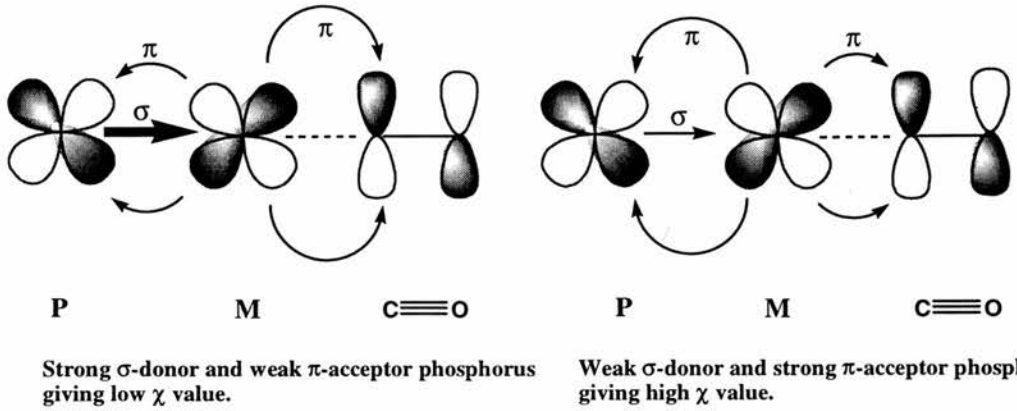

Strong σ-donor and weak π-acceptor phosphorus giving low χ value.

Weak σ-donor and strong π-acceptor phosphorus giving high χ value.

Figure 2.3 Electronic effects on the phosphorus-metal-carbonyl bonds (the orbitals of the σ bonds are not represented).

Tolman's steric parameter is known as the ligand cone angle θ. The cone angle for a symmetrical phosphine ligand (three identical substituents) is measured as the apex angle of a cylindrical cone centred at 2.28 Å from the P atom and touching the van der Waals radii of the outermost atoms of the ligand (Figure 2.4). The minimum cone angle, i.e. with no degree of freedom for the substituents, is always considered. For unsymmetrical phosphines, the cone angle is obtained as an average of the different substituents. Other attempts to define a parameter describing the steric effect in molecules include the solid angle Ω,[29, 30] pocket angle,[31] and molecular mechanics.[32]

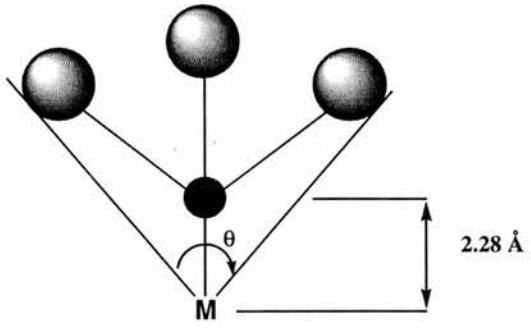

Figure 2.4 Tolman's cone angle θ.

Recently Casey and co-workers, followed by van Leeuwen's group, developed a simpler method to determine the steric effects of bidentate phosphine ligands complexed to a metal centre. They proposed that the four substituents and the backbone rigidity of the two phosphorus atoms determine the steric properties of

diphosphines. The principle is based on the fact that a diphosphine ligand will adopt a particular geometry/ angle in a complex because of its steric and flexibility constraints (Figure 2.5). For example for a square planar complex or apical-equatorial (ae) co-ordination in a trigonal bipyramidal structure a diphosphine with a bite angle (Figure 2.6) of 90° would be preferred. For a tetrahedral complex and for a bisequatorial (ee) co-ordination in the trigonal bipyramidal (TBP) structure, bite angles of 109° and 120° would be respectively preferred.

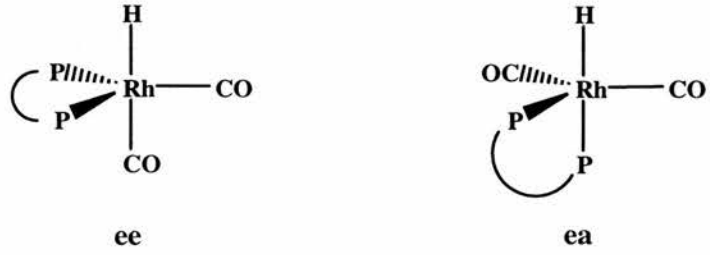

Figure 2.5 Equatorial-equatorial (left) or equatorial-apical co-ordination in a TBP structure.

They introduced the "natural bite angle" β_n and the ligand flexibility range, which are determined by the ligand backbone and the phosphorus substituents only. They are therefore independent of any electronic preferences of the metal. The natural bite angle is determined by minimising the strain energy of the metal-diphosphine fragment with a P-M-P bending force constant of 0 kcal mol^{-1} rad^{-2}.

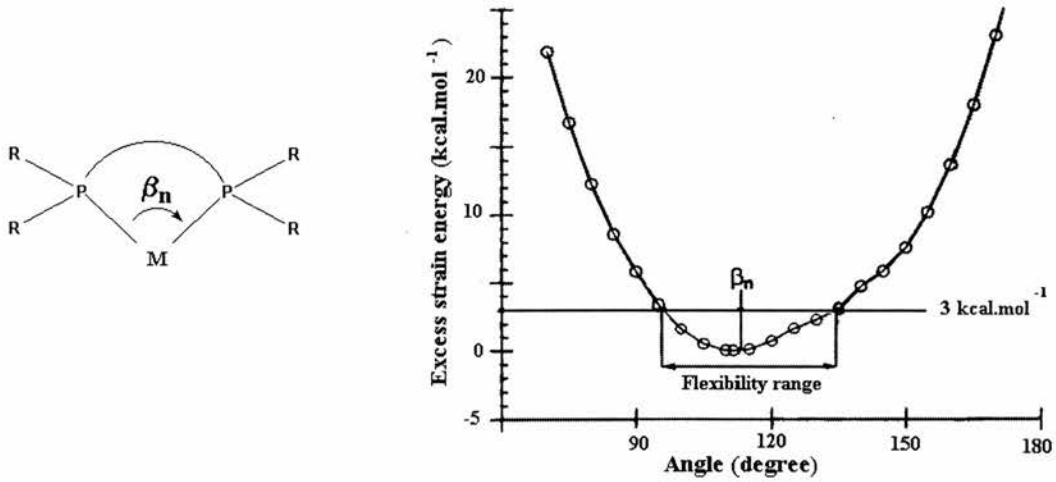

Figure 2.6 Bite angle β_n of a diphosphine ligand and energy diagram for calculation of the 'flexibility range'.

A potential energy diagram can then be drawn by calculating the strain energy at a given bite angle with a large bending force constant toward the metal (Figure 2.6). The flexibility range is determined from this diagram by taking the angle values within a 3 kcal mol^{-1} excess strain energy range.

2.3 Diphosphine ligands in rhodium hydroformylation system.

The hypothesis that the intermediate determining the regioselectivity of the hydroformylation reaction was the complex with two triphenylphosphine ligands[5, 15, 16] in the equatorial plane[33] (Figure 2.5) triggered a lot of interest in bidentate ligand chemistry. One could imagine that a chelating ligand would favour the bidentate $[HRh(CO)L_2]$ complex (Figure 2.5) instead of the less selective monodentate $[HRh(CO)_2L]$ species. Early results were however disappointing. The bidentate ligands available in the 1970's (e.g. dppe, dppp, dppb in Figure 2.7) did not enhance the regioselectivity of the reaction.[34-36] On the contrary, lower selectivities to the linear isomer were found (l:b around 2:1).

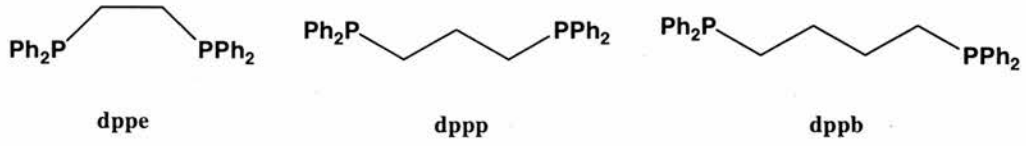

Figure 2.7 Simple bidentate diphenylphosphine ligands.

The first improvement in the regioselectivity of the reaction using bidentate ligands was reported by Consiglio in 1973. It was shown that DIOP (**7**) could lead to l:b ratios between 5 and 13:1 in the hydroformylation of internal or terminal alkenes (e.g. pent-1-ene, oct-1-ene, etc.).[37] But one had to wait a decade before new regioselective ligands were synthesised. In 1981 Hughes and Unruh (Celanese) reported high l:b ratios (5-8:1) using DIOP and trans-dppm-cyb (**8**) ligands for the hydroformylation of hex-1-ene.[38] Similar ligands to **8** (e.g. **9** and **10**) gave poor selectivities.

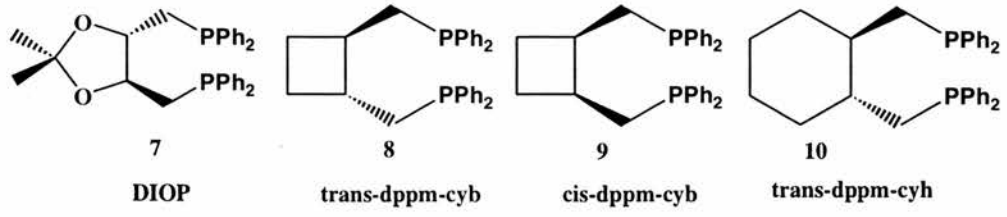

Figure 2.8 Diphosphine ligands used by Unruh and co-workers.

One year later Unruh again, and Christenson studied diphosphines based on a ferrocene moiety (Figure 2.9).[39] The substituted 1,1'-bis(diphenylphosphino) ferrocene (dppf) (**11**) showed interesting reactivities and selectivities during the hydroformylation of hex-1-ene when using a dppf:Rh ratio over 1.5 (see Table 2.1).

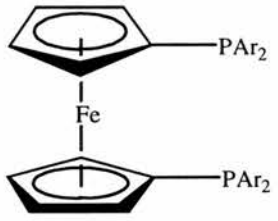

11 Ar = Ph
12 Ar = *p*-CF_3-ChH_4
13 Ar = *m*-F-C_6H_4
14 Ar = *p*-Cl-C_6H_4

Figure 2.9 Substituted 1,1'-bis(diphenylphosphino) ferrocenes (dppf).

Table 2.1 Hydroformylation of hex-1-ene catalysed by dppf Rhodium complexes at 110°C, and 7.9 bar CO/ H_2 1:1.

dppf: Rh ratio	*l:b ratio*	*Heptanal* %	*2-methylhexanal* %	*2-hexene* %	*Hexane* %
1.0	2.1	54.2	25.6	19.2	1.0
1.5	5.1	82.5	16.1	0.5	0.9
3.0	5.2	82.6	15.9	0.6	0.9

Unruh and coworkers thus speculated that the selectivity was induced by a rhodium complex with three phosphorus atoms, i.e. where one dppf ligand chelated to the each rhodium, and another bridges two rhodium atoms. These types of complex, where all three phosphines are in equatorial sites were indeed identified by ^{31}P NMR studies in solution at varied dppf/Rh ratios. It should be noted however that these experiments were carried out at a rhodium concentration two or three times higher than the actual catalytic situation and that no CO pressure was applied. Indeed, re-examination of the dppf-Rh system by van Leeuwen showed that the main species formed in situ in 'standard conditions' was $[RhH(dppf)(CO)_2]$ with ee and ea coordination in rapid equilibrium.[40]

Unruh and coworkers also studied the properties of electronically modified dppf. To do so they synthesised compounds with electron withdrawing substituents at the meta or para positions of the phenyl groups (Figure 2.9). It was found that both

rate and selectivity increased with increasing χ value (i.e. decreasing basicity) (Table 2.2). Another plausible explanation not known at the time is that the electron withdrawing ligands and the large bite angle of dppf favours ee isomers, which are often more selective (see further on).

Table 2.2 Effect of ligand basicity on the selectivity in the hydroformylation of hex-1-ene at 110°C and 7.9 bar CO/H_2 (1:1).

Ligand	*χ-value*	*l:b ratio*	*Relative rate*	*Heptanal %*	*2-methyl hexanal %*	*2-hexene %*	*Hexane %*
11(dppf)	4.3	5.4	7.2	80.8	15.0	3.7	0.5
12	5.6	6.8	9.3	82.3	12.1	5.0	0.6
13	6.0	8.0	13.7	83.9	10.4	5.0	0.7
14	6.4	11.4	13.8	85.3	7.5	6.4	0.8

Such rate increase can be explained as follow. One can speculate that the decrease π-back donation to the phosphine, and so to the metal, enhances the formation of the linear alkyl intermediate. However, the full kinetic of the catalytic process is required to demonstrate such hypothesis.

One must keep in mind that the real selectivity of the reaction to the linear aldehyde is determined not by the l:b ratio but by the amount of products. When decreasing the basicity of the ligands, an increase in the selectivity for the linear aldehyde, heptanal, as well as for the isomerisation product, hex-2-ene, were observed to the detriment of the branched aldehyde, 2-methyl hexanal. Two factors are in fact contributing to the increase of the l:b ratio. Firstly, the terminal alkyl intermediates are more favoured, as indicated by the greater selectivity for heptanal. On the other hand, isomerisation products are formed by β-hydrogen abstraction of hydrogen in the branched alkyl-rhodium species. Hence an increase of hex-2-ene is related to a decrease of branched aldehyde, consequently it gives higher l:b ratio, but not an overall increase in selectivity to the derived linear product.

Devon et al. (Eastman Kodak Company) reported in 1987 a new class of diphosphine ligand, the 2,2'-bis(phosphinomethyl)-1,1'-biphenyls which showed very high selectivity for linear aldehyde during rhodium-catalysed hydroformylation.[41] The best known ligand in this class is the diphosphine 2,2'-bis(diphenylphosphinomethyl)-1,1'-biphenyl or BISBI compound (**15**).

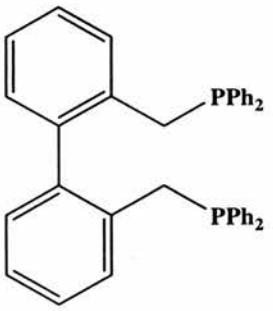

15

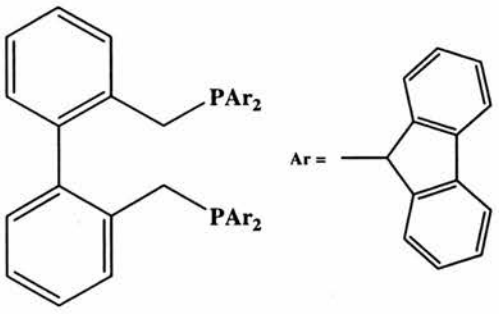

16

Figure 2.10 2,2'-bis(diphenylphosphinomethyl)-1,1'-biphenyl or BISBI (left) and 2,2'-bis(dibenzophosphinomethyl)-1,1'-biphenyl (right).

Hydroformylation of propene using rhodium complexes of BISBI (P/Rh ratio 2.4) was reported to give excellent l:b ratio (25:1) and very high rate (Table 2.3). Interestingly lower temperature increased the amount of linear aldehyde. In a later patent they described that using 2,2'-bis(dibenzophosphinomethyl)-1,1'-biphenyl (**16**), an l:b ratio of 288:1 could be reached.[42]

Table 2.3 Hydroformylation of propene using several ligand including BISBI at 16 bar CO/H_2 (1/1), 125°C, 5 bar propene, [Rh] = 1.5 mmol dm^{-3}, P/Rh = 2.4/1

Ligand	*Rate/ Mol.(Rh mol)$^{-1}$ .h^{-1}*	*l:b ratio*
BISBI	3650	25.1
DIOP	3250	4.0
Dppf	3800	3.6
TPP	5930	2.4
dppb	790	2.5
dppp	610	0.8
trans-dppmcyb	3200	4.4

Casey and co-workers have published extensively on the catalytic behaviour of such ligands.[43, 44] By comparison of the effect of the chelate bite angle of ligands in the TBP with the selectivity of the reaction, they first suggested that higher selectivity could be obtained with ligands with wider bite angles.[43] Crystal data and spectrometric measurements demonstrated a bisequatorial mode of coordination of the diphosphine in [HRh(CO)(BISBI)(PPh_3)] and [$HRh(CO)_2$(BISBI)]. To classify this kind of ligand they introduced the concept of the natural bite angle (see section

2.2) and calculated the natural bite angle and the flexibility of several diphosphine ligands. Hydroformylation of hex-1-ene was carried out with rhodium complexes with various diphosphine ligands and the selectivity/ bite angle relationship was then studied.

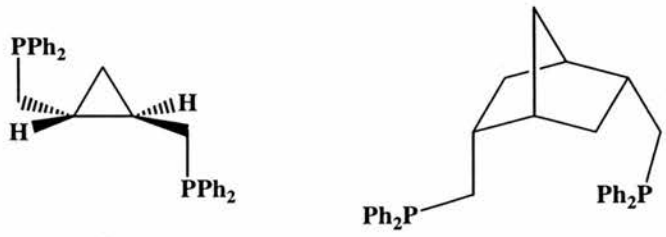

trans-dppm-cyp **2,5-dppm-cyp**

17 **18**

Figure 2.11 Bidendate phosphine ligands.

Table 2.4 Results of the hydroformylation of 1-hexene with various diphosphine ligands at 34°C, 6 bar CO/ H_2 (1:1) with a diphosphine/ rhodium ratio of 1:1.

Diphosphine Ligand	*Natural Bite Angle/ βn*	*Ligand Flexibility*	*l:b Ratio*	*ee:ea*
Dppe	85 °	70-95 °	2.1	0:100
DIOP	102 °	90-120 °	8.5	-
17	107 °	93-131 °	12.1	37:63
BISBI	113 °	92-155 °	66.5	100:0
18	123 °	110-145 °	2.9	-

Interestingly, except for the norbornyl ligand, a correlation between natural bite angle and l:b ratio is evident. This exception was attributed to the inability of the latter diphosphine (supposedly too wide) to form stable bidentate complexes with rhodium. Casey and co-workers then postulated two hypotheses. They suggested that either complexes with ee configuration could lead to higher l:b ratios, or that wider bite angles allowed a more effective steric bulk of the diphosphine around the metal leading to a better selectivity for the linear aldehydes.

It is believed that the regio-chemistry of rhodium-catalysed hydroformylation of linear alkenes is mainly determined at the stage of Rh-H addition to the alkene.[1] Indeed, many studies have demonstrated that in 'normal' catalytic conditions the insertion of the alkene was irreversible or at least strongly favours the alkyl

complex.[44-46] The geometry and steric environment of the rhodium-alkene hydride complex and the square planar 4-coordinate alkyl-rhodium intermediate seem to be very important in controlling the regioselectivity of the reaction. Thus these complexes are presumably affected by the bite angle of a chelating ligand. Brown and Kent showed in early studies that in solution the five co-ordinate complex $[RhH(PPh_3)_2(CO)_2]$ with a TBP structure exists as a mixture of two geometric isomers with the phosphines co-ordinated equatorial-equatorial (ee) or equatorial-axial (ea) in a ratio of 85:15 (see complexes ee and ea in Figure 2.5)[33]. Thus, the diphosphine can adopt either an ea or an ee configuration in the trigonal bipyramidal structure. Chelates with natural bite angle of 90° (like dppe) and 120° (like BISBI) are more likely to adopt respectively an ea and ee structure. However, as shown by van Leeuwen and co-workers,[47] the actual bite angle strongly depends on electronic properties of the ligand itself, the metal and other ligands.

Hence a steric difference between ee and ea configurations and their subsequent intermediates could explain the regioselectivity, molecular mechanics calculations were investigated.[44, 48, 49] However they failed to support such explanations. Electronic considerations were then suggested. BISBI and other chelates were thus modified with electron withdrawing groups to study the electronic properties of such ligands in hydroformylation (Figure 2.12).[50, 51]

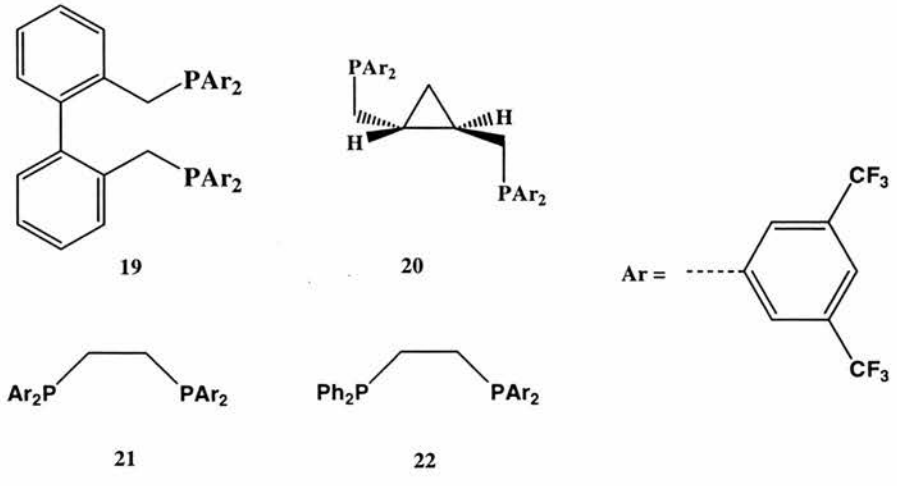

Figure 2.12 Electronically modified ligands.

As found previously (see dppf), functionalisation of the BISBI aryl groups by m-trifluromethyl substituents (higher χ-values) gave as much as 5-fold rate increase and 2-fold selectivity increase to the linear aldehyde. Modified trans-dppm-cyp (**17**)

and dppe were also studied. The diphosphine ratios of ee:ea coordination were measured in the TBP structure at room temperature in related iridium complexes .

Table 2.5 Regioselectivity of the hydroformylation of hex-1-ene catalysed by rhodium diphosphine catalysts.

Ligand	*l:b ratio*	*ee:ea ratio*
BISBI	66:1	100:0
19	123:1	100:0
Trans-dppm-cyp **17**	12.1:1	37:63
20	17.7:1	90:10
dppe	2.6:1	0:100
21	1.3:1	0:100
22	4.2:1	0:100

As shown in Table 2.5 an electron-withdrawing substituent on an equatorial phosphine increased the linear selectivity of the catalyst while, when introduced in the apical position, a decrease of the n:i ratio was observed. The selectivity to the linear isomer was lower when using **21** than when using dppe. Therefore the electron-withdrawing substituent of the phosphine in the axial position had a greater (negative) influence on the complex than the ligand in equatorial position (positive effect). To confirm that ligands with high χ value co-ordinating in ee configuration led to higher selectivity, the disymmetric dppe derivative **22** was synthesised. It was shown (NMR techniques) that the more electron-withdrawing phosphorus atom was in the equatorial position and the more electron donating phosphorus ligand was in the axial position as mechanics calculation demonstrated.[51] Indeed, the hypothesis was confirmed since the linear selectivity with this disymmetric ligand was increased by a factor two.

To study the exact influence of the natural bite angle on the regioselectivity of hydroformylation, van Leeuwen et al synthesised a range of new diphosphine ligands based on xanthene-type backbones (Figure 2.13).[47, 52-54] The bite angles and flexibility of these bidentate phosphines were determined using Casey's calculations. Variation of the substituent at the 9-position of the backbone gave a range of diphosphines with similar steric and electronic properties but with various bite angles all near 110°. All xantphos ligands with the exception of **24** with a very large bite

angle (131.1°) gave high regio-selectivity and low isomerisation activities. **24** probably behaved like norbornyl in Casey's studies and did not form a bidentate chelate.[43, 44] When considering the linear aldehyde selectivity instead of the l:b ratio, the xanthene type diphosphine ligands were in fact more regioselective than BISBI due to the lower level of isomerisation in the former.

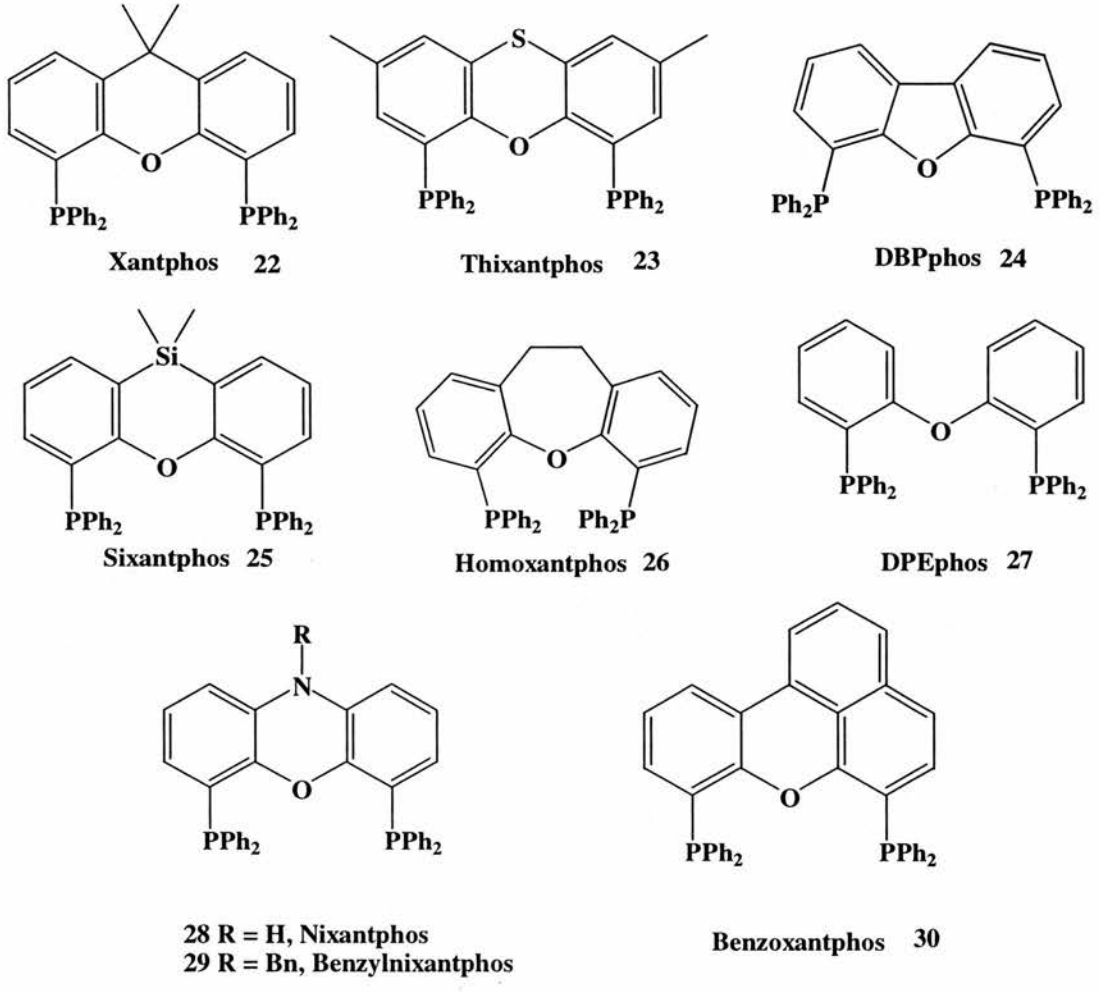

Figure 2.13 Xantphos type ligands.

A clear correlation between both the selectivity and the rate of reaction with the increasing bite angle was found. Surprisingly the ee:ea values (obtained by calculation from ^{1}H NMR) could not be correlated to the natural bite angle and the overall regioselectivity. Therefore in the xantphos system a bis equatorial coordination is not a key parameter in the regioselectivity of the reaction.

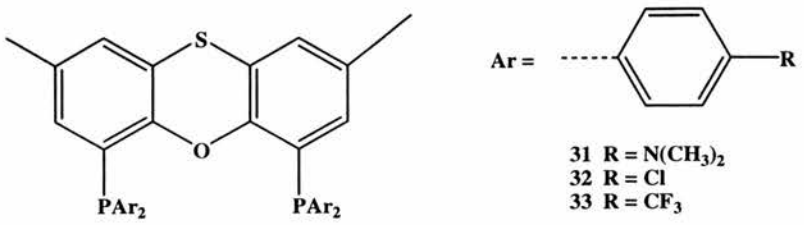

Figure 2.14 Electronically modified Thixantphos.

Para substitution of the aryl groups of the phosphines with donor or acceptor substituents led to the different conclusions than suggested for dppf and BISBI. Indeed although higher l:b ratios increased with the χ-value of the phosphine ligands, the overall selectivity to the linear aldehyde stayed unchanged (increase of isomerisation products). A same correlation was however found between the basicity of the ligand and the ee:ea ratio as electron withdrawing ligands favoured the ee configuration.

Table 2.6 Results of the hydroformylation of 1-octene at 80°C, p = 20 bar CO/H_2, (1:1), ligand/Rh = 5, substrate/ Rh =637, [Rh] = 1.0 mM, [a] TOF in (mol aldehyde)(mol of Rh)$^{-1}$ h^{-1}.

Ligand	*Bite angle βn*	*χ*	*l : b ratio*	*Nonanal %*	*Isom. %*	*TOF[a]*	*Ratio ee:ea*
26	102.0	-	8.5	88.2	1.4	36.9	3:7
34	107.9	-	14.6	89.7	4.2	74.2	7:3
25	108.5	-	34.3	94.4	2.9	76.5	6:4
23	109.6	-	56.6	93.7	4.7	94.1	7:3
22	111.4	-	52.2	94.5	3.7	187	7:3
36	113.2	-	49.8	94.3	3.8	162	8:2
29	114.1	-	50.6	94.3	3.9	154	7:3
28	114.2	-	69.4	94.9	3.7	160	8:2
30	120.6	-	50.2	96.5	1.6	343	6:4
BISBI	122.6	-	80.5	89.6	9.3	-	100:0
24	131.1	-	3	71	5.5	125	
31	-	1.7	44.6	93.1	4.8	28	1:1
32	-	5.6	67.5	91.7	6.9	66	85:15
33	-	6.4	86.5	92.1	6.8	158	9:1

As the bite angle was still closely related to the regioselectivity, van Leeuwen and co-workers speculated that the regioselectivity was more likely to be determined by some steric factors. They suggested that the effective increasing steric bulk of the ligand with increasing bite angle caused the steric congestion around the rhodium centre. This effect led to the increase in the regioselectivity by favouring the less sterically demanding linear alkyl intermediate.

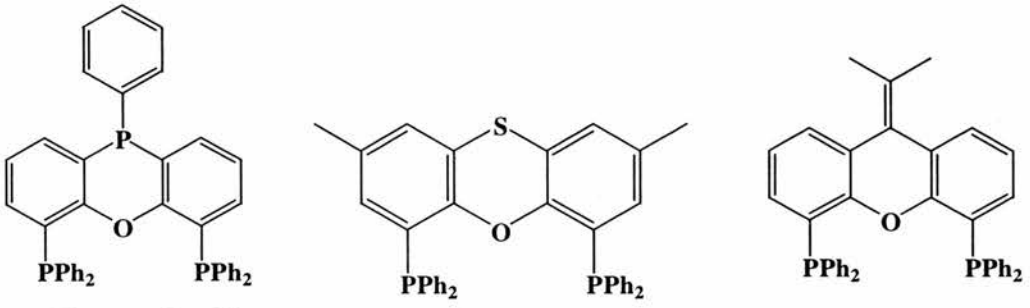

Phosxantphos 34 **Thixantphos 23** **Isoproxantphos 35**

bite angle 107.9 **109.6** **113.2**

Figure 2.15 Xantphos diphosphine used in the kinetic studies of the ^{13}CO dissociation.

The kinetics of the ^{13}CO dissociation from the [(diphosphine)RhH(^{13}CO)] complexes was investigated.[54] No correlation between the ee:ea ratios of the three diphosphine hydride rhodium complexes studied with the regioselectivity of the reaction and the kinetics of ^{13}CO dissociation, was found. Thus, although the intermediate complex [(diphosphine)RhH(CO)(alkene)] could not be observed, van Leeuwen *et al* suggested that CO dissociation from the ee and ea isomers resulted in the formation of the same four coordinate intermediate **36.** Either alkene coordination or hydride migration thus would determine the regioselectivity. Therefore it was suggested that the alkene attack on the intermediate **36**, *via* a square pyramidal transition state, **37** controlled the regioselectivity. Increasing the bite angle of the diphosphine in the four coordinate complex **36** consequently widened the steric bulk around the rhodium centre and hampered the approaching alkene. Wide bite angle should therefore favour the less sterically demanding pro-linear transition state **36 l** and give the linear product of reaction. However, the angle between the two Rh-P bonds in the intermediate **36** can not alone explain the selectivity for either the pro-linear or pro-branched transition state. Indeed molecular models showed that the

diphosphine's backbone interacts with the intermediate species **38 l & b** constraining the phenyl substituents on the phosphorus in such a way that the pro-linear complex **38 l** is favoured.

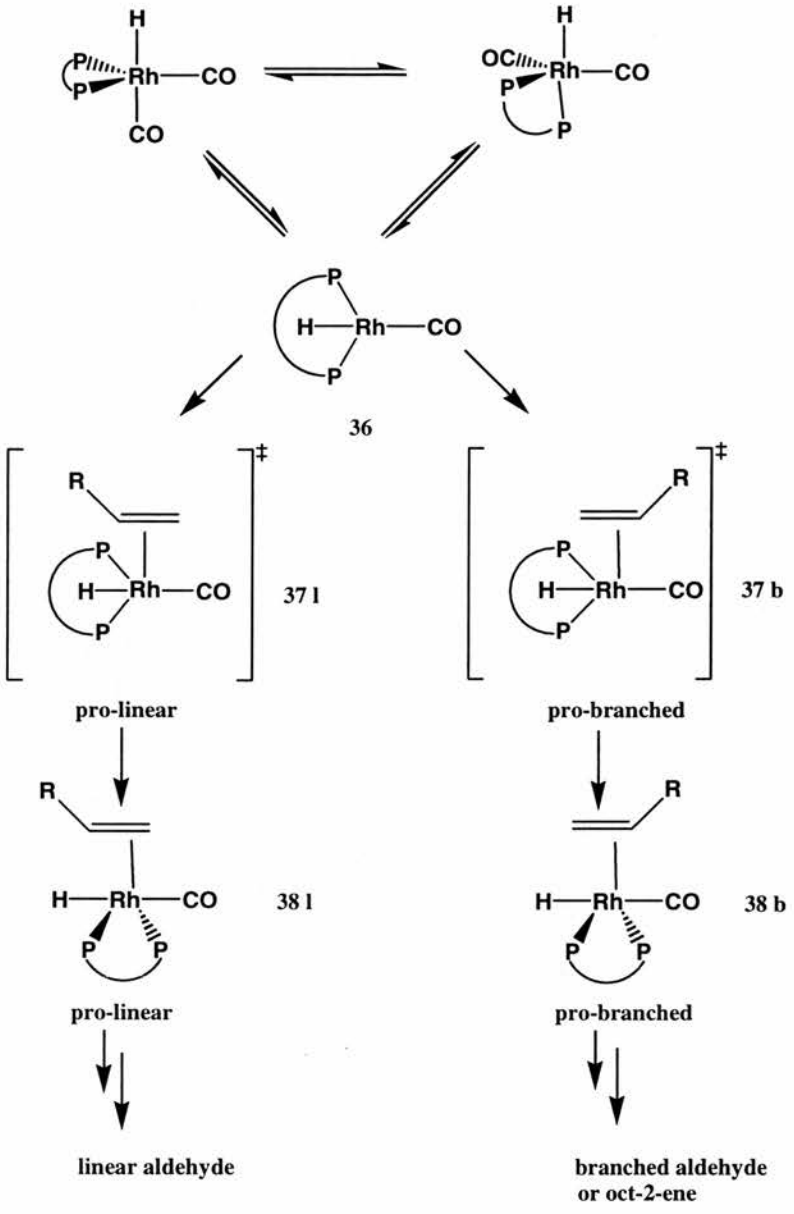

Scheme 2.5 Mechanism proposed by van Leeuwen and co-workers determining the regioselectivity of hydroformylation reaction.

2.4 Diphosphite ligands.

Bryant and co-workers (Union Carbide Corporation) were the first to report improved selectivity using (di)phosphite ligands for hydroformylation.[24, 25, 55] So far only bulky diphosphites had shown high regioselectivity. Although the reaction rates of the bulky monophosphite-based catalysts were often higher, diphosphite systems showed superior rate to the TPP-based catalyst. Moreover, since a lower ligand/ rhodium was necessary when using diphosphites rather than TPP, these ligands were industrially interesting and still are. As mentioned above, diphosphite ligands led to much slower hydroformylation reaction than bulky monophosphites. Indeed, the latter form mono-ligand complexes, which for electronic and steric reasons are more active catalysts than the chelate phosphites.

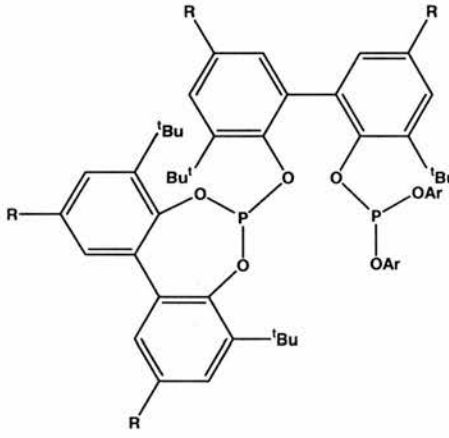

39a R = OMe, $(OAr)_2$ = 
39b R = ^{t}Bu, Ar = 4-C_6H_4Cl
39c R = ^{t}Bu, Ar = C_6H_5

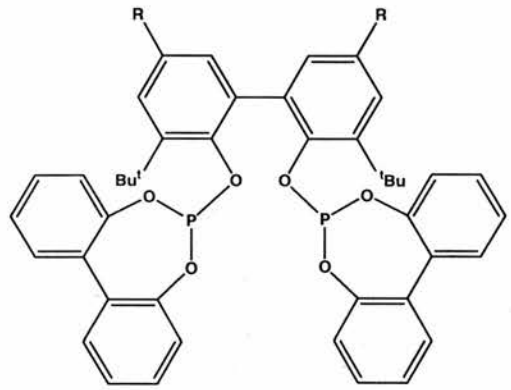

40 a R = OCH_3
40 b R = ^{t}Bu

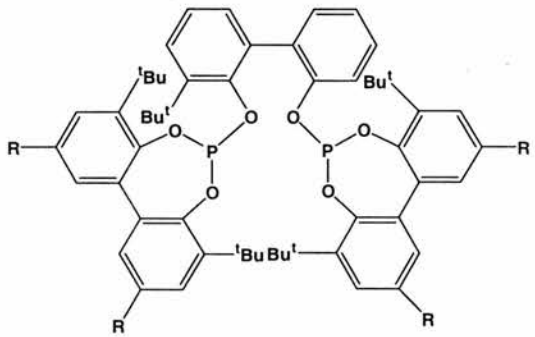

41a R = OMe
41b R= ^{t}Bu

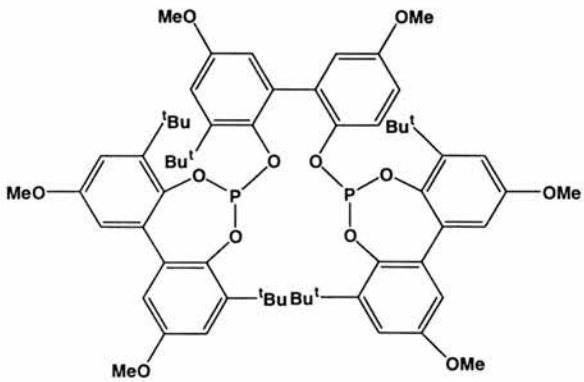

42

Figure 2.16 Diphosphites with bisphenol backbones used by Union Carbide for the hydroformylation of alkenes.

No real trend can yet be drawn to synthesise diphosphite ligands with good regioselectivity. However the exact structures of the diphosphite ligands seem to determine their regioselectivity towards linear or branched aldehydes. Indeed the bridge (backbone) and the bulkiness of the chelates are often decisive. The bite angle of these ligands probably also take part in the selectivity although no comparative studies have been published so far. Van Leeuwen and co-workers[56] studied the hydroformylation of oct-1-ene and styrene using Union Carbide's diphosphite-based rhodium catalysts. Although the bisphenol bridge seems to be important in the synthesis of regioselective ligands, it is not sufficient by itself. While ligands **39** and **40** gave high aldehyde linearity (l:b up to 50:1) for the rhodium-catalysed hydroformylation of but-1-ene and propene, poor selectivity was obtained for the structurally similar ligand **41** (l:b of 3.). The lack of steric bulk of the backbone is probably responsible for the decrease of selectivity. Whilst ligand **42** is probably too sterically hindered (low rate), ligand **43** seems to be too small to induce high regioselectivity.

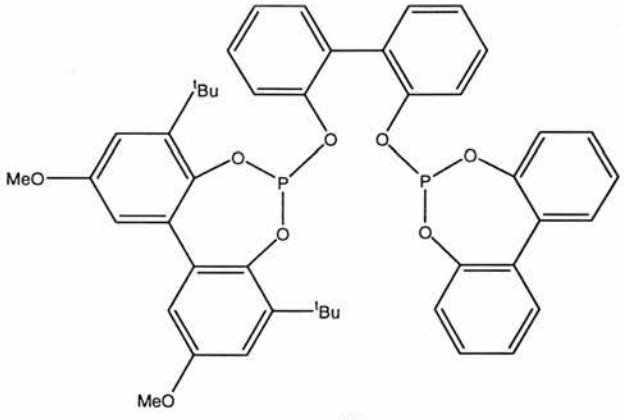

43

Figure 2.17 Less hindered diphosphite ligands

Usually bulky bisphenol-type diphosphites were found to coordinate on equatorial-equatorial position in the complexes RhH(CO)(diphosphite) (e.g. **39**) (determination through NMR technique).

More flexible ligands with alkyl backbones did not generally give good selectivities (Figure 2.18). Interestingly, ligand **45a** with the propyl bridge (n=3) gave a reasonable l:b ratio of 3.8:1. However the ligands with the ethyl or butyl linkage (n=2 and 4) were not regioselective. Ligands **46** resulted in faster rates but low selectivities, which could be explained by their inability to form chelates and hence they behaved as bulky-mono-phosphite ligands. Ligand **46b** gave a high rate

for the hydroformylation of but-2-ene but with only a l:b ratio of 0.5. Whilst an equatorial-axial conformation in the rhodium carbonyl complexes was determined through NMR techniques for **44a, 44b** afforded an ee complex.

Union Carbide and Mitsubishi reported respectively the use of the diphosphite **47** and **48** for the hydroformylation of alkenes.[57] This compound can be seen as an intermediate between the bisphenol and alkyl backbone. Interestingly, high linearities (l:b up to 20:1) for the hydroformylation of internal and terminal alkenes were found.

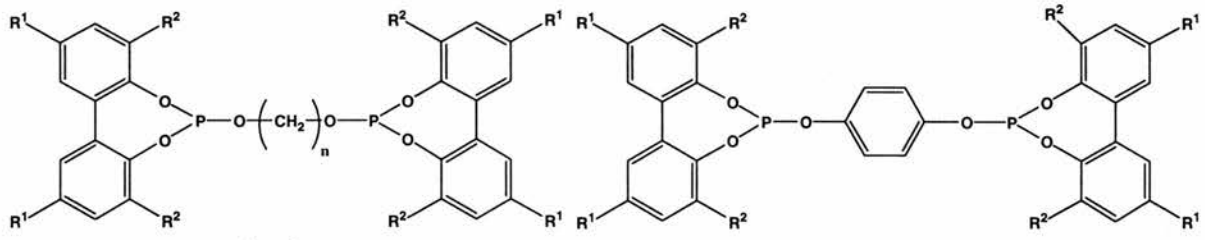

44a $R^1 = R^2 = H$, n = 2
44b $R^1 = R^2 = H$, n = 3
45a R^1 = OMe, $R^2 = {}^tBu$, n = 2
45b R^1 = OMe, $R^2 = {}^tBu$, n = 3
45c R^1 = OMe, $R^2 = {}^tBu$, n = 4

46a $R^1 = R^2 = H$
46b R^1 = OMe, $R^2 = Bu^t$

Figure 2.18 Diphosphites with alkyl/aryl backbones used by Union Carbide for the hydroformylation of alkenes.

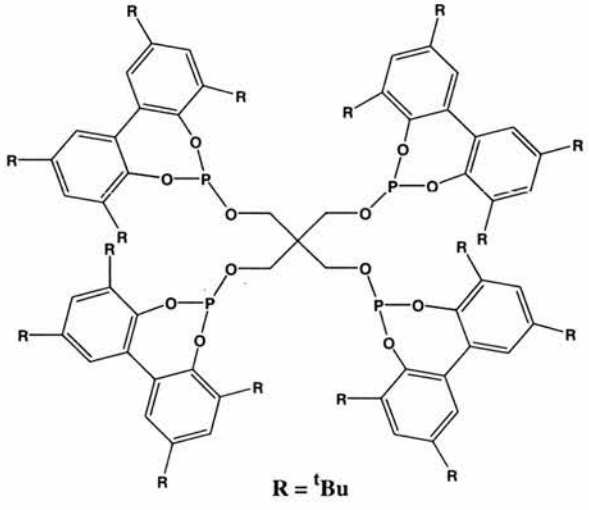

$R = {}^tBu$

47

Figure 2.19 Union carbide ligand.

The kinetic studies (hydroformylation of oct-1-ene) of the regioselective diphosphites showed a first order dependency of the alkene and rhodium concentrations and a negative order with respect to CO pressure. A negligible

dependency of H_2 pressure in the reaction rate was noticed. These results indicate that the alkene addition is the rate-determining step, or is at least involved in a pre-equilibrium (see Section 2.1).

Table 2.7 Hydroformylation of alkenes catalysed by rhodium phosphite species.[24, 25, 55, 56]

Ligand	*T °C*	*P CO/H₂ Bar*	*Alkene*	*Isomer. %*	*Initial rate*[a]	*l:b*
39a	70	2.5[b]	But-1-ene		2400	50
39a	71	6.7 [b]	But-1-ene		730	35
39b	80	20	Oct-1-ene	n.d.	3375	19
40a	74	4.5	propene		402	53
40a	80	20	Oct-1-ene	18	3600	>100
40b	80	20	Oct-1-ene	27	6.120	51
41a	70	7 b	But-1-ene		1480	3.2
41b	80	20	Oct-1-ene	13	520	1.2
42	70	7 b	But-1-ene		160	6.3
42	70	4.3	propene		20	2.1
43	70	4.3	propene		280	1.2
44a	80	20	Oct-1-ene	n.d.	11.100	1.6
44b	80	20	Oct-1-ene	20	1550	2.2
45a	90	7.1	But-1-ene		1620	2.3
45b	90	7.1	But-1-ene		1320	3.8
45c	90	7.1	But-1-ene		1070	2.2
46b	90	7.1	But-1-ene		3660	2.0
46b	90	7.1	But-2-ene		1140	0.5
47	90	7.1	But-1-ene		1650	9.9
47	90	7.1	But-2-ene		65	2.8

Reaction conditions: 0.1-1 mM Rh, L/Rh = 10-20/1, [alkene] = 0.5-1 M in toluene, [a]: initial rate in mol.(mol Rh)$^{-1}$.h^{-1}, [b] : ratio CO/H_2 = 1/2; n.d.: not detected.

No straightforward correlation between the ee or ea configurations in the rhodium complex [HRh(CO)(diphosphite)] and the regioselectivity was found (see examples above). Nevertheless, improved regioselectivity towards the linear

aldehydes was obtained when using diphosphite ligands owning an ee configuration, though ea configuration led very often to low selectivity.

Using the diphosphite **39c**, high regioselectivity to the linear aldehydes (84 % of the aldehydes) during hydroformylation of styrene was obtained. Although there was nothing surprising for alkenes such as oct-1-ene, high regioselectivity to the linear aldehydes for the styrene is unusual (see section 2.1). This change of regioselectivity can be explained by the enhanced isomerisation rate (β-H elimination), which often characterised phosphite ligands (high χ values), and the reaction condition applied i.e. high temperature (120°C), low CO pressure (5 bar), and high H_2 pressure (30 bar). Gladfelter and Moasser showed that alkene insertion (oct-1-ene) was reversible even at room temperature and suggested that the regioselectivity of the reaction was not determined by the formation of the alkyl rhodium complexes.[58] However, these high isomerisation rates were found under mass transfer limiting conditions. Although hydroformylation of longer chain alkenes such as oct-1-ene by diphosphites **39** or **40** rhodium complexes gave n:i ratio up to 27:1, as much as 27 % (**40b**) of the products of the reaction were found to be isomerisation compounds. This flattering ratio is indeed not reflected in the overall selectivity of the reaction.

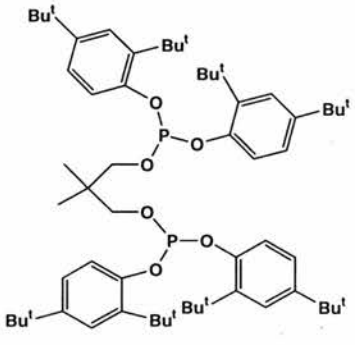

48

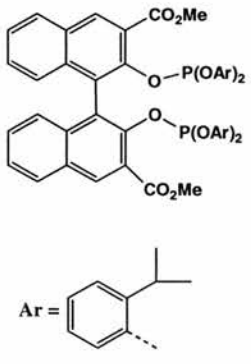

49

Figure 2.20 Active diphosphites for the hydroformylation of internal alkenes.

The high proportion of isomerisation products led to attempts to hydroformylate internal alkenes to linear aldehydes. Union Carbide Corporation,[23, 55] Mitsubishi Chemical Corporation,[57] Du Pont and DSM[59] have patented diphosphite ligands showing interesting properties for the hydroformylation of internal alkenes. Recently Börner *et al* reported the use of ligands similar to **46** for the rhodium

catalysed hydroformylation of n-octene with high rates (TOF up to 4760 (mol aldehyde)(mol catalyst)$^{-1}$.h^{-1}) and selectivity to n-nonanal up to 68 %.

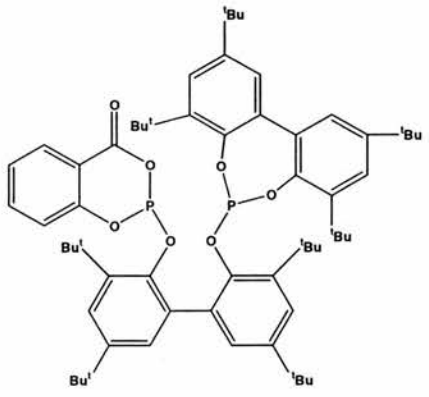

50

Figure 2.21 Börner 's ligand for the rhodium catalysed hydroformylation of n-octene.

2.5 Asymmetric hydroformylation.

In the last few decades, the synthesis of enantiomerically pure compounds has stirred considerable interest in chemistry and biochemistry. Since asymmetric hydroformylation can be a powerful tool to introduce enantiomeric aldehydes in molecule many attempts were carried out. A successful application is found for example in the synthesis of Ibuprofen. Indeed, hydroformylation of functionalised substrates such as styrene or vinyl acetate lead preferentially to the branched aldehydes (Figure 2.22) with formation of stereocentre on α of the carbonyl group.

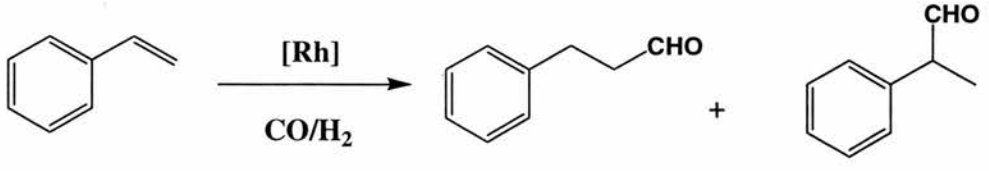

Figure 2.22 Hydroformylation of styrene.

However until now, not many enantiomeric catalytic systems have reached this goal. This can be partially explain by the difficulties encountered so far in determining the mechanistic aspects of the asymmetric hydroformylation, and thus in designing an efficient ligand. We will focus in this section on a few ligands leading to high stereoselectivity in asymmetric hydroformylation. Excellent reviews on the

subject can be found in the literature.[1, 60] Chiral diphosphite and phosphine-phosphite chelates are efficient ligands with moderate to high enantioselectivity. Both types of rhodium complex were characterized by NMR and IR techniques as the resting state of the catalyst $[HRh(P\text{-}P)(CO)_2]$ with a trigonal bipyramidal configuration. The complexes adopting only one diastereomeric conformation are believed to be more enantioselective.[49, 61, 62] Diphosphine ligands on the contrary were found to induce lower enantioselectivity. This result is however surprising as they are among the most efficient ligands in homogeneous catalysis.[60] Chiral ligands as EPHOS[63]and DIOP[64] (Figure 2.23) hardly gave enantiomeric excess over 30 % in the hydroformylation of styrene. So far the best result with diphosphine ligands (ee of 58 %) have been obtained by the quite simple BDPP ligand.[53, 65-67]

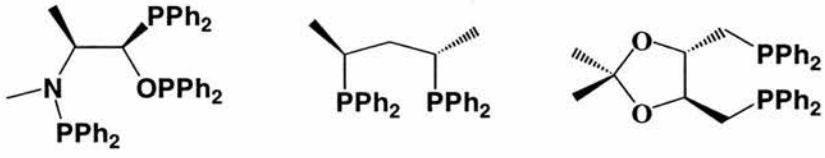

EPHOS **BDPP** **DIOP**

Figure 2.23 Diphosphine chiral ligands for asymmetric hydroformylation.

Babin and Whiteker for Union Carbide[68] were the first to report high asymmetric induction in the hydroformylation of alkenes. Bulky diphosphites UC PP* ligands were used to reach enantiomeric selectivity up to 90 % using styrene as substrate. Van Leeuwen and co-workers carried on the work with modified ligands.[69] High enantioselectivities were obtained with the enantiopure ortho-substituted bisphenol-containing diphosphites **52** and the binaphthol equivalent formed from the (2R, 4R)-pentane-2, 4-diol and respectively bisphenol and (S) binaphthol. 93 % of branched products with ee up to 87 % for the (S) aldehyde was reached during the hydroformylation of styrene. However, due to the low temperature of the reaction (25°C), the rates were poor (TOF= 9 mol styrene $(mol\ Rh)^{-1}h^{-1}$).[61]

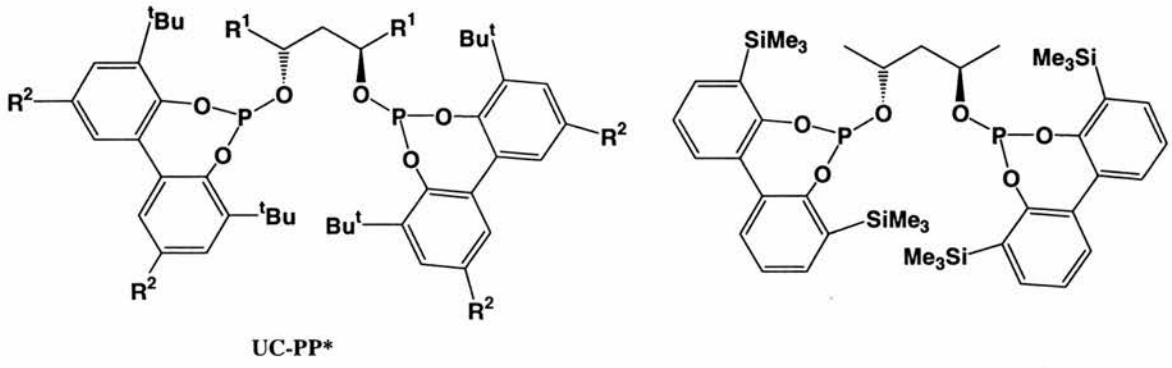

Figure 2.24 Union Carbide UC PP diphosphite ligand (left) ant the ortho-substituted bisphenol-containing diphosphites of van Leeuwen and co-workers (right).*

The structural and chiral variation brought to the diphosphites led to the conclusion that the ligand configuration and the selectivity were closely related. Indeed the chain length and chirality of the backbone as well as the steric bulk of the substituents (e.g. on the bisphenols) and the chirality of the terminal groups determined the enantioselectivity. The eight-membered ring complexes provided better asymmetric induction than its seven or nine counterparts and were likely to adopt a bis–equatorial coordination mode. More interestingly, a chiral cooperativity of the central backbone (determining the absolute configuration) and the terminal groups was found.[1, 61, 69, 70]

Diphosphite ligands based on sugar backbones (Figure 2.25) were also shown to be efficient ligands for the asymmetric hydroformylation of vinylarenes. High regio- and enantioselectivity (up to 98.8 and 91 % respectively) under mild conditions were obtained.[71]

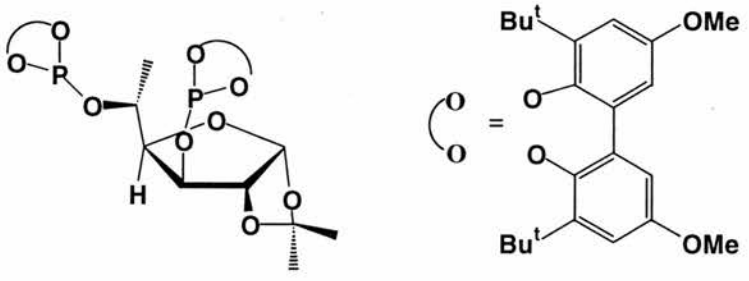

Figure 2.25 Diphosphite ligands based on sugar backbone.[71]

Phosphine-phosphite rhodium catalysts provide other successful catalytic system for asymmetric hydroformylation. The first and still probably the best asymmetric system so far was discovered by Takaya, Nozaki *et al.* They used the

chiral phosphine- phosphite ligands (R,S)- and (R,R)-BINAPHOS to induce high enantioselectivity (ee over 90 %) in the hydroformylation of numerous alkene substrate.[72-75] For example, hydroformylation of styrene using (R, S) BINAPHOS gave 94 % ee to S aldehyde with a conversion >99 % and branched to linear ratio of 86/14 (reaction condition 60°C, CO/ H_2 50/50 bar, 43h)[72, 74].

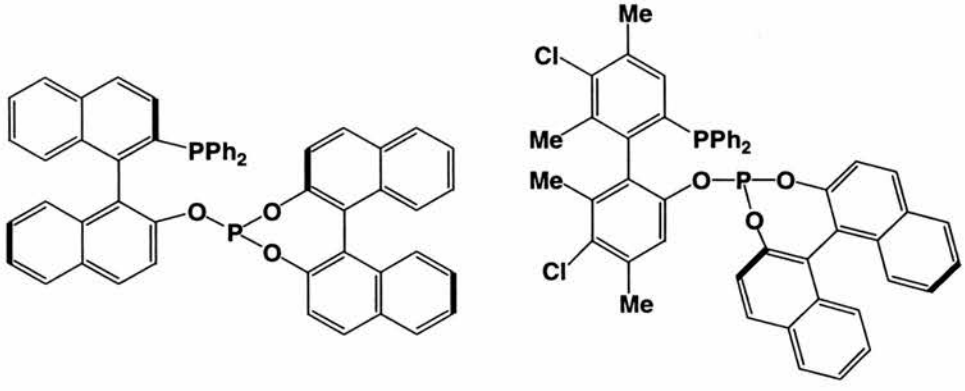

(R, S)- BINAPHOS **(S, R)- BIPHEMPHOS**

Figure 2.26 BINAPHOS and related ligand.

Interestingly, the alkene insertion step for styrene in the [$RhH(CO)_2$(R,S-BINAPHOS)] system was shown to be irreversible at pressures between 20 and 100 bar. Under a total pressure of 1 bar partial reversibility was found.[76] Another excellent ligand is the related (S,R)-BIPHEMPHOS. This ligand gave an ee of 94 % for the (S) enantiomer with a conversion of styrene of 95 % and a l:b ratio of 92/8. The (R,R) diastereoisomer was however unsuccessful (ee of 16 %).[72, 74] In these phosphite-phosphine rhodium catalysts the enantioselectivity was predominantly controlled by the absolute configuration of the bridge (biphenyl or binaphthyl). It was found that an opposite absolute configuration of the binaphthyl and biphenol moieties gave the highest ee. Contrary to the diphosphite ligands, the favoured chelation mode in the hydrido-rhodium complex [$HRh(P\text{-}P)(CO)_2$] was an equatorial-axial configuration. Amazingly, the phosphine occupied an equatorial position and the phosphite moiety an apical one. This result is contradictory to the donor and acceptor properties (see section 2.1). Using another type of phosphine (chiral)-phosphite ligand (Figure 2.27), van Leeuwen and co-workers found this time an equatorial- axial configuration for respectively the phosphite and the phosphine moieties.[77] This configuration favoured the branched aldehyde as required. Although their ligands were less selective (ee up to 63 % with R^1 = 1-Naphtyl), they reached the same conclusions about the factors influencing the enantioselectivity.

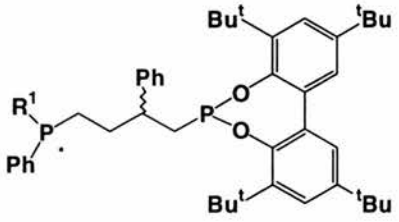

R^1 = 1-Naphtyl
= 2-Anisyl

Figure 2.27 van Leeuwen and co-workers phospine-phosphite ligands.

Recently Wills and Cole-Hamilton reported the asymmetric hydroformylation of vinyl acetate and styrene with rhodium complexes of a novel type of phosphorus-donor ligand named ESPHOS (Figure 2.28).[78] This chelate showed high regio- and enantioselectivity for the hydroformylation of the vinyl acetate (respectively 88 % (branched) and ee of 94 %), but no asymmetric induction was found for the reaction with styrene.

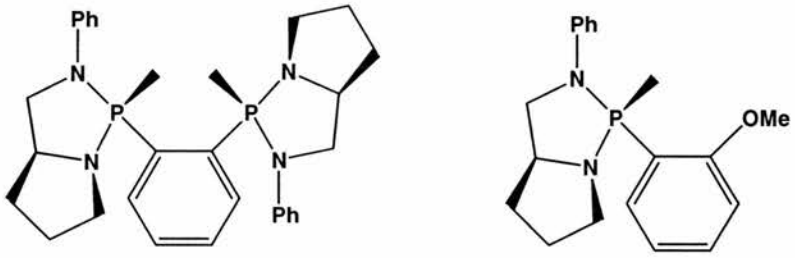

Figure 2.28 ESPHOS (right) and SEMI-ESPHOS (left) ligand.

Interestingly, the hydroformylation of the vinyl acetate under the same conditions using the SEMI-ESPHOS ligand gave low yields of essentially racemic products. Another important result reported was the formation of alcohol products (with vinyl acetate as substrate) by prolonged reaction time and higher pressure (40 bar) and temperature (80°C) (Figure 2.29). Up to 58.8 % of alcohol products was obtained with an enantioselectivity excess of 84 % (up to 89 %).

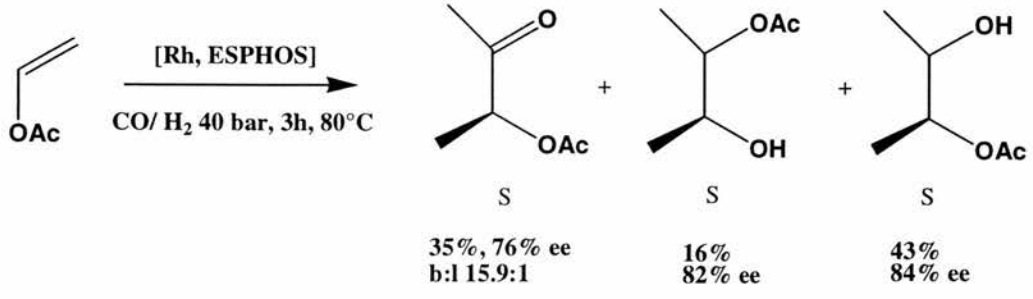

Figure 2.29 Hydroformylation of vinyl acetate followed by reduction.

2.6 Rhodium catalysed hydroformylation with alkyl-phosphine ligands.

The most predominant phosphines in the catalytic rhodium hydroformylation type reaction have been arylphosphines. Alkylphosphines, on the other hand, have been studied less extensively. It has recently become apparent that some of their properties, in particular the greater electron donating ability compared to arylphosphines, can be utilised.[79] Phosphine ligands allowed the direct reduction of aldehydes to alcohols but only under forcing conditions with higher hydrogen pressure.[79, 80] However, recently Cole-Hamilton and co-workers reported that it was possible to hydrocarbonylate alkenes to alcohols under mild conditions by using electron donating trialkylphosphine ligands with rhodium catalysts in protic solvents (Figure 2.30).[79, 81-84]

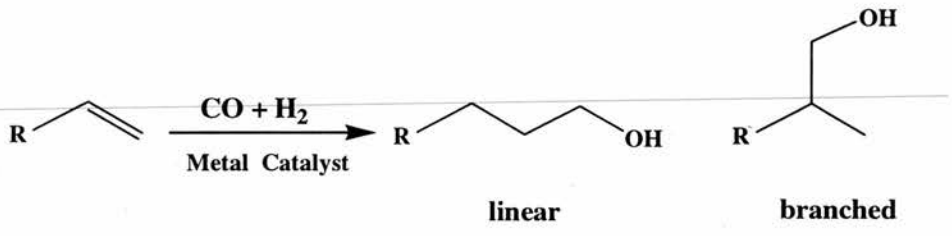

Figure 2.30 Hydrocarbonylation of alkenes by rhodium alkyl phosphine complexes in protic solvent.

While hydroformylation of hex-1-ene in toluene by $[RhH(PEt_3)_3]$ at 40 bar CO/H_2 1:1 and 120°C (oven) gave mainly aldehydes even after 16 hours, it was found that in primary, secondary and tertiary alcohol solvents, alcohols were the only products after 2 hours of reaction, no aldehydes were observed. Similar results were reported for the hydroformylation of ethene, propene, and allyl alcohol. Mechanistic investigations on rhodium-catalysed hydroformylation/ reduction of hex-1-ene to the C7 alcohols (heptan-1-ol and 2-methyl hexanol) with $[RhH(PEt_3)_3]$ or $[HRh(CO)(PEt_3)_2]$ in ethanol showed that aldehydes were not the intermediates in the formation of the alcohols in these particular conditions.

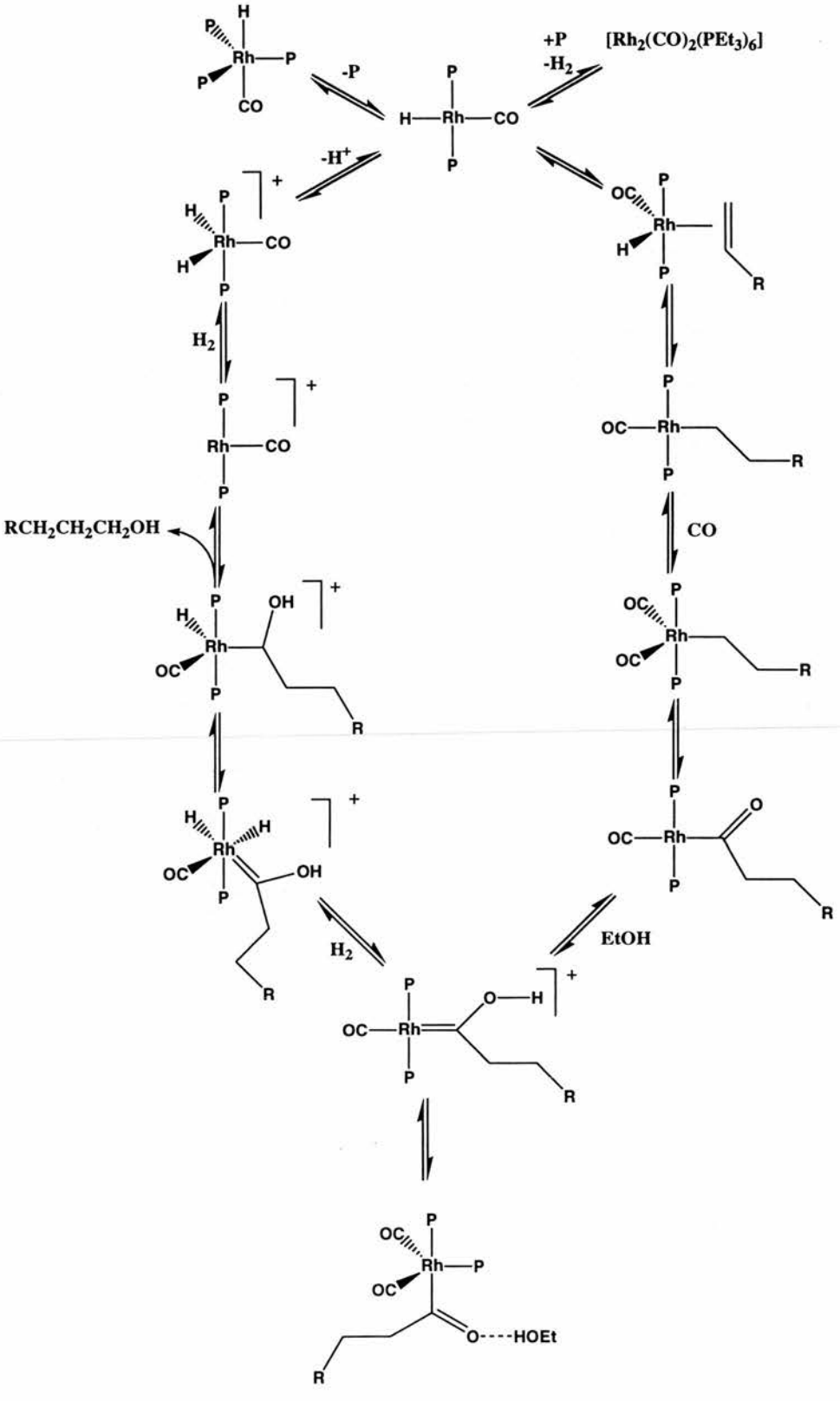

Scheme 2.6 Mechanism proposed for the hydroformylation of alkene to alcohols.

The catalytic mechanism, which has been proposed in accordance with labelling studies, is shown in Scheme 2.6. The first step is the non-oxidative addition

of the double bond (alkene) to the complex followed by insertion into the Rh-H bond. Then a non-oxidative addition of CO and its insertion in the Rh-alkyl bond occur. The protonation of the acyl carbon atom in species B gives the hydroxycarbene complex, C. The process was thought to occur due to the higher electron density on the metal caused by the electron donating trialkylphosphines. The oxidative addition of H_2 to the hydroxycarbene complex is followed by migration of H to give a hydroxylalkyl, D, and reductive elimination to give heptanol as the primary product and $[Rh(CO)(PEt_3)_2]^+$. Recycling of the catalyst involves oxidative addition of H_2 followed by deprotonation.

2.7 Bimetallic rhodium species

Stanley and co-workers reported that the ligand **53 rac** (Figure 2.31) formed a bimetallic complex with rhodium, which was an active and regioselective catalyst for the hydroformylation reaction of hex-1-ene.[85, 86] This complex afforded a l:b ratio of 27.5 with a selectivity to the linear aldehyde of 82 % (products of isomerization and hydrogenation respectively 8 % and 3 %).

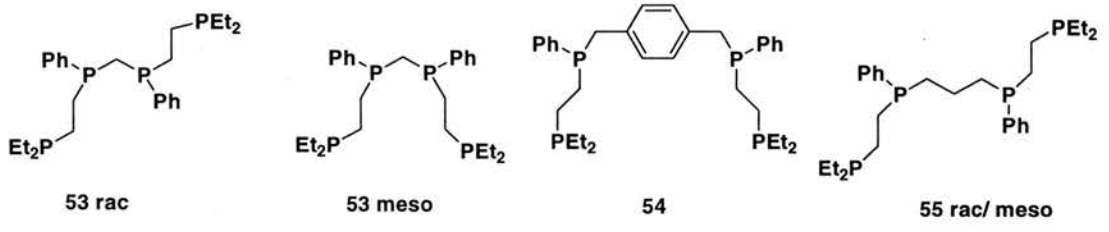

Figure 2.31 Tetraphosphines compounds used by Stanley and co-workers.

They suggested that the mechanism of reaction occurred via a co-operative mechanism in a bimetallic species (Scheme 2.7). An X-ray structure of **56** and spectroscopic evidence of unusual dicationic bimetallic rhodium (II) complexes supported the hypothesis. It was proposed that the formation (elimination) of the aldehydes occurred through intramolecular hydride transfer from the rhodium hydride to the rhodium acyl species in intermediate **F** (Scheme 2.7). Comparative studies with ligands possessing similar structures (**53 meso, 54, 55**) indicated that only this particular ligand was selective to the aldehydes and thus underwent a different mechanism of reaction. Importantly, alkene inhibition of the catalytic reaction occurred at high concentration. This effect supported the hypothesis of a bimetallic co-operative mechanism hence bis-acyl species could be formed and so prevented the hydride transfer.

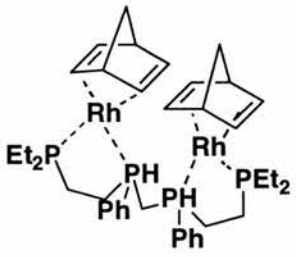

56

Figure 2.32 Crystalline rhodium complex.

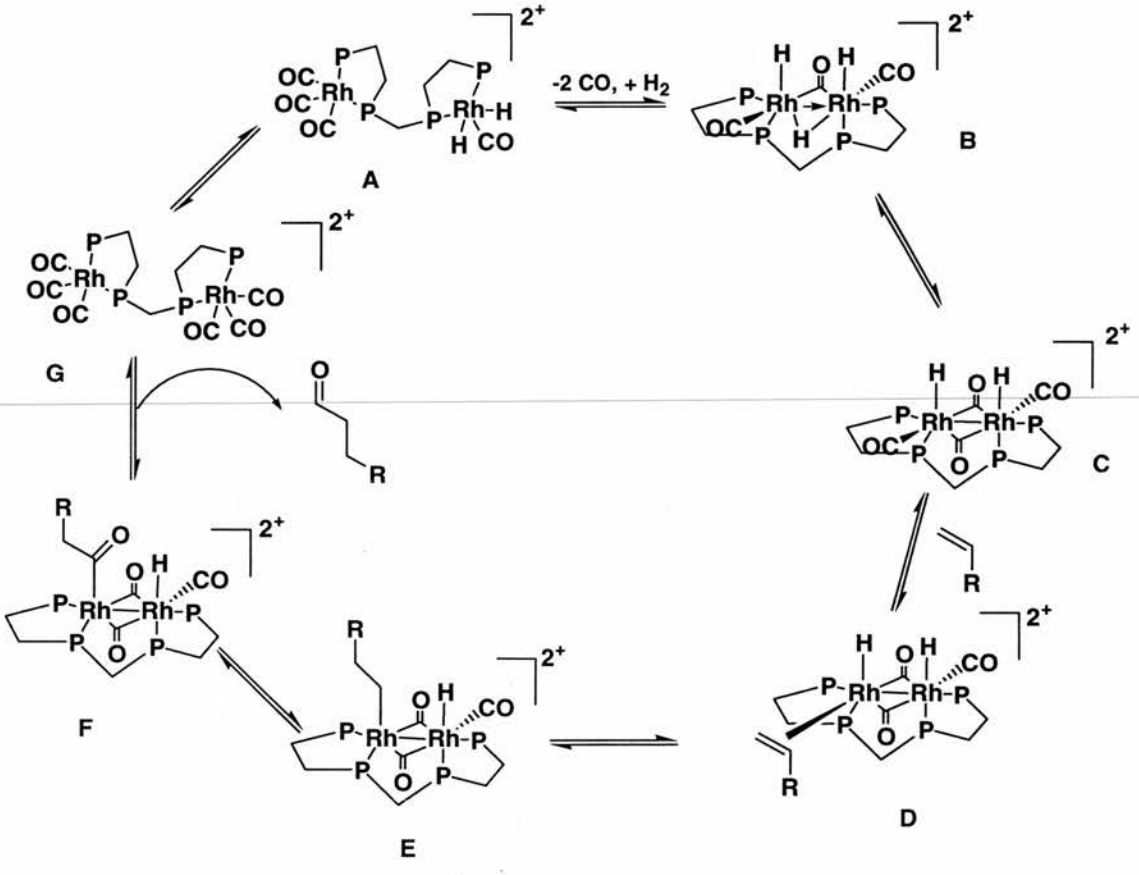

Scheme 2.7 Proposed bimetallic mechanism in the hydroformylation of alkenes.

2.8 Recycling processes of metal complexes.

Industrially, rhodium catalysts are only used when a process allows the recovery of the expensive complexes. For low boiling point products like C3-C5 aldehydes, separation of the system can be achieved by direct distillation. Unfortunately, the stability of the rhodium catalyst does not exceed 150°C, and this limits the use of distillation processes. Biphasic systems have stirred a lot of interest

since the 1970's since separation of products and catalyst should be facilitated as they are in different phases. An environmentally benign and very successful process is the aqueous biphasic system developed by Ruhrchemie/Rhône-Poulenc.[26, 27] The combination of a water-soluble ligand (TPPTS: triphenylphosphine tri-sulfonate) with a rhodium precursor affords an active recyclable catalyst for the hydroformylation of propene and butene. However the poor solubility of longer alkenes chain (> C5) in water limits also the extension of the process. The use of surfactant-based catalysts allowed a better solubility of the alkenes and therefore a better activity.[87-91] BISBI **57** [92, 93] and xantphos **58** [94] ligands modified to micelle-type compounds showed enhanced rates (up to a factor 14 for **58**) and good selectivity (l:b up to 50:1 for **58**) in the biphasic hydroformylation of oct-1-ene.

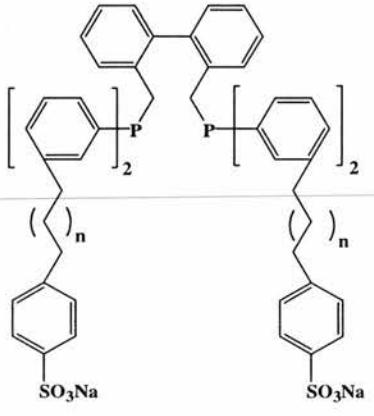

57

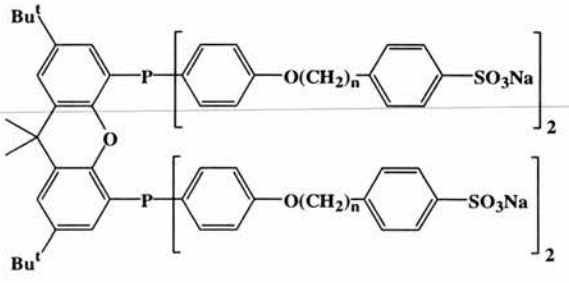

58

Figure 2.33 BISBI [92, 93] (left) and xantphos[94] (right) ligands modified to micelle-type compounds.

Thermoregulated phase-transfer catalysis was also applied to hydroformylation of long chain alkenes or styrene. This process is based on the inverse temperature-dependant solubility of the ligand called 'smart ligands' in the water and organic phase. At a given temperature the water-soluble catalyst transfers into the organic phase containing the substrate leading to hydroformylation reaction. So recovery of the catalyst is obtained by cooling of the reaction medium. A series of poly(ethylene oxide)-substituted triphenylphosphine ($Ph_{3-m}P[C_6H_4$-p-$(OCH_2CH_2)_nOH]_m$ was used for the hydroformylation of long chain alkenes (C6 to C12).[95] Interestingly, similar rates of reaction were found for hexene and dodec-1-ene indicating that, as expected, the reaction took place in the organic phase. This system could be used 5 times

without significant loss of activity. No information on the regioselectivity of the reaction was however given. An octylpolyglycol-phenylene-phosphite[96] (Figure 2.34) and a chiral polyether-phosphite ligands derived from (S)-binaphtol[97] (Figure 2.34) were used respectively for the hydroformylation and the asymmetric hydroformylation of styrene. Both ligands formed active complexes with rhodium species showing high catalytic activity and regioselectivity. Enantiomeric excess up to 25 % was obtained for the polyether-phosphite system as expected for this type of ligand. However, slow leaching of the metal occurred.

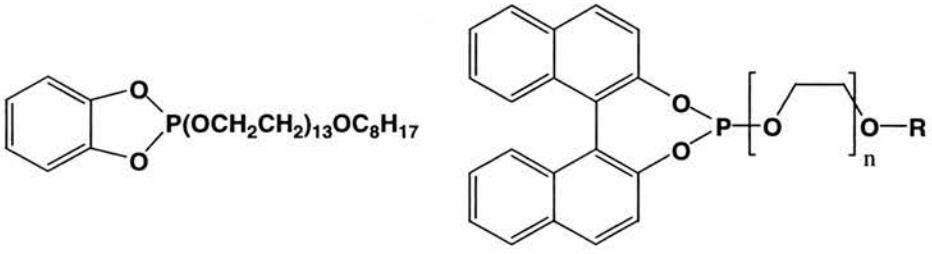

Figure 2.34 Octylpolyglycol-phenylene-phosphite (right) and chiral polyether-phosphite (left) ligands.

On the contrary, in fluorous biphasic phase system, long chain alkenes are soluble at high temperature and thus the recovery of the catalyst (which stays in principle in the fluorous phase) is facilitated.[98, 99] Using the fluorous-soluble ligand $P[CH_2CH_2(CF_2)_5CF_3]$ and rhodium catalyst, hydroformylation of dec-1-ene and ethene was performed. The selectivity for the linear C11 aldehyde was about 72 %. Recovery of the different phases was successfully executed nine times. Although leaching of the rhodium and ligand occurred (1.18 ppm per mole of aldehyde), a total turnover number of 35,000 mole of aldehyde/mole of rhodium was reached. Unfortunately the cost of such fluorous solvent inhibits its industrial application.

Ionic liquids are a promising system to recover homogeneous catalysts. Chauvin *et al*,[100] and recently Salzer, Wasserscheid and co-workers[101] showed the ability of such biphasic system to give active and recyclable hydroformylation process. High activity and regioselectivity (l:b = 16:1) with no detectable leaching of the metal, were obtained using an ionic phosphine ligands with a cobaltocenium backbone (Figure 2.35) for the hydroformylation of oct-1-ene.

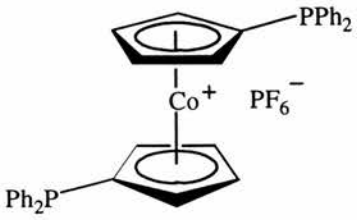

Figure 2.35 Active and regioselective ionic phosphine ligands with a cobaltocenium backbone for hydroformylation in an ionic liquid.

Another way to overcome the problematic recovery of the catalyst is to use a heterogeneous solid catalyst. Numerous attempts have been made to immobilise rhodium complexes on polymeric or on inorganic supports. However in many cases the rates and/ or selectivity were slow and leaching of the catalyst occurred.[102-105] One recent successful system is the immobilisation of rhodium-xantphos complexes on silica gel reported by van Leeuwen and co-workers (Figure 2.36). Despite a slow reaction rate for the hydroformylation of oct-1-ene, the system could be recycled 8 times without significant loss of rhodium or activity and high linearity to the aldehyde (> 90 %) was obtained.[106]

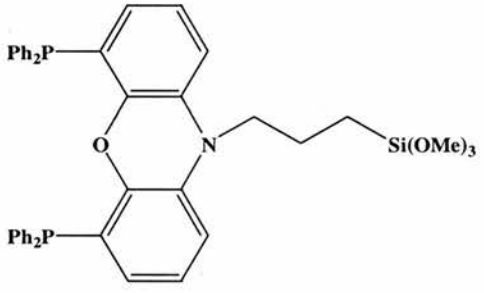

Figure 2.36 Xantphos type ligand immobilised on silica gel.

An in between system is the supported aqueous phase catalysis (SAPC) process. A thin film of water adhering to a high-surface-area hydrophilic support is the active media for catalytic reaction. The activity and robustness of the system are highly dependent of the thickness of the water. Water-soluble phosphines were successfully used for the hydroformylation of alkenes.[107-109] Whilst TPPTS ligands showed low selectivity and a decrease of activity after 4 runs, xantphos-type ligand (Figure 2.37) maintained high regioselectivity (l:b 40:1) and activity at least 10 consecutive runs for oct-1-ene hydroformylation.[110]

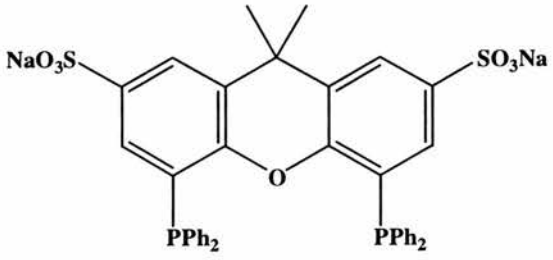

Figure 2.37 Water soluble xantphos-type ligand.

The recent developments of novel dendritic catalysts as described in Chapter 1 show that this is an alternative recycling route to heterogeneous and biphasic systems. However more intensive research must be develop to acquire such attractive goal.

A new reaction medium, intensively developed in the last decade, is the supercritical fluids. In this system there are no phase boundaries as in the biphasic system, moreover gas and organic products present good solubilities. Supercritical CO_2 ($scCO_2$) in particular has stirred a lot of interest due to its non-toxicity and low cost. Hence it is not surprising that it was chosen as a highly suitable media for hydroformylation reaction with cobalt[111] or rhodium complexes. Nevertheless, such system requires large investment to be developed to in an industrial scale due to the pressurisation and subsequent depressurisation processes needed. Leitner[112-114] and Erkey[115] studied the effect of perfluoroalkyl-substituted aryl-phosphines (Figure 2.38) in the hydroformylation of oct-1-ene in $scCO_2$. High activity and regioselectivity to the linear aldehyde were obtained (conversion > 99 %, l:b ratio up to 5.6).[112-114] Interestingly the phosphite ligand **60** showed a high overall selectivity for the linear products (l:b ratio of 8.5:1) which is unusual for this kind of ligand (see section 2.1).

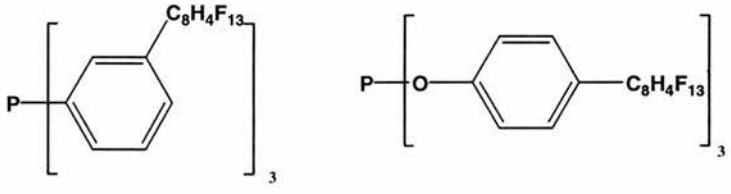

59 **60**

Figure 2.38 Perfluoroalkyl-substituted aryl-phosphines[112-114] used in the hydroformylation of oct-1-ene in $scCO_2$.

High enantioselectivities (ee > 94 %) and regioselectivities (> 88 %) were as well obtained using perfluoroalkyl-modified BINAPHOS (Figure 2.39) as ligand in the

hydroformylation of toluene.[116] Leitner and co-workers recycled their catalyst system up to 5 times without consequent loss of catalytic performance.

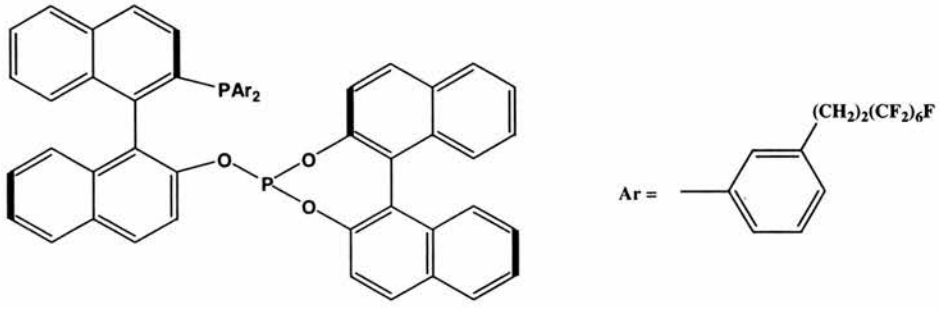

(R,S)-3-H^{2}F^6-BINASPHOS

Figure 2.39 Stereoselective perfluoroalkyl-modified BINAPHOS as ligand in the hydroformylation of toluene in sCO_2.

Cole-Hamilton and co-workers reported the hydroformylation of hex-1-ene and oct-1-ene in $scCO_2$ using respectively soluble and insoluble complexes of rhodium[117, 118] and continuous flow process using an ionic liquid biphasic system.[119] The ligands of the soluble system were simple rhodium alkyl phosphine (PEt_3) (l:b ratio of 2.4). Rhodium complexes of triphenylphosphite and long alkyl chain on aryl-phosphite or phosphine showed good activity despite being insoluble in the reaction medium. Linear to branched ratios up to 10:1 were reported. Mono-sulfonated triphenyl phosphines were used as ligands in imidazolium-type ionic liquid for the hydroformylation of oct-1-ene under CO_2 supercritical conditions. This system allows continuous flow homogeneous catalysis with complete separation of the products from the catalyst. Slow depressurisation of the $scCO_2$ solution in another vessel precipitated the products while the catalytic solution remained in the reactor vessel. Good reactivities and selectivities (l:b over 6:1) systems for the phosphite based system were found.

2.9 References for Chapter 2.

1 P. W. N. M. van Leeuwen and C. Claver, 'Rhodium Catalysed Hydroformylation', Kluwer Academic Publishers, Dordrecht, 2000.

2 O. Roelen, Ger. Pat., 849,548, 1938, .

3 O. Roelen, *Chem. Zentr.*, 1953, 927.

4 J. F. Young, J. A. Osborn, F. A. Jardine, and G. Wilkinson, *J. Chem. Soc., Chem. Commun.*, 1965, 131.

5 D. Evans, J. A. Osborn, and G. Wilkinson, *J. Chem. Soc. A.*, 1968, 3133.

6 G. Schiller, Germ. Pat., 965,605, 1956, Chem. Verwertungsges. Oberhausen.

7 V. L. Hughes, Br. Pat., 801,734, 1958, Esso Res. Eng. Comp.

8 J. L. Vidal and W. E. Walker, *Inorg. Chem.*, 1981, **20**, 249.

9 H. M. Colquhoun, D. J. Thompson, and M. T. Twigg, 'Carbonylation-direct Synthesis of Carbonyl Compounds', Plenum, 1991.

10 R. F. Heck and D. S. Breslow, *J. Am. Chem. Soc.*, 1962, **84**, 2499.

11 C. D. Frohning and C. W. Kohlpaintner, 'Applied Homogeneous Catalysis with Organometallic Compounds', Cornils, B., Herrmann, W.A., VCH, Weinheim, 1996.

12 L. H. Slaugh and D. Mullineaux, *Chem. Abs.*, 1966, **64**, 15745.

13 L. H. Slaugh and D. Mullineaux, U. S. Pat., , 1966, Shell Oil Company.

14 L. H. Slaugh and D. Mullineaux, *J. Organomet. Chem.*, 1968, **13**, 469.

15 C. K. Brown and G. Wilkinson, *J. Chem. Soc. A*, 1970, 2753.

16 D. Evans, G. Yagupsky, and G. Wilkinson, *J. Chem. Soc. A*, 1968, 2660.

17 F. H. Jardine, *Polyhedron*, 1982, **1**, 569.

18 R. F. Heck, *J. Am. Chem. Soc.*, 1962, **83**, 4023.

19 R. Lazzaroni, A. Raffaelli, R. Settambolo, S. Bertozzi, and G. Vituli, *J. Mol. Catal.*, 1989, **50**, 1.

20 R. L. Pruett and J. A. Smith, *J. Org. Chem.*, 1969, **34**, 327.

21 P. W. N. M. van Leeuwen and C. Roobeek, *J. Organomet. Chem.*, 1983, **258**, 343.

22 P. W. N. M. van Leeuwen and C. Roobeek, U.S. Pat., 4,467,116, 1983, Shell Oil Company.

23 E. Billig, A. G. Abatjoglou, D. R. Bryant, R. E. Murray, and J. M. Mathers, U. S. Pat., 4,769,498, 1986, Union Carbide Co.

24 E. Billig, A. G. Abatjoglou, and D. R. Bryant, U. S. Pat., 4,769,498, 1988, Union Carbide Co.

25 E. Billig, A. G. Abatjoglou, and D. R. Bryant, , 4,748,261, 1988, Union CarbideCorporation.

26 E. Kuntz, Fr. Pat., 2,314,910, 1977, Rhône-Poulenc.

27 E. Kuntz, *E. D. CHEMTECH*, 1987, **17**, 570.

28 C. A. Tolman, *J. Am. Chem. Soc.*, 1970, 2953.

29 D. White, B. C. Taverner, P. G. L. Leach, and N. J. Coville, *J. Organomet. Chem.*, 1994, 205.

30 D. White, B. C. Taverner, N. J. Coville, and P. W. Wade, *J. Organomet. Chem.*, 1995, **495**, 41.

31 Y. koide, S. G. Bott, and A. R. Barron, *Organometallics*, 1996, **15**, 2213.

32 T. L. Brown, *Inorg. Chem.*, 1992, **31**, 1286.

33 J. M. Brown and A. G. Kent, *J. Chem. Soc., Perkin Trans. II*, 1987, 1597.

34 C. U. Pittman Jr. and A. Hirao, *J. Org. Chem.*, 1978, **43**, 640.

35 A. R. Sanger, *J. Mol. Cata.*, 1977/8, **3**, 221.

36 A. R. Sanger, *J. Mol. Cata.*, 1977/8, **3**, 101.

37 G. Consiglio, C. Botteghi, C. Salomon, and P. Pino, *Angew. Chem.*, 1973, **85**, 665.

38 O. R. Hughes and J. D. Unruh, *J. Mol. Cat.*, 1981, **12**, 71.

39 J. D. Unruh and J. R. Christenson, *J. Mol. Cata.*, 1982, **14**, 19.

40 U. Nettekoven, P. C. J. Kamer, M. Widhalm, and P. W. N. M. van Leeuwen, *Organometallics*, 2000, **19**, 4596.

41 T. J. Devon, G. W. Phillips, T. A. Puckette, J. L. Stavinoha, and J. J. Vanderbilt, U. S. Pat., 4,694,109, 1987, Eastman Kodak Company.

42 T. J. Devon, G. W. Phillips, T. A. Puckette, J. L. Stavinoha, and J. J. Vanderbilt, U. S. Pat., 5,344,988; 5,332,846, 1994, Eastman Chemical Company.

43 C. P. Casey, G. T. Whiteker, M. G. Melville, L. M. Petrovich, J. A. Gavney Jr., and D. R. Powell, *J. Am. Chem. Soc.*, 1992, **114**, 5535.

44 C. P. Casey and L. M. Petrovich, *J. Am. Chem. Soc.*, 1995, **117**, 6007.

45 R. Lazzaroni, G. Ucello-Barretta, and M. Benetti, *Organometallics*, 1989, **8**, 2323.

46 A. van Rooy, E. N. Orij, P. C. J. Kamer, and P. W. N. M. van Leeuwen, *Organometallics*, 1995, **14**, 34.

47 L. A. van der Veen, M. D. K. Boele, F. R. Bregman, P. C. S. Kamer, P. W. N. M. van Leeuwen, F. Goubitz, J. Fraanje, H. Schenk, and C. Bo, *J. Am. Chem. Soc.*, 1998, **120**, 11616.

48 T. Matsubara, N. Koga, Y. Ding, D. G. Musaev, and K. Morokuma, *Organometallics*, 1997, **16**, 4828.

49 D. Gleich, R. Schmid, and W. A. Herrmann, *Organometallics*, 1998, **17**, 2141.

50 C. P. Casey, L. E. Paulsen, E. W. Beuttenmueller, B. R. Proft, L. M. Petrovich, and B. A. Matter, *J. Am. Chem. Soc.*, 1997, **119**, 11817.

51 C. P. Casey, E. L. Paulsen, E. W. Beuttenmueller, B. R. Proft, B. A. Matter, and D. R. Powell, *J. Am. Chem. Soc.*, 1999, **121**, 63.

52 M. Kranenburg, Y. E. M. van der Burgt, P. C. J. Kamer, and P. W. N. M. van Leeuwen, *Organometallics*, 1995, **14**, 3081.

53 P. Dierkes and P. W. N. M. van Leeuwen, *J. Chem. Soc., Dalton Trans.*, 1999, 1519.

54 L. A. van der Veen, P. H. Keeven, G. C. Schoemaker, J. N. H. Reek, P. C. J. Kamer, P. W. N. M. van Leeuwen, M. Lutz, and A. L. Spek, *Organometallics*, 2000, **19**, 872.

55 E. Billig, A. G. Abatjoglou, and D. R. Bryant, U.S. Pat., 4,668,651, 1987, Union Carbide Corporation.

56 A. van Rooy, P. C. J. Kamer, P. W. N. M. van Leeuwen, K. Goubitz, J. Fraanje, N. Veldman, and A. L. Spek, *Organometallics*, 1996, **15**, 835.

57 K. Sato, J. Karawagi, and Y. Tanihari, Jpn. Kokai Tokkyo Koho JP, 07,278,040, 1996, Mitsubishi.

58 B. Moasser, W. Gladfelter, and D. C. Roe, *Organometallics*, 1995, **14**, 3832.

59 P. M. Burke, J. M. Garner, W. Tam, K. A. Kreutzer, and A. J. J. Teunissen, MWO, 97/33854, 1997, DSM/ Du Pont.

60 F. Agboussou, J. F. Carpentier, and A. Montreux, *Chem. Rev.*, 1995, **95**, 2485.

61 G. J. H. Buisman, L. A. van der Veen, A. Klootwijk, W. G. J. de Lange, P. C. J. Kamer, P. W. N. M. van Leeuwen, and D. Vogt, *Organometallics*, 1997, **16**, 2929.

62 D. Gleich and W. A. Herrmann, *Organometallics*, 1999, **18**, 4354.

63 Y. Pottier, A. Mortreux, and F. Petit, *J. Organometal. Chem.*, 1989, **370**, 333.

64 C. Salomon, G. Consiglio, C. Botteghi, and P. Pino, *Chimia*, 1973, **27**, 215.

65 A. M. Masdeu-Bultó, A. Orejon, A. Castellanos, S. Castillón, and C. Claver, *Tetrahedron Asymmetry*, 1996, **7**, 1829.

66 M. Diéguez, M. M. Pereira, A. M. Masdeu-Bultó, C. Claver, and J. C. Bayón, *J. Mol. Cat.*, 1999, **143**, 111.

67 A. Castellanos-Páez, S. Castillón, C. Claver, P. W. N. M. van Leeuwen, and W. de Lange, *Organometallics*, 1998, **17**, 2543.

68 J. E. Babin and G. T. Whiteker, W.O. Pat., 93/03830, 1992, Union Carbide Corporation.

69 G. J. H. Buisman, E. Vos, P. C. J. Kamer, and P. W. N. M. van Leeuwen, *J. Chem. Soc., Dalton Trans.*, 1995, 409.

70 A. van Rooy, J. N. H. de Bruijn, and K. F. Roobeek, *J. Organomet. Chem.*, 1996, **507**, 69.

71 M. Diéguez, O. Pàmies, A. Ruiz, S. Castillón, and C. Claver, *J. Chem. Soc. , Chem. Commun.*, 2000, 1607.

72 N. Sakai, S. Mano, K. Nozaki, and H. Takaya, *J. Am. Chem. Soc.*, 1993, **115**, 7033.

73 N. Sakai, K. Nozaki, and H. Takaya, *J. Chem. Soc., Chem. Commun.*, 1994, 395.

74 K. Nozaki, N. Sakai, T. Nanno, T. Higashijima, S. Mano, T. Horiuchi, and H. Takaya, *J. Am. Chem. Soc.*, 1997, **119**, 4413.

75 T. Horiuchi, T. Ohta, E. Shirakawa, K. Nozaki, and H. Takaya, *J. Org. Chem.*, 1997, **62**, 4285.

76 T. Horiuchi, T. Ohta, E. Shirakawa, K. Nozaki, and H. Takaya, *Organometallics*, 1997, **16**, 2981.

77 S. Deerenberg, P. C. J. Kamer, and P. W. N. M. van Leeuwen, *Organometallics*, 2000, **19**, 2065.

78 S. Breeden, D. J. Cole-Hamilton, D. F. Foster, G. J. Schwarz, and M. Wills, *Angew. Chem. Int. Ed.*, 2000, **39**, 4106.

79 M. C. Simpson and D. J. Cole-Hamilton, *Coord. Chem. Rev.*, 1996, **155**, 163.

80 P. Eilbracht, L. Bärfarcker, C. Buss, C. Hollmann, B. E. Kitsos-Rzychon, C. L. Kranemann, T. Rische, R. Roggenbuck, and A. Schmidt, *Chem. Rev.*, 1999, **99**, 3329.

81 J. K. MacDougall, D. J. Cole-Hamilton, and M. J. Green, Eur. Pat., 420510, 1991,

82 J. K. MacDougall, M. C. Simpson, and D. J. Cole-Hamilton, *Polyhedron*, 1993, **12**, 2877.

83 J. K. MacDougall, M. C. Simpson, and D. J. Cole-Hamilton, *J. Chem. Soc., Dalton Trans.*, 1994, 3061.

84 J. K. MacDougall, M. C. Simpson, M. J. Green, and D. J. Cole-Hamilton, *J. Chem. Soc., Dalton Trans.*, 1996, 1161.

85 M. E. Broussard, B. Juma, S. G. Train, W.-J. Peng, S. A. Laneman, and G. G. Stanley, *Science*, 1993, **260**, 1784.

86 R. C. Matthews, D. K. Howell, W.-J. Peng, S. G. Train, W. D. Treleavan, and G. G. Stanley, *Angew. Chem. Int. Ed.*, 1996, **35**, 2253.

87 B. Fell and G. Papadogianakis, *J. Mol. Catal.*, 1991, **66**, 143.

88 B. Fell and G. Papadogianakis, *J. Mol. Catal. A: Chem.*, 1995, **101**, 179.

89 H. Ding, B. E. Hanson, T. Bartik, and B. Bartik, *Organometallics*, 1994, **13**, 3761.

90 H. Ding and B. E. Hanson, *J. Chem. Soc., Chem. Commun.*, 1994, 2747.

91 T. Bartik, H. Ding, B. Bartik, and B. E. Hanson, *J. Mol. Catal. A: Chem.*, 1995, **98**, 117.

92 H. Ding, J. X. Kang, B. E. Hanson, and C. W. Kohlpaintner, *J. Mol. Catal. A: Chem.*, 1997, **124**, 21.

93 B. E. Hanson, H. Ding, and C. W. Kohlpaintner, *Catal. Today*, 1998, **42**, 421.

94 M. Schreuder Goedheijt, B. E. Hanson, J. N. H. Reek, P. C. J. Kamer, and P. W. N. M. van Leeuwen, *J. Am. Chem. Soc.*, 2000, **122**, 1650.

95 X. Zheng, J. Jiang, X. Liu, and Z. Jin, *Catalysis Today*, 1998, **44**, 175.

96 R. Chen, X. Liu, and Z. Jin, *J. Organomet. Chem.*, 1998, **571**, 201.

97 J. A. J. Breuzard, M. L. Tommasino, M. C. Bonnet, and M. Lemaire, *J. Organomet. Chem.*, 2000, **616**, 37.

98 I. T. Horváth and J. Rábai, *Science*, 1994, **266**, 72.

99 I. T. Horváth, G. Kiss, R. Cook, J. E. Bond, P. A. Stevens, J. Rábai, and J. Mozeleski, *J. Am. Chem. Soc.*, 1998, **120**, 3133.

100 Y. Chauvin, Y. Mussmann, and H. Olivier, *Angew. Chem.*, 1995, **107**, 2941.

101 C. C. Brasse, U. Englert, A. Salzer, H. Waffenschmidt, and P. Wasserscheid, *Organometallics*, 2000, **19**, 3818.

102 S. Wieland and P. Panster, *Catal. Org. React.*, 1994, **62**, 383.

103 M. O. Farrell, C. H. van Dyke, L. J. Boucher, and S. J. Metlin, *J. Organomet. Chem.*, 1979, **172**, 367.

104 K. Nozaki, Y. Itoi, F. Shibahara, E. Shirakawa, T. Otha, H. Takaya, and T. Hiyama, *J. Am. Chem. Soc.*, 1998, **120**, 4051.

105 K. Nozaki, F. Shibahara, Y. Itoi, E. Shirakawa, T. Otha, H. Takaya, and T. Hiyama, *Bull. Chem. Soc. Jpn.*, 1999, **72**, 1911.

106 A. J. Sandee, L. A. van der Veen, J. N. H. Reek, P. C. J. Kamer, M. Lutz, A. L. Spek, and P. W. N. M. van Leeuwen, *Angew. Chem. Int. Ed.*, 1999, **38**, 3231.

107 B. B. Bunn, T. Bartik, B. Bartik, W. R. Bebout, T. E. Glass, and B. E. Hanson, *J. Mol. Catal.*, 1994, **94**, 157.

108 M. Schreuder Goedheijt, P. C. J. Kamer, and P. W. N. M. van Leeuwen, *J. Mol. Cat.*, 1998, **134**, 243.

109 M. J. Naughton and R. S. Drago, *J. Catal.*, 1995, **155**, 383.

110 A. J. Sandee, V. F. Slagt, J. N. H. Reek, P. C. J. Kamer, and P. W. N. M. van Leeuwen, *J. Chem. Com., Chem. Commun.*, 1999, 1633.

111 J. W. Rathke, R. J. Kingler, and T. R. Krause, *Organometallics*, 1991, **10**, 1350.

112 S. Kainz, D. Koch, W. Baumann, and W. Leitner, *Angew. Chem. Int. Ed.*, 1997, **36**, 1628.

113 S. Kainz and W. Leitner, *Catal. Lett.*, 1998, **55**, 223.

114 D. Koch and W. Leitner, *J. Am. Chem. Soc.*, 1998, **120**, 13398.

115 D. R. Palo and C. Erkey, *Organometallics*, 2000, **19**, 81.

116 G. Franciò and W. Leitner, *J. Chem. Soc., Chem. Commun.*, 1999, 1663.

117 I. Bach and D. J. Cole-Hamilton, *J. Chem. Soc., Chem. Commun.*, 1998, 1463.

118 M. F. Sellin and D. J. Cole-Hamilton, *J. Chem. Soc., Dalton Trans.*, 2000, 1681.

119 M. F. Sellin, P. B. Webb, and D. J. Cole-Hamilton, *J. Chem. Soc., Chem. Commun.*, 2001, 781.

Chapter Three: Building of dendritic molecules on a polyhedral oligosilsesquioxane core.

3 Building of dendritic molecules on a polyhedral oligosilsesquioxane core.

3.1 Introduction.

The aim of the work is to develop a catalytic system in which the catalytic species are separable from the products of reaction. The use of a macromolecule like a dendrimer should allow the reaching of that goal (see chapter 1). In tackling this project a number of factors need to be considered, the design of the dendrimer itself, the selection of the catalytic species incorporated into it and the tuning of the surface functional groups to allow it to ligate in the desired way. In this chapter we will focus on the building of suitable dendritic molecules and their functionalisation by substituents, which will allow ligation of metal complexes. Morris and co-workers previously carried out the development of a dendrimer based on a polyhedral silsesquioxane core in our department.[1] During their work, it became apparent that the groups introduced in successive generations, i.e. chloro- and vinyl-silane substituents, would be easily functionalisable by phosphorus type species. We have firstly extended the synthesis of this type of compound to obtain variable dendritic structure. Simple organic/ inorganic reactions then allowed introducing different phosphorus substituents on the periphery. This will consequently vary the density and number of functional groups on the exterior, hence allowing the number and nature of the coordination sites to the metal to be varied. Alkyl- and arylphosphine, as well as phosphite are excellent ligands in catalytic reactions and more precisely for hydroformylation. More significantly the resulting dendrimers are predicted to have similar chemical (and electronic properties) to 'small molecule' phosphine complexes. Hence the dendrimer is acting merely as a means to enlarge the catalyst sufficiently so that it can be recovered by ultrafiltration, but does not prevent catalytic reaction from occurring.

3.2 The core.

The core structure on which we have developed our dendritic molecules is the cubic polyhedral oligosilsesquioxane (Figure 3.1). The use of a silsesquioxane as the core of the dendrimer has been chosen as it will pass on certain advantageous characteristics to the entire molecule, namely a rigid framework that has similar properties to heterogeneous siloxane catalyst supports.

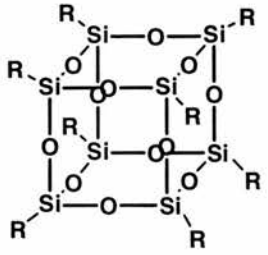

Figure 3.1 Cubic polyhedral oligosilsesquioxane molecule or POSS cube with R groups (R = H, C_6H_6, etc.).

Above all, because this POSS is a cube with a functional group at each corner, means there are eight sites from which to develop the dendrimer. Most dendrimers are only based on tetravinylsilane, tetraallylsilane, pentaerythritol or propyl amino compounds with only four such sites.[2-5] Using the POSS cube as a framework, the species can be built upon as dendrimers in three dimensions and by the second generation the introduction of 72 substituents is possible (Figure 3.2)[1] instead of 36 for dendrimers based on tetrahedral cores. This would provide an ordered array of functional groups crowded on a globular surface. Overcrowding on the periphery may limit the extension of the dendrimer (see the 'stardust effect' discuss in Chapter 1) in fewer generations than those prepared with other cores. Moreover the size and rigidity of the core and so of the different generations, should allow a better recovery of the dendrimer by ultrafiltration techniques.

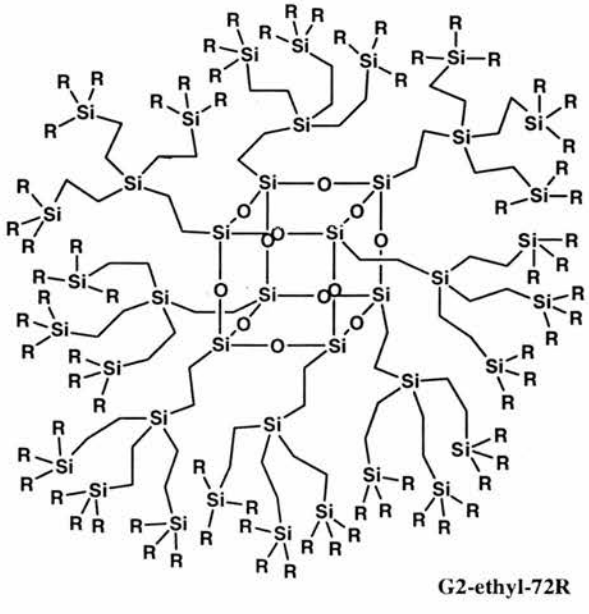

Figure 3.2 A 72-functionalised POSS developed by Morris and co-workers (R = Cl or $CH{=}CH_2$).

3.3 Building of successive generation dendrimers.

3.3.1 First generation dendrimer.

Polyhedral octavinyl octasilsesquioxane is commercially available or easily synthesised[6, 7] from hydrolysis of readily available trichlorovinylsilane in a water/ acetone medium (Figure 3.3). Slow precipitation of the compound over one month yielded after filtration 30-35 % of the octavinylsilsesquioxane, which we shall call the zeroth generation dendrimer or G0. In order to eliminate all trace of water, which causes side-reactions and cross-linking in the subsequent reactions, the compound was dried under vacuum at 60°C for 15 minutes before any other reaction. Successive hydrosilylation-alkenylation of the compound allowed the building of a dendrimer up to 72 arms.[1] At this stage, the overcrowding of the outer substituents led to incomplete functionalisation.

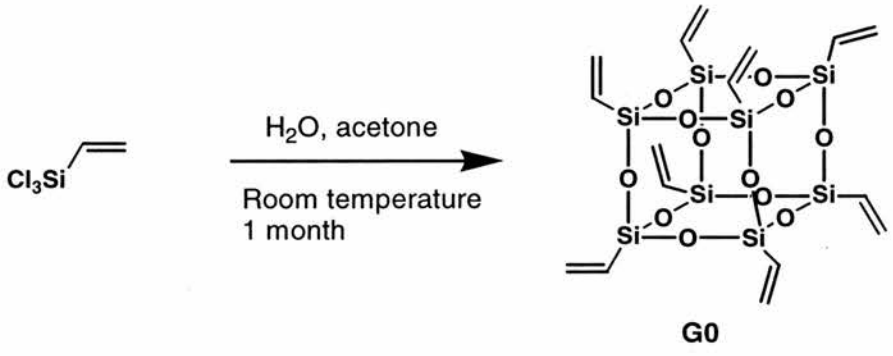

Figure 3.3 Synthesis of polyhedral octavinyl octasilsesquioxane G0.

The hydrosilylation of G0 by different silanes ($HSiCl_3$ and $HSiMeCl_2$ in excess[a]) catalysed by Speier's catalyst, H_2PtCl_6, allowed the introducing of substituents on the dendrimer with quantitative yields (over 98 %). For the first generation, the reaction was performed in diethyl ether under reflux for 8 hours and then at room temperature overnight (white precipitate apparent). The bulkiness of the POSS cube prevented the unwanted β-addition to the vinyl groups. The solvent and the excess of silane were removed under vacuum. White crystalline products were obtained. Trichlorosilane yielded 24 'reactive' chlorosilane groups, while dichloromethylsilane gave 16 chloro groups on the outer shell of the first generation dendrimer G1 (Figure 3.4). ^1H and ^{13}C NMR techniques were used for the characterisation of the products at this stage of the reaction as any unreacted vinyl

[a] this excess corresponds to an excess of reactive compare to the number of functionalisable groups on the dendrimer. This is valid for all synthesis in this chapter.

groups were easily spotted (^{1}H NMR δ 5.6 ppm). No further characterisation of the chloro compounds was carried out.

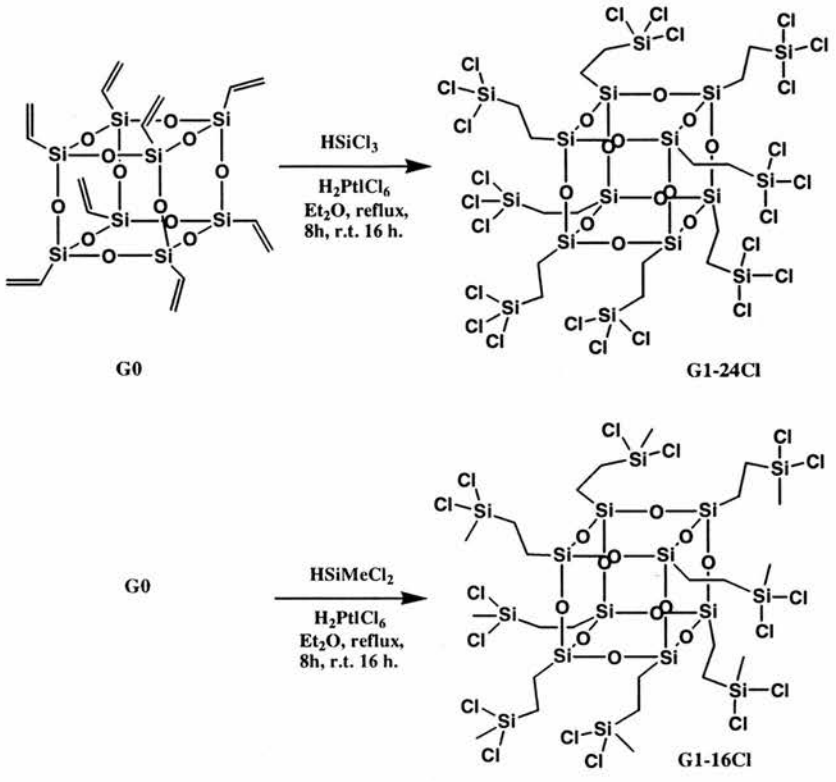

Figure 3.4 Synthesis of 24 or 16 Chloro-functionalised POSS.

The high sensitivity towards water of the chlorosilane forced us to use inert atmosphere and dried solvents to prevent intra- or intermolecular-crosslinking of the silanol formed by contact with water. Chloro-functionalised G1 could be then modified by introduction of vinyl or allyl groups through nucleophilic substitution of the chloro groups by Grignard reagents used in large excess. Compounds with 16- and 24-vinyl or allyl groups (G1-16vinyl, G1-24vinyl, G1-16allyl, G1-24allyl) were prepared (Figure 3.5 and Figure 3.6). High yields (over 80 %) were obtained after work-up and purification using silica gels columns. G1-16vinyl and G1-24vinyl were isolated as white solids in respectively 85 % and 81 % yield. G1-16allyl and G1-24allyl were recovered respectively in 90 % and 88 % yield as colourless oils. NMR techniques and microanalysis were used to characterise the products. Quantitative conversions were found.

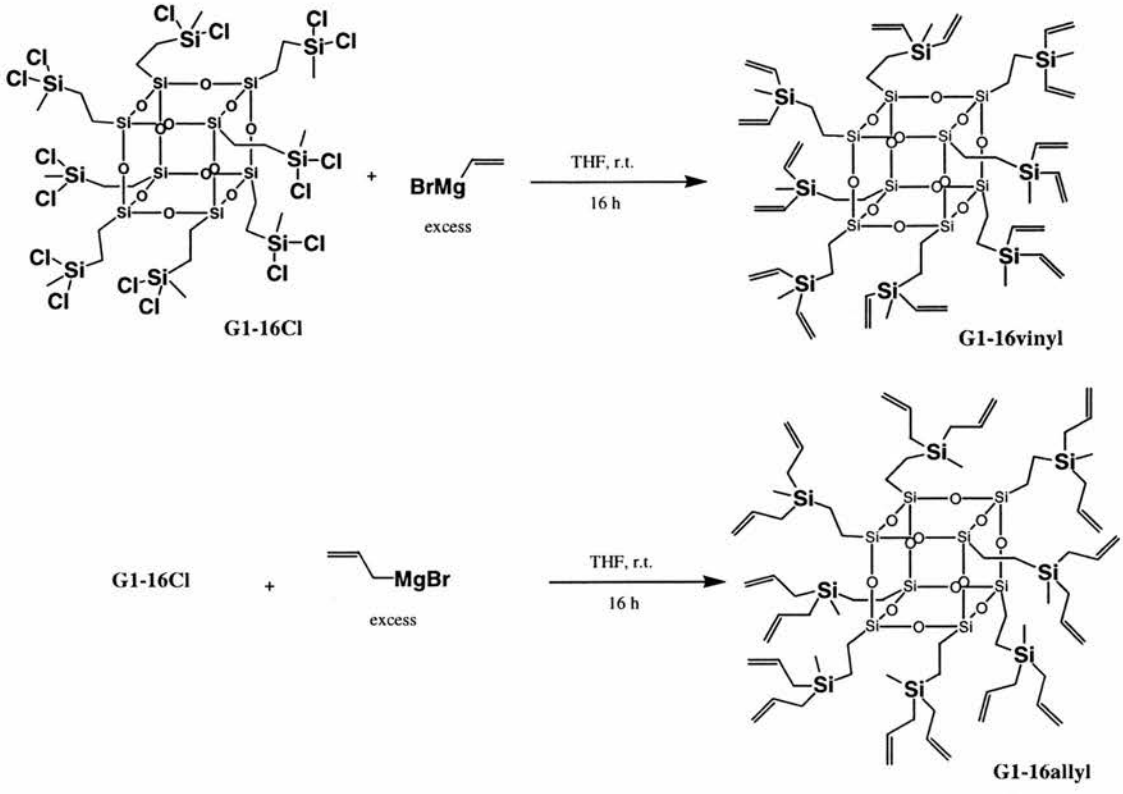

Figure 3.5 Synthesis of the 16-vinyl and 16-allylPOSS.

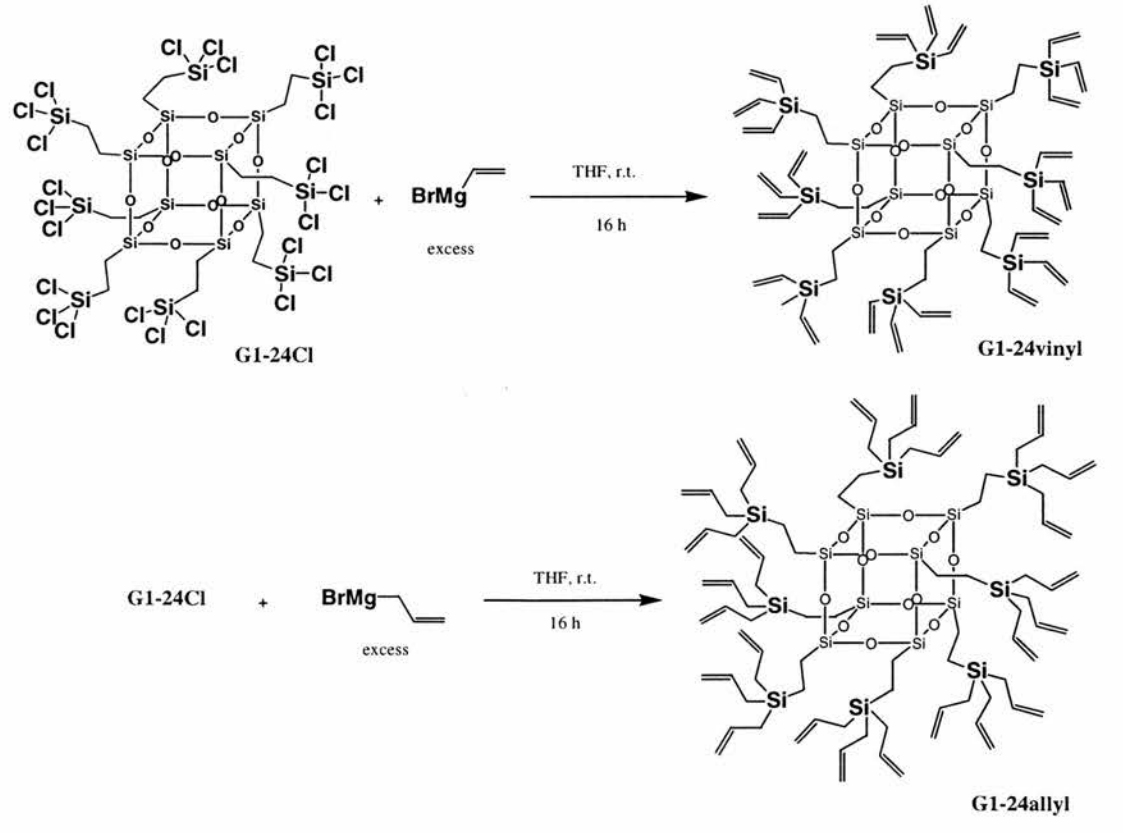

Figure 3.6 Synthesis of the 24-vinyl and 24-allyl POSS.

The 16-vinyl functionalised POSS (G1-16vinyl in Figure 3.5) was partially characterised by single crystal X-ray diffraction (see Appendix I). The silsesquioxane core is in fact more like a sphere than a cube since the oxygen atoms (edge of the cube) actually lies outside the perpendicular joining the silicon atoms. Only partial refinement was obtained due to the extensive disorder of the carbon atoms of the vinyl and methyl groups at the periphery of the dendrimer. Crystals were obtained by recrystallisation in cold petroleum ether (40-60). In a previous work Morris and co-workers obtained a crystal structure of the 24-vinyl POSS (G1-24vinyl).[1] Only partial refinement for the vinyl groups was also achieved.

It was found, in contrast to previous studies,[1] that neutralisation (aqueous solution of ammonium chloride) of the excess Grignard reagents led to possible polymerisation. A careful addition of the reaction mixture to the cold acidified water phase was chosen to limit the formation of base leading to the destruction of the framework. The vinyl POSS compounds were particularly sensitive. Moreover they were relatively sensitive to air and light possibly because the proximity of the numerous reactive vinylsilane groups could lead to oligomerisation reaction. During the synthesis, it became apparent that the vinyl magnesium bromide used in the functionalisation to vinyl POSS had to be extremely pure to avoid partial or total polymerisation of the vinyl groups. Unfortunately the partial polymerisation was often difficult to trace and led to many problems (low reactivity, low solubility, etc.) Preparation of our own batch of vinyl magnesium bromide and conservation in a cold and dark place under inert atmosphere allowed the use of the reactants for months whilst Aldrich products were most of the time defective. Crystalline 16-vinyl POSS was indeed obtained with a batch of our own vinyl magnesium bromide.

3.3.2 Second generation dendrimer.

Second generation vinyl POSS (48 and 72 groups) were obtained from the reaction of G1-24vinyl or G1-24allyl with $HSiMeCl_2$ and $HSiCl_3$ and subsequent addition of the vinyl magnesium bromide in excess. When starting from G1-24vinyl, reaction with $HSiCl_3$ (Et_2O, reflux 27 h, yield 90 %) and CH_2=CHMgBr (THF, room temperature, 24 h) as described by Morris and co-workers[1] gave the compound G2-ethyl-72vinyl (Figure 3.2, R = vinyl) as a white solid in 45 % yield, a value which is higher than the one previously reported (21 %).[1] It is believed that this improved

yield was due to the higher quality of vinyl magnesium bromide leading to less side reactions such as polymerisation or oligomerization. The intermediate 72-chloro compound was isolated as a white solid. However since both successive reactions gave only partial conversion the characterization of the final vinyl product (^{1}H NMR) was extremely difficult.

From the G1-24allyl POSS, different reaction conditions were used as the solubility and reactivity of the starting materials and product differed. Indeed, toluene was used as solvent in the hydrosilylation reaction ($HSiMeCl_2$ and $HSiCl_3$) since the use of diethyl ether led to fast precipitation of partially functionalised product. The use of THF as solvent led to an intractable mixture. This mixture was found to react with the Grignard species to give quantitative yield of the corresponding G2-propyl-48vinyl POSS (Figure 3.7). However since the characterization of the mixture was extremely difficult (large amount of solvent present), the use of THF was abandoned.

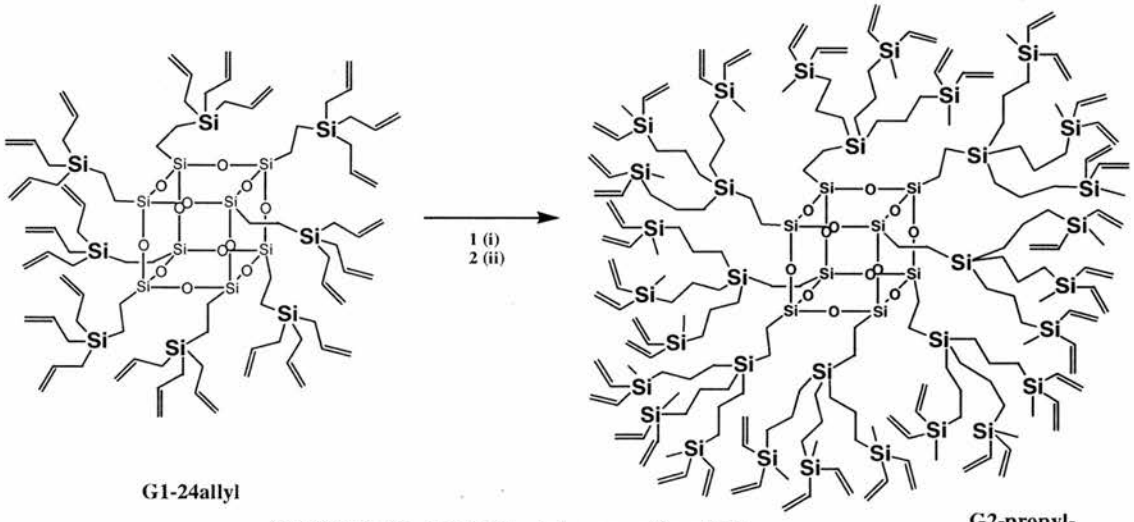

Figure 3.7 Synthesis of a 48-vinyl functionalised POSS from the 24-allyl compound.

Longer reaction times (up to 96 h) were needed as the allyl groups were found to be less reactive toward hydrosilylation than their vinyl counterparts. However these 48- and 72-chloro compounds were isolated as white solids in quantitative yield (>95 % and >92 % respectively).

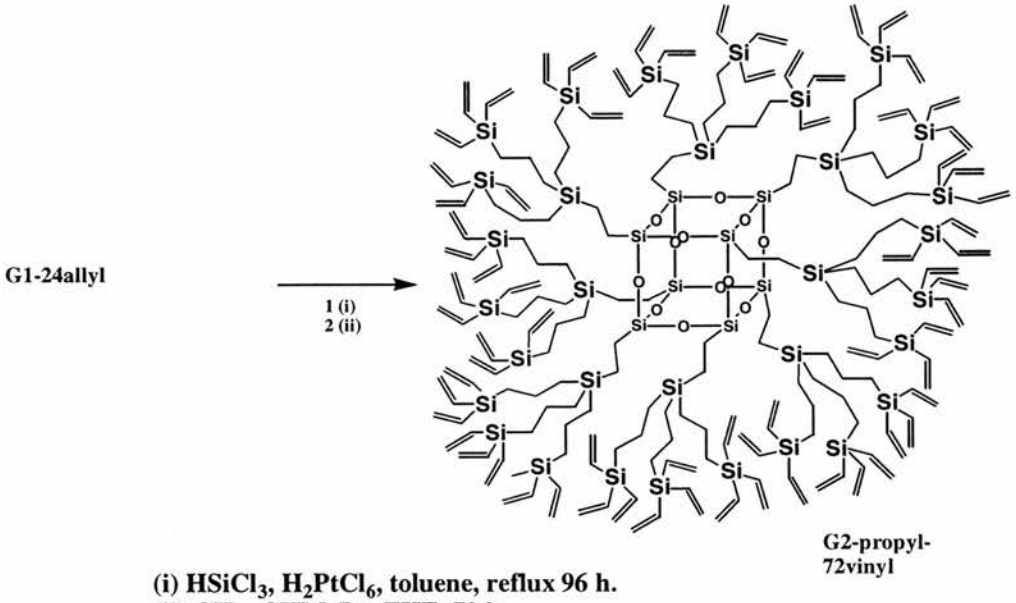

(i) $HSiCl_3$, H_2PtCl_6, toluene, reflux 96 h.
(ii) CH_2=CHMrBr, THF, 72 h.

Figure 3.8 Synthesis of a 72-vinyl functionalised POSS from the 24-allyl POSS.

At this stage, although the ^{1}H NMR showed traces of β-substitution (^{1}H NMR $MeCl_2SiC\mathbf{H}(CH_3)$- or $MeCl_2SiC\mathbf{H}_2CH_2$-) it was difficult to determine the relative amount of α- or β-substitution of the chlorosilane. Treatment with vinyl magnesium bromide gave the corresponding G2-propyl-48vinyl and G2-propyl-72vinyl (Figure 3.7 and Figure 3.8) as heavy oily products in respectively 70 % and 58 % yields. NMR and microanalysis showed conversions respectively of >95 % and 70 % (considering 100 % as fully functionalised 48- or 72-chloro arms). Numerous defects were clearly present in the 72-branched molecules. This 72-vinyl compound was particularly unstable, since it formed an insoluble tar with time.

3.4 Introduction of phosphorus atoms on the periphery.

3.4.1 Alkyl- or arylphosphine POSS.

Two routes, a radical addition on the alkenyl groups and a nucleophilic substitution of the chlorine atoms of the chlorosilanes, have been considered to introduce phosphine into the framework of the dendrimers. Using these two methods, we have synthesized a series of phosphine-based dendrimers with terminal PR_2 groups (R= Me, Et, hexyl, Cy, Ph, $C_6H_3(CF_3)_2$). The phosphorus atoms were separated by a spacer of three, five or seven atoms, the central one of which was a silicon atom. The compounds were characterized by MALDI-TOF (Matrix Assisted Laser Desorption Ionization- Time Of Flight) mass spectrometry. The air sensitivity

of the phosphine compounds led sometimes to low resolution or oxidative increments. However, this technique was used as a valuable and successful tool to determine the conversion of the reactions.

3.4.1.1 Radical addition onto the alkenyl groups.

The first synthesis used was the radical reaction of dialkyl- or diaryl-phosphines onto the double bonds of the vinyl-functionalised dendrimers. A radical reaction was performed to affect an anti-Markownikoff type addition of the phosphine to the alkenes so that it would promote the desired terminal phosphine groups. Similar work had been previously carried out with the octavinyl octasilsesquioxane and diethylphosphine[8] and dimethylphosphine[9] leading to POSS compounds with eight phosphine moieties (Figure 3.9).

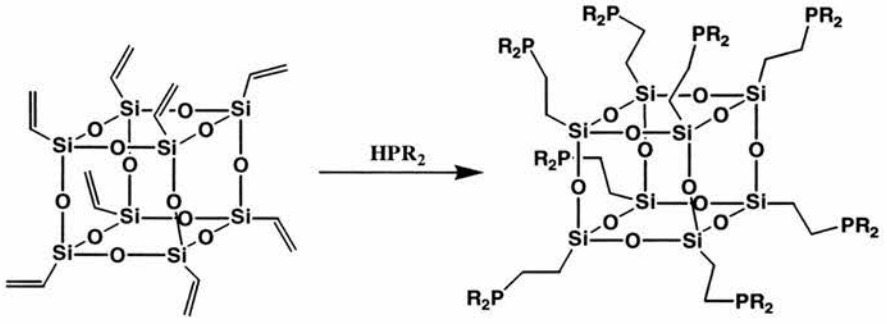

Figure 3.9 Radical addition of HPR_2 (R = Me,[10] Et[8]) onto the octavinyl octasilsesquioxane.

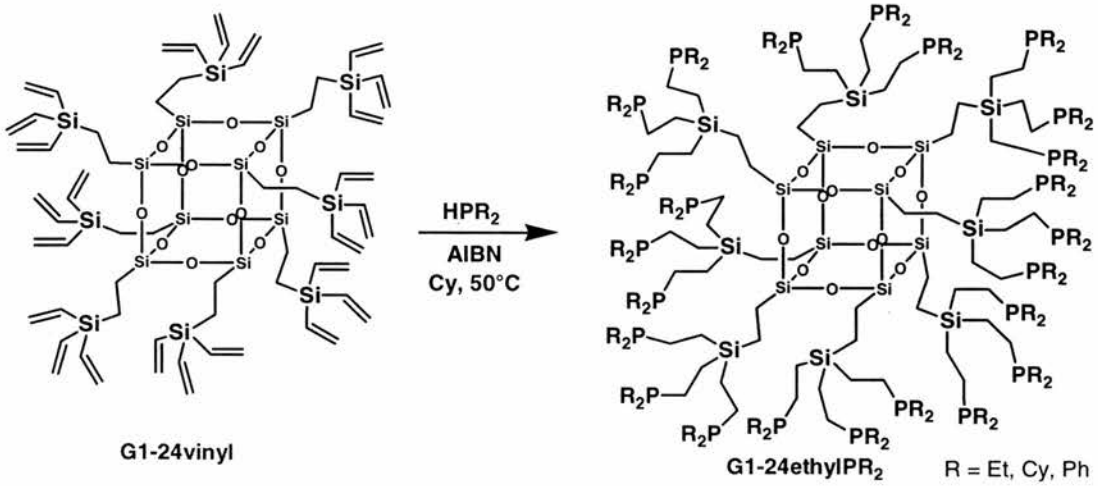

Figure 3.10 Radical addition of HPR_2 (R = Et, Cy, Ph) onto the 24-vinyl POSS.

The 24-vinyl POSS molecules were reacted in this way with $HPEt_2$, $HPPh_2$, $HPCy_2$ in cyclohexane (Figure 3.10). The reaction was initiated by AIBN (azoisobutylnitrile). The addition of $HPEt_2$ was incomplete after 5 days at 50°C

despite 20 mole percent excess of diphosphine. 25 % and 35 % of the vinyl groups of G1-24vinyl and G2-ethyl-72vinyl (Figure 3.2, R = vinyl) respectively remained unreacted as indicated by a multiplet centred at δ 6 ppm in the ^{1}H NMR spectrum to the protons of the vinyl groups. The new products were white powders that were very thermally stable but that decomposed rapidly in air or non-degassed solvent. The ^{31}P NMR spectra clearly showed if any oxidation had taken place (signal at δ 40.3 ppm after exposure to the air). A single signal was found at δ –15.6 ppm attributed to the bound CH_2-diethylphosphine. It is significant that the peak due to triethylphosphine would be found around δ –20 ppm and that of the starting phosphine ($HPEt_2$) at δ –54.5 ppm. The addition of larger quantities of phosphine (3 fold excess) and longer time of reaction (8 days) increased the conversion to 96 % for the 24-branched compound. The solvent and the excess of phosphine were removed under vacuum to give an oily colourless product. The product was characterised by NMR (^{31}P δ –15.6 ppm) and MALDI-TOF techniques. Although no vinylic protons were detected by ^{1}H NMR, the mass spectrum showed that a majority of 23 to 24 arms were converted to diphosphine groups. As shown in Figure 3.13 (right) two main broad signals were found at m/z 3582 {M-(PEt_2)} and 3676 (m/z expected 3677). In a first spectrum with the same batch of product but with different conditions of analysis (no sodium salt was added), it was found that the matrix interfered with the product giving higher m/z values (Figure 3.13, left). One can suggest two explanations for these contradictory results. Firstly it is possible that some of the vinyl groups oligomerized (intramolecular) during the reaction or during the preparation of the vinyl compound since that reaction occurred when using poor quality Grignard reagent. Two possible mechanisms for the oligomerisation reaction are shown in Figure 3.11 and Figure 3.12. These reactions could also explain the different ^{31}P resonances found for a same dendrimer. The first oligomerisation reaction could be the addition of the radical phosphine species on α of the silicon leading to the formation of a 5-member ring (Figure 3.11). However this reaction is unlikely to happen since the synthesis of smaller analogues of the dendrimer did not lead to such oligomerisation (see Section 3.5).

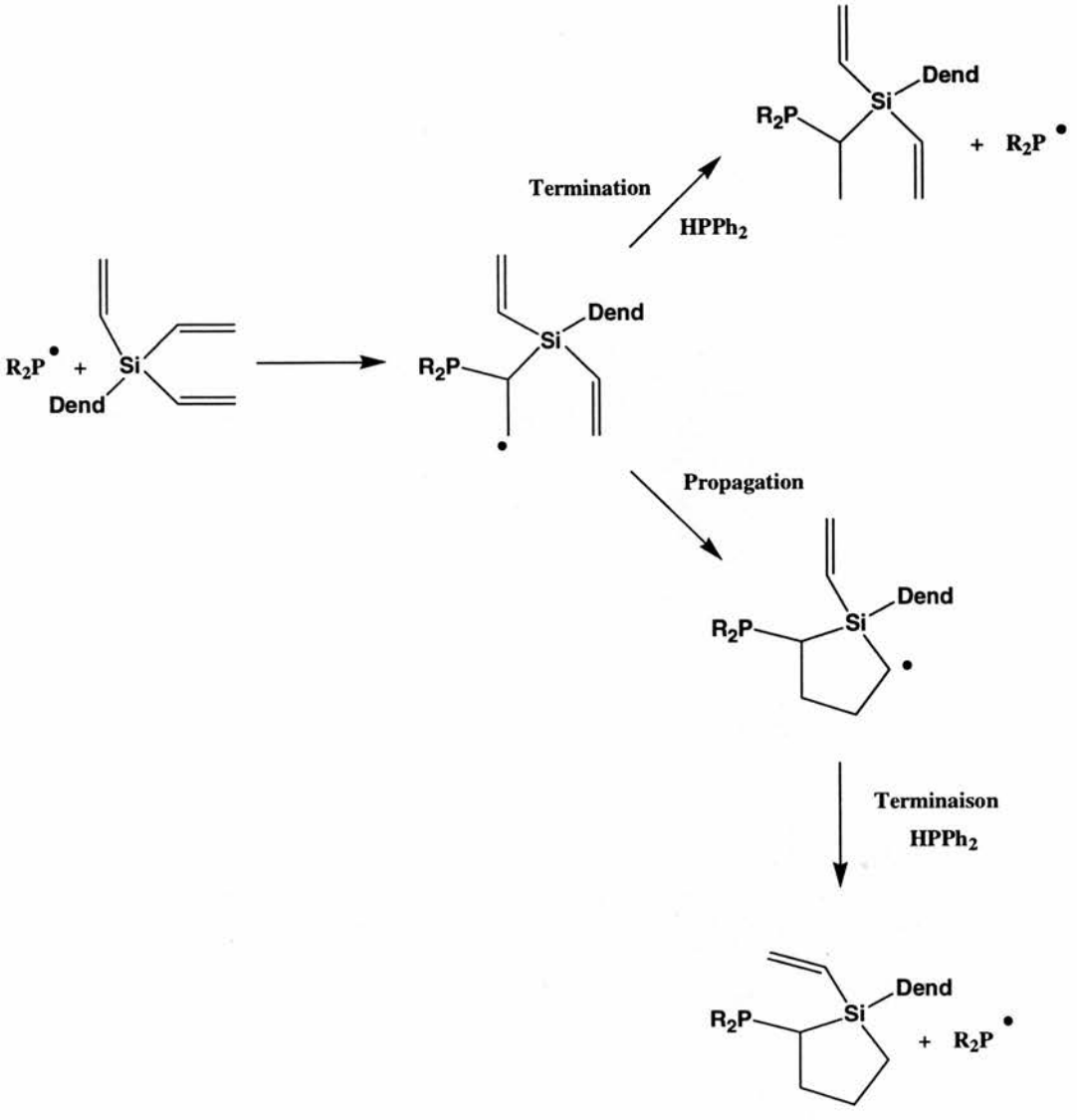

Figure 3.11 Possible oligomerisation of the vinyl groups on a same arm during the radical addition of HPR_2.

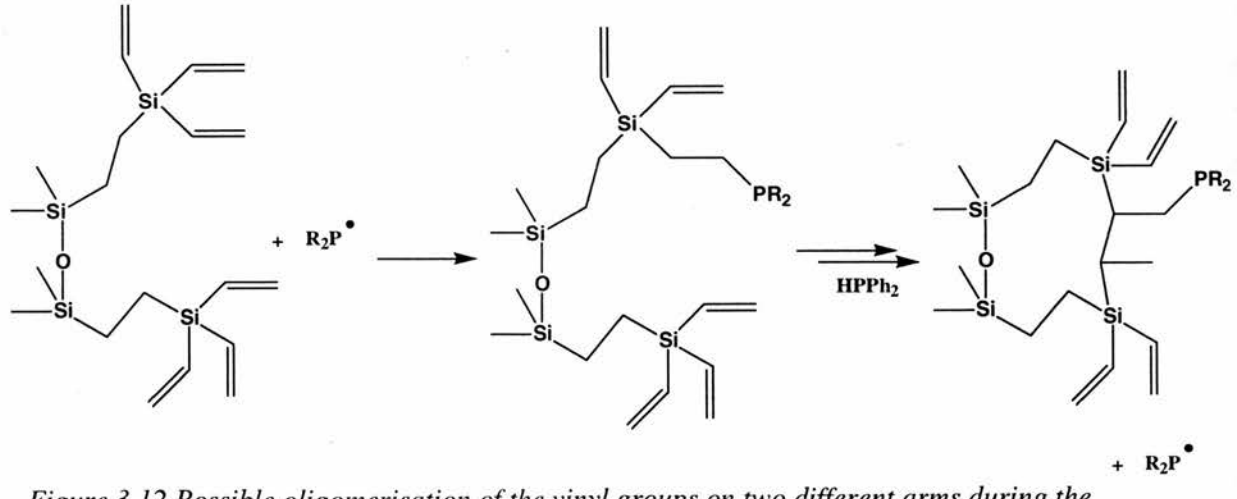

Figure 3.12 Possible oligomerisation of the vinyl groups on two different arms during the radical addition of HPR_2.

The second oligomerisation reaction considered is the propagation of the reaction to another arm of the cube as shown in Figure 3.12. This reaction would lead to the formation of a 11-membered ring (shown on the Figure 3.12) or a 12-membered ring.

On the other hand, to explain these contradictory characterisations of the dendrimer, one can suggest that fragmentation occurred during the MALDI-TOF analysis. Indeed as shown in other synthesis/ analysis (see below) and in the MALDI-TOF spectra shown in Figure 3.13, fragmentation probably occurred during the MALDI-TOF analysis. The comparison of the two spectra in Figure 3.13 clearly indicates that fragmentation occurred since, using the same batch of product, the spectrum on the left shows only two major peaks, while the spectrum on the right (different analytic conditions) shows different peaks corresponding to different loading of phosphine species on the dendrimer.

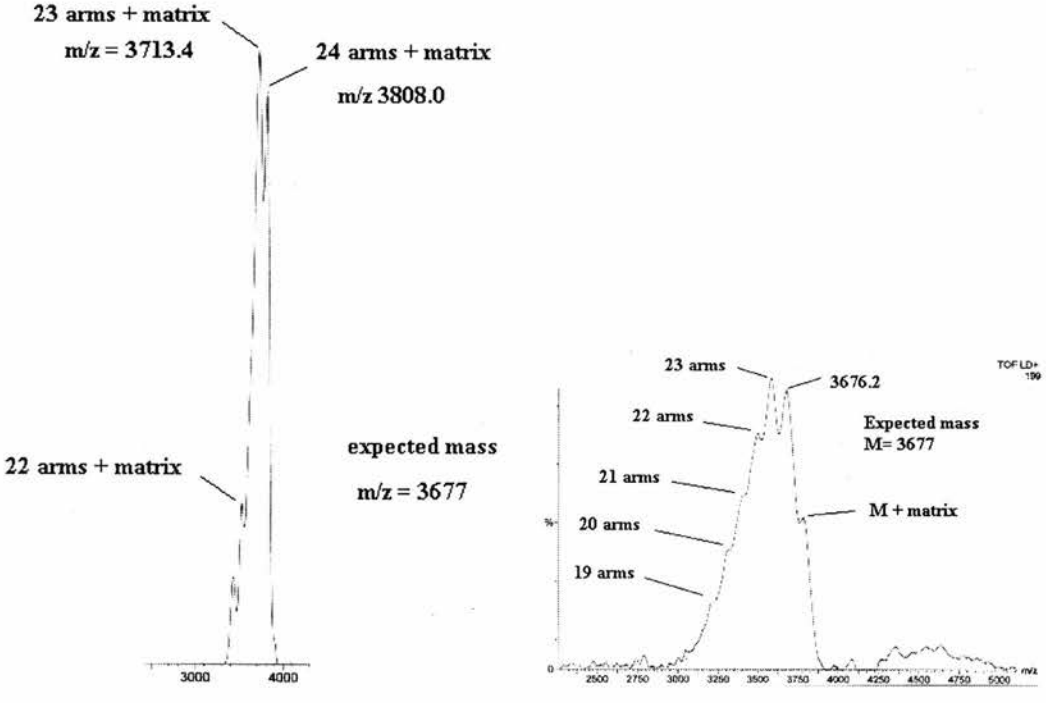

Figure 3.13 MALDI-TOF spectra of G1-24ethylPEt$_2$ compound.

Attempts to synthesise the G2-ethyl-72ethylPEt$_2$ (Figure 3.2, R = $(CH_2)_2PEt_2$) did not give complete functionalisation. A maximum conversion of 84 % was obtained after 3 weeks (determined by ^{1}H NMR) (^{31}P δ –16.4ppm). As the product (yield 56 %) was accompanied by precipitation of uncharacterised products, no attempt was made to synthesise it again.

The radical addition was extended to the G1-24allyl POSS. The product obtained (Figure3.14) was a colourless oil in 98 % yield with a conversion reaching 87 % after 15 days. The conversion was calculated from the MALDI-TOF, which showed a broad signal centered at m/z = 3730 corresponding to 21 arms functionalised (m/ z expected = 4014). However this conversion differs with that suggested by the ^{1}H NMR since no alkenyl protons were detected. It is therefore, as discussed above, difficult to determine the exact conversion. Interestingly various ^{31}P chemical shifts were found at δ -22.1, -23.3 (low intensity for both), -23.5, -23.7 (average intensity), -24.2 (high intensity) and two others at δ –28.2 and –29.3 ppm (low intensity), suggesting that the phosphine groups are in different environments in the POSS molecule.

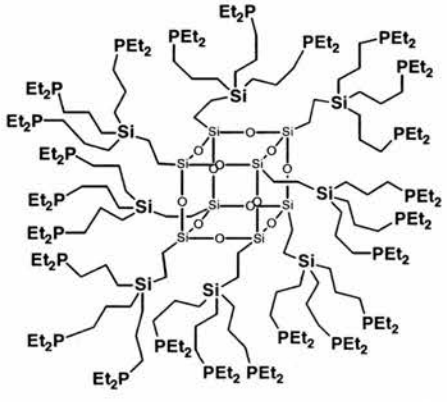

Figure 3.14 A 24-diethylphosphine functionalised dendrimer built upon the 24-allylPOSS.

The synthesis of G1-16ethylPEt$_2$ and G2-propyl-48ethylPEt$_2$ was also carried out (shown in respectively in Figure 3.15 and Figure 3.16). G1-16ethylPEt$_2$ and the 2nd generation dendrimer, G2-propyl-48 ethylPEt$_2$, were respectively built upon G1-16vinyl and G2-propyl-48vinyl by addition of diethylphosphine moieties. The G1 and G2 dendrimers containing diethylphosphine moieties were isolated as oily products (the G2 dendrimer was less liquid like) in quantitative yields and with conversions of respectively >99 % (6 days, ^{1}H NMR, MALDI-TOF) and >96 % (12 days, ^{1}H NMR). The MALDI-TOF spectrum of G1-16ethylPEt$_2$ showed a peak at m/z 2922 (m/z expected 2861) possibly corresponding to the oxide {M + 3 × 'O'}. However the 2nd generation product could not be characterised by MALDI-TOF since a broad peak centred at m/z 3693 was found (m/z expected 8502). A single ^{31}P chemical shifts was found at δ –14.9 ppm for the 16-branched product, while for the 48 arm molecule two broad signals were detected at δ –15.8 and –16.1 ppm indicating different environments for the G2 phosphine-containing dendrimer.

The diethyl dendrimers were sensitive to air and extremely soluble in most organic solvents except in polar ones like ethanol.

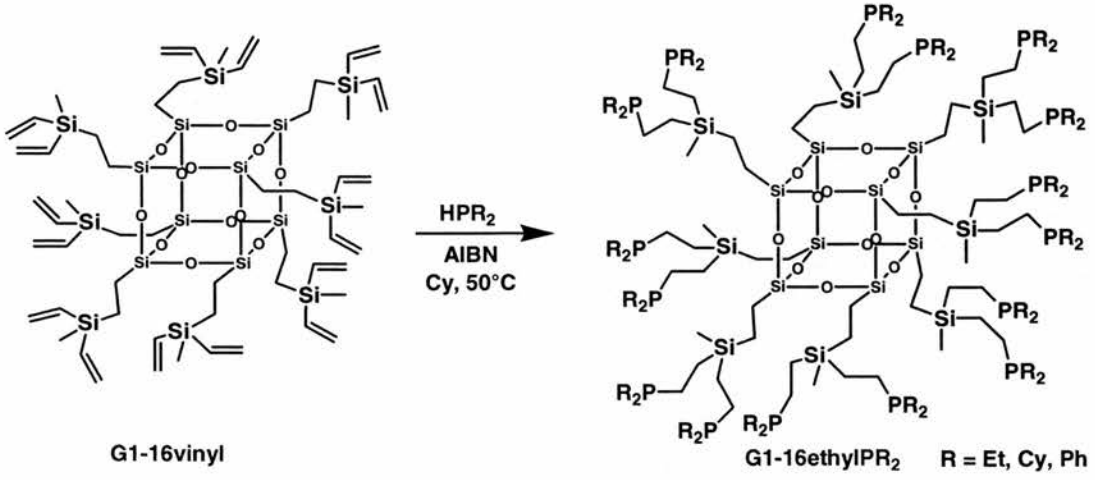

Figure 3.15 Synthesis of 16-functionalised diphosphine POSS.

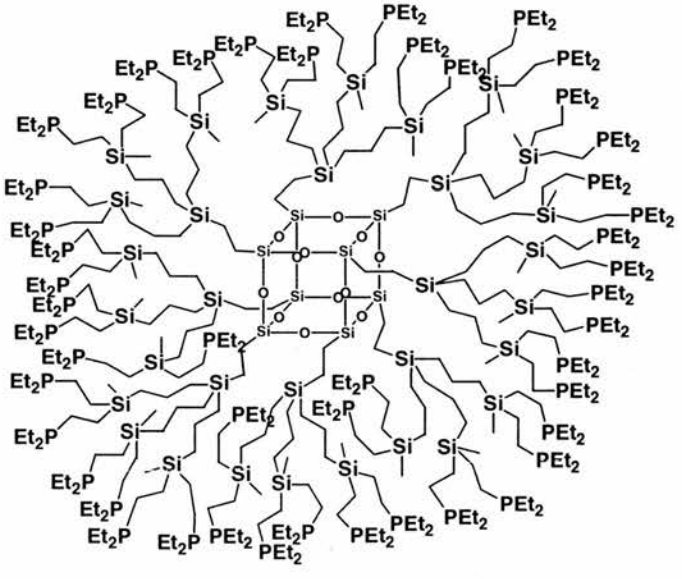

Figure 3.16 A 48-diethylphosphine-containing dendrimer built on G2-propyl-48vinyl POSS.

Dicyclohexyl phosphine was as well reacted with G1-16vinyl and G1-24vinyl. As the substitution of the 24 vinyl compound failed (conversion of 55 % determined by ^{1}H NMR and MALDI-TOF techniques), the synthesis of the smaller 16-branched compound was carried out. After 10 days at 50°C with an excess of diphosphine (3-4 fold) and AIBN as radical initiator, and after removal at 110°C under vacuum (0.1 mm Hg) of the excess of phosphine, an air sensitive product was

obtained. The compound, G1-16ethylPCy$_2$ (Figure 3.15), was a colourless low melting point solid. A single ^{31}P chemical shift was detected at δ 4.1 ppm corresponding to the expected $CH_2P(Cy)_2$ bond ($HPCy_2$ resonates at δ -27.5 ppm). Although the ^{1}H NMR spectrum did not show unreacted double bonds (<1 %), characterization of the compound by MALDI-TOF showed that approximately 12 arms were functionalised. This quite low conversion (75 %) was partially explained by the mediocre quality of the vinyl POSS used as similar results were found for diphenylphosphine compounds using the same batch (see below). It is believed that the vinyl POSS contained some intramolecular oligomerised double bonds. However it was not attempted to improve the conversion using a better starting material.

A randomly dispersed diethyl- and dicyclohexyl-phosphine functionalised POSS was synthesized by addition to the crystalline G1-16vinyl POSS of $HPCy_2$ (phosphine/ vinyl ratio of 1.5:1) followed by $HPEt_2$ (1 equivalent to the vinyl groups) 3 days later. Excess of phosphines were removed under vacuum with heating to give a quantitative yield of the derivatised dendrimer as a colourless oil. The product contained 68 % of dicyclohexylphosphine groups and 32 % of diethylphosphine substituents (determined by ^{1}H and ^{31}P NMR). No vinyl groups were detected in ^{1}H NMR. Attempt to prepare a 50/50 mixture failed, as the only phosphine groups incorporated were diethyl groups (better reactivity and less steric hindrance). In this both phosphines were introduced at the same time in the reaction mixture.

Following the same experimental method, the reaction with diphenylphosphine was carried out (10 days, 50°C) to give the corresponding diphosphine-functionalised POSS. Quantitative yield (over 97 %) and excellent to good conversions for respectively G-16ethylPPh_2 (Figure 3.15) (complete conversion determined by ^{1}H NMR and microanalysis) and G2-propyl-48ethylPPh_2 (conversion 77 % determined by ^{1}H NMR) (Figure 3.18). However, only 60 % conversion (^{1}H NMR and MALDI-TOF) was reached for the 24 arms counterpart, G1-24ethylPPh_2, probably due to steric crowding. The ^{31}P NMR spectra showed that the phosphine groups in the same dendrimer for the three compounds were not equivalent. Indeed two major and a minor peaks for the 16-branched dendrimer were found at δ -9.6, -9.7 ppm (major) and δ -14.4 ppm. A broad signal centred at δ –9.8 ppm for G2-propyl-48ethylPPh_2 and at –9.0 ppm for G1-24ethylPPh_2 were detected ($HPPh_2$ δ –

39.7 ppm). The excess of phosphine was removed at 120°C under vacuum or by silica gel column chromatography (eluent gradient of petroleum ether/ diethyl ether). Although lower yields were obtained using chromatography (86 %), no change in the conversion of the product was found. These compounds were low melting point solids, sensitive to air and extremely soluble in most organic solvents except in polar ones like ethanol. Although the ^{1}H NMR spectra and the microanalysis did not show the presence of unreacted vinyl groups in the 16-arm compounds, G1-16ethylPPh$_2$, further characterisation by MALDI-TOF techniques showed the loading of mainly 14, 15 or 16 phosphine groups (Figure 3.17). It is thus believed the fragmentation occurred during the analysis. The compound was found partially oxidised (occurred during the analysis process) since mass increments of 16 due to the oxygen atoms were shown in the spectrum giving the distribution of mass shown in Figure 3.17. The multiplet at the right inside of the spectrum corresponds to the fully functionalised dendrimer (16 arms) with a central peak showing oxidation of 8 of the 16 phosphine species.

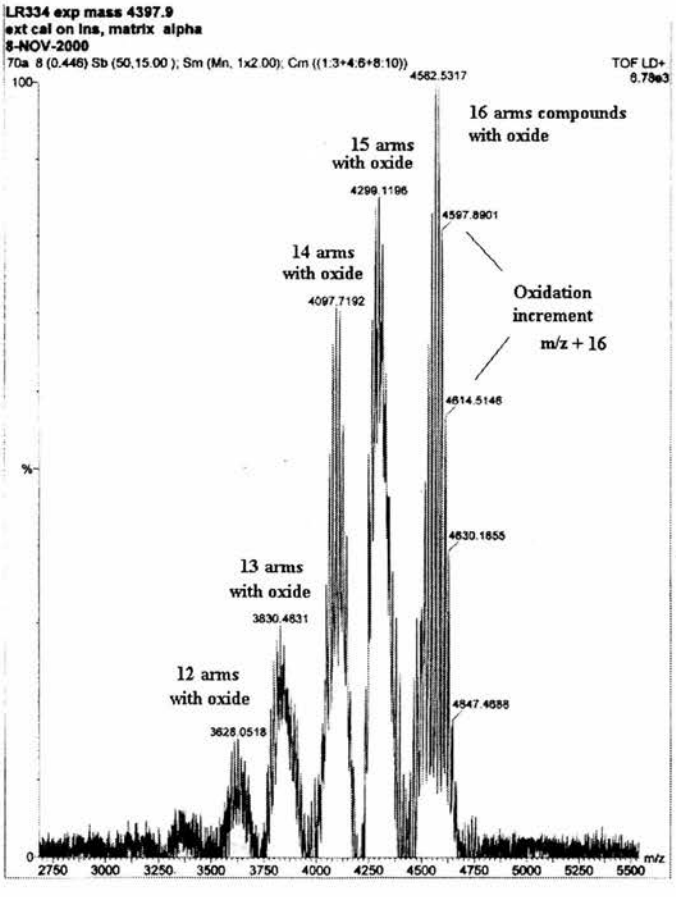

Figure 3.17 MALDI-TOF spectrum of the G1-16ethylPPh$_2$ POSS (Figure3.12, R = Ph).

A partially functionalised G1-16ethylPPh$_2$ POSS was synthesised from G1-16vinyl POSS of mediocre quality. Although no double bonds were observed in the ^{1}H NMR spectra, the integration of the protons showed partial loading (>90 %). Functionalisation of 12 arms only of the compound was determined by MALDI-TOF. The partial conversion is believed to arise from partial condensation of the vinyl groups occurred during the radical addition of the phosphine compound (see discussion above) or more likely during the synthesis of the vinyl-functionalised POSS. However, as discussed above, partial fragmentation during the mass spectroscopy analysis is likely to occur since the conversion determined by ^{1}H NMR differed from the results obtained in the MALDI-TOF analysis.

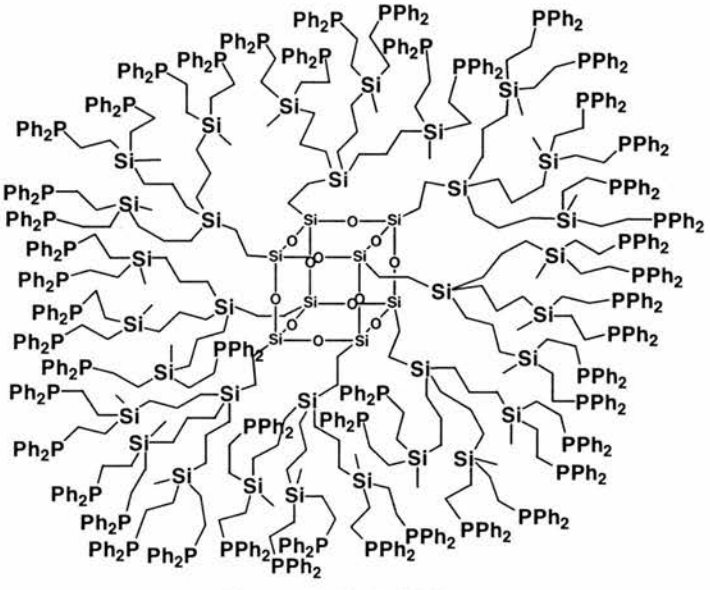

Figure 3.18 A G2 48-diphenylphosphine dendrimer built from the G2- propyl-48vinyl POSS.

Whist radical addition of diethylphosphine to the allyl POSS was successfully achieved albeit with lower reactivity, addition of HPPh$_2$ failed even after 2 weeks under heating and several additions of radical initiator (conversion 56 % determined by ^{1}H NMR) (^{31}P NMR δ -17.3 ppm). It is believed that this poor conversion is probably due to the lesser reactivity of the allyl silane.

Attempt to introduce arylphosphines with electron withdrawing groups into the periphery of the dendrimer was also carried out. The bis [3,5 (trifluoromethyl)phenyl]phosphine **3** (Figure 3.19) (^{31}P NMR δ -39.3 ppm) was

synthesised by addition of two equivalents of the prepared Grignard compound **1** to $(Et_2N)PCl_2$ and subsequent chlorination (HCl) and reduction by $LiAlH_4$.[11]

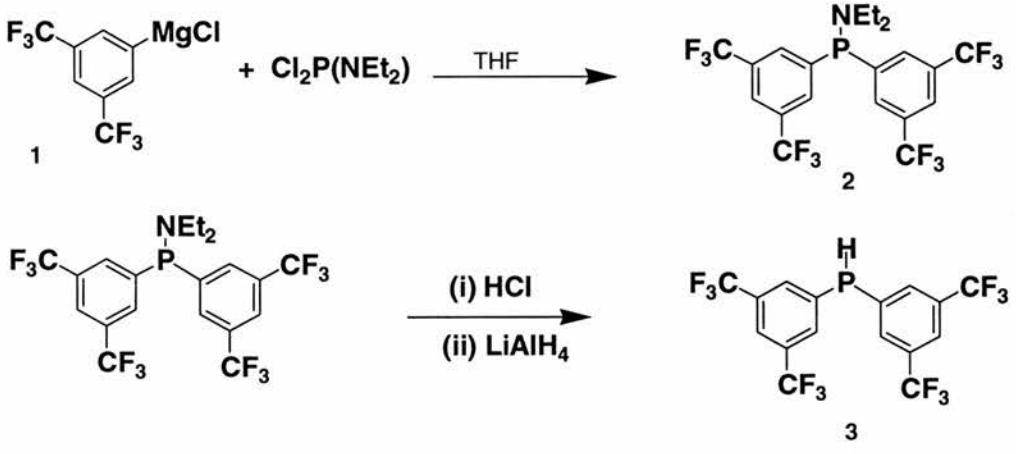

Figure 3.19 Synthesis of bis [3,5 (trifluoromethyl)phenyl]phosphine.

Such compounds are indeed very interesting as ligands since the electron withdrawing groups improve the selectivity of the hydroformylation reaction (see Chapter 2). In addition, Casey and co-workers showed that this effect depends on the relative binding sites of the two P atoms, equatorial-equatorial or equatorial-axial, in the 5 coordinate rhodium intermediates.[11] The characterisation of the active rhodium complex in the dendrimer (ee or ea configuration) could then be facilitated by the use of such a ligand. The complete radical addition of the fluorinated arylphosphine on the G1-16vinyl compound however failed since 25% of unreacted vinyl groups were still present after 1 month and numerous consecutive additions of AIBN. The substituted POSS compound (G1-16ethylPAr$_2$, Ar = 3,5-$C_6H_3(CF_3)_2$) showed four ^{31}P chemical shifts at δ -6.6, -6.9, -7.0 and -12.9, indicating the complexity of the phosphorus environment of such compound. As expected these ^{31}P NMR resonances are shifted to higher frequency by an average of 2-3 ppm compared with the diphenylphosphine analogue POSS. The low conversion may possibly be explained by the steric bulk of such compound although the substituents are in the meta-position. A modification of the electronic properties of the P-H bond may also be considered, as trifluoromethyl are electron-withdrawing groups.

The analysis of the various dendrimers derived from radical addition of several phosphines to various unsaturated dendritic molecules are summarised in Table 3.1.

Table 3.1 Phosphine functionalised POSS prepared by radical addition of di-alkyl or aryl phosphine.

Dendrimer	*^{31}P NMR* δ *(ppm)*	*conversion* %	*yield* %
G1-16ethylPEt$_2$	-15.2 (br)	>99 [a, b]	99
G1-24ethylPEt$_2$	-15.9. -16	>96 [a, b]	97
G2-propyl-48ethylPEt$_2$	-15.8, -16.1[c]	>90 [a, b]	96
G2-ethyl-72ethylPEt$_2$	-15.6 (br)	65 [a, b]	85
G1-24propylPEt$_2$	-23.6, -23.9, -24.3 [c]	>87 [a, b]	98
G1-16ethylPCy$_2$	4.1 (br)	75 [a]	98
G1-24ethylPCy$_2$	4.1 (br)	55 [a]	95
G1-16ethylPCyEt	-14.9, 4.8	98 [a]	95
G1-16ethylPPh$_2$	-9.4, -9.5	>99 [a, b]	95
G1-24ethylPPh$_2$	-9.5 (br)	60 [a, b]	95
G1-propyl-48ethylPPh$_2$	-9.9 (br)	84 [a]	75
G1-16propylPPh$_2$	-17.3	56 [a]	96
G1-16ethylPAr$_2$ Ar = 3,5-C$_6$H$_3$(CF$_3$)$_2$	-6.6, -6.9, -7.0, -12.9	75 [a]	92

[a] :^{1}H NMR, [b] : MALDI TOF, [c] : major peaks

3.4.1.2 Nucleophilic substitution on the chlorosilane dendrimers.

The second reaction considered was a nucleophilic substitution of the chlorine atoms of the Cl-functionalised dendrimers. Deprotonation of three different methyl phosphine compounds to form nucleophilic lithium dialkyl- or diarylphosphino methyl salt or addition of phosphine alcohols were carried out.

The first reaction tested used LiCH$_2$P(CH$_3$)$_2$ as the nucleophile. This reagent was prepared by reaction of P(CH$_3$)$_3$ with Bu^{t}Li.[12-14] Stoichiometric additions of this compound to G1-24Cl (Figure 3.20) and G2-ethyl-72Cl (Figure 3.2) were carried out. First attempts used the G1-24Cl as substrate. Because of difficulties in

determining the conversion of the substrate (^{1}H NMR) due to the overlapping of the proton resonances and the poor resolution (broad signal), we used a subsequent reaction to characterise the product. It was decided to add methyllithium at the end of the reaction since this compound combined a high reactivity and small size. After 24 hours, it was found that at least 22 % of the chlorosilane were unreacted as the ^{1}H NMR showed clearly the formation of methylsilane groups at 0.1 ppm. The result suggested that the steric bulk of the dendrimer (steric hindrance, back-folded arms) hamper the reaction since both chlorosilane and the phosphorus compound are highly reactive species. Higher conversion was obtained after 36 hours (> 90 %). The elimination of the LiCl salts was obtained by precipitation in dichloromethane. Addition of 5 to 10 % excess of $LiCH_2P(CH_3)_2$ led to numerous problems. The purification of the products was difficult and, as will be described in Chapter 4, its use as ligands for hydroformylation led to poor results. In an attempt of purification, the addition of ethanol at the end of reaction led to poorly soluble products. It is thought that the ethoxide formed with the excess of reagent may have led to polymerisation of the POSS framework.

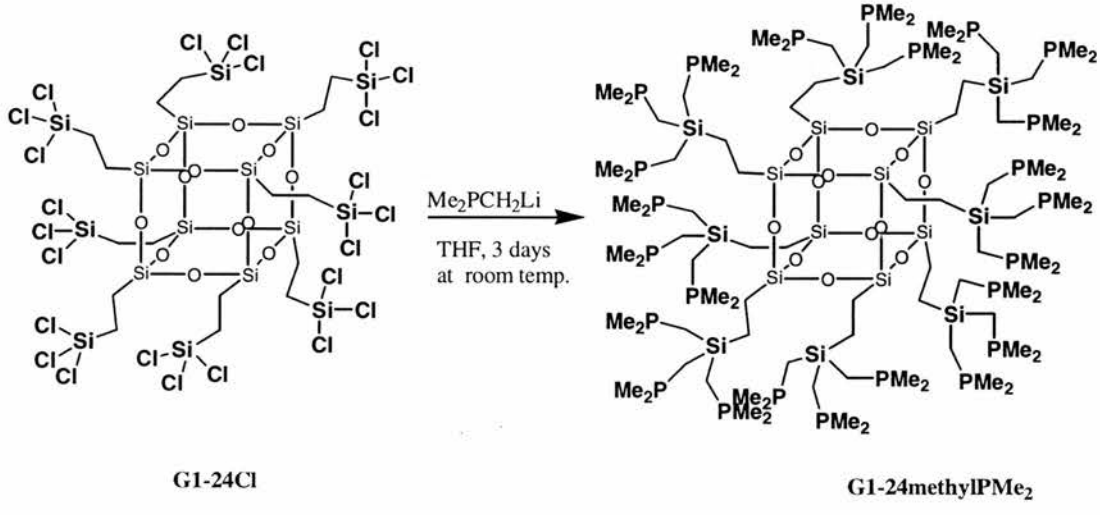

Figure 3.20 Synthesis of a 24-dimethylphosphine POSS.

The ^{31}P NMR spectrum showed a single signal at –54.5 ppm attributed to the bound CH_2-$P(Me)_2$. $P(Me)_3$ (hydrolysis of the lithium salt) and the starting phosphine are expected respectively around –61 ppm and –42 ppm. The white product decomposed rapidly in air or non-degassed solvent to form the oxide. The MALDI-TOF spectrum of the compounds showed the high conversion of the product (>95%) (Figure 3.21) (m/z expected 2667). However due to extremely sensitivity to moisture and air, low

resolution was obtained. The product showed lower solubility than the diethylphosphine compounds previously synthesized.

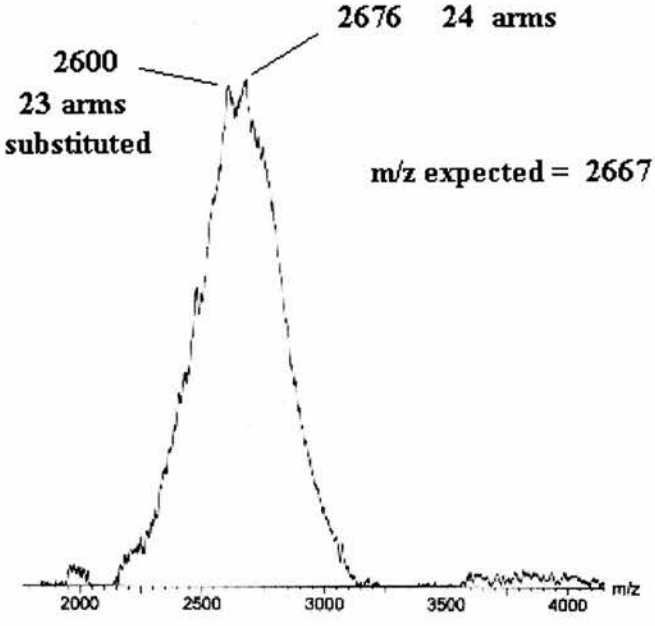

Figure 3.21 MALDI-TOF spectrum of 24-dimethylphosphine POSS.

Addition to the G2-ethyl-72Cl compound led to slow precipitation (over 3 days) of a compound, which could not be characterized due to its poor solubility. ^{31}P NMR of the crude material showed a single signal at δ –54.4 ppm. The precipitate was collected and washed with small amount of the solvent (THF) to give a solid corresponding to a 80 % yield (for a supposed 100 % conversion). It is believed that this compound was difficult to characterize because of the poor quality of the previously used 24-vinyl POSS. However no more attempts were made to synthesize the product.

The substitution by di-n-hexylphosphine groups was also carried out by addition of $LiCH_2P(C_6H_{13})_2$ on the G1-24Cl dendrimer. $LiCH_2P(C_6H_{13})_2$ was prepared by addition of the Grignard $C_6H_{13}MgBr$ to methyldichlorophosphine ($PMeCl_2$) and subsequent lithiation by ^tBuLi.[12-14] However it was found that the latter reaction did not give complete conversion (78 % after 5 days determined by ^{31}P and ^1H NMR). As the elimination of side-products, e.g. $MeP(Hex)_2$, could be not achieved (product with similar solubility to the starting materials), the reagent was then used without further purification. Addition in excess to the G1-24Cl POSS gave after 3 days a colorless low melting point solid (^{31}P NMR δ -36.3 ppm). The conversion reached 90 % to the desired dihexylphosphine POSS (^1H NMR) since the

integration of the ^{1}H NMR spectrum showed an excess of CH_3 groups (δ_H 0.95 ppm) compare to CH_2 (hexyl) groups (δ_H 1.4 and 1.3 ppm). This can be easily explained by the reaction between the 24-Cl functionalised dendrimer and the unreacted Bu^tLi of the reactant. It appears that 10 % of the silicon chloride bonds have been substituted by some Bu^t groups. Once more, the purification of the product was not easy. The long alkyl chains (hexyl groups) improve the solubility of the dendrimer in hexane hence the purification by washing is not so efficient. A 40 % yield of the compound was obtained in this way (after removing of LiCl). Occasionally, a signal at δ -41.4 ppm corresponding to free $PMe(C_6H_{13})_2$ (hydrolysis of the lithium salt) could also be found, $LiCH_2P(C_6H_{13})_2$ being expected at δ –24.6 ppm. No further work was carried out to improve the preparation of this compound hence the synthesis of the product was not successful at all steps (see also Chapter 4). The ^{31}P NMR spectrum of the reaction product showed a signal at δ –36.3 ppm attributed to the bound CH_2-$P(C_6H_{13})_2$.

Using a similar reaction, attempts to functionalize the dendrimer with diphenylphosphine were carried out (Figure 3.22). $LiCH_2P(C_6H_5)_2$- TMEDA was prepared by addition of n-butyllithium and TMEDA to methyldiphenylphosphine.[15] TMEDA was used as a means of improving the difficult deprotonation of CH_3PPh_2 (TMEDA chelates the lithium atom of the Bu^nLi leading to enhance basicity). After 3-5 days of reaction, only partial substitution (70 % determined by ^{1}H NMR, MALDI-TOF) (Figure 3.23) was reached when using G1-24Cl. The reaction required a small excess of the phosphine salt to prevent the formation of side products (TMEDA in some form was present as shown by ^{1}H NMR signals at δ 5.9 and 3.1 ppm). The ^{31}P NMR spectrum showed a singlet signal at δ -23.9 ppm attributed to the bound CH_2-PPh_2. $MePPh_2$ (hydrolysis of the lithium salt) and the starting material $LiCH_2PPh_2$-TMEDA complex were expected respectively at δ –26.7 ppm and δ 1.9 ppm. The product decomposed rapidly in air or non-degassed solvent. However ^{1}H NMR and MALDI-TOF techniques clearly indicated the low loading of diphenylphosphino groups. It is believed that this was caused by the steric hindrance of the introduced diphenyl phosphine groups. In a similar work with a tetravinylsilane core, van Leeuwen and co-workers also could not obtain complete substitution by $LiCH_2P(C_6H_5)_2$/TMEDA of their second generation dendrimer with

36 endgroups on the periphery (see Chapter 1).[16] Washing of the product by petroleum ether gave the compound in 93 % yield.

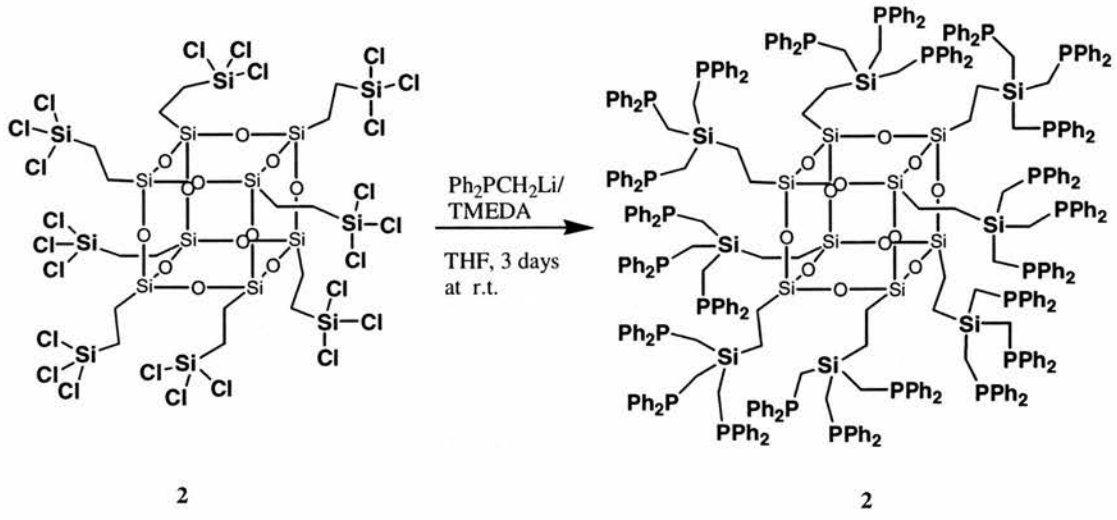

2 2

Figure 3.22 Synthesis of a 24-diphenylphosphine functionalised POSS by nucleophilic addition of TMEDA-LiCH$_2$PPh$_2$.

As the complete substitution of the 24-Cl POSS failed, we prepared the homologue with 16 arms G1-16methylPPh$_2$ (Figure 3.25). Good conversion was obtained (> 95%) as shown by ^{1}H NMR and MALDI-TOF techniques. A major peak was found in the mass spectrum at m/z = 4176 (m/z expected 4173.5). Interestingly, fragmentation clearly occurred since a peak at m/z [M-(PPh$_2$)] is identified in the mass spectrum. Indeed, if partial substitution had happened one would expect m/z values of {M-(CH$_2$PPH$_2$)+Cl} or at least {M-(CH$_2$PPH$_2$)+OH}. Some peaks of the MALDI-TOF spectrum were particularly difficult to assign since m/z values did not match any calculated substitution or fragmentation mass. It is therefore extremely difficult to determine the exact conversion since ^{1}H NMR spectra are often difficult to analyze. Once again an excess of phosphorus-containing reagent allowed a better conversion to the desired phosphine substituents. However the elimination of the excess nucleophile and TMEDA was extremely difficult under these circumstances. Neither vacuum techniques nor washing were found efficient to purify the products (excellent solubility in diethyl ether). The use of silica gel column chromatography (eluent: gradient of petroleum ether/ diethyl ether) improved the purification of the product. Good purity products were obtained in 60-70 % yields. This purification process was not optimized and could be certainly improved by modification of the

size of the column and the gradient of the eluents. The ^{31}P NMR spectrum showed two resonances at δ –22.6 and –22.7 ppm.

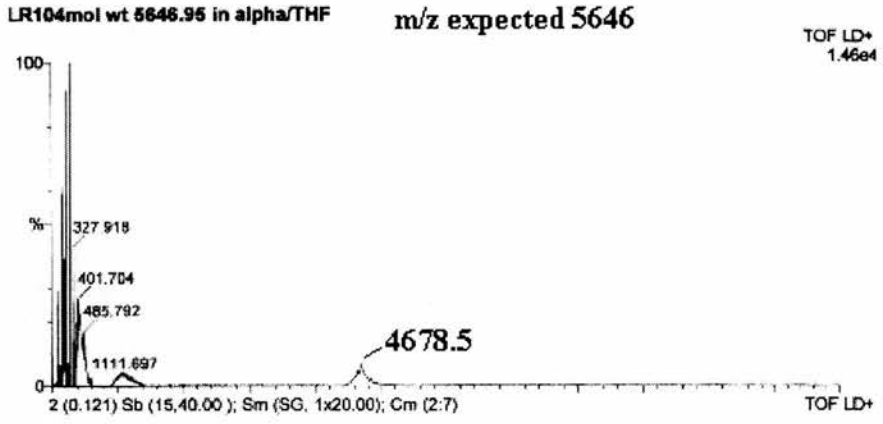

Figure 3.23 G1-24methylPMe$_2$ POSS non fully functionalised.

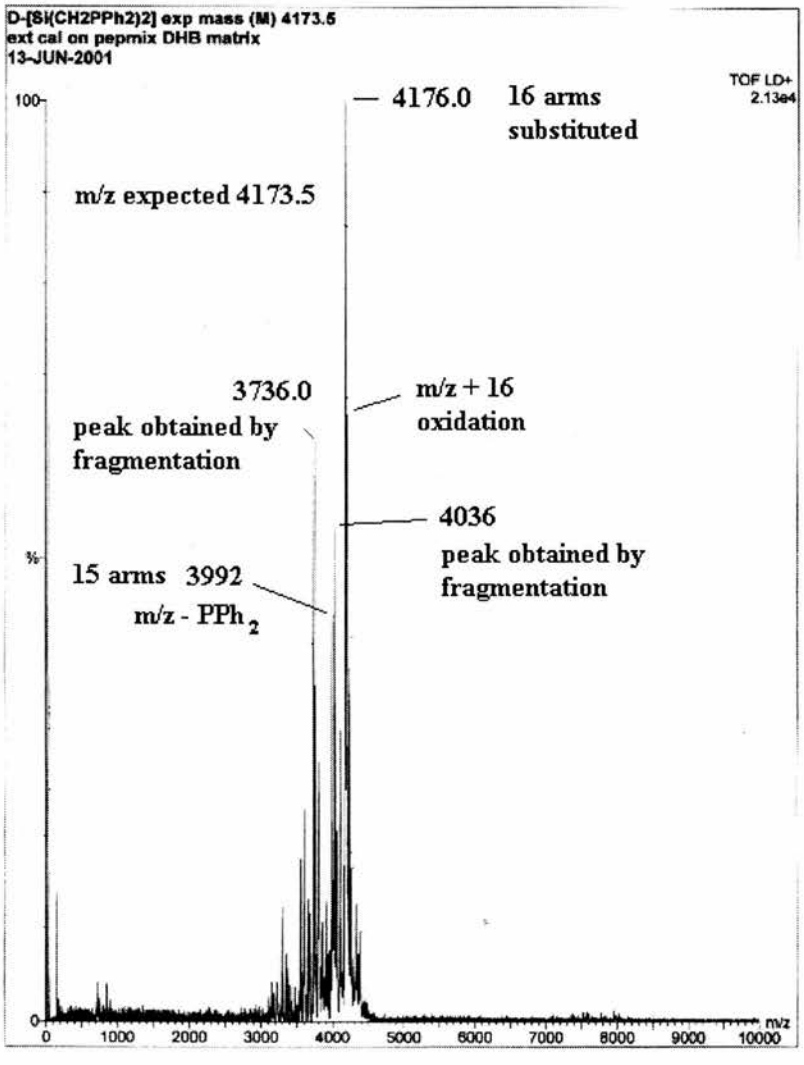

Figure 3.24 MALDI-TOF spectrum of G1-16methylPPh$_2$ POSS (Figure 3.25).

Diphenylphosphino alcohol compounds were also used to introduce phosphine moieties into the dendrimer. Addition of these alcohols to the 16-chloro POSS G1-16Cl in the presence of base to led to diphenylphosphine-containing dendrimers with different length spacers between the phosphorus atoms (Figure 3.25). Diphenylphosphino methanol, produced by reaction of paraformaldehyde with diphenylphosphine (120°C, *in situ*),[17] was added in excess (3 to 1) to the 16-chloro POSS in the presence of triethylamine. Good conversion was obtained after 6 days (only 60 % after 2 days). After purification through silica gel column chromatography (eluent: petroleum ether/ diethyl ether gradient), a 76 % yield of a colourless non-crystalline product was isolated. ^{1}H NMR and MALDI-TOF (Figure 3.26) showed that an average of 14 arms (of the possible16) contained the diphenylphosphine species (conversion > 86 %). Once again partial fragmentation occurred since peaks at m/z {M-X(CH_2PPh_2)} are found (X = 0, 1,2,3, etc.). A single signal in ^{31}P NMR was found at δ -13.6 ppm confirming the presence of the phosphine species.

Table 3.2 Phosphine functionalised POSS prepared by nucleophilic substitution reactions.

Dendrimer	*Synthetic method*	*^{31}P NMR δ (ppm)*	*conversion %*	*yield %*
G1-24methylPMe_2	2[c]	-54.5	>95[f,g]	97
G2-ethyl-72methylPMe_2	2[a]	-54.4	nd[f]	80
G1-24methylP(hex)$_2$	2[a]	-36.3 (br)	90[d]	40
G1-16methylPPh_2	2[a]	-22.6 (br)	>95[d,e]	70
G1-24methylPPh_2	2[a]	-23.9	>70[d,e]	93
G1-16methoxyPPh_2	3[b]	-13.6 (br)	>86[d,e]	76
G1-16ethoxyPPh_2	3[b]	-22.3, -22.5	>92[d,e]	85
G1-16propylPPh_2	4[c]	-16.1, -16.2, -16.4	>85[d,e]	75

[a]: reaction of R_2PCH_2Li with –Si$MeCl_2$ derivatised dendrimer, [b]: reaction of $Ph_2P(CH_2)_nOH$ with –Si$MeCl_2$ derivatised dendrimer, [c] : reaction of $Ph_2P(CH_2)_3MgBr$ with –Si$MeCl_2$ derivatised dendrimer, [d]: ^{1}H NMR, [e]:.MALDI TOF, [f] : not determined (poor solubility).

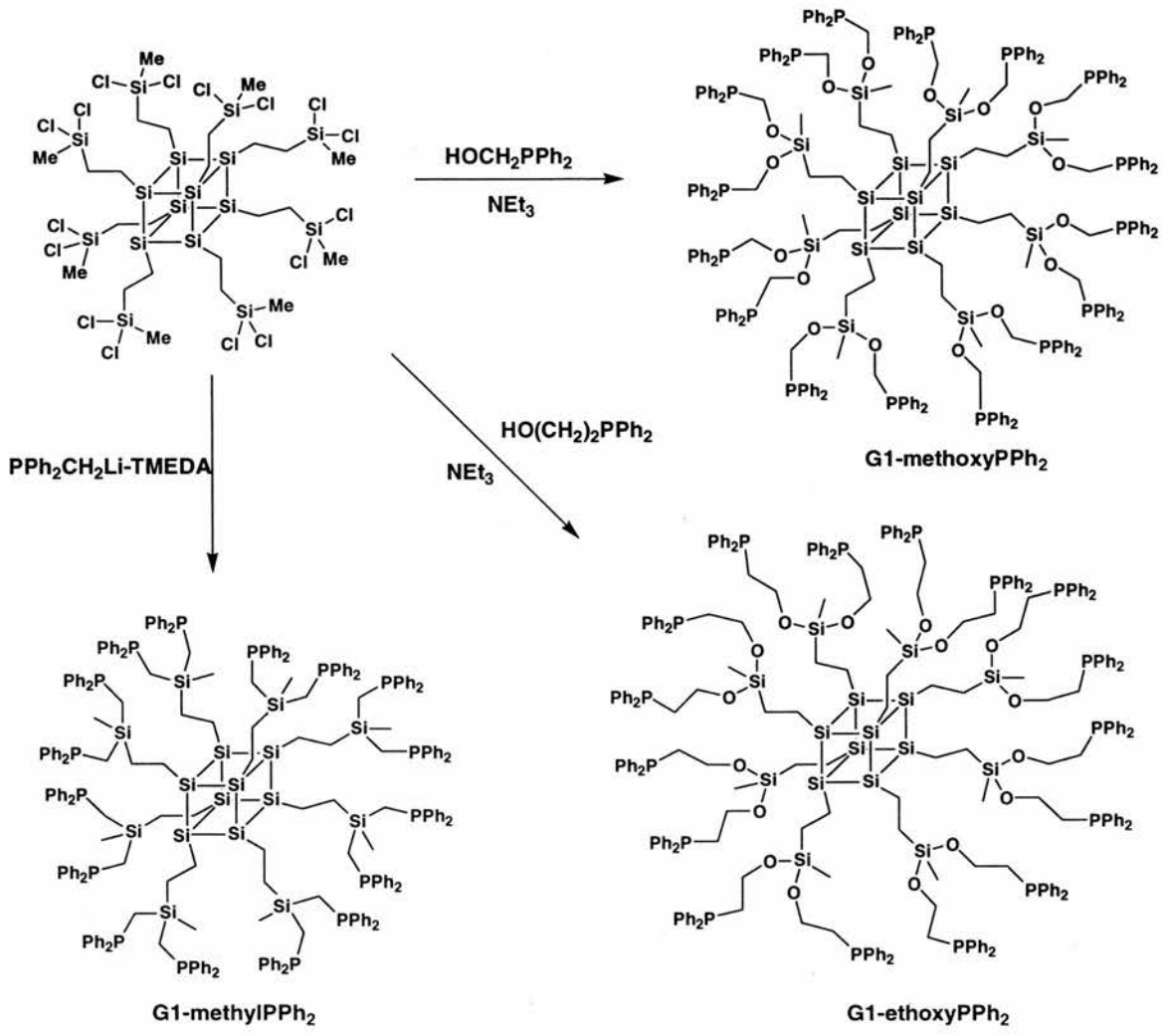

Figure 3.25 Synthesis of POSS with 16 diphenylphosphine groups (the oxygen atom at the edge of the cube are missing for simplification).

To vary the chain length between the phosphorus atoms, addition of 2-diphenylphosphino ethanol in excess to G1-16Cl was also carried out (Figure 3.25). Compound **4** was prepared in 85 % yield by lithiation of triphenylphosphine (formation of PPh_2PLi and PhLi), followed by addition to 2-chloroethan-1-ol at –78°C (^{31}P δ –23.6 ppm) (Figure 3.27).[18] The phosphine compound was reacted for 5 days with the 16-chloro POSS and the product purified by silica gel column chromatography to give a non-crystalline solid in 85% yield. The dendrimer was characterized by NMR and MALDI-TOF techniques. Good conversion was found since a average of 14-15 arms were converted to the phosphine species (conversion > 92 % determined by ^{1}H NMR).

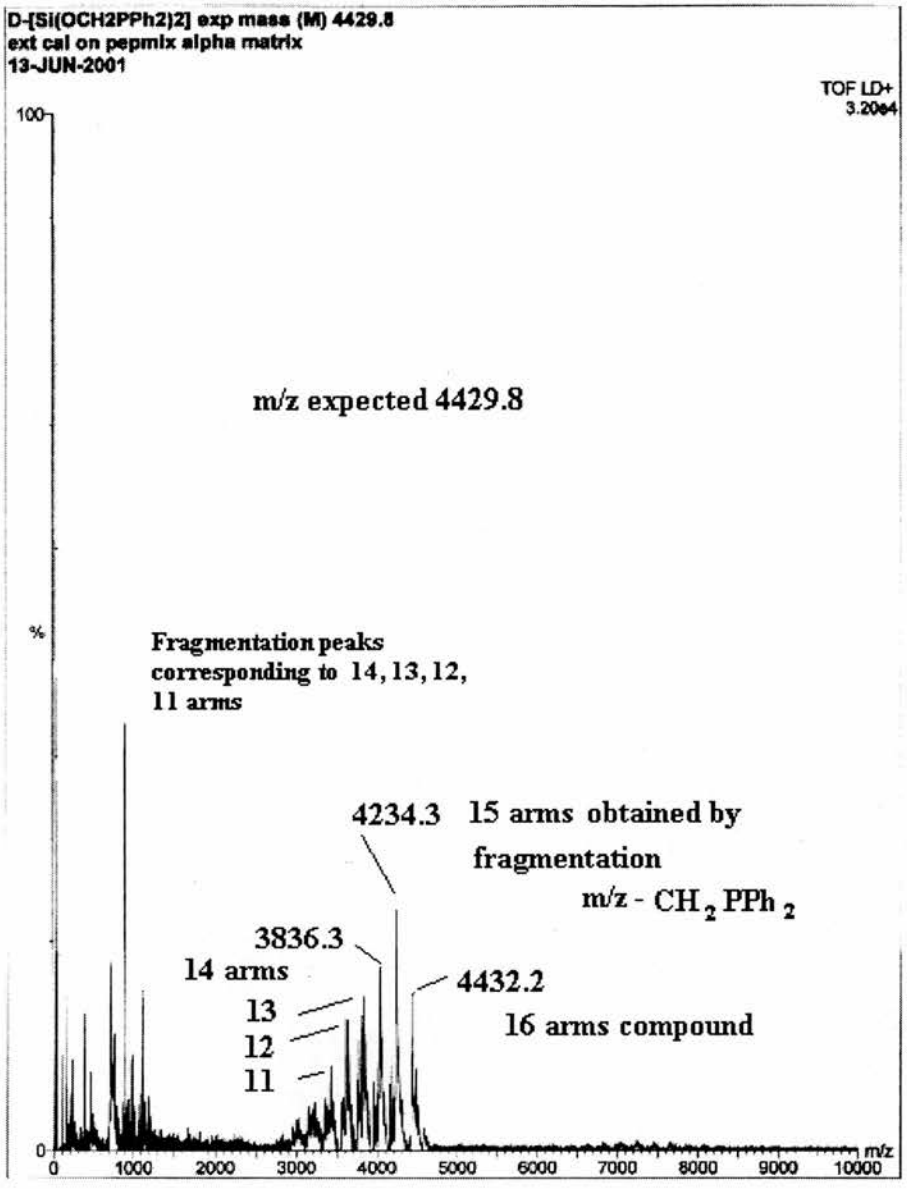

Figure 3.26 MALDI-TOF spectrum of G1-16methoxyPPh$_2$ POSS (Figure 3.25).

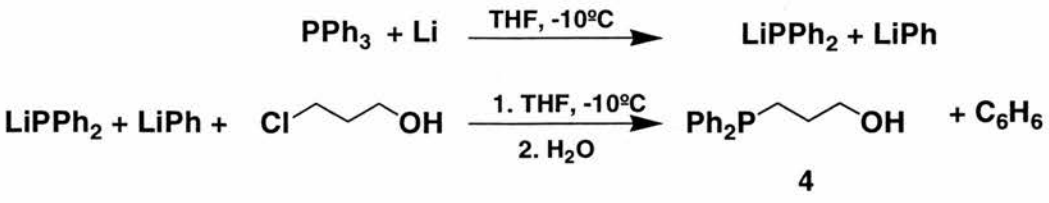

Figure 3.27 Synthesis of 2-diphenylphosphino ethanol.

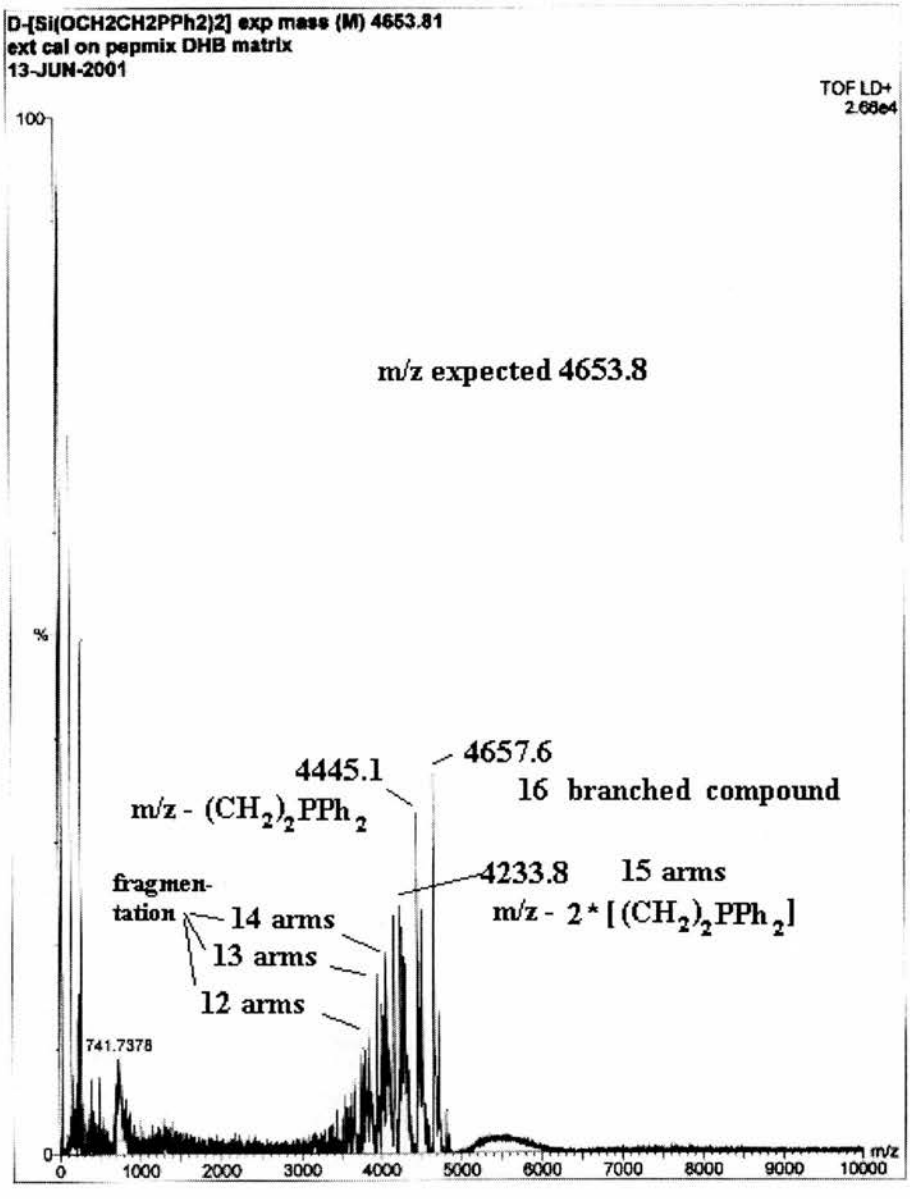

Figure 3.28 MALDI-TOF spectrum of G1-16ethoxyPPh$_2$ POSS (Figure 3.25).

The MALDI-TOF spectrum showed a large distribution of peaks (Figure 3.28). However in this case it is clear that partial decomposition occurred during the MALDI-TOF analysis since peaks at {M-X($CH_2CH_2PPh_2$)} are found (X = 0, 1, 2, 3, etc.) when expecting peaks at {M-X[($OCH_2CH_2PPh_2$)+Cl]} or at least at {M-X[($OCH_2CH_2PPh_2$)+OH]} if partial substitution had happened. The ^{31}P NMR showed two broad signals centered at δ -22.3 and –22.5 ppm indicating that the phosphorus atoms were in a similar environment. These products were found more sensitive to decomposition as the Si-O-C bonds are more easily hydrolyzed (see Chapter 4).

To obtain a more stable compound (than the compound with siloxane linker) with a 7 atom spacer between the two phosphorus atoms, we reacted the Grignard species $ClMgCH_2CH_2CH_2PPh_2$ (**6**) with the 16-chloro POSS. Reaction of lithium diphenylphosphide (n-butyllithium and diphenylphosphine) with a large excess of 1,3 dichloropropane (Figure3.29) yielded the chlorophosphine compound **5** (yield 85%, ^{31}P δ -15.9 ppm), which was then reacted with magnesium to give **6**.[19]

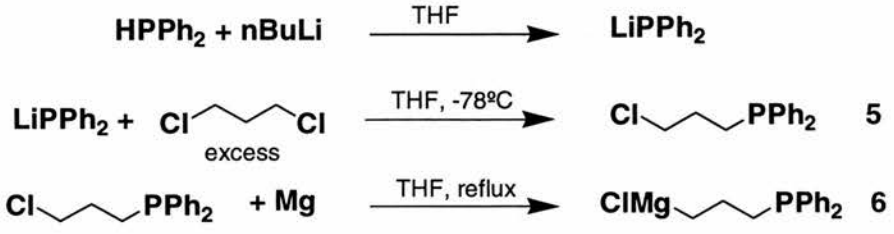

Figure 3.29 Preparation of 3-diphenylphosphinopropyl magnesium chloride.

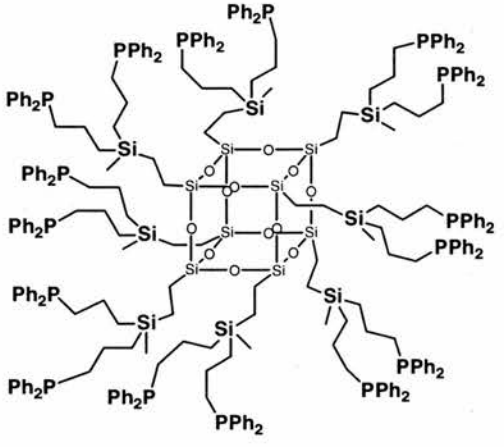

Figure 3.30 16-diphenylphosphine containing dendrimer with a spacer of 7 atoms between the phosphorus atoms.

The addition of an excess (3 fold) of the Grignard compound to the 16-Cl POSS afforded, after 36 hours a partially functionalised POSS, G1-16propylPPh$_2$), with $SiCH_2CH_2CH_2PPh_2$ groups (conversion 76 %). After 4 days only a slight increase of the conversion was obtained since 86 % (^1H NMR) of the chloride were substituted. The compound was then isolated after work up as a colourless non-crystalline solid in 75% yield. Four ^{31}P chemical shifts were found at δ -16.1, -16.2, -16.3, -16.4 ppm indicating the different environments of the phosphorus atoms.

3.4.2 Phosphite functionalised POSS.

To introduce phosphite substituents on the outer shell of the dendrimer, another approach was considered due to the reactivity/ chemistry of such compounds. It was decided to functionalised the POSS with hydroxy groups to obtain a multi-site nucleophilic molecule which could easily be reacted with chlorophosphite compounds. Although Morris and coworkers showed that POSS molecules could be functionalised with silanol groups,[20] the sensitivity of the Si-O-P bonds to moisture caused us to seek another way of introducing the hydroxy groups. Introduction of alkoxy substituents to the POSS was developed in our group[21] based on previous work using hydroboration.[22] Addition of an excess of borane compound (9-BBN) to the G1-16allyl POSS gave the borane substituted POSS, which was subsequently reacted with H_2O_2 and an aqueous sodium hydroxide solution to yield the 16-hydroxy POSS (Figure 3.32). The intermediate borane compound was not characterized. The elimination of by-products (cyclo-octanediol) and trace of water from the final reaction was obtained by passing the products through a silica gel column with dried solvents. First the by-product was eluted with THF, then a gradient of THF-pyridine allowed the recovery of the hydroxy POSS in reasonable yield (60 %). The product was a colourless non-crystalline solid, which was characterized by NMR and MALDI-TOF techniques. Quantitative conversion was demonstrated. The total removal of solvent was extremely difficult to achieve even under vacuum using a hot water bath. Thus, as a polar solvent was required to elute the products, pyridine was chosen since it was one of the reactants of the subsequent reaction, i.e. introduction of phosphite moieties. Indeed, 2,2'-biphenol was reacted with an excess of PCl_3 to give the 2,2'-bisphenoxyphosphorus chloride (yield 79 %, ^{31}P NMR δ 180.4 ppm) (Figure 3.31).[23]

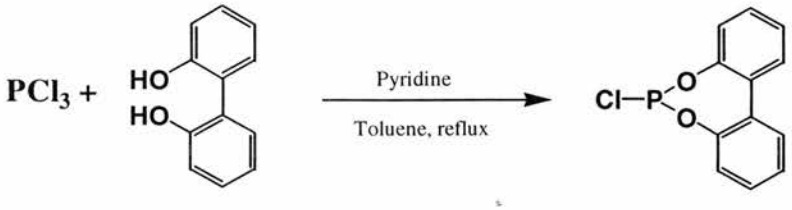

Figure 3.31 Synthesis of 2,2' bisphenoxyphosphorus chloride.

Slow addition of the hydroxy POSS dissolved in pyridine to the chlorophosphite compound (1.5 excess) in a toluene/ pyridine mixture (high dilution) gave the desired compound. Purification and removal of the excess of chlorophosphite was acquired

by column chromatography. The product was a colourless non-crystalline compound (yield 45 %). A conversion higher than 94% was determined by ^{1}H NMR. Characterization of the phosphite POSS was extremely difficult due to its sensitivity to moisture. MALDI-TOF failed to give any information since two peaks were detected at m/z 722 and at m/z 1333 while the m/z expected was 5358. The ^{31}P NMR spectra showed two peaks at δ 140.0 and 139.7 corresponding to the expected phosphite species.

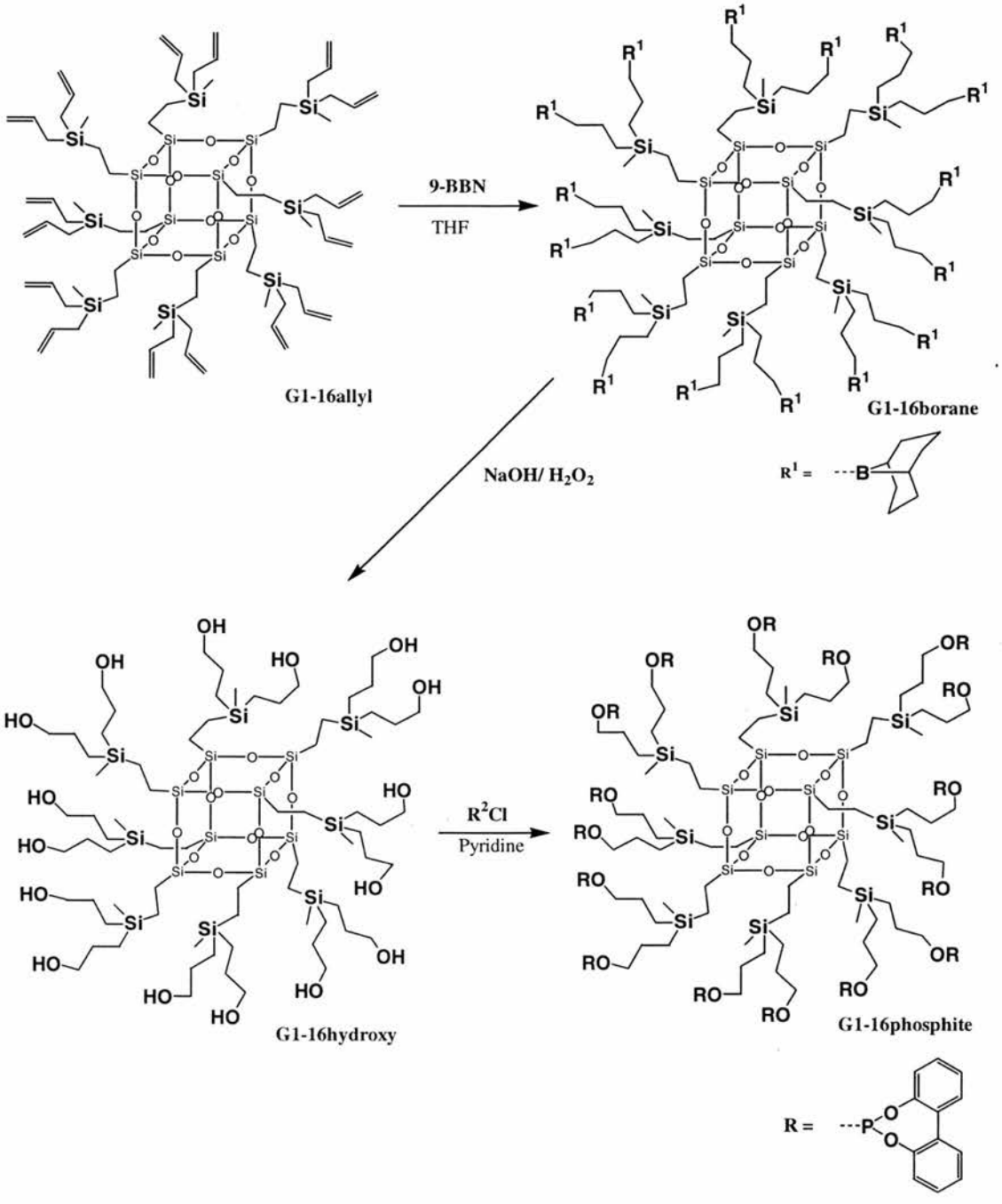

Figure 3.32 Synthesis of phosphite-containing POSS.

3.4.3 Preparation of chiral phosphorus species, a SEMI-ESPHOS type compound.

Attempts to synthesize a chiral phosphorus species which could be introduced into the framework of the dendrimer were carried out. The chiral compound considered (Figure 3.33) was a similar species to the SEMI- ESPHOS ligand prepared by Wills and co-workers (see Chapter 2, section 2.5).[24] While the ESPHOS ligand induced high asymmetry in the hydroformylation of vinyl acetate, the SEMI ESPHOS showed poor enantioselectivity. To investigate the chelate properties of the diphosphine of our dendrimer, i.e. to see whether or not two SEMI-ESPHOS on the dendrimer could ligate in a way similar to the ESPHOS compounds and so induce asymmetry, it was thus decided to attempt to functionalize the POSS with a species similar to SEMI ESPHOS. As the successful introduction of compounds to the outer shell of the dendrimer necessitated highly reactive species, we tried to synthesize the cycloaminophosphine **8,** which could be then grafted to the dendrimer by radical addition.

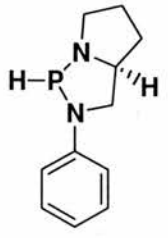

8

Figure 3.33 A chiral phosphine based on a SEMI-ESPHOS model, 3-phenyl-1,3diazaphosphabicyclo[3.3.0]octane.

The chiral moiety (S)-2anilinomethyl pyrrolidine **10** was prepared by addition of aniline to L-Glutamic acid (60 % yield) and subsequent reduction by $LiAlH_4$ (85% yield, absolute configuration S).[25] Addition to PCl_3 in the presence of pyridine yielded the chloro phosphorus compound **11** in 85 % yield. The product was a crystalline white solid, which was extremely sensitive to moisture. Two ^{31}P chemical shifts were found at δ 150.3 ppm (70 %) and δ 142.3 ppm (30 %) showing the formation of two compounds, possibly diastereoisomers.

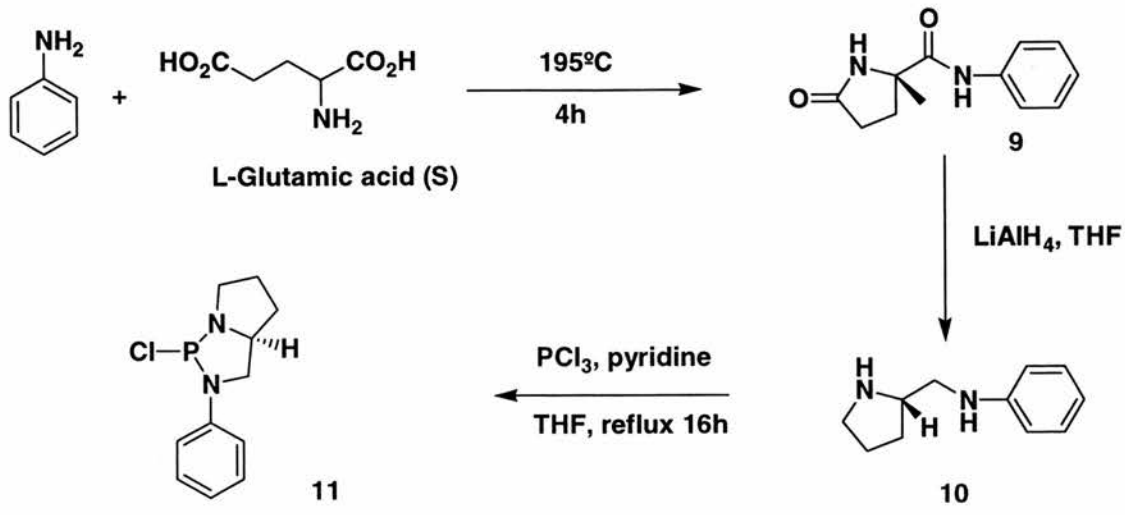

Figure 3.34 Synthesis of chiral chlorodiazaphosphine compounds 9.

Unfortunately, the reduction of the chlorodiazaphosphine compound by $LiAlH_4$ [26] or tri-n-butyltin hydride[27] failed since uncharacterized materials were obtained showing no phosphorus signal in the ^{31}P NMR spectra. No further characterization was carried out. The successful reduction of this type of compound is indeed extremely difficult to achieve without destruction of the phosphorus-nitrogen bonds since it necessitates bulky substituents on the two nitrogen atoms.[26]

3.5 Synthesis of diphenylphosphinoethyl silane compounds.

To compare the properties of the diphenylphosphine functionalised dendrimers with smaller but similar molecules, we prepared the di- and tetra(diphenylphosphino ethyl)silane compounds **12** and **13** shown in Figure 3.35. These ligands were synthesized by radical addition (AIBN as radical initiator) of $HPPh_2$ to the corresponding dimethyldivinylsilane and tetravinylsilane.[28] Total conversion was achieved for both compounds. Interestingly these parent molecules showed different solubility in cyclohexane that of the larger molecule since they precipitated after a few hours in the reaction medium. The solvent of the reaction was thus changed to toluene. More importantly the reactions were much faster than for the dendrimer, since the reaction was completed after 3 hours at 50°C (10 days for the dendrimer).

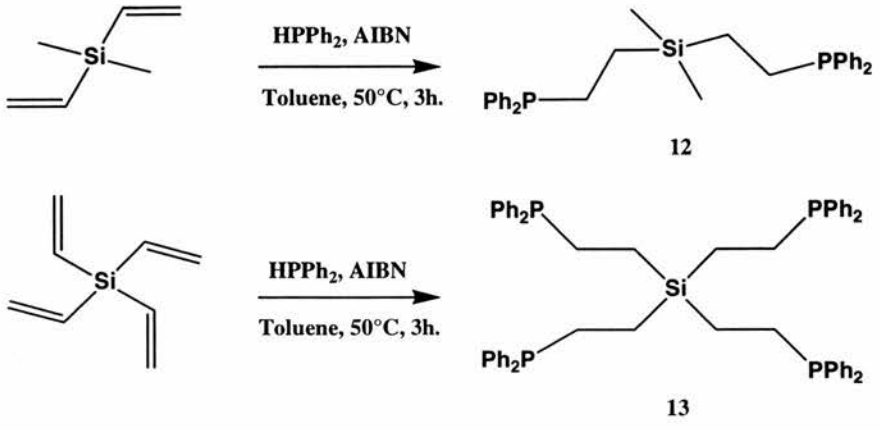

Figure 3.35 Synthesis of diphenylphosphinoethyl silane compounds

This difference in rate is further evidence that the vinyl groups of the dendrimer are difficult to approach for the phosphine reagent due to the steric hindrance in the dendrimer and also the probable phenomenon of back-folding of the arms.

The compounds were isolated as white crystalline compounds in quantitative yields. A single ^{31}P NMR chemical shift, identical for both compounds, was found at δ -9.5 ppm. An X-ray crystal structure of the tetra(diphenylphosphinoethyl)silane compound was obtained showing the diphenylphosphine moieties group two by two (see Chapter 5 and Appendix II).

3.6 Conclusions.

It was shown that 1st and 2nd generation dendrimers with functionalisable endgroups could be built on a POSS core. Compounds with 16- or 24-vinyl or allyl groups (G1) and 48- and 72-vinyl POSS (G2) and their intermediate chlorosilane compounds were synthesised often in good yields and characterised by ^{1}H, ^{13}C NMR and microanalysis. However, MALDI-TOF or E.I mass spectrometry failed to give satisfactory results. The poor resolution given by these techniques was likely due to the instability of the numerous alkenyl groups on the periphery, which are easy polymerizable substituents. The later functionalisation of these compounds by phosphorus species, however, gave well resolved in MALDI-TOF spectra. The vinyl moieties of the different dendrimers are extremely sensitive to polymerisation leading to many problems during their synthesis and storage. The less reactive allyl groups gave more stable products although a better longevity of both products was

found under inert atmosphere in the dark. It was thus decided that the higher generation dendrimers would be synthesised using the allyl compounds.

Solvents, and in particular THF, were found extremely difficult to remove from both the chloro and alkene compounds. Although the dendrimers acted as host apparently for the solvent and water molecules, silica gel column chromatography using petroleum ether as eluent allowed a satisfactory purification of the products. Traces of solvents and water in the 2^{nd} generation dendrimers with vinyl end groups were particularly difficult to remove.

The introduction of longer alkyl chain alters the physical properties of the molecule. The products are either solids (vinyl groups) or oils (allyl groups). More importantly, a longer linker between successive generation modifies the size of the molecule involving less steric congestion on the periphery. Functionalisation or growing of the dendrimer is then facilitated despite the lower reactivity of the allyl moieties.

Diverse routes were successfully applied to introduce phosphorus species onto the dendritic molecules. Alkyl- or arylphosphine and phosphite compounds were grafted to the external layers of the dendrimer. Various dendritic generations (1^{st} and 2^{nd}) were also functionalised with these compounds. Most of these compounds were characterized by NMR and mass spectroscopy techniques (MALDI-TOF) showing good to high conversion. The characterization was sometimes difficult since ^{1}H NMR and MALDI-TOF showed limitations. Indeed as expected for oligomer type molecules the NMR resolution of such compounds is often low. Moreover, since fragmentation occurs during the MALDI-TOF analysis it is somewhat difficult to determine the exact number of functionalised arms.

Dendritic molecules with different spacers (3, 5 or 7 atoms) between the diphosphine moieties were synthesized. This is important as the activity and selectivity of diphosphine compounds in catalytic reactions are often correlated to the structure of the phosphine ligands. It is important to note that relatively different ^{31}P chemical shifts were obtained with the different spacers between the two phosphines. The more noticeable effects are found with the 16-diphenylphosphine functionalised dendrimers. Indeed when passing from a spacer of 3 to 5 and then 7 carbon atoms the chemical shift of the phosphorus atoms changes from –23.6 to -9.4 and –16.2 ppm respectively (see Table 3.3). There is nothing surprising about this observation since these electronic properties are also found in the equivalent small molecules.

However, since the basicity of the phosphine varied with the different bridges, some different interaction might occur between the metal and phosphine species when they are used as ligands for catalysis. In addition, substitution of a carbon by an oxygen atom in the 5 atom spacer compounds (see Table 3.3) also led to a shift of the ^{31}P resonance of –4 ppm compared with the all carbon analogue. This shift was –6 ppm for the 7 atom spacer.

Table 3.3 16-diphenylphosphine functionalised POSS and their ^{31}P NMR chemical shifts.

Dendrimer	*Endgroup*	*Synthetic method*	*^{31}P NMR δ (ppm)[a]*	*Spacer atoms[b]*
G1-16ethylPPh$_2$	$(CH_2)_2PPh_2$	1[c]	-9.4	5
G1-16methylPPh$_2$	CH_2PPh_2	2[d]	-22.6	3
G1-16methoxyPPh$_2$	OCH_2PPh_2	3[e]	-13.6	5
G1-16ethoxyPPh$_2$	$O(CH_2)_2PPh_2$	3[e]	-22.5	7
G1-16propylPPh$_2$	$(CH_2)_3PPh_2$	4[f]	-16.2	7

a: major peak, b: number of atoms between the two phosphorus atoms on a same arm, c: radical addition of $HPPh_2$ with –SiMe(Vinyl)$_2$ derivatised dendrimers in presence of AIBN, d: reaction of Ph_2PCH_2Li/ TMEDA with $-SiMeCl_2$ derivatised dendrimer, e: reaction of $Ph_2P(CH_2)_nOH$ with $-SiMeCl_2$ derivatised dendrimer, reaction of $Ph_2P(CH_2)_3MgBr$ with $-SiMeCl_2$ derivatised dendrimer.

Although nucleophile substitution reactions necessitated one less reaction step (addition of the alkenyl groups to the chloro POSS) than the radical addition, the purification and the loss of possible costly phosphine intermediates used in excess were not in favour of this type of reaction. Indeed, whilst diphenylphosphine could be recovered from the radical addition (by distillation or by column chromatography), the diphenylphosphine methanol or the Grignard compound $MgBr(CH_2)_3PPh_2$ were lost during the process.

3.7 References for Chapter 3.

1 P.-A. Jaffrès and R. E. Morris, *J. Chem. Soc., Dalton Trans.*, 1998, 2767.

2 L. L. Zhou and J. Roovers, *Macromolecules*, 1993, **26**, 963.

3 A. W. van der Made and P. W. N. M. van Leeuwen, *J. Chem. Soc., Chem Commun.*, 1992, 1400.

4 D. Seyferth, D. Y. Son, A. L. Rheingold, and R. L. Ostrander, *Organometallics*, 1994, **13**, 2682.

5 F. J. Feher and T. A. Budzichowski, *Polyhedron*, 1995, **14**, 3239.

6 T. N. Voronkov, R. G. Martynova, and V. I. Belyi, *Zh. Obshch. Khim.*, 1979, **49**, 1522.

7 T. N. Martynova and V. P. Korchkov, *Zh. Obshch. kim.*, 1982, **52**, 1522.

8 G. Schwarz, D. J. Cole-Hamilton, and R. E. Morris, *ISHC conference, abstract*, 1998.

9 S. Lücke, K. Stoppek-Langner, J. Kuchinke, and B. Krebs, *J. Organomet. Chem.*, 1999, **584**, 11.

10 S. Lücke, K. Stoppek-Langner, B. Krebs, and M. Läge, *Z. Anorg. Allg. Chem.*, 1997, **623**, 1243.

11 C. P. Casey, L. E. Paulsen, E. W. Beuttenmueller, B. R. Proft, L. M. Petrovich, and B. A. Matter, *J. Am. Chem. Soc.*, 1997, **119**, 11817.

12 D. J. Peterson and H. R. Hays, *J. Org. Chem.*, 1965, **30**, 1939.

13 H. H. Karsch and H. Schmidbaur, *Z. Naturforsch.*, 1977, **32b**, 762.

14 H. H. Karsch, *Z. Naturforsch.*, 1979, **34b**, 1178.

15 D. J. Peterson, *J. Organometal. Chem*, 1967, **8**, 199.

16 D. de Groot, P. G. Emmerink, C. Coucke, J. N. H. Reek, P. C. J. Kamer, and P. W. N. M. van Leewen, *Inorg. Chem. Commun.*, 2000, **3**, 711.

17 M. Slany, M. Bardaji, A.-M. Caminade, B. Chaudret, and J.-P. Majoral, *Inorg. Chem.*, 1997, **36**, 1939.

18 D. Chantreux, J.-P. Gamet, R. Jacquier, and J. Verducci, *Tetrahedron*, 1984, **40**, 3087.

19 E. Arpac and L. Dahlenburg, *Z. Naturforsch.*, 1980, **35b**, 146.

20 P. I. Coupar, P.-A. Jaffrès, and R. E. Morris, *J. Chem. Soc., Dalton Trans.*, 1999, 2183.

21 X. Zhang, K. J. Haxton, L. Ropartz, D. J. Cole-Hamilton, and R. E. Morris, *manuscript submitted.*

22 C. Kim, S. Son, and B. Kim, *J. Organometal. Chem.*, 1999, **588**, 1.

23 G. J. H. Buisman, E. Vos, P. C. J. Kamer, and P. W. N. M. van Leeuwen, *J. Chem. Soc., Dalton Trans.*, 1995, 409.

24 S. Breeden, D. J. Cole-Hamilton, D. F. Foster, G. J. Schwarz, and M. Wills, *Angew. Chem. Int. Ed.*, 2000, **39**, 4106.

25 J. M. Brunel, T. Constancieux, and G. Buono, *J. Org. Chem.*, 1999, **64**, 8940.

26 R. B. King and P. M. Sundaram, *J. Org. Chem.*, 1984, **49**, 1784.

27 E. E. Nifantiev, S. F. Sorokina, A. A. Borisenko, A. A. Zavalishina, and L. A. Vorobjeva, *Tetrahedron*, 1981, **37**, 3183.

28 W. Schalk, P. Wirth, G. E. M. Dannenberg, and V. Schmied-Kowarzik, Deutsches Pat., DE 1118781, 1959, Koppers Co.

Chapter Four: Hydroformylation/ hydrocarbonylation reactions catalysed by dendritic rhodium alkylphosphine complexes.

4 Hydroformylation/ hydrocarbonylation reactions catalysed by dendritic rhodium alkylphosphine complexes.

4.1 Introduction

The design of the catalyst support needs to ensure that the active species is exposed enough to perform its duty, but at the same time that it is sufficiently bound to ensure leaching is kept to a minimum. In a dendrimer-based catalyst, the number of catalytic sites can be controlled by the design of the dendrimer. As the number of branches increases radially, the number of potential metal binding sites also increases. As the crowding of the outer surface of exposed functional groups is directly related to the degree of branching, the potential for producing a multidentate ligand is evident. Thus, the size of the dendrimer will allow it to function as a tuneable ligand with the ability to vary the number of metals bound.

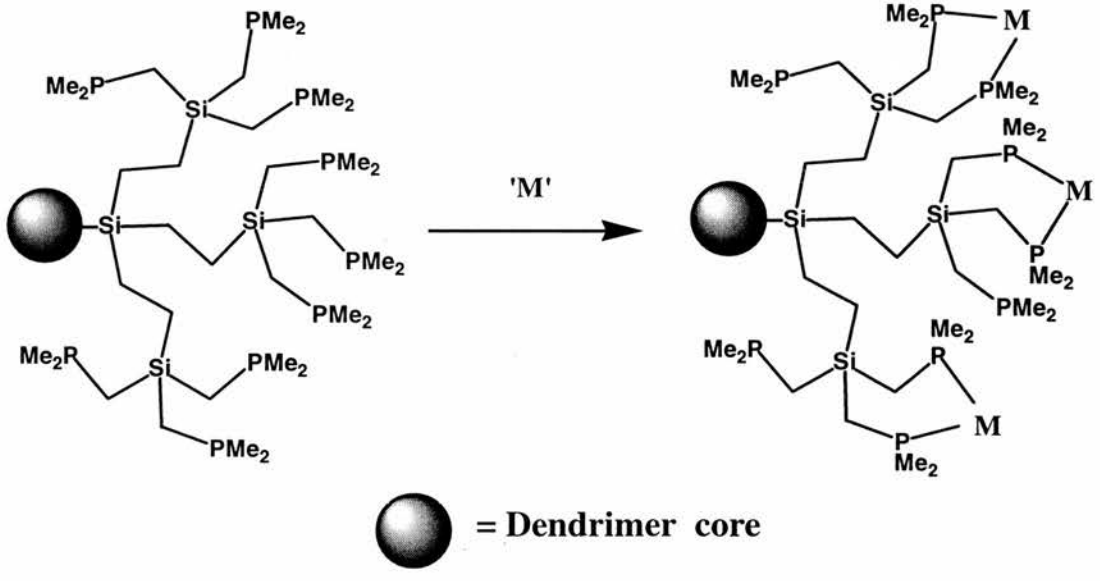

Figure 4.1 Expected bidendate chelation of the phosphine containing dendritic ligand to a metal species ('M').

The dendritic species can be considered a large ligand able to act as a multidentate species. The increase of branching and complexity of the molecule may lead to different reactivity of the complexes formed on the periphery of the dendrimer. Whether the dendritic ligand will bind on the metal centre (rhodium) in a bidendate or tridendate way or will form a dinuclear rhodium species will be of great interest.

Trialkylphosphine ligands are effective ligands to rhodium catalysts providing alcohols from terminal alkenes under pressure of CO/H_2 (Figure 4.2) (see Chapter 2). Using a protic solvent and mild conditions, Cole-Hamilton and co-workers showed that this hydrocarbonylation reaction did not necessarily proceed through aldehyde intermediates. [1, 2]

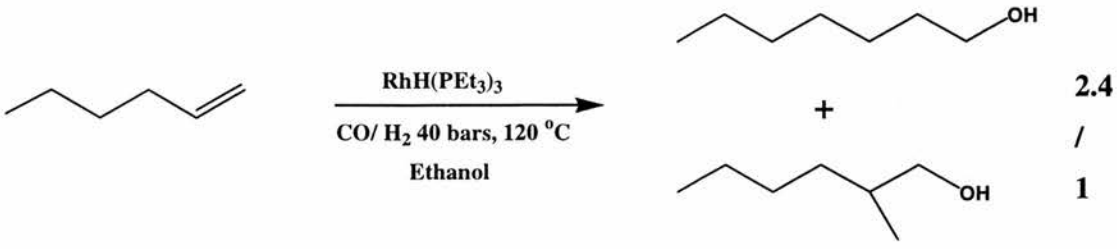

Figure 4.2 Hydroformylation of hex-1-ene catalysed by [$RhH(PEt_3)_3$] in ethanol.

This reaction has been chosen for testing the ability of dendrimer bound alkyl phosphines to act as suitable ligands to rhodium, since simple product analysis will be diagnostic. If the ligand binds and a trialkylphosphine rhodium complex is formed, alcohols (heptan-1-ol and 2-methylhexan-1-ol from hex-1-ene) will be the hydrocarbonylation products, whilst if binding does not occur, the products will be aldehydes and acetals. In addition, since hydrocarbonylation can give two different regio isomers of the product (linear and branched), any changes in the balance of the products brought about by the environment of the dendrimer surface will be apparent.

4.2 Results and discussion

4.2.1 Dimethyl and dihexylphosphine functionalised dendrimers as ligands.

The catalytic activity of the phosphine-functionalised dendrimers as ligands for the hydrocarbonylation of alkenes was not studied previously. Our first results were based on dimethyl- and dihexyl-phosphine functionalised POSS. It was shown that the rhodium-dendrimer complexes derivatised with $-CH_2PMe_2$ or $-CH_2PHex_2$ were efficient for the catalytic hydrocarbonylation of hex-1-ene to heptan-1-ol and 2-methylhexan-1-ol. Thus, the dendrimers must be bound to the rhodium since only reactions involving trialkylphosphine complexes give alcoholic products.[1]

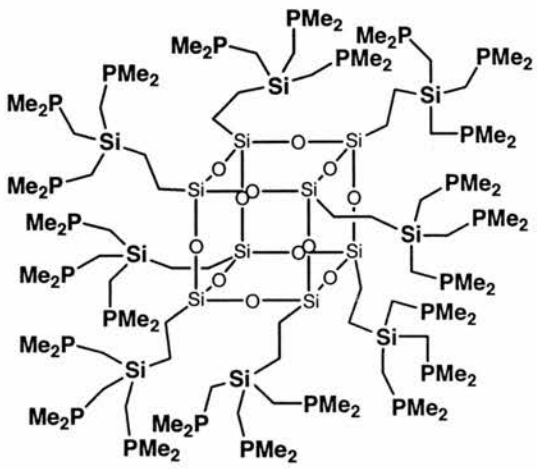

G1-24methylPMe$_2$

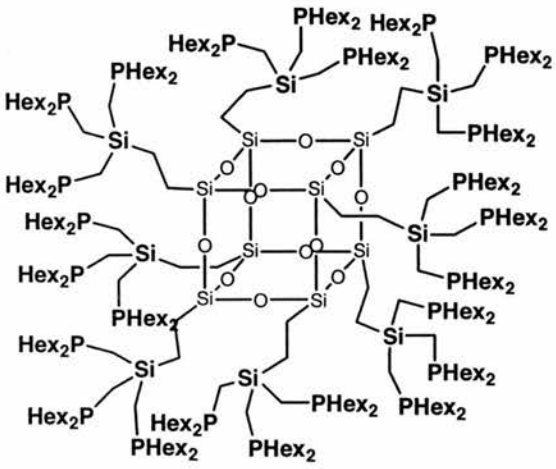

G1-24methylP(Hex)$_2$

Figure 4.3 First generation 24-dimethyl- or dihexylphosphine-containing POSS.

Both rhodium complexes of the G1-24methylPMe$_2$ (Figure 4.3) and G2-ethyl-72methylPMe$_2$ (Figure 4.4) showed good activity for the hydroformylation at the optimal conditions found previously.[1] The reactions were carried out at 120°C (heating jacket) for 16 h in an autoclave stirred using a stirrer bar under a CO/H$_2$ atmosphere of 40 bar. [Rh$_2$(O$_2$CMe)$_4$] was the rhodium precursor catalyst with a phosphine/rhodium ratio of 3/1. A substrate/ rhodium ratio of 207/1 was used ([Rh] = 8.0×10^{-3} mol.dm^{-3}).

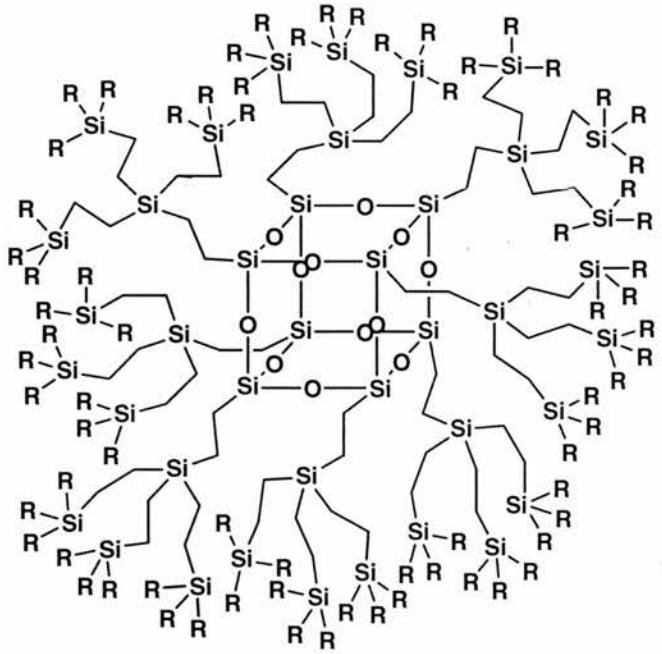

R = CH$_2$PMe$_2$

G2-ethyl-72methylPMe$_2$

Figure 4.4 Second generation 72-dimethylphosphine-containing POSS.

In order to compare the results of the hydrocarbonylation of hex-1-ene catalysed by dendritic rhodium complexes, we carried out the hydrocarbonylation reaction using trimethylphosphine as ligand in similar conditions. After 16 hours of reaction the only products detected were the linear and branched alcohols, respectively heptan-1-ol and 2-methylhexan-1-ol. The regioselectivity was found similar to the previous studies[1] with a linear to branched ratio (l:b) of 2.4:1.

The G1-24methylPMe$_2$ ligand was not soluble in ethanol. However after addition of [$Rh_2(O_2CMe)_4$] (Phosphine/Rh ratio of 3/1), the colour of the solution changed gradually (during 3 hours under stirring) from green to red-brown with partial dissolution of the dendritic complex into solution. A homogeneous solution was obtained after 16 hours stirring. This change indicated that the complete complexation of the transition metal by the phosphine occurred.

The hydroformylation of hex-1-ene using [$Rh_2(O_2CMe)_4$] and G1-24methylPMe$_2$ as catalyst complex in ethanol gave mainly C_7 alcohols (over 94 %) as expected if the dendrimer were bound to rhodium. The substrate was totally converted to products. It is interesting to note that both the heterogeneous and homogeneous prepared catalytic solutions (i.e. after 2-3 h or 16 h of pre-stirring) gave similar results indicating that the same species were formed under the catalytic condition. Heptan-1-ol and 2-methylhexan-1-ol were found as products of the reaction (determined by gas chromatography (GC)) in a ratio of 2.1:1. Some traces of C_7 aldehydes and diethyl acetals formed from C_7 aldehydes and ethanol) have also been detected in some cases. It is important to note that the products were analysed by GC and that the sensibility of the detectors was not very high. Traces of isomerisation of the substrate (hex-2-ene, hex-3-ene) were hardly detected (see Section 4.2.2). The solutions recovered after reaction were clear yellow mixtures although a yellow precipitate was present sometimes. This yellow solid was observed when a large amount of the liquid phase was found between the glassware and the autoclave wall thus increasing the concentration and so the precipitation of the complexes in the glassware vessel. After exposure to air, another precipitate appeared corresponding probably to the formation of non-chelating phosphine oxide dendrimer. When using a dendrimer formed by using an excess of $LiCH_2PMe_2$ (not totally removed from the dendritic product in this case), total conversion was hardly reached and the linear to branched selectivity dropped to 1.5:1. Side products, i.e. aldehydes and diethyl acetals were then detected (5 to 10 %). This decrease of

selectivity was probably due to formation of base and/or a nucleophile (ethanoate formed by deprotonation, etc.) leading to a non selective rhodium species.

Interestingly, after 4 hours of reaction using the G1-24methylPMe$_2$ dendrimer as ligand, the conversion reached 95 % whilst the products of reaction were mainly aldehydes (heptan-1-al and 2-methylhexan-1-al) in 80 % yield (l:b ratio of 1.8:1) indicating that the reaction proceeded in two steps. The other products were the alcohols (14 %) with a l:b ratio of 4.6:1. This result clearly showed that the aldehydes were first formed, and were then reduced to the alcohols (Figure 4.5), the linear isomer being faster hydrogenated as expected since the l:b ratios of aldehydes and alcohols were disymmetric. The overall linear to branched selectivity was 2.2:1, which was similar to that obtained after the longer reaction time. This result is thus in contradiction with the earlier studies showing the direct formation of alcohol products.[1] It is important to note that, in the former investigations, the autoclave was placed cold into an oven and not stirred. This may possibly lead to different reaction conditions. The mechanism of hydroformylation and subsequent hydrogenation is discussed in Section 4.3.

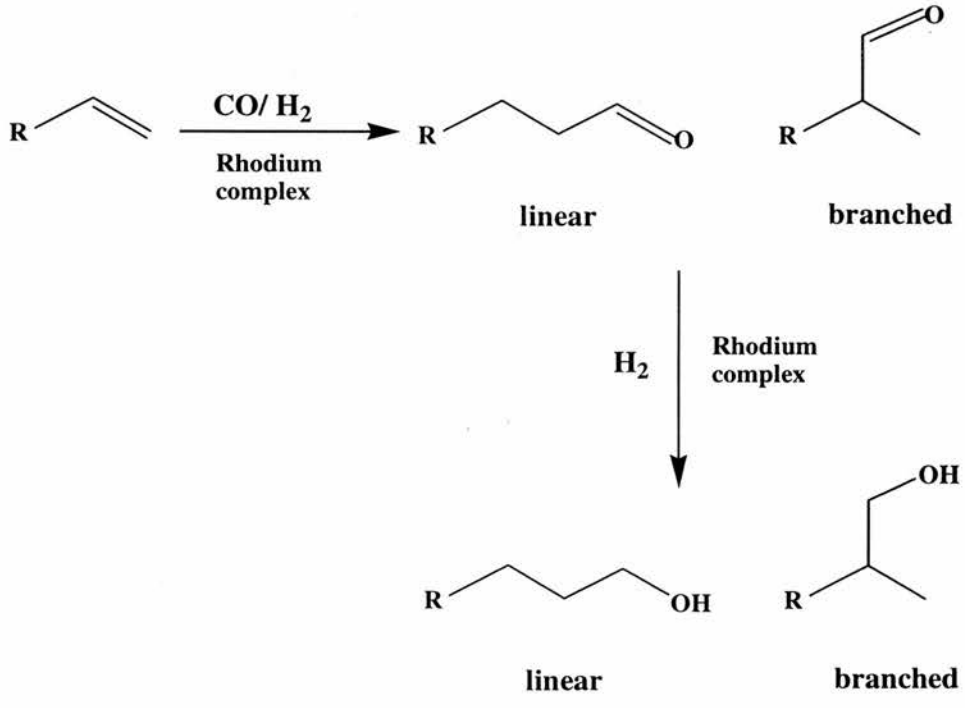

Figure 4.5 Hydroformylation of alkene and subsequent hydrogenation catalysed by rhodium/ alkylphosphine dendrimer complexes to form alcohol products.

Lower concentrations of Rh-dendrimer complexes increase the amount of side products (i.e. diethyl acetals). Indeed the hydroformylation of hex-1-ene produced 5 % of diethyl acetals (from C7 aldehydes) when the concentration of rhodium was reduced to 4.4×10^{-3} mol.dm^{-3} (standard concentration 8.0×10^{-3} mol dm^{-3}) (P/Rh = 3/1) (Table 4.1). Since the hydrogenation rate generally depends on the amount of catalyst, slower reaction was thus obtained with lower concentration of rhodium leading to possible side reaction of the aldehydes with the solvent (ethanol).

Table 4.1 Hydrocarbonylation reactions of hex-1-ene catalysed by Rh complexes of POSS derived dimethyl- and dihexylphosphine dendrimers.

Ligand	*[Rh] (10^{-3} mol.dm^{-3})*	*Time h*	*Conv. %*	*Aldehydes %*	*Alcohols %*	*l:b ratio*
PMe_3	8	16	> 99	-	99	2.4
G1-24methylPMe_2	8	16	> 99	tr [a]	98	2.1
G1-24methylPMe_2	8	4	> 95	80	14	2.2 [b]
G1-24methylPMe_2	4.4	16	> 99	5[c]	94	2.1
G2-ethyl-72methylPMe_2	8	16	> 99	2	97	2.4
G1-24methylP$(Hex)_2$	8	16	> 99	tr [a]	99	2.4

Reaction conditions: catalyst prepared in situ from $[Rh_2(O_2CMe)_4]$ and alkylphosphine species, P/Rh = 3/1, substrate 8.3×10^{-3} mole, ethanol (4 cm^3), 120°C, CO/H_2 40 bar.

[a] : traces not quantified, [b] : overall linear to branched ratio of alcohols and aldehydes, [c] : diethylacetals of the C7 aldehydes.

The 72-dimethylphosphine functionalised POSS, G2-ethyl-72methylPMe_2, was also used as ligand for the catalytic hydrocarbonylation of hex-1-ene. The catalytic solution (dendrimer and $[Rh_2(O_2CMe)_4]$ in ethanol) was mostly heterogeneous. The slow complexation overnight (colouring red-brown) allowed a partial improvement of the solubility. After the catalytic reaction, a precipitate was apparent on the glassware of the autoclave probably indicating that the reaction was partially heterogeneous. The conversion of the substrate reached a value over 99 %.

The catalytic reaction provided mainly C_7 alcohols as expected (heptan-1-ol and 2-methylhexanol) and small amount of heptanal diethylacetal (2 %). Traces of isomerisation products were also detected but not quantified. The l:b ratio of the alcohols obtained was 2.4:1 (Table 4.1). This regioselectivity is higher than the one found for the 1st generation dendrimer. However, this increased selectivity was unlikely to due to any effects of the dendrimer since the use of trimethylphosphine as ligand led to a l:b ratio of 2.4:1 in identical conditions.[1] It is thus thought that the lower ratio obtained for the 1st generation dendrimer arose from the fact that traces of unreacted $LiCH_2P(CH_3)_2$ affect the active catalytic species in a negative way as described above.

Hydroformylation of hex-1-ene in ethanol was carried out using the dendrimer containing dihexylphosphine moieties (G1-24methylP$(Hex)_2$ shown in Figure 4.3) under the same conditions (CO/H_2 40 bar, 120°C, 16 h, $[Rh_2(O_2CMe)_4]$ = 8.0×10^{-3} mol.dm^{-3}, P/Rh = 3/1, substrate/rhodium ratio = 207/1). The number of phosphines contained on the dendrimer was measured by ^{1}H NMR spectroscopy (see Chapter 3). After 16 hours, the conversion of the substrate was higher than 99 % (GC). As expected the main products of reaction were heptan-1-ol and 2-methylhexan-1-ol in a ratio of 2.4:1. No trace of aldehydes or side-products were detected. The regioselectivity of the reaction (l:b ratio of 2.4:1) is as expected for this kind of ligand. It seems here that the bulkiness of the dendrimer and the long alkyl chain of the phosphine moieties do not affect the catalytic selectivity.

4.2.2 Diethyl- and dicyclohexylphosphine functionalised dendrimers as ligands.

Hydrocarbonylation of hex-1-ene, oct-1-ene, non-1-ene and prop-2-en-1-ol catalysed by rhodium complexes formed from $[Rh_2(O_2CMe)_4]$ or $[Rh(acac)(CO)_2]$ and diethylphosphine functionalised dendrimers were carried out at 120°C and 40 bar of CO/H_2 in ethanol. G1-16ethylPEt_2, G1-24ethylPEt_2 (Figure 4.6) and G1-24propylPEt_2 and the 2nd generation POSS with 48 phosphine groups (G2-propyl-48PEt_2) (Figure 4.7) were used as ligands in this study.

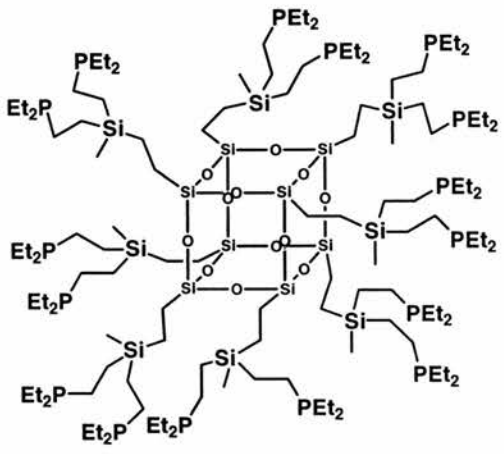

G1-16ethylPEt$_2$

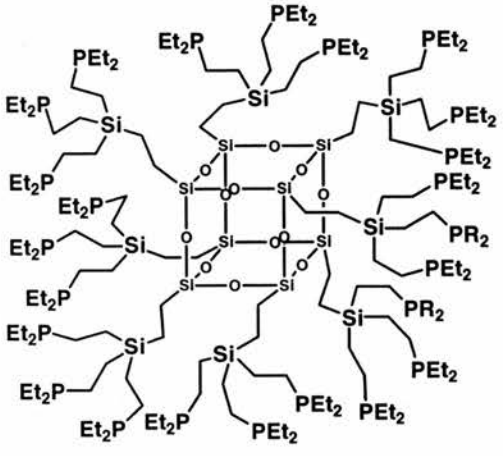

G1-24ethylPEt$_2$

Figure 4.6 First generation POSS functionalised by diethylphosphine groups used as ligands of rhodium complexes for the hydroformylation of alkene.

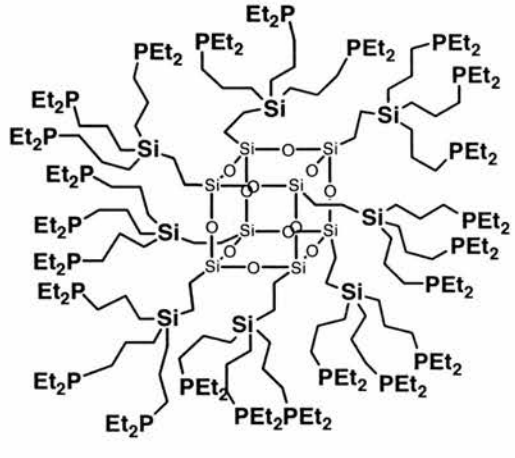

G1-24propylPEt$_2$

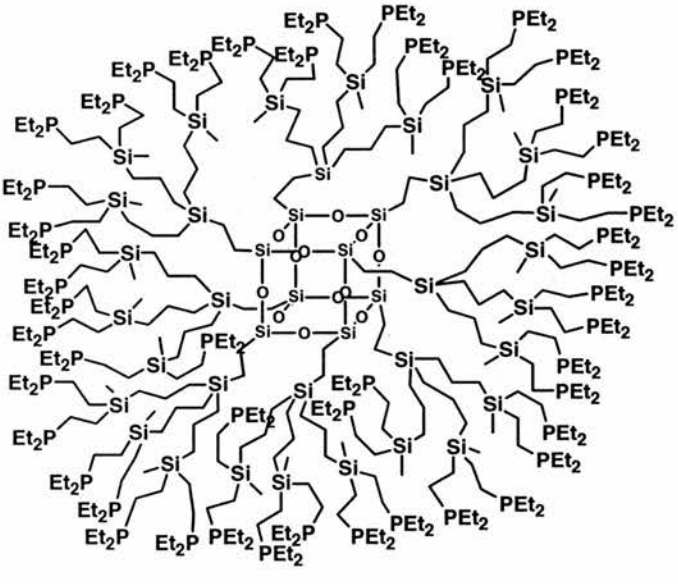

G2-propyl-48PEt$_2$

Figure 4.7 1st and 2nd generation POSS functionalised by diethylphosphine groups used as ligands of rhodium complexes for the hydroformylation of alkene.

Two reactor systems were used to conduct the experiments. A simple autoclave as mentioned before was firstly used to determine preliminary results. Kinetic studies were then performed on a specially designed autoclave owned and operated by CATS (the Catalyst Evaluation and Optimisation Service) (see Chapter 6 for full description). The reliability of the system encouraged us to carry out all experiments with this autoclave. Indeed, since all parameters of the reaction (stirring, heating, pressure, product analysis) are monitored, the comparison of the reactivity

and selectivity of the reaction is much more reproducible and accurate. In addition, higher rates of reaction were obtained since stirring is maintained by using a specially designed mechanical stirrer. This allows efficient gas transport into the solution.

4.2.2.1 Catalytic solutions.

The catalytic solutions were prepared from rhodium-based complexes and the phosphine-containing dendrimer in ethanol in a Schlenk tube and then injected into the autoclave under argon or directly under syngas (CO/H_2, ratio 1/1). The phosphine/rhodium ratios used varied from 3/1 to 6/1 while the rhodium concentration was kept at 8.0×10^{-3} mol.dm^{-3}. None of the dendrimers used, i.e. G1-16ethylPEt$_2$, G1-24propylPEt$_2$, G1-24ethylPEt$_2$, G2-propyl-48ethylPEt$_2$, were soluble in the reaction solvent (ethanol). When using the [$Rh_2(O_2CMe)_4$] based catalyst and G1-24ethylPEt$_2$ dendrimer (ratio 3/1) a brown homogeneous solution was obtained after 3-4 hours, while a yellow solution was obtained with [$Rh(acac)(CO)_2$] and the dendritic ligand (< 1 h). Bubbling of CO/H_2 into the former brown solution led to a clear yellow solution (incorporation of CO into the complexes). Interestingly lower phosphine/rhodium ratios (below 3 to 1) led to the formation of gels when using the rhodium-based complex [$Rh(acac)(CO)_2$] or under CO/H_2 atmosphere using [$Rh_2(O_2CMe)_4$]. The gels precipitated with time to form insoluble materials, which could not be dissolved again even at higher temperature or on addition of excess ligands. It is believed that cross-linking between two dendrimers, i.e. two phosphine groups of two different dendritic ligands bind to the same rhodium atom, occurred leading to insoluble 'oligomeric' species. Steric hindrance of such complex would then prevent the new complexation of a phosphine ligand on the metal centre on addition of excess ligand.

The G1-16ethylPEt$_2$ and G1-24propylPEt$_2$ dendrimers were readily complexed with [$Rh(acac)(CO)_2$] in the ethanol solution leading to fast dissolution in the mixture while the 2nd generation dendrimer necessitated stirring during the night to obtain a homogeneous mixture. Solubility/complexation properties of the different dendrimers are thus different depending on their structure. The more crowded dendrimers (in increasing order G1-16ethylPEt$_2$, G1-24propylPEt$_2$, G1-24ethylPEt$_2$, G2-propyl-48ethylPEt$_2$) seemed less likely to form homogeneous catalytic solutions.

4.2.2.2 Hydrocarbonylation of terminal alkenes.

4.2.2.2.1 Hydrocarbonylation of hex-1-ene and non-1-ene catalysed by rhodium/G1-24ethylPEt$_2$ species.

As expected on the basis of studies with PEt_3 the only carbonylation products of hex-1-ene in ethanol using the catalytic solution with G1-24ethylPEt$_2$ and [$Rh_2(O_2CMe)_4$] or [Rh(acac)(CO)$_2$] (P/Rh = 4/1 or 6/1) were heptan-1-ol and 2-methylhexan-1-ol (120°C, 40 bar H_2/CO (ratio 1/1)).[1] Total conversion of the substrate was obtained after 16 hours in a batch autoclave while only 6 hours were necessary using the CATS rig. The increased turnover can be explain by the better stirring process of the CATS reactor leading to better mass transport of the gas reactants among the gas-liquid interface. Interestingly the linear to branched ratio (3.1:1) was slightly higher than for PEt_3 (2.4:1) under identical conditions, perhaps suggesting that the large dendrimer-based ligand was exerting some steric control over the reaction. The analysis of the products of reaction by the CATS service showed that small amounts of isomerisation products (hex-2-ene and hex-3-ene < 2 %) were formed during the catalytic process. These isomerisation products, as discussed in Chapter 2, were formed *via* the branched alkylrhodium species by β-H-elimination.

Table 4.2 Hydrocarbonylation reactions catalysed by Rh complexes of POSS derived 24-diethylphosphine dendrimer G1-24ethylPEt$_2$.

substrate	*Reaction time*	*Conv. %*	*Aldehydes %*	*Alcohols %*	*l:b ratio (alcohol)*	*Rate constant (10^{-4} s^{-1})*
hex-1-ene	16[a] or 8[b]	> 99	tr	98	3.1	3.7
non-1-ene	16[a]	> 99	tr	98	2.6	-

Reaction conditions: catalyst prepared in situ from [$Rh_2(O_2CMe)_4$] and dendrimer (Rh = 4.0 × 10^{-5} mol, P/Rh = 4/1), substrate 8.0 × 10^{-3} mole (hex-1-ene 1 cm^3, non-1-ene 1.4 cm^3), solvent 4 cm^3, 120°C, CO/H_2 40 bar.

[a] : batch autoclave, [b] : CATS rig.

The graph representing the consumption of syngas (CO/H_2) during the hydrocarbonylation of hexe-1-ene is shown in Figure 4.8. An inflection at the

beginning of the graph and a long tail at the end may indicate that different reactions occurred. Based on the results obtained with G1-24methylPMe$_2$ (see also below), the hydrocarbonylation is thus probably a two step reaction with hydroformylation followed by subsequent hydrogenation of the aldehydes. Such a mechanism would explain the traces of aldehydes found in the reaction products. A first order rate constant of rate of reaction of 3.7×10^{-4} s^{-1} was calculated for this reaction.

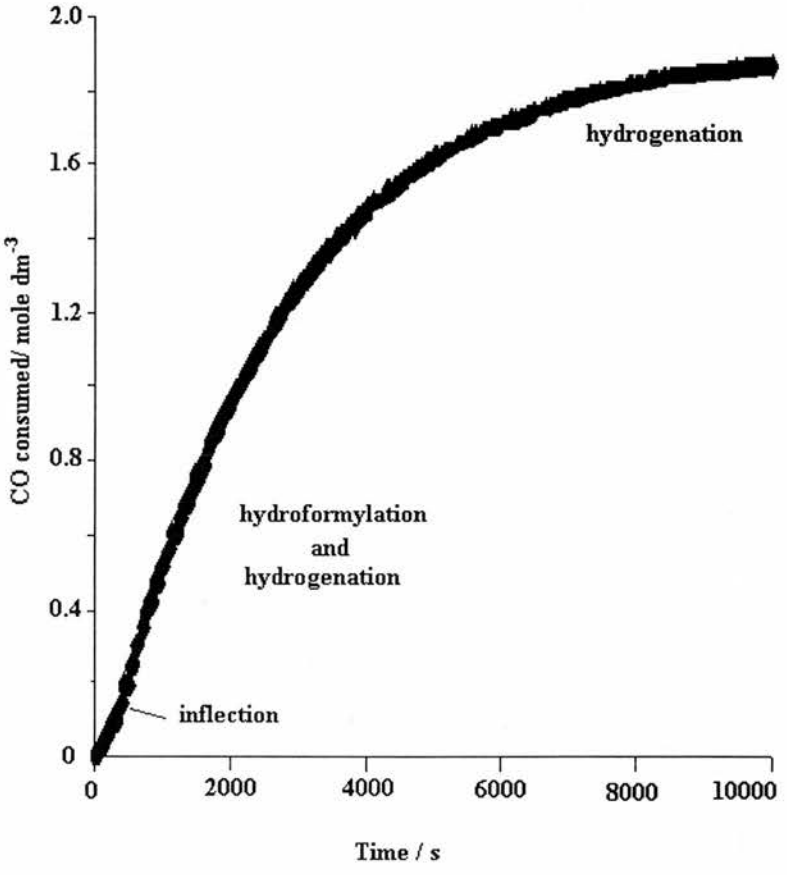

Figure 4.8 Kinetics of the hydrocarbonylation of hex-1-ene in ethanol at 120°C at 40 bar of CO/H$_2$ catalysed by the complexes [Rh (CO)$_2$(acac)]/G1-24ethylPEt$_2$.

The reduced rate at the end of the reaction could arise from the increased CO pressure and reduced H_2 pressure (two equivalents of H_2 are consumed for 1 equivalent of CO) since the reaction is positive order in H_2 pressure and negative order in CO pressure.

The hydrocarbonylation of non-1-ene (in similar conditions) led to the formation of decan-1-ol and 2-methylnonan-1-ol in 98 %. A linear to branched ratio of 2.6:1 was obtained. Traces of aldehydes and 2- and 3-nonene were also detected.

After reaction, the catalytic mixtures were bright yellow solutions although the use of batch autoclave occasionally led to formation of a yellow precipitate (see above).

4.2.2.2.2 Hydrocarbonylation of oct-1-ene by various diethylphosphine-functionalised dendrimers.

The hydrocarbonylation of oct-1-ene catalysed by the complexes formed by the rhodium-based complex [Rh(acac)$(CO)_2$] and the diethylphosphine-containing dendrimers (G1-24ethylPEt_2, G1-16ethylPEt_2, G1-24propylPEt_2, G2-propyl-48ethylPEt_2) led to the formation of nonan-1-ol and 2-methyloctan-1-ol as the only products of carbonylation.

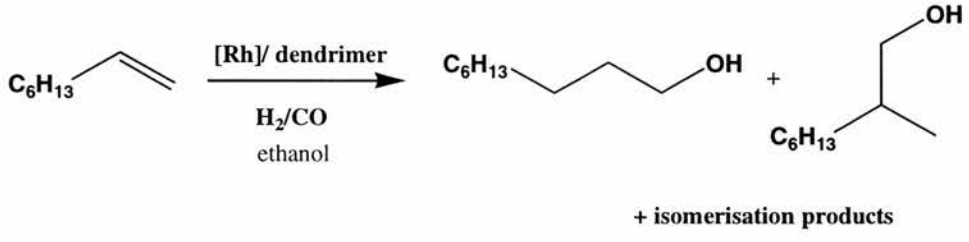

Figure 4.9 Hydrocarbonylation of oct-1-ene by rhodium/ diethylphosphine-containing dendrimer species in ethanol.

The complexes were initially formed in a Schlenk tube and injected to the autoclave when homogeneous solutions were obtained. All complexes formed from ligands G1-24ethylPEt_2 (7 atoms between the phosphorus atoms, 3 P atoms/ Si), G1-16ethylPEt_2 (7 atoms between the P atoms, 2 P atoms/ Si), G2- propyl-48PEt_2 (2^{nd} generation, 7 atoms between the P atoms, 2 P atoms/ Si) and G1-24propylPEt_2 (9 atoms between the P atoms, 3 P atoms/ Si) showed similar selectivity to the linear alcohol nonan-1-ol (*ca* 73 %), with a linear to branched ratio of *ca* 3:1. Therefore, it is likely that the active complexes formed during hydroformylation were very similar. This result differs from those obtained with the diphenylphosphine dendrimers, which led to different selectivities when using different spacers between the two phosphorus atoms (see Chapter 5). Small amounts of isomerisation products (oct-2-ene, oct-3-ene and oct-4-ene) were detected (1.8 to 3.1 % in total). For the first generation dendrimer a decreasing rate (see Table 4.3) was observed when using ligands G1-24propylPEt_2 (longer spacer atoms), G1-16ethylPEt_2 (only 16 phosphine groups) and G1-24ethylPEt_2 respectively. It seems then that crowding at the

dendrimer surface led to a slower reaction. However, the 48-branched diethylphosphine POSS, G2-propyl-48ethylPEt$_2$, led to slightly higher reactivity than its similar 1st generation counterparts G1-16ethylPEt$_2$ and G1-24ethylPEt$_2$ with a spacer of two carbons between the silicon and phosphorus atoms.

The reaction probably did not proceed through direct formation of alcohols since aldehydes (6.1 %, i.e. 10.5 % of the total amount of products) were found after 1 hour of reaction (conversion 57.9 %) when using G1-24propylPEt$_2$ as ligand. In addition, since the linear to branched ratio for the alcohols and the aldehydes were respectively of 3.8:1 and 1:3, and so disymmetric, a two steps reaction is likely to have occurred. The overall linear to branched ratio (aldehyde and alcohols) was indeed identical to the longer reaction time (2.9:1).

Table 4.3 Hydrocarbonylation reactions of oct-1-ene catalysed by Rh complexes of POSS derived diethylphosphine dendrimers.

Ligand	*time*	*k*	*Conv.*	*Isom.*	*Nonan-1-ol*	*l:b ratio*
	h	*10^{-4} s^{-1}*	*%*	*%*	*%*	
G1-16ethylPEt$_2$	8	1.5	> 99.9	3.1	73.5	3.1
G1-24ethylPEt$_2$	8	1.7	> 99.9	2.1	73.2	3.1
G1-24propylPEt$_2$	4	3.7	> 99.9	1.4	72.8	2.9
G1-24propylPEt$_2$	1	-	57.9	0.6	40.3[a]	3.8
G2-propyl-48ethylPEt$_2$	8	2.1	> 99.9	2.6	72.8	3.0

Reaction conditions: [Rh(acac)(CO)$_2$] = 4.0 × 10^{-5} mole, P/Rh = 6/1, toluene (4 cm^3) heated under CO/H$_2$ (6 bar) for 1 h. Substrate oct-1-ene (8.3 x 10^{-3} mol) injected and pressure increased to CO/H$_2$ 40 bar, 120°C. Pressure kept constant through mass flow controller and feed from a ballast vessel. Pressure drop in ballast vessel monitored every 5 s.

[a] : nonan-1-al 6.1 %, aldehyde l:b = 0.33

Interestingly after reaction with the three 1st generation dendritic ligands, yellow (crystalline) suspended solids were sometimes found. A similar formation of a crystalline solid was noticed when bubbling CO/H$_2$ through a solution of the G1-24ethylPEt$_2$ dendrimer and [Rh(acac)(CO)$_2$] in ethanol to study the NMR spectrometry of the complex. This precipitation (NMR study) only occurred after

partial evaporation of the solvent. It was then attempted to isolate the crystals for X-ray crystallography characterisation. However the solid, which was extracted, did not diffract.

4.2.2.2.3 Hydroformylation and hydrocarbonylation reactions using dicyclohexyl-phosphine functionalised dendrimers.

Dendrimers G1-16ethylPCy$_2$ and G1-16ethylPCy$_{0.64}$Et$_{1.36}$ (Figure 4.13) with dicyclohexyl-phosphine moieties were used as ligands for the hydroformylation/ hydrocarbonylation of oct-1-ene.

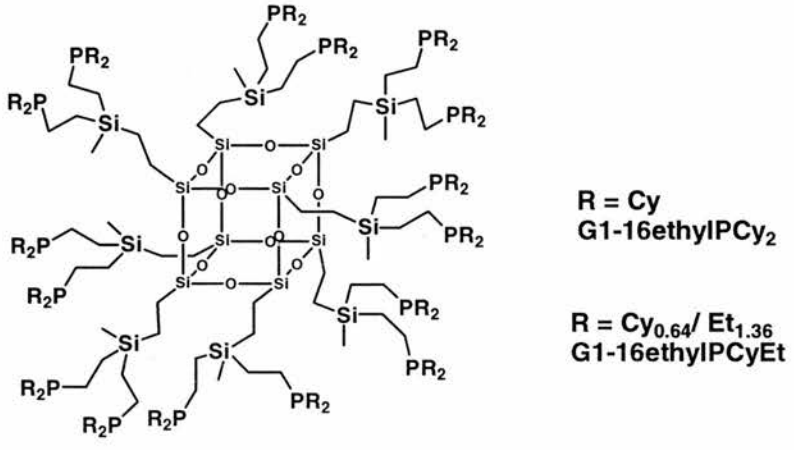

Figure 4.10 Dicyclohexylphosphine-containing POSS used as ligands for the hydroformylation of oct-1-ene.

Hydroformylation in toluene at 120°C and 10 bar of syngas by the complex formed from [Rh(acac)(CO)$_2$] and G1-24ethylPCy$_2$ (only 12 branches substituted) led to the formation of nonan-1-al (57.2 %) and 2-methyloctan-1-al (40.3 %). A poor selectivity to the linear aldehyde, l:b ratio of only 1.4, was obtained. It is believed that the bis ligand species responsible for the selectivity could not formed due to the steric hindrance of such dicyclohexylphosphine ligands. When using the di-substituted diethyl and dicyclohexylphosphine dendrimer (G1-16ethylPCyEt) as ligand of the rhodium-based catalyst derived from [Rh(acac)(CO)$_2$] for the hydrocarbonylation of oct-1-ene, in ethanol at 120°C under 40 bar of syngas, the alcohols (59.9 % of nonan-1-ol and 32.4 % of 2-methyloctan-1-ol) were the main products of reaction. A slightly higher linear to branched ratio was obtained (l:b = 1.8:1). This value is however low compared to those obtained from the

diethylphosphine dendrimers showing that the catalytic active species were affected by the bulky cyclohexyl substituents.

Table 4.4 Hydroformylation or Hydrocarbonylation of octe-1-ene catalysed by [Rh(acac)(CO)$_2$]/ dicyclohexylphosphine-containing dendrimers.

Ligand	*Solvent*	*Time h*	*k 10^{-4} s^{-1}*	*Conv. %*	*Nonan -1-ol %*	*Nonan-1-al %*	*l:b ratio*
G1-16ethylPCy$_2$	toluene[a]	5	1.9	> 99.9	-	57.2	1.4
G1-16ethylPEtCy	ethanol[b]	8	2.4	> 99.9	59.9	-	1.8

Reaction conditions: [Rh(acac)(CO)$_2$] = 4.0×10^{-5} mole, P/Rh = 6/1, substrate 8.3×10^{-3} mole, solvent (4 cm^3), 120°C.

[a] :Rh = 2.0×10^{-5} mole, CO/ H_2 10 bar, [b] :Rh = 4.0×10^{-5} mole, CO/ H_2 40 bar.

4.2.2.3 Hydrocarbonylation of prop-2-en-1-ol

The synthesis of butane-1,4-diol is an important industrial process since the diol is used as an intermediate in the formation of tetrahydrofuran and of polyester resins.[3] The hydrocarbonylation in protic solvent of prop-2-en-1-ol was thus carried out. The products expected from prop-2-en-1-ol are butane-1,4-diol and 2-methylpropane-1,3-diol if the reaction followed a similar pathway that of the hydrocarbonylation of hex-1-ene. However the reaction carried out in ethanol led to butane-1,4-diol in 60.8 % yield and to the branched alcohols 2-methylpropan-1-ol and 2-methylpropane-1,3-diol in respectively 26.1 % and 4.4 % (Figure 4.11 and Table 4.5). The other products detected (see Table 4.5 and Appendix III) were 2-methylpropan-1-al (2.5 %), propanol (1.4 %), 2-methylprop-2-en-1-ol (0.3 %) 4-hydroxybutan-1-al (0.5 %), 2-methylprop-2-en-1-al (0.2 %). Traces of propan-1-al, 2-methyl-3-hydroxypropan-1-al and the cyclics γ-butyrolactone (0.4 %) and 2,3-dihydrofuran were also among the products with 3.4 % of undetermined products. The linear to branched ratio (taking account of all the different products) was 1.8:1. This distribution of products is indeed similar to early studies carried out by Cole-Hamilton and co-workers.[2] 2-methylpropan-1-ol was indeed the major branched product observed in these studies when prop-2-en-1-ol was the substrate. The

production of 2-methylpropan-1-ol as the major branched product requires some explanations since it cannot be a direct product of the hydrocarbonylation of the substrate.

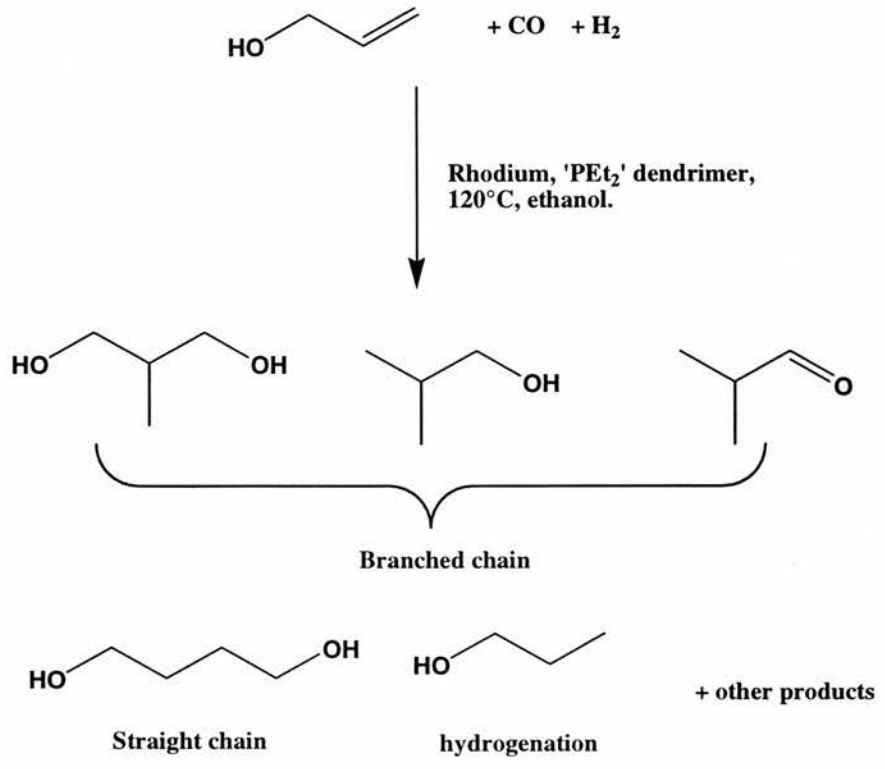

Figure 4.11 Major products obtained from the hydrocarbonylation of prop-2-en-1-ol in ethanol catalysed by [Rh(acac)(CO)$_2$]/G1-24ethylPEt$_2$ complexes.

The formation of 2-methylpropan-1-ol (C4 compound) must indeed involve dehydration at some point of the reaction followed by hydrogenation. It was previously proposed that the hydrocarbonylation of hex-1-ene and prop-2-en-1-ol in protic solvents using PEt_3 as ligand may involve a single step reaction to the alcohols *via* a hydroxycarbene intermediate (see Chapter 2, Section 2.5).[1, 2] The mechanism of formation of 2-methylpropan-1-ol proposed was thus occurring *via* this intermediate to form 2-methylpropan-1-al, which was then hydrogenated to 2-methylpropan-1-ol (Scheme 4.1). Evidence was indeed presented that the dehydration step occurred from the hydroxycarbene intermediate.[2]

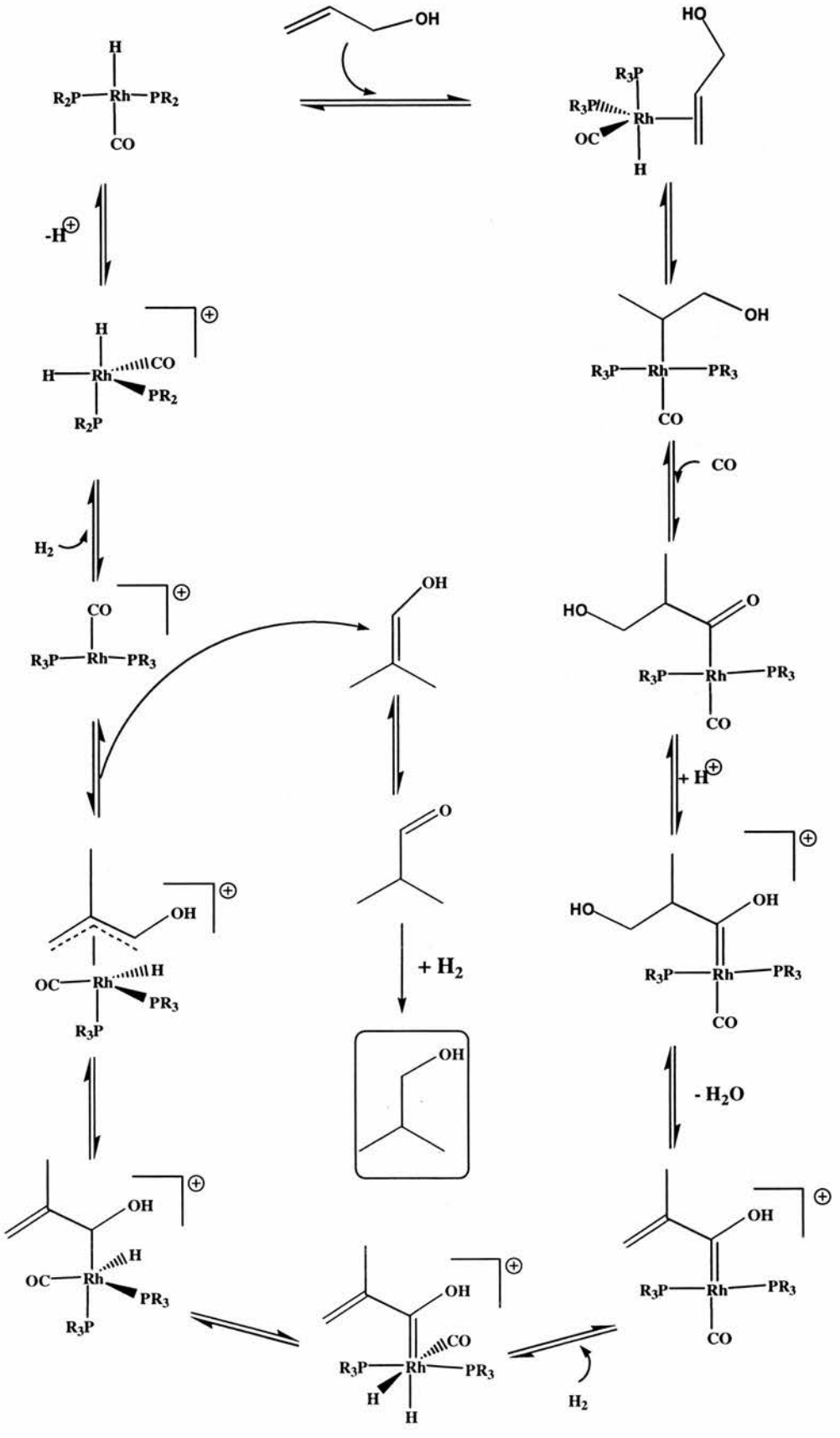

Scheme 4.1 Postulated mechanism for the production of 2-methylpropan-1-ol via the hydroxycarbene intermediate.

Table 4.5 Hydrocarbonylation of prop-2-en-1-ol catalysed by rhodium/G1-16ethylPEt2 complexes at 120°C and 40 bar H_2/CO.

Solvent	*T*	k_1 [a]	k_2 [b]	*Conv.*	*BDO*	*MPO*	*MPD*	*MPA*	*HBA*
	h	10^{-3} s^{-1}	10^{-3} s^{-1}	%	%	%	%	%	%
Ethanol	2	1.2	-	99.9	60.8	26.1	4.4	2.5	0.5
Ethanol	0.25	-	-	67.5	14.1	3.6	1.8	15.6	25.0
Ethanol	-	-	-	100	20.9	5.4	2.7	23.2	37.1
THF	3	1.2	0.23	99.8	59.3	17.1	5.5	8.0	4.1
THF	9	-	-	99.9	64.9	21.9	6.9	1.1	0.2

Reaction conditions [Rh(acac)$(CO)_2$] (4.0×10^{-5} mole), G1-24ethylPEt_2 (1.0×10^{-5} mol) , solvent 4 cm^3, substrate 1 cm^3 (14.7×10^{-3} mol), 120°C, 40 bar H_2/CO.

[a] : k_1 = rate constant for the hydroformylation step, [b] : k_2 = rate constant for the hydrogenation step.

BDO = 1,4-butanediol, MPO = 2-methylpropan-1-ol, MPD = 2-methylpropane-1,3-diol, MPA = 2-methylpropan-1-al, HBA= 4-hydroxybutan-1-al.

Full detail of the distribution of the products is given Appendix III.

However in our reaction after 15 minutes, more than 67 % of the substrate had reacted, with the aldehydes being the major products. Normalising this conversion to 100 %, 37.1 % of the products was the linear aldehyde 4-hydroxybutan-1-al while the main branched product was 2-methylpropan-1-al. Only 20.9 % and 5.4 % of the products were respectively butane-1,4-diol and 2-methylpropan-1-ol (Figure 4.12). The reaction thus clearly occurred by a sequential pathway, i.e. hydroformylation to the aldehyde and subsequent hydrogenation to the alcohol (Figure 4.5). For the linear product this implies that the hydroxycarbene mechanism is not operative under these conditions (or at least not exclusively). For the branched aldehyde this is less certain since 2-methylpropan-1-al is an intermediate in the formation of 2-methylpropan-1-ol by the proposed hydroxycarbene route. The low amount of the expected branched aldehyde, 2-methyl-3-hydroxypropan-1-al (1.4 % for a 100% normalised conversion), and of its hydrogenated product, 2-methylpropane-1,3-diol (2.7 % for a 100% normalised conversion) showed that these products were probably not the intermediates in the

formation of 2-methylpropan-1-al and 2-methylpropan-1-ol (see Table 4.5 and Appendix III).

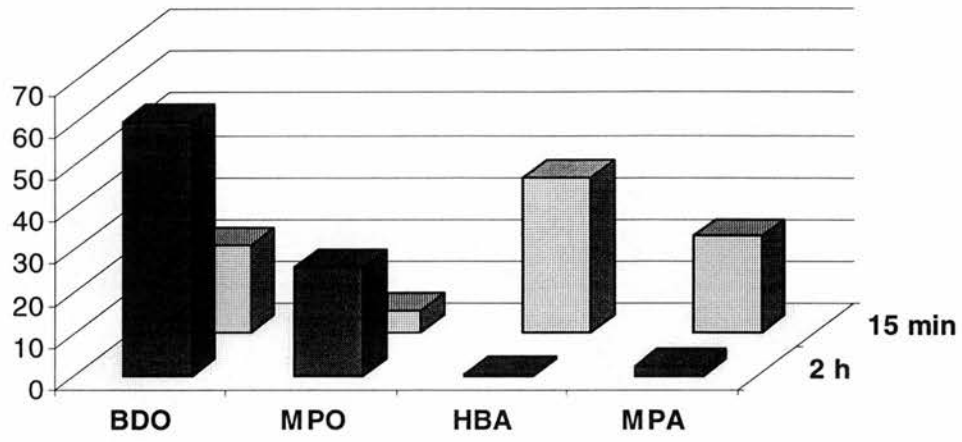

Figure 4.12 Distribution of the major products of the hydrocarbonylation prop-2-en-1-ol in ethanol catalysed by Rh dendritic complexes after 15 minutes and 2 hours.

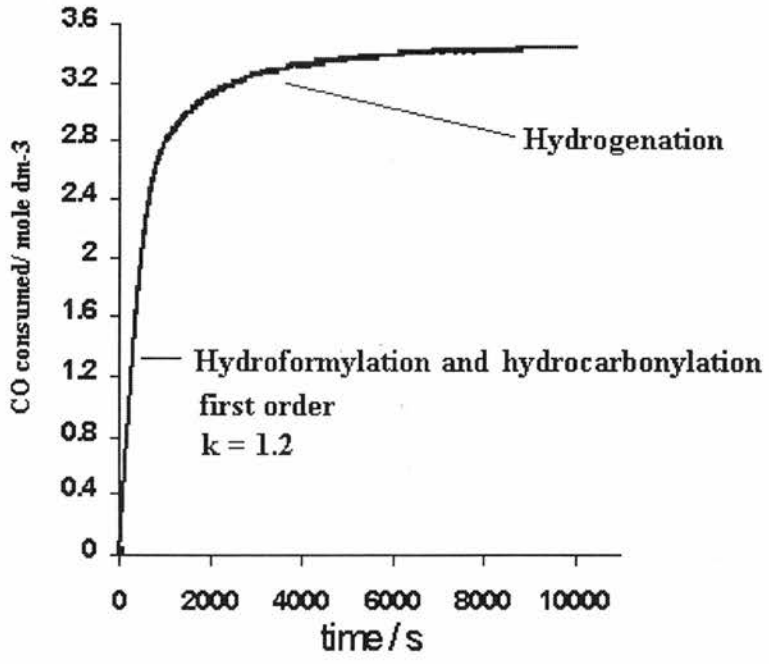

Figure 4.13 Kinetic of the hydrocarbonylation of prop-2-en-1-ol catalysed by [Rh(CO$_2$)(acac)]/ G1-24ethylPEt$_2$ at 120°C and 40 bar (H$_2$/CO) in ethanol (k in 10^{-3} s^{-1}).

As shown in the graph in Figure 4.13 corresponding to the gas consumption during the hydroformylation of prop-2-en-1-ol in ethanol catalysed by the complex formed between [Rh(acac)$(CO)_2$] and dendrimer G1-24ethylPEt_2, two reaction regimes are visible. Firstly, a hydroformylation reaction occurred with possibly a concurrent hydrocarbonylation reaction (see below), followed by a slower hydrogenation process giving a long tail curb. A first order reaction was found for the first step ($k_1 = 1.2 \times 10^{-3}$ s^{-1}).

In the early studies Cole-Hamilton and co-workers proposed that 2-methylpropan-1-ol was formed *via* a protonated acyl intermediate (see above) since the mechanism of the hydrocarbonylation reaction suggested included this intermediate in a one step reaction process.[2] The mechanism of formation of butane-1,4-diol is different in our study, so it is also possible that 2-methylpropan-1-ol is produced by a different process.

2-methylprop-2-en-1-al can be considered as an intermediate in the formation of 2-methylpropan-1-ol since a simple hydrogenation would lead to the alcohol product (Figure 4.14).

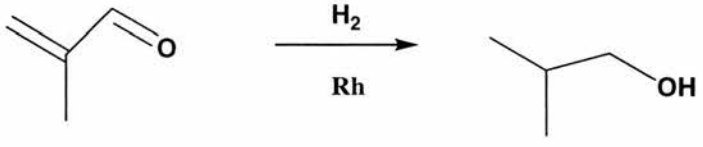

Figure 4.14 Hydrogenation of 2-methylprop-2-en-1-al to 2-methylpropan-1-ol.

Two possible mechanisms of formation of this conjugated compound were considered. The first mechanism involved the acylrhodium complex as shown in Scheme 4.2. Dehydration on the rhodium complex and subsequent oxidative addition of H_2 followed by reductive elimination would give 2-methylprop-2-en-1-al. An equivalent dehydration on the linear alkylrhodium complex would not be favoured since no conjugated species can be formed.

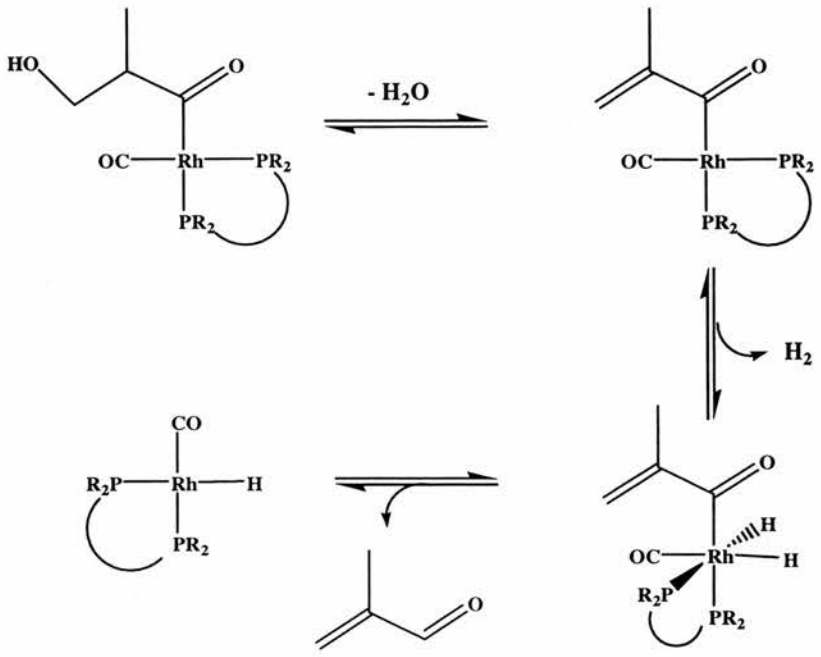

Scheme 4.2 Possible mechanism of formation of 2-methylprop-2-en-1-al via a branched alkylrhodium complex.

The second mechanism of formation of the conjugated compound implies a simple dehydration of 3-hydroxy-2-methylpropan-1-al[4] formed by hydroformylation of the substrate (Scheme 4.3).

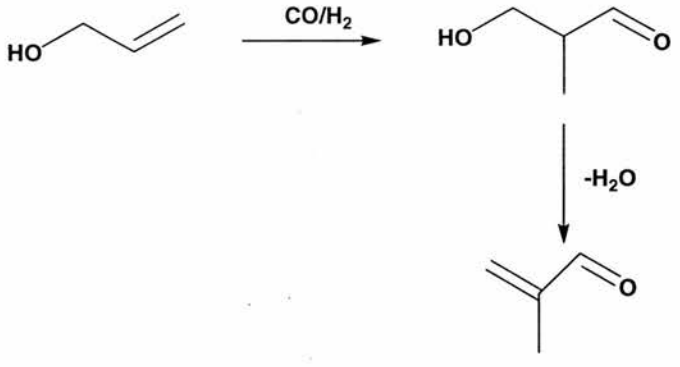

Scheme 4.3 Possible route to the formation of 2-methylprop-2-en-1-al.

However Cole-Hamilton and co-workers showed that the products of hydroformylation of 2-methylprop-2-en-1-al did not correspond to 2-methylpropan-1-ol (< 5 %) when used as the only substrate in similar conditions.[2] One would then rule out these two mechanisms. However in our case, 2-methylprop-2-en-1-al and 2-methyl-3-hydroxypropan-1-al were found as products of reaction (this was not the case in the previous studies) when the reaction was stopped after 15 min (respectively in 2 % and 1.3 % of the total products). Although the amounts of

products were low, one may have to consider the formation of 2-methylpropan-1-ol via a rapid dehydration and hydrogenation in these particular conditions.

Another possible mechanism of formation of 2-methylpropan-1-ol considered by Cole-Hamilton and co-workers was the dehydration of 2-methylpropane-1,3-diol followed by hydrogenation (Scheme 4.4). However the products obtained from 2-methylprop-2-en-1-ol under catalytic conditions were carbonylation products and no important hydrogenation of the substrate was found (< 5 %).[3] In addition, the dehydration of the diol is less likely since no conjugated system would be formed (2-methylprop-2-en-1-ol represented only 0.4 % of the products after 15 minutes of reaction).

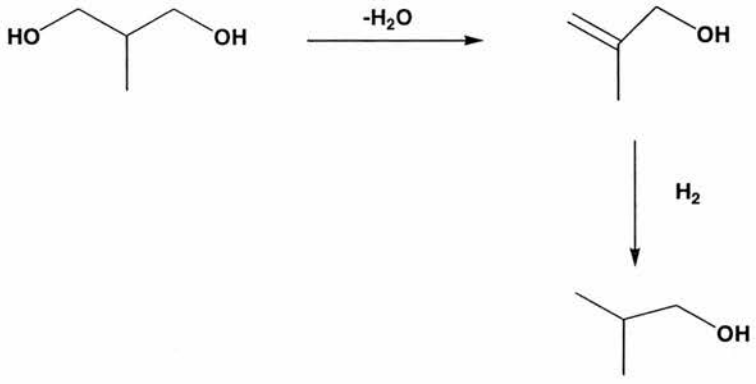

Scheme 4.4 Possible route of formation of 2-methylpropan-1-ol via hydrogenation of 2-methylprop-2-en-1-ol.

One other alternative is possible. The linear butane-1,4-diol may be formed through a two step process, whilst the branched product could be formed through the hydroxycarbene route. The relative rate of protonation of the acyl intermediate and oxidative addition of H_2 to the same intermediate determine which route will be followed (Scheme 4.5). The branched acyl intermediate complex has its hydroxy proton in such a position that it may act to protonate the carbonyl oxygen via a six membered transition state. This may greatly enhance the rate of formation of the hydroxycarbene intermediate. For the linear acyl complex, the equivalent intermediate would involve a seven membered ring, which would not be expected to give such a rate enhancement.

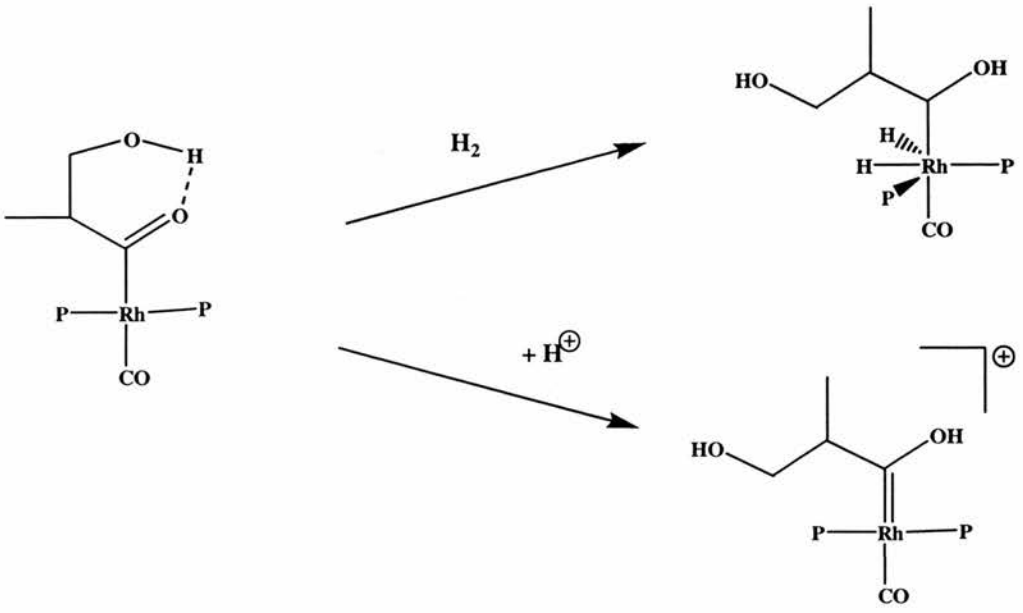

Scheme 4.5 Addition of H_2 to the branched acyl intermediate versus formation of the hydroxycarbene species (P = phosphine species).

If this explanation is correct, there is clearly fine balance between the "normal" hydroformylation mechanism and the hydroxycarbene route. Further evidence for this comes from the observation of 2-methyl-3-hydroxypropan-1-al after short reaction times, since this must come from the "normal" hydroformylation pathway via the branched acyl intermediate. This suggests that both pathways are occurring for the branched aldehyde.

The similarity in rate between protonation and H_2 addition to the acyl intermediate may allow an explanation of the differences observed between this dendrimer based catalyst and a catalyst involving PEt_3. The reaction involving PEt_3 were carried out under conditions of severe gas transfer limitation (no stirring) whilst those with dendrimer involve rapid stirring. The rate of H_2 addition to the complex will be much slower for the PEt_3 reaction because the concentration of H_2 is depleted, despite the similar pressure. Protonation will thus compete effectively with H_2 addition. When gas transfer is more efficient (dendrimer reactions), the rate of H_2 addition will be greatly increased and will predominate over protonation.

The formation of the cyclic compound γ-butyrolactone can be explained by the intramolecular attack of the terminal hydroxy group on the acyl C atom (see Scheme 4.6). Subsequent hydrogenation of the lactone and dehydration led to the 2,3-dihydrofuran compound. Propanol could either arise from isomerisation of the

substrate to give propanal (indeed propanal was found as a product after 15 min) followed by hydrogenation or it could be directly formed by hydrogenation of the substrate.

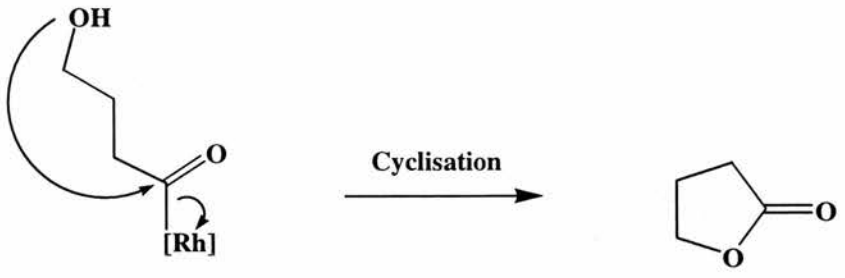

Scheme 4.6 Simplified cyclisation of the straight chain acylrhodium complexes to form γ-butyrolactone.

The hydrocarbonylation of prop-2-en-1-ol in THF (see Table 4.5 and Appendix III) gave similar results with the formation of butane-1,4-diol (64.9 % after 9 h), 2-methylpropan-1-ol (21.9 %) and 2-methylpropane-1,3-diol (6.9 %). Interestingly the selectivity (include all the linear and branched products) was somewhat higher in THF (l:b = 2.2:1 instead of 1.8:1 in ethanol). The rate of formation of the desired alcohol products was much lower (*ca* half) in the less polar solvent despite a similar rate of hydroformylation ($k_1 = 1.2 \times 10^{-3}$ s^{-1}) being found (first order reaction). The hydrogenation step was much slower in THF ($k_2 = 0.23 \times 10^{-3}$ s^{-1}) (first order reaction). Similar results were previously found with simple alkylphosphines (PEt_3).[3] Unfortunately the determination of the (small) amount of 2-methylprop-2-en-1-al could not be achieved due to the partial overlapping of this compound and THF in the GC. Nevertheless it seemed that a higher formation of 2-methylpropane-1,3-diol (6.9 % instead of 4.4 % in ethanol) was obtained in THF to the detriment of 2-methylpropan-1-ol and other dehydrated products (23.1 % instead of 29.1 % in ethanol) indicating that dehydration occurred slightly more slowly in this solvent or that the hydroxycarbene route was less favoured in THF.

Shorter reaction time (3 h instead of 9 h) confirmed that the reaction proceeded in two steps since higher amounts of the aldehyde products were detected in the short reaction (see Table 4.5).

4.3 Mechanistic considerations.

To clarify the mode of chelation of the dendritic structure, i.e. whether or not bidendate or tridentate coordination of the phosphine to the rhodium centre occurred or if bimetallic species were formed, a ^{31}P NMR study of the dendritic rhodium complexes was carried out. The ^{31}P NMR spectrum of the solution formed under CO/H_2 from the $[Rh(acac)(CO)_2]$/G1-24ethylPEt$_2$ species (P/Rh = 4/1) showed several species in solution. Two resonances were observed under 1 atmosphere of CO/ H_2 at room temperature in ethanol solution (Figure 4.15).

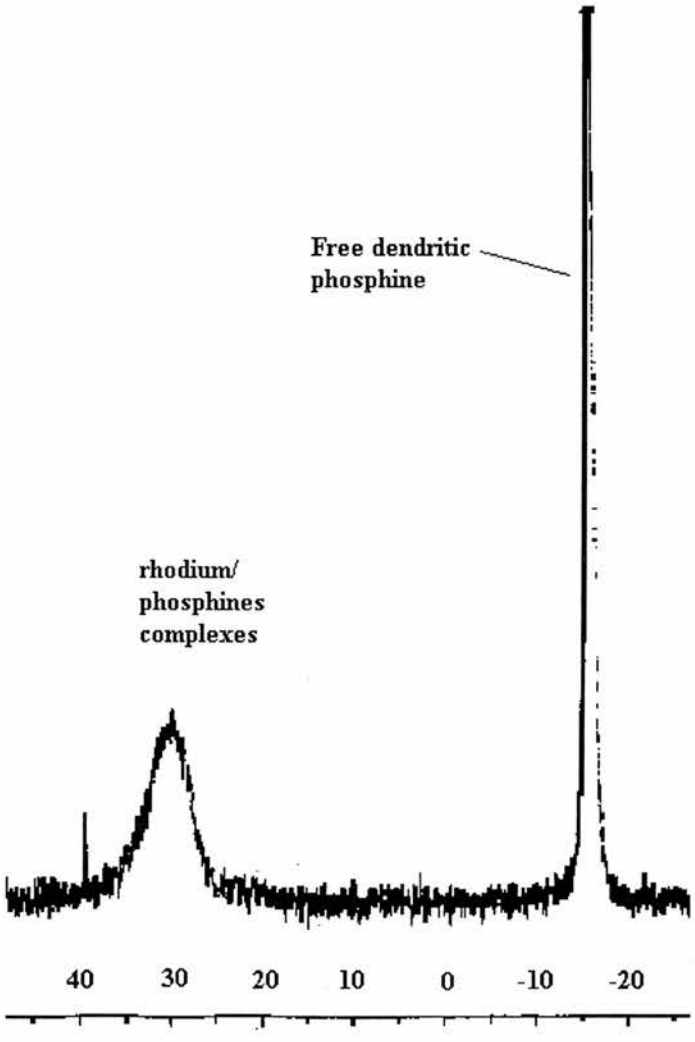

Figure 4.15 ^{31}P NMR spectrum of $[Rh(acac)(CO)_2]$/G1-24ethylPEt$_2$ species (P/Rh = 4/1) under 1 atmosphere of CO/H_2 in ethanol at 25°C.

One signal was found corresponding to the free P atoms (G1-24ethylPEt$_2$ resonates at δ_P -16.0 ppm) (with at half maximum = 50 Hz) and the other resonance centred at δ_P 29.6 ppm (broad signal, width at half maximum = 660 Hz) was attributed to $[RhH(CO)_2(P)_2]$ ($[RhH(CO)_2(PEt_3)_2]$ resonates at δ_P 24.5 ppm)[2] or $[RhH(CO)(P)_3]$

species ([RhH(CO) (PEt_3)$_3$] resonates at δ_P 26.2 ppm)[2] (P = Dend-PR_2, Dend for dendrimer). However since the integration of the signal indicated a distribution of 2 to 2 for the free P atoms and the rhodium species, it is believed that the dominating rhodium complexes was more likely [$RhH(CO)_2(P)_2$]. At –50°C (Figure 4.16), the resonance of the free P atoms stayed unchanged while the rhodium complex species showed some asymmetric broadening suggesting fluxionality within the bound complex. The fact that the resonances for the Rh bound P atoms are broad at all temperatures suggests that there are different coordination environments.

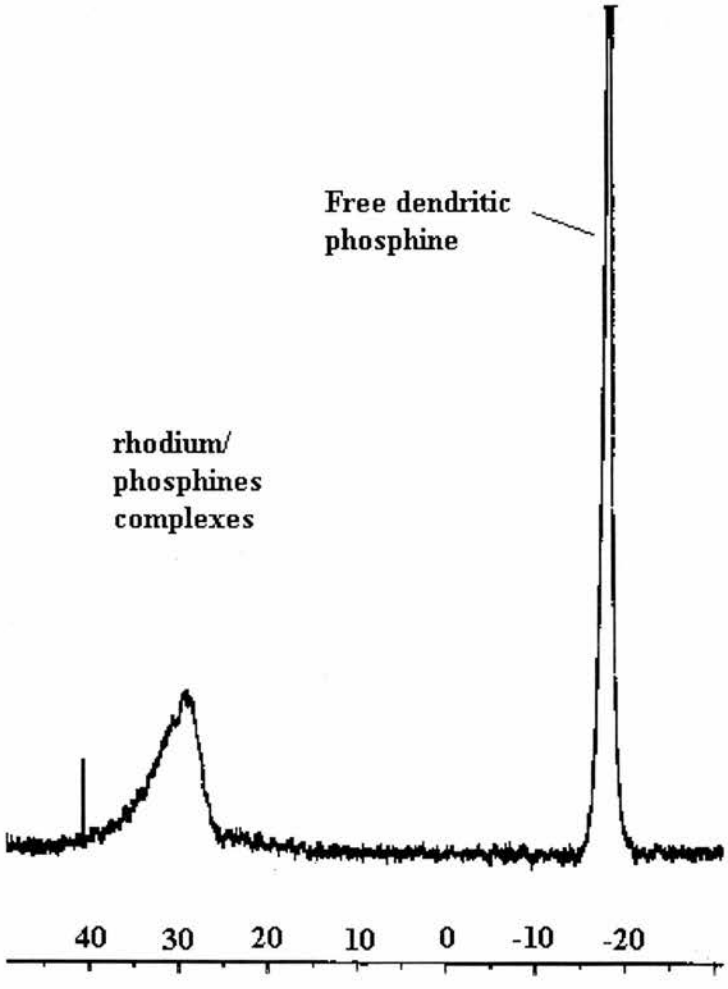

Figure 4.16 ^{31}P NMR spectrum of [Rh(acac)$(CO)_2$]/G1-24ethylPEt_2 species (P/Rh = 4/1) under 1 atmosphere of CO/H_2 in ethanol at -50°C.

The mechanism of formation of the aldehydes is believed to be similar to that proposed by Wilkinson[5, 6]. This mechanism was discussed in Chapter 2. Since we could not identify the species, i.e. probably [$RhH(CO)_2(P)_2$] or [$RhH(CO)(P)_3$] under resting condition, we have simplified the mechanism of reaction by introducing a ligand L which could be either CO or a phosphine species. In addition, it is believed

that the rhodium complexes presented in this mechanism might interchange at some points a phosphine and CO ligands.

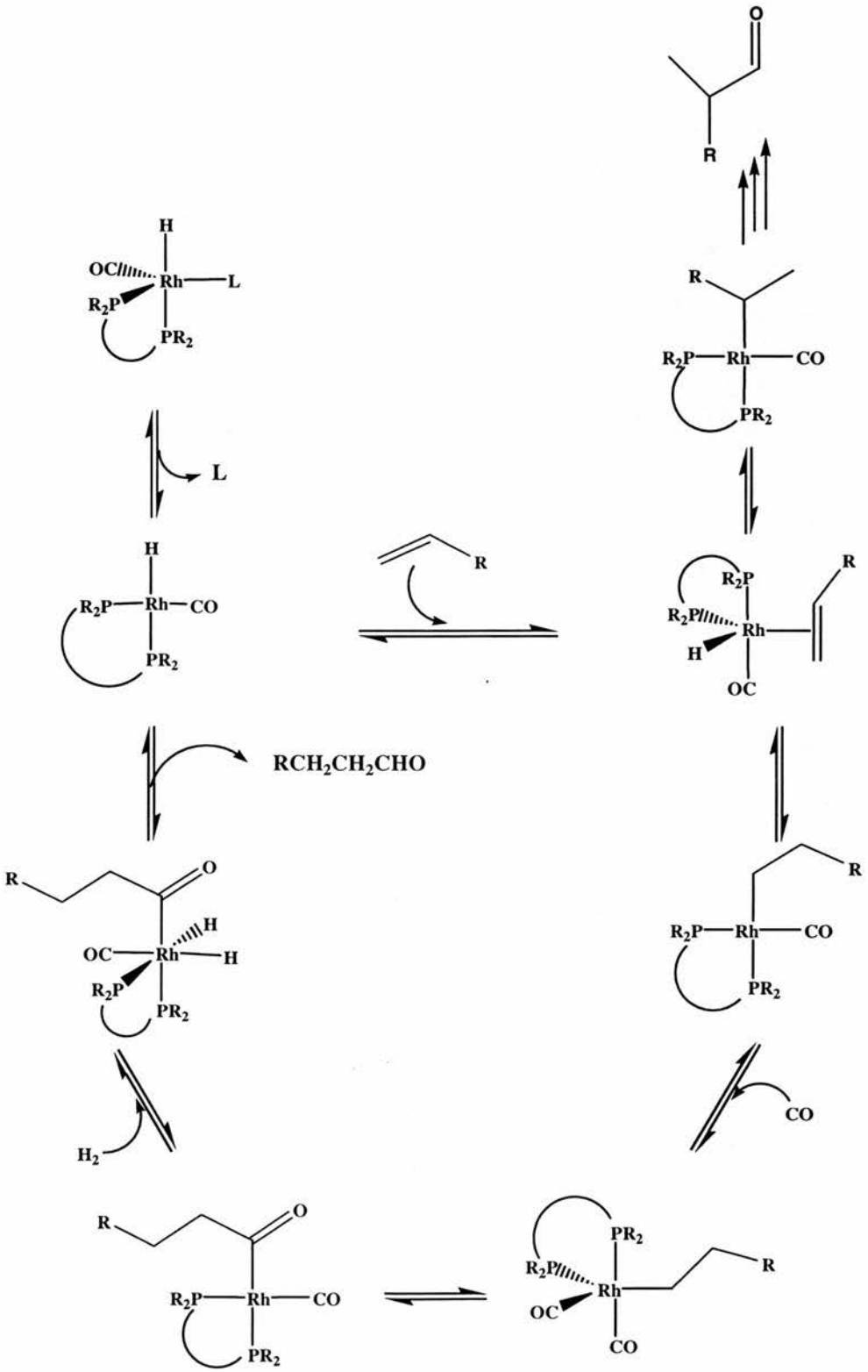

Scheme 4.7 Proposed mechanism for the hydroformylation of alkenes by rhodium/ dialkylphosphine-containing dendrimer in ethanol. L = Dend-PR_2 or CO.

The mechanism proposed from labelling studies for the hydrogenation of the aldehyde[1] is shown in Scheme 4.8. Two parallel routes were considered since labelling studies showed different distribution of the deuteriated compounds. The upper cycle in Scheme 4.8 corresponds to the formation of alcohols by the mechanism expected for hydrogenation of an aldehyde via an hydroxylalkyl intermediate. The second mechanism proposed is via a protonated acyl intermediate. Since the reaction occurred in two steps in our study, and so no protonated acyl intermediates seemed to be formed, it is likely that the main mechanism of hydrogenation is via the formation of hydroxylalkyl species (upper cycle in Scheme 4.8).

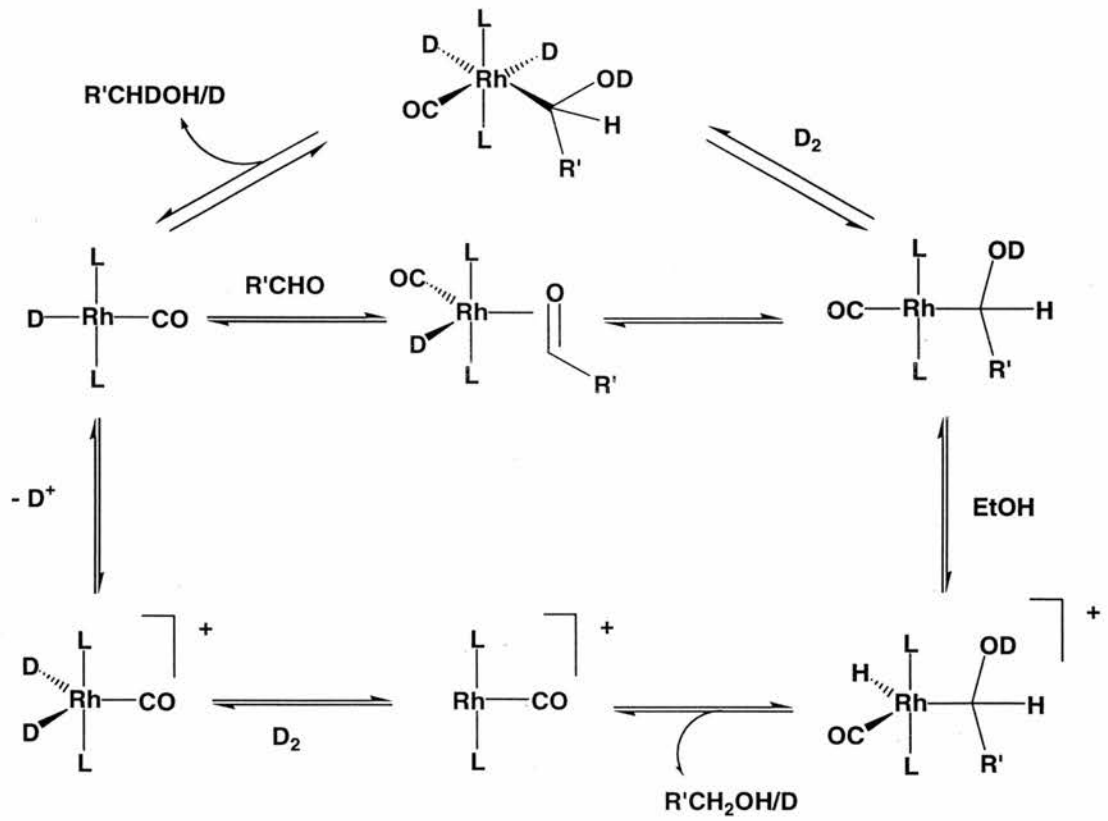

Scheme 4.8 Proposed hydrogenation mechanism of heptanal catalysed by [RhD(CO)(PEt$_3$)$_3$] using D_2/ CO in ethanol (L = PEt$_3$,, R' = C_6H_{13}).[1]

4.4 Conclusion.

These 1st and 2nd generation alkylphosphine dendrimers were successfully applied as ligands for the hydrocarbonylation of linear alkenes leading, in some cases to slightly higher l:b ratios in the alcohols products than with free triethylphosphine ligand (3.1:1 for the triethylphosphine type dendrimers instead of 2.4:1). The reaction was shown to occur *via* formation of the aldehydes and subsequent hydrogenation to the alcohols. This result contrasts with those obtained in previous studies.[1, 2]

The hydrocarbonylation of propen-1-ol using the dendritic ligand G1-24ethylPEt$_2$ led to the formation of identical products (mainly butane-1,4-diol and 2-methylpropan-1-ol) to those obtained with the free PEt$_3$ species. However the formation of the linear alcohol (butane-1,4-diol) clearly occurred via a two step reaction i.e. hydroformylation to form 4-hydroxybutan-1-al and subsequent hydrogenation to the diol. The formation of 2-methyl-propan-1-ol was suggested to occur *via* a hydroxycarbene route.

The different functionalised dendrimers showed different properties depending upon the phosphine on the outer shell, and the complexity of the dendrimer itself. As indicated previously, hexyl and ethyl groups on the phosphine allowed a better solubility than their methyl equivalents (solubility in toluene for example). Indeed whichever diethylphosphine dendrimer was used, its ability to form homogeneous systems with rhodium complexes was higher than its dimethylphosphine counterpart. It seems that long alkyl chain on the dendrimer increases the solubility of the dendrimers.

Understanding the effect of the dendrimer structure in the rates and selectivity of hydroformylation reaction is not straightforward since the different generation dendrimers may show different properties depending on the phosphine endgroups. Whist the dendrimer generation did not seem to modify the selectivity of the hydroformylation reaction, the branching pattern had a large influence on the reaction rate. Indeed, the number of functional groups and the length of the bridge between the phosphines were determinant factors in the reactivity of the rhodium complexes formed leading to different rate of reaction.

4.5 References for chapter 4.

1 M. C. Simpson, A. W. S. Currie, J. A. Andersen, M. J. Green, and D. J. Cole-Hamilton, *J. Chem. Soc., Dalton Trans.*, 1996, 1793.

2 J. K. MacDougall, M. C. Simpson, M. J. Green, and D. J. Cole-Hamilton, *J. Chem. Soc., Dalton Trans.*, 1996, 1161.

3 A. M. Brownstein, *Chemtech.*, 1991, 506.

4 J. C. U. Pittman and W. D. Honnick, *J. Org. Chem.*, 1980, **45**, 2132.

5 D. Evans, J. A. Osborn, and G. Wilkinson, *J. Chem. Soc. A.*, 1968, 3133.

6 D. Evans, G. Yagupsky, and G. Wilkinson, *J. Chem. Soc. A*, 1968, 2660.

Chapter Five: Hydroformylation reactions catalysed by dendritic rhodium arylphosphine or phosphite complexes.

5 Hydroformylation reactions catalysed by dendritic rhodium arylphosphine or phosphite complexes.

5.1 Introduction.

The hydroformylation of long chain alkenes to form aldehydes is an important industrial process.[1] However the use of rhodium complexes, which show high reactivity and selectivity, is restrained by the cost of such transition metals. The full recovery of such catalyst is therefore essential. No efficient recovery process is however yet successfully applied to industrial scale for long chain alkenes (see Chapter 2). The use of dendrimers could help to overcome this problem since their size may allow recycling using ultrafiltration techniques (see Chapter 1).

Since two major products are formed during the hydroformylation reaction (linear and branched aldehydes), the design of a ligand favouring one of the isomers (mainly the linear aldehyde) has triggered a considerable amount of interest and research. So far not many rhodium catalytic systems have shown high regioselectivity, only bidendate phosphine chelates such as BISBI[2] and Xantphos[3] type ligands allowed high regioselectivity (ratio up to 50:1 to the linear aldehyde) (see Chapter 2). A few bulky diphosphite ligands also showed some interesting selectivity coupled with high activities (see Chapter 2).

In this chapter, we will show that 1st and 2nd generation polyhedral octasilsesquioxane (POSS) dendrimers containing diphenylphosphine moieties at their periphery were successfully used as ligands of rhodium species for the hydroformylation of oct-1-ene. Unexpected high regioselectivity to the linear aldehyde was found for a specific type of POSS dendritic ligand (16 diphenylphosphine-containing dendrimer, spacer of 5 atoms between the P atoms) while the other dendritic ligands prepared showed lower selectivity.

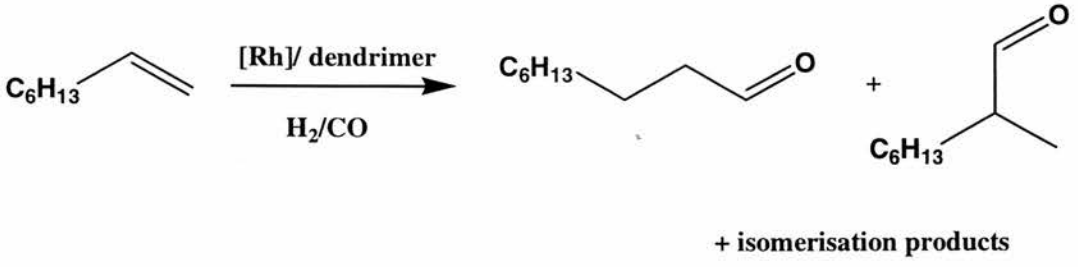

Figure 5.1 Hydroformylation of oct-1-ene in toluene catalysed by [Rh(acac)(CO)$_2$]/phosphine-containing dendrimers.

Unfortunately we were not able to carry out recycling experiments because of the lack of a suitable ultrafiltration membrane compatible with hydroformylation reactions (high temperature, high pressure, organic solvents).

5.2 Hydroformylation reaction using 16-diphenylphosphine-containing dendrimers G1-16ethylPPh$_2$.

The 16-diphenylphosphine functionalised dendrimer, G1-16ethylPPh$_2$ (Figure 5.2), was used as ligand for rhodium ([Rh(acac)(CO)$_2$] as metal source) for the hydroformylation of oct-1-ene under CO/H$_2$ pressure (ratio 1:1). The reactions were carried out in toluene (4 cm^3) at various temperature (80°C to 120°C) and pressure (10 to 20 bar) at a fixed rhodium concentration (2.0×10^{-5} mol, [Rh] = 3.77×10^{-3} mol dm^{-3}) in order to determine the optimised conditions of reaction. The effect of the phosphine/rhodium ratio on the reaction was also investigated since various ratios (P/Rh = 2 to 10.8/1) were used.

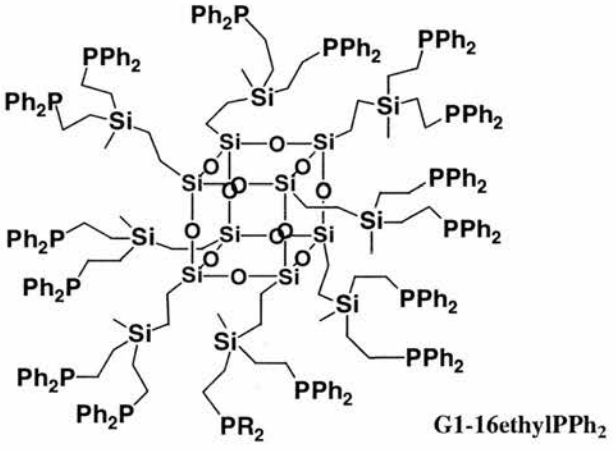

Figure 5.2 A 16-diphenylphosphine functionalised dendrimer, G1-16ethylPPh$_2$, used as ligand for rhodium in the hydroformylation of oct-1-ene.

As previously discussed in Chapter 4, the catalytic solutions were prepared beforehand and injected into the autoclave. The autoclave was then pressurised to the desired H$_2$/CO (syngas) pressure. The catalytic solutions formed (phosphine-containing dendrimers and [Rh(acac)(CO)$_2$] in toluene) were homogeneous yellow-orange mixtures depending on the concentration of rhodium and/or dendrimer. Interestingly the total complexation of the dendritic phosphines to the metal centre was obtained only after a few seconds and was accompanied by the appearance of bubbles in the solution (replacement of CO by a phosphorus species in the metal-

based catalyst). Under H_2/CO pressure these solutions turned bright yellow and remained like this until after hydroformylation reaction. Low phosphine/rhodium ratios (≤ 2.5/1) led to the formation of an insoluble solid (*via* a gel). A similar precipitation occurred under H_2/CO pressure when using a P/Rh ratio below 3/1. Attempts to dissolve the precipitate back in solution failed. It is believed that, as discussed in Chapter 4, a phenomenon of cross-linking between the different dendrimers, i.e. through the binding of phosphine groups to different rhodium atoms, occurred leading to oligomeric dendritic species.

The reactions were carried out using different batches of G1-16ethylPPh$_2$ ligand since a first synthesis led to incomplete conversion to the desired dendrimer (12 arms substituted over 16). This partially functionalised ligand will be named 'A' in this chapter. The second type of dendritic ligands used (different batches) was shown to have more than 15 arms functionalised (ligand named 'B').

A first set of experiments was carried out in a batch autoclave using ligand A at 80°C under 20 bar of H_2/CO with a phosphine/rhodium of 5.4/1. After 3.5 hours of reaction the conversion to the aldehydes, nonan-1-al and 2-methyloctan-1-al, was only 55 %. However, the selectivity to the linear aldehyde was relatively high since a linear to branched ratio (l:b) of 6.3:1 was obtained. Such high regioselectivity was unexpected. Indeed, such potentially bidentate ligand with a spacer of 5 atoms (or more) between the two P atoms (considering two phosphorus species on the same dendrimer arm) were shown only highly selective when constrained as for the BISBI[2] and Xantphos[3] type ligands (see Chapter 2 and section 5.3 & 5.5 for discussion).

To optimise the catalytic reaction conditions, the reactions were performed in the CATS rig, which allows the characterisation of the products (see Chapter 4 and Chapter 6) to be determined clearly. Using similar conditions (20 bar of H_2/CO, 80°C, P/Rh = 5.4/1) but allowing the completion of the reaction (< 24 h), a comparable linear to branched ratio was obtained (l:b = 6.6:1) with a selectivity to the linear aldehyde, nonan-1-al, of 83.9 %. As shown by the long reaction time, the rate of reaction was very low (initial Turn Over Frequency of 0.02 mole of oct-1-ene s^{-1}). A first order dependency in substrate and rhodium was determined for this reaction. Higher temperatures, i.e. 100°C and 120°C (H_2/CO 10 bar), increased the

reaction rate allowing the completion of the reaction respectively in 4 and 2 hours (see Table 5.1 and Figure 5.3).

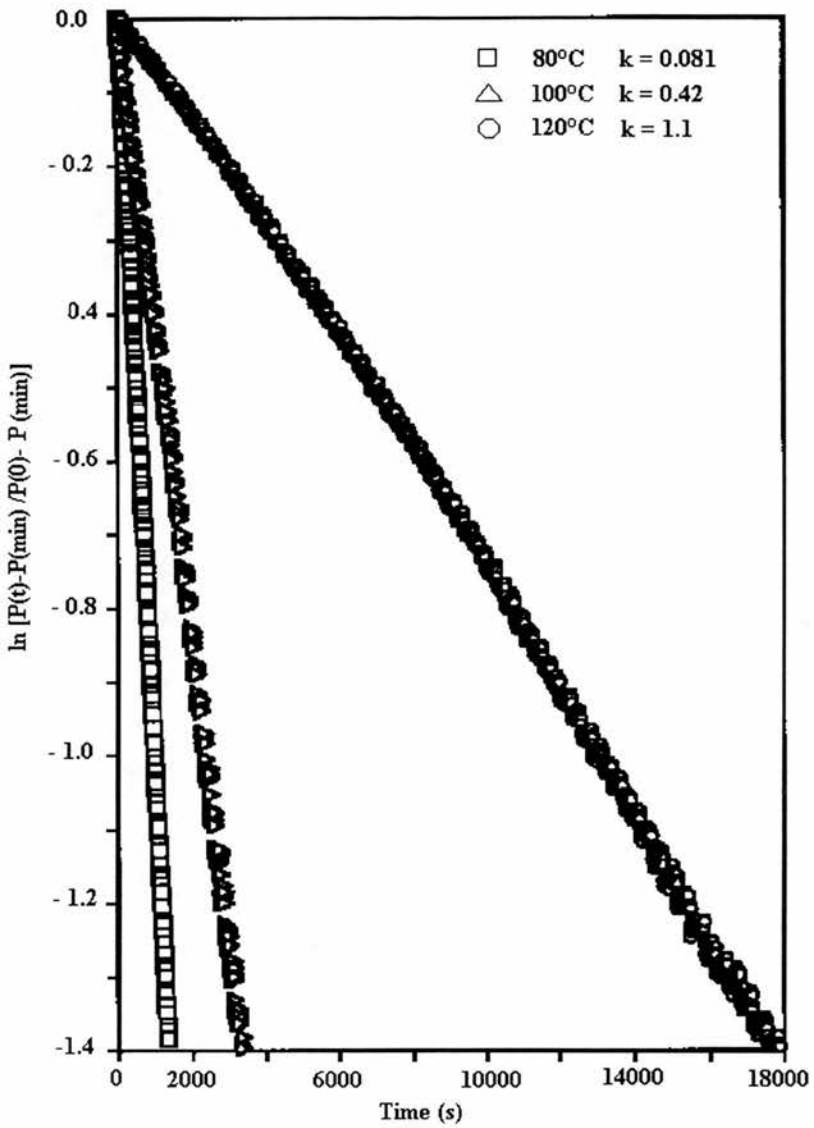

Figure 5.3 Effect of the temperature on the rate of hydroformylation of oct-1-ene using G1-16ethylPPh$_2$ as ligand (k in 10^{-3} s^{-1})([Rh] = 3.77 × 10^{-3} mol.dm^{-3}, P/Rh = 5.4/1, H_2/CO 10 bar).

These reaction temperatures combined with lower CO/H_2 pressure (10 bar) led also to an increased selectivity to the linear aldehyde (up to 85.6 %) with an interesting l:b ratio of 12:1. Even higher selectivity was obtained under these conditions (120°C, 10 bar) with the more crowded dendrimer B since 86.0 % of the products was nonan-1-al with a l:b ratio of 13.9/1. It thus appears that, for a given P/Rh ratio (5.4/1), both the rate constant (from 0.081 × 10^{-3} to 1.1 ×10^{-3} s^{-1}) and l:b

ratio (from 6.6 to 12) markedly increased when the pressure was lowered (compare entries 5 and 6 or 4 and 7 in Table 5.1) or the temperature increased (compare entries 2, 4, 5).

Table 5.1 Results of hydroformylation reactions of oct-1-ene using G1-16ethylPPh$_2$ ligands.

Entry	*Ligand*	*T* ^oC	*P* *bar*	*t* *h*	*k* 10^{-3} s^{-1}	*Conv.* %	*Isom.* %	*l:b*	*Nonan-1-al* %
1	B[a]	120	10	2	1.2	> 99.9	6.6	13.9	86
2	A[b]	120	10	2	1.1	> 99.9	6.3	12.0	85.6
3	A[b]	120	10	0.2	1.1	56.7	6.6	15.4	48.5, 86[c]
4	A[b]	100	10	4	0.42	> 99.9	5.0	10.8	86.2
5	A[b]	80	10	19	0.08	> 99.9	6.0	8.8	83.5
6	A[b]	80	20	24	0.05	>99.9	2.5	6.6	83.9
7	A[b]	100	20	6	0.33	> 99.9	3.2	7.5	84.7

Reaction conditions: [Rh(acac)(CO)$_2$] (2.0×10^{-5} mol), toluene (4 cm^3), heated under CO/H$_2$ (6 bar) for 1 h. Oct-1-ene (8.3×10^{-3} mol) injected and pressure increased. Pressure kept constant through mass flow controller and feed from a ballast vessel. Pressure drop in ballast vessel monitored every 5 s.

[a] G1-16ethylPPh$_2$ dendrimer with 15 arms functionalised, P: Rh = 6:1.

[b] G1-16ethylPPh$_2$ dendrimer with 12 arms functionalised P: Rh = 5.4:1.

[c] based on the amount of oct-1-ene consumed.

Such rate increase is easily explained since the rate of reaction is directly related to the reaction temperature, and the lower gas pressure, i.e. CO, frees some vacant coordination site allowing the reaction to occur more quickly (see Chapter 2).[1] The increase of the l:b ratio under these conditions is caused by two related effects. Firstly, increasing the temperature or decreasing the gas pressure increased indeed the amount of linear aldehyde to reach a maximum of 86 % (compare for example entries 2 and 6 in Table 5.1). On the other hand, the amount of branched aldehyde decreased with higher temperature or lower gas pressure, while the amounts of isomerised substrate (2-& 3- & 4-octene) increased (compare entries 5 and 6 or 1 and 4). These two effects can be related to the enhanced isomerisation process. Indeed isomerisation of the substrate, *via* β-H-elimination in the alkylrhodium complex, occurs if a vacant site is freed, which is favoured by low CO pressure or high

temperature (increased rate of isomerisation). Whilst β-H-elimination with the linear alkylrhodium species can only reform the initial substrate, the branched alkylrhodium complex can undergo a β-H-elimination giving the terminal alkene, and so potentially the linear aldehyde, or it can lead to the isomerised substrate, oct-2-ene, to the detriment of the branched aldehydes. Therefore whilst the amount of linear aldehyde and isomerisation products increase, the amount of branched isomer, 2-methylhexan-1-al, decreases. Oct-3-ene and oct-4-ene were formed by isomerisation of respectively oct-2-ene and oct-3-ene. The complete distribution of isomerisation products is given in Appendix IV.

In all cases, traces of hydrogenated product, nonan-1-ol (< 0.4 %), and substrate, octane (0.5-1.4 %), were detected (see Appendix IV for details).

Table 5.2 Results of hydroformylation reactions of oct-1-ene varying the phosphine/rhodium ratios using G1-16ethylPPh$_2$ ligands.

Ligand	*P/Rh*	*k*	*Conv.*	*Isom.*	*l:b*	*Nonanal*
		10^{-3} s^{-1}	*%*	*%*		*%*
A	3.6	0.95	> 99.9	7.1	11.9	84.3
A	5.4	1.1	> 99.9	6.3	12	85.6
A	10.8	1.5	> 99.9	6.6	12.2	85.2
B	6	1.2	> 99.9	6.6	13.9	86.0
B	2	0.52	> 99.9	35.5	3.4	48.4

Reaction conditions: Rh(acac)(CO)$_2$] (2.0 x 10^{-5} mol), toluene (4 cm^3), heated under CO/H_2 (6 bar) for 1 h. Oct-1-ene (8.3 x 10^{-3} mol) injected and pressure increased. Pressure kept constant through mass flow controller and feed from a ballast vessel. Pressure drop in ballast vessel monitored every 5 s. Total reaction time, 2 h.

The effect of the phosphine/rhodium ratio under fixed reaction conditions (10 bar of H_2/CO, 120°C, [Rh] = 3.77 × 10^{-3} mol.dm^{-3}) was also studied. It was found that the dendrimer could only support a limited amount of rhodium species since when a P/Rh ratio of 2/1 was used, the precipitation of a metallic residue occurred with lowering in the rate constant and in the aldehyde l:b ratio (3.4:1) (see Table 5.2). This can be related to the formation of oligomeric complexes discussed above. Interestingly, increasing of the P/Rh ratio from 3.6 to 10.8/1 (ligand A) led to higher rate constant (see Figure 5.4) while the l:b ratio stayed virtually invariant at *ca.* 12 -

the upper limit that we have observed for this particular dendrimer composition. It is thus believed that the rhodium is strongly bound to the dendrimer, probably *via* 2 P atoms, and that steric constraint prevents the coordination of extra P atoms to block vacant sites and inhibit the reaction, as is observed when using triphenylphosphine.

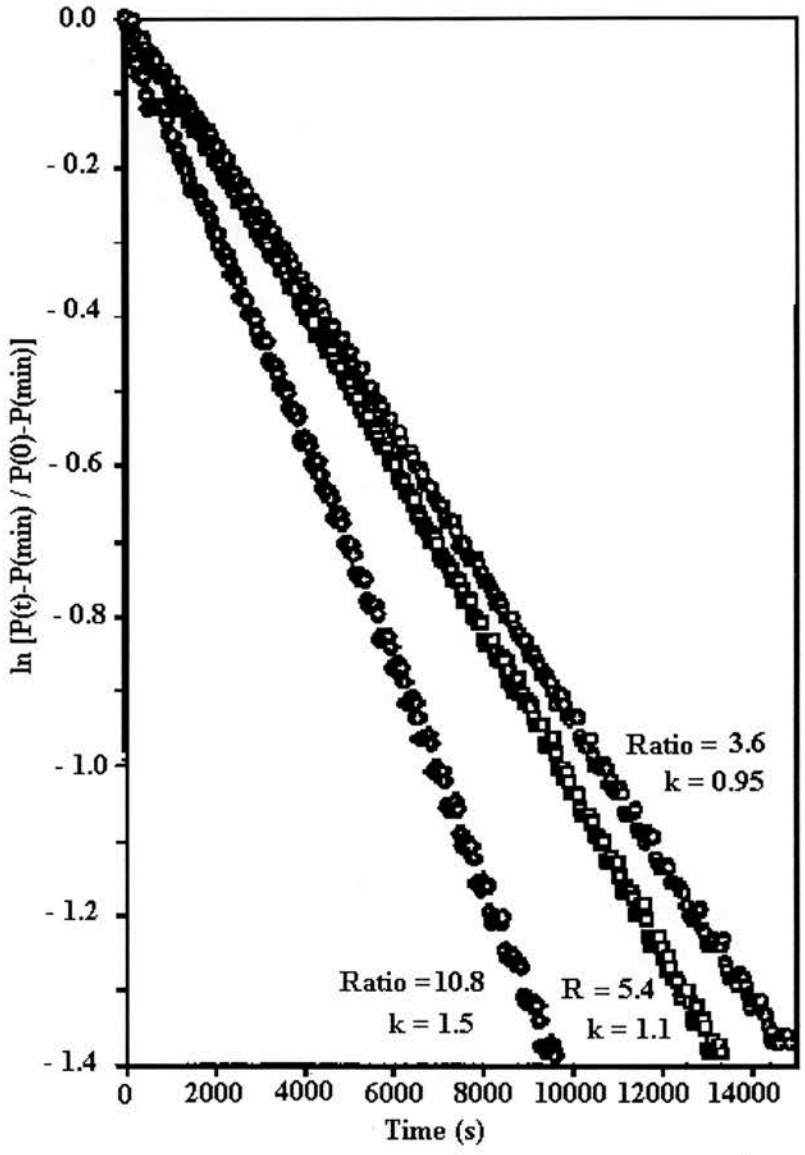

Figure 5.4 Effect of the phosphine/rhodium ratio on the rate of hydroformylation of oct-1-ene using G1-16ethylPPh$_2$ as ligand (k in 10^{-3} s^{-1})(120°C, H_2/CO 10 bar).

Lower diphenylphosphine loading on the dendrimer A (average value of 12 PPh_2 groups) gave a slightly lower l:b ratio (12.0:1) than the more completely substituted dendrimer B (15 substituted arms) (l:b ratio 13.9:1). Thus the steric crowding on the dendrimer periphery seems to play an important role in the selectivity of the reaction. This different ratio is however mainly related to the

isomerisation process since the regioselectivity to the linear aldehyde was similar for both dendritic ligands (85.6 % for A, 86.0 % using B).

The intrinsic l:b ratio (15.4:1) for the hydroformylation of oct-1-ene by rhodium complexes of G1-16ethylPPh$_2$ was obtained by running the hydroformylation over a short period (0.2 hour). Longer time reaction runs are contaminated with 2-methyloctan-1-al formed through hydroformylation of the oct-2-ene.

5.3 Comparative studies with parent molecule ligands.

In order to determine the exact influence of the dendrimer structure on the reactivity and selectivity of the catalytic reaction, the hydroformylation of oct-1-ene using parent molecules of the dendrimer was carried out. Indeed, a linear to branched ratio this high (l:b = 13:9) would be very unusual for an unconstrained ligand of this size and certainly shows that a positive dendrimer effect was operating. Indeed when comparing the results obtained with the dendrimer and so-called parent molecules this dendrimer effect is clearly apparent.

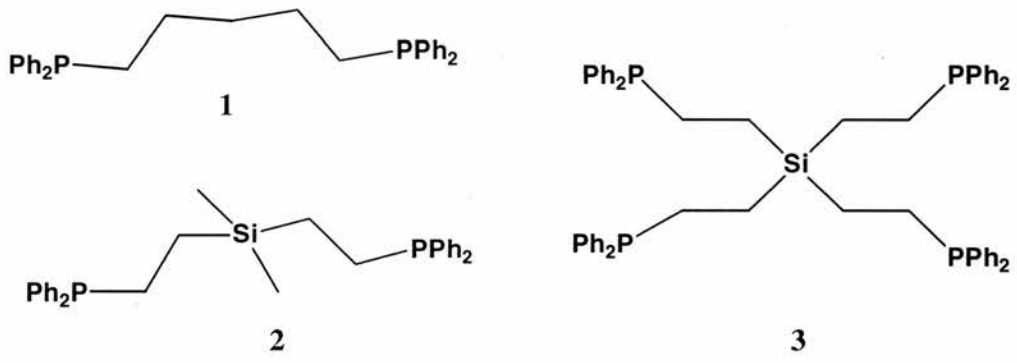

Figure 5.5 'Parent' molecule ligands used in hydroformylation reaction.

1,5-bis(diphenylphosphino)pentane (**1**), di(diphenylphosphinoethyl)dimethyl silane (**2**), and tetra(diphenylphosphinoethyl)silane (**3**) were used as ligands under identical conditions to those used for the dendrimer ([Rh(acac)(CO)$_2$] 2.0 x 10^{-5} mol, P/Rh = 6/1, 120°C, H$_2$/CO 10 bar). The results of the reactions are reported in Table 5.3. Whilst the dendrimer gave a selectivity to the linear aldehyde, nonan-1-al, of 86 %, the small molecules **1**, **2** and **3** respectively led to 70.1, 72.7, and 77.4 % selectivity to the desired aldehyde. The rates of reaction using the small molecules

were , however, higher than those found when using the dendritic ligand (see Table 5.3).

Table 5.3 Comparative study in the hydroformylation reaction of oct-1-ene using the parent model ligands.

Ligand	*k* 10^{-3} s^{-1}	*Conv.* %	*Oct-2-ene* %	*3&4-Octene* %	*Nonanal* %	*l:b ratio*
G1-16ethylPPh$_2$ A	1.5	> 99.9	6.1	0.26	85.6	12.0
G1-16ethylPPh$_2$ B	1.2	> 99.9	6.3	0.26	86	13.9
1	3.6	> 99.9	10.6	0.83	70.1	3.4
2	3.0	> 99.9	5.8	0.90	72.7	3.8
3	2.1	> 99.9	6.2	0.40	77.4	5.2

Reaction conditions: Rh(acac)$(CO)_2$] (2.0 x 10^{-5} mol), P/Rh = 6/1, toluene (4 cm^3), heated under CO/H_2 (6 bar) for 1 h. Oct-1-ene (8.3 x 10^{-3} mol) injected and pressure increased. Pressure kept constant through mass flow controller and feed from a ballast vessel. Pressure drop in ballast vessel monitored every 5 s. Total reaction time 2 h, 120°C, CO/ H_2 10 bar.

It is clear that the dendrimer offers higher selectivity with lower rate compared with the small molecules. It is also important to note that the selectivity using **3**, which can be thought of as the first generation dendrimer was better than the diphosphine, **2**. The ligand **2** was also found more selective than the less hindered ligand **1**. As expected for the more sterically crowded phosphine ligand **3,** the rate constant, which was 3.0×10^{-3} s^{-1} for **2**, dropped to 2.1×10^{-3} s^{-1} (P/Rh = 6/1). Therefore, comparing the small molecules with the dendrimer, it is clear that the increase of steric crowding around the core leads to higher l:b ratios. Interestingly, extensive studies carried out by van Leeuwen and co-workers showed that a compound derived from tetravinylsilane containing 16 Ph_2P arms, but with only one CH_2 spacer between the silicon and phosphorus atoms (i.e. $R_2Si(CH_2PPh_2)_2$) gave no special enhancement over the small molecule analogue ($Me_2Si(CH_2PPh_2)_2$) with a l:b ratio of 2.3:1 (see Chapter 1).[4]

Comparing the product distribution from the dendrimer based catalyst to those arising from catalysts based on **2** and **3** suggests that the dendrimer catalysts isomerised oct-1-ene at a lower rate and also more selectively to oct-2-ene (P/Rh = 6/1) (see Table 5.3 and Appendix IV). Indeed there was significantly less oct-3-ene

and oct-4-ene formed with the dendrimer catalysts (0.26 % in total for A or B) than for **2** and **3** (respectively 0.4 % and 0.9 %) (see Appendix IV for full details). In addition, there was no 2-propylhexanal and virtually no 2-ethylheptanal (0.07 %) formed with the dendrimer catalysts whilst **2** and **3** led respectively to 0.13 % and 0.03 % of 2-propylhexanal and 1.19 % and 0.37 % of 2-ethylheptan-1-al. Therefore the dendrimer crowding clearly disfavoured the hydroformylation of internal alkenes. These combined observations account for the better selectivity of the dendrimer-based catalyst towards nonan-1-al.

Table 5.4 Effects of the rhodium/ phosphine ratio in the hydroformylation of oct-1-ene using the small molecule model ligands.

Ligand	*P/Rh ratio*	*k* 10^{-3} s^{-1}	*Conversion* %	*Isom.* %	*l:b ratio*	*Nonan-1-al* %
1	3	3.0	> 99.9	20.6	1.9	51.9
1	6	3.6	> 99.9	6.7	3.4	70.1
2	1	1.6	> 99.9	19.3	3.4	62.7
2	2	2.8	> 99.9	10.3	3.5	68.9
2	6	3.0	> 99.9	6.7	3.8	72.7
2	12	3.1	> 99.9	8.1	4.0	70.2
3	2	2.1	> 99.9	18.3	2.3	55.9
3	6	2.1	> 99.9	6.6	5.2	77.4
3	12	2.4	> 99.9	6.1	6.3	79.9

Reaction conditions: $[Rh(acac)(CO)_2]$ (2.0×10^{-5} mol), toluene (4 cm^3), heated under CO/H_2 (6 bar) for 1 h. Oct-1-ene (8.3×10^{-3} mol) injected and pressure increased. Pressure kept constant through mass flow controller and feed from a ballast vessel. Pressure drop in ballast vessel monitored every 5 s. Total reaction time 2 h, 120°C, CO/H_2 10 bar.

It would also appear that the units $RMeSi(CH_2CH_2PPh_2)_2$ (R = dendrimer or Me) and $Si(CH_2CH_2PPh_2)_4$ were capable of acting as chelating ligands whereas **1** was not (see Table 5.4). Even with a $H_2C(CH_2CH_2PPh_2)_2$ to Rh ratio of 1.5/1 a small amount of "sticky" solid precipitate was formed and there was low selectivity (52 %) to nonan-1-al. On increasing the ratio of $H_2C(CH_2CH_2PPh_2)_2$ to Rh to 3:1 (P/Rh = 6/1), the selectivity to nonan-1-al was increased to 70 % and the final solution was found as a normal clear, bright yellow coloured product. These observations suggest

that ligand **1** is capable of behaving as a monodentate ligand. In contrast, with a $Si(CH_2CH_2PPh_2)_4$ to Rh ratio of 1/2 (P/Rh = 2/1) and even a $Me_2Si(CH_2CH_2PPh_2)_2$ to Rh ratio of 0.5/1 (P/Rh = 1/1) the final product was the usual bright yellow solution with no solid precipitate. In the later case the low rate constant, which was *ca.* half that when ratios of $Me_2Si(CH_2CH_2PPh_2)_2$ to Rh were higher than one, suggests there was a phosphine "starvation" effect in this experiment.

For both small molecule ligands with silicon as central atom the selectivity to nonan-1-al improved, as expected, on increasing the P/Rh ratio. Indeed using **3**, which can be considered as a small dendritic structure (see Section 5.5), the selectivity to nonan-1-al rose from 55.9 to 79.9 % when phosphine/rhodium ratios of respectively 2/1 to 12/1 was used. This trend clearly confirms the strong bidentate chelate of the dendrimer to the rhodium species since no such effects was found with the dendritic ligand.

5.4 Effect of the dendritic structure on the hydroformylation reaction of oct-1-ene.

5.4.1 Hydroformylation reaction using the ligand G1-24methylPPh$_2$.

The dendrimer G1-24methylPPh$_2$ (incomplete substitution, i.e. 60 % functionalised) (Figure 5.6) was also used as ligand for the hydroformylation of hex-1-ene using $[Rh(acac)(CO)_2]$ or $[Rh_2(O_2CMe)_4]$ as metal-based precursor. The preliminary experiments were performed in an autoclave containing a stirrer bar and heated by a heating jacket. The catalytic solutions were prepared beforehand and then injected in the autoclave allowing control of the homogeneity of the mixture. The dendritic ligands formed rhodium/phosphine complexes in toluene as shown by the rapid change of colour of the solution. The solutions obtained were found as dark-red or red-orange homogeneous mixtures when using respectively $[Rh_2(O_2CMe)_4]$ and $[Rh(acac)(CO)_2]$.

The catalytic reactions, using hex-1-ene as substrate (8.0×10^{-3} mol), were carried out at 120°C and 40 bar of H_2/CO (1/1) at various rhodium concentrations (4.0×10^{-3} to 8.0×10^{-3} mol.dm^{-3}) and phosphine/rhodium ratios (1.5/1 to 4/1) to give the expected aldehydes, heptan-1-al and 2-methylhexan-1-al. The products of reaction were analysed by gas chromatography techniques (GC). The best selectivity

to the linear aldehyde (67.5 % for a calculated total conversion, see Table 5.5) was obtained for a phosphine/rhodium of 3/1 with a linear to branched ratio of 2.3:1.

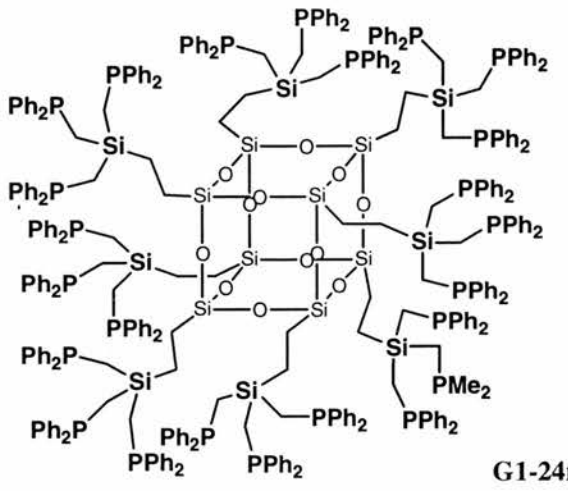

Figure 5.6 24-diphenylphosphine functionalised POSS dendrimer (only 60% substituted).

Below a P/Rh ratio of 3/1, the l:b ratio slightly decreased to reach values around 2:1. The different concentrations of catalyst tested (4.0×10^{-3} to 8.0×10^{-3} mol.dm^{-3}) led to similar selectivity and rate of the reactions. In all cases, small amounts of isomerised substrate (< 4 %), i.e. hex-2-ene and hex-3-ene, were detected.

Interestingly similar selectivity (l:b ratio of 2.3/1) was reported by van Leeuwen and co-workers using a silane-based dendrimer with 12 to 24 -CH_2PPh_2 endgroups or the parent molecule $Me_2SiCH_2PPh_2$ (see Chapter 2).[4]

Table 5.5 Hydroformylation of hex-1-ene catalysed by rhodium complexes formed with the G1-24methylPPh$_2$ dendritic ligand.

Solvent	*[Rh]* 10^{-3} *mol dm*$^{-3}$	*P/Rh*	*Time* *h*	*Conv.* *%*	*Aldehydes* *%*	*Alcohols* *%*	*l:b ratio*[a]
Toluene	8	3	2.5	95	92	-	2.3
Toluene	8	4	2.5	95	92	-	2.3
Toluene	4	3	2.5	89	86	-	2.4
Toluene	8	2	4	>99	96	-	2.0
Toluene	8	1.5	4	>99	97	-	1.9
Ethanol	8	4	16	>99	93	5	1.8

Reaction conditions: [$Rh_2(O_2CMe)_4$] or [Rh(acac)$(CO)_2$], solvent 4 cm^3, hex-1-ene 8.0×10^{-3} mol, 120°C, H_2/CO 40 bar.

[a] : linear to branched ratio of aldehyde only.

The hydroformylation reaction of hex-1-ene catalysed by rhodium complexes formed by G1-24methylPPh$_2$ and [Rh$_2$(O$_2$CMe)$_4$] in ethanol (red-brown solution) was also performed at 120°C with 40 bar of CO/H$_2$ (phosphine/rhodium ratio of 4/1). The products of reaction were mostly, as expected, heptan-1-al and 2-methylhexan-1-al (93 % in total). The linear to branched ratio was found lower, i.e.1.8:1, than the one obtained when the reaction was carried out in toluene because disymmetric hydrogenation to the alcohols (5 %) occurred. Indeed a higher l:b ratio (3.3:1) in the alcohol distribution was found, indicating that hydrogenation of the linear aldehyde was faster that of the branched isomer.

Since the regioselectivity of the reaction was different using the dendritic ligand, G1-methylPPh$_2$, or the G1-16ethylPPh$_2$ dendrimer, it was decided to compare the latter ligand with other 16-branched dendrimers.

5.4.2 Hydroformylation reaction using 16-diphenylphosphine substituted POSS dendrimers.

To investigate the effect of the dendritic structure on the hydroformylation reaction various POSS dendrimers (Figure 5.7, 5.8 and 5.9) with 16 functionalised arms were used as ligands for the hydroformylation of oct-1-ene. The reactions were carried out using the CATS rig in the optimal conditions found for G1-16ethylPPh$_2$, i.e. using [Rh(acac)(CO)$_2$] (2.0×10^{-5} mole) as metal-based complex, a temperature of 120°C and at 10 bar of CO/H$_2$ (phosphine/rhodium ratio of 6/1).

5.4.2.1 Hydroformylation reaction using G1-16methylPPh$_2$.

As discussed previously the catalytic solution was prepared in a Schlenk tube before use. The dendritic ligand G1-16methylPPh$_2$ (Figure 5.7) and the rhodium-based complex readily formed a bright yellow homogeneous solution when dissolved in toluene indicating fast complexation of the phosphorus atoms to the metal centre. As expected the G1-16methylPPh$_2$ dendritic ligand showed similar results in the hydroformylation of oct-1-ene to those of its counterpart G1-24methylPPh$_2$, since the supposed 24-branched dendrimer had only partially been converted to the phosphine species.

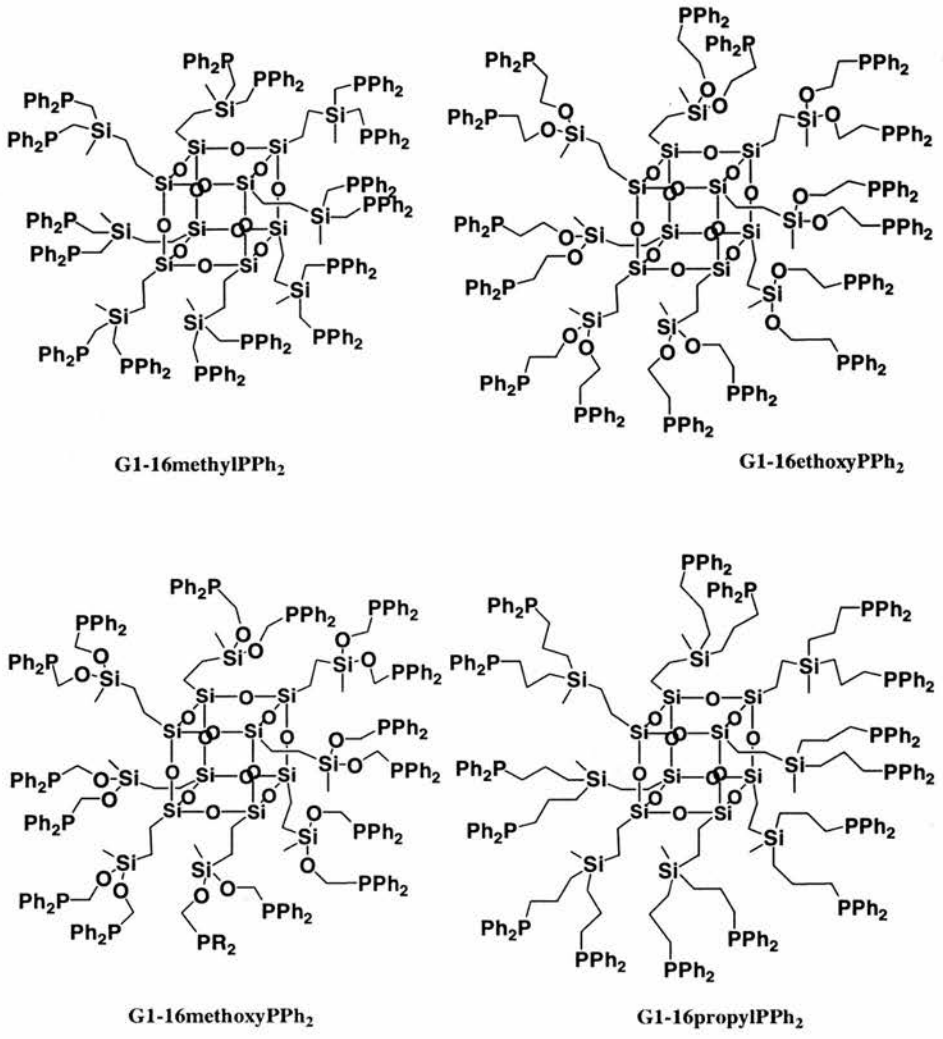

Figure 5.7 1st generation dendrimer with 16 diphenylphosphine groups on the periphery.

The selectivity to the linear aldehyde was 68.5 % with G1-16methylPPh$_2$ (see Table 5.6) compared to 67.5 % for the G1-24methylPPh$_2$ ligand (Table 5.5). The different reaction conditions used (pressure of 10 bar instead of 40 bar used previously) should not have influenced too much this regioselectivity and so altered this comparison. However, as expected the amount of isomerisation products increased with the lower pressure from 3 % at 40 bar to 12.1 % at 10 bar. This increase of side products is at the detriment of the branched aldehydes, 2-methyloctan-1-al, which fell from 29.3 % to 16.3 % at respectively 40 and10 bar, allowing a better l:b ratio in these reaction conditions (l:b = 3.4:1 instead of 2.3:1 at 40 bar). However the dendritic ligand (G1-16methylPPh$_2$) did not hydroformylate the internal alkenes at a high rate since only 1.19 % of 2-ethylheptan-1-al and 0.09 % of propylhexan-1-al were found as products of the reaction.

The dendritic ligand G1-16methylPPh$_2$ led, therefore, to lower regioselectivity to the linear aldehyde compared to its counterpart G1-16ethylPPh$_2$ (86 % of nonan-1-al). It seems thus that the dendrimers with a spacer of 3 atoms between the two phosphorus atoms (i.e. G1-16methylPPh$_2$, G1-24methylPPh$_2$ and van Leeuwen's studies[4]) do not allow the formation of selective phosphine/rhodium complexes. It is believed that these dendritic compounds probably formed a high proportion of mono-phosphine complexes, which are not regioselective catalytic species. This conclusion is emphasised by the fact that the rate of reaction with this G1-16methylPPh$_2$ is *ca* 6 times higher than for the G1-16ethylPPh$_2$ dendritic ligand (see Table 5.6). In addition, the high amount of isomerised substrate combined with high rate of hydroformylation of the internal alkenes (highest rate of all the dendritic catalyst discussed in this chapter) showed that this dendrimer was not highly selective toward the substrate. However, since different ^{31}P NMR resonances were found for the two dendrimers, respectively δ -9.4 and δ -22.6 ppm for G1-16ethylPPh$_2$ and G1-16methylPPh$_2$, it is believed that the different basicity of the phosphine species could also influence the selectivity of the reaction.

Table 5.6 Hydroformylation reactions catalysed by Rh complexes of POSS derived dendrimer diarylphosphines.

Ligand	*t* *h*	*rate* *10^{-3} s^{-1}*	*Conv.* *%*	*Isomer.* *%*	*Nonanal* *%*	*l:b* *ratio*
G1-16methylPPh$_2$	0.3	6.2	> 99.9	12.1	68.5	3.9
G1-16ethylPPh$_2$ A	2	1.1	> 99.9	6.4	85.6	12.0
G1-16ethylPPh$_2$ B	2	1.2	> 99.9	6.6	86.0	13.9
G1-16ethylPAr$_2$[a]	2	1.1	> 99.9	20.0	73.0	15.0
G1-16methoxyPPh$_2$	2	0.7	> 99.9	9.0	76.2	5.7
G1-16propylPPh$_2$	2	1.5	> 99.9	5.1	78.0	5.0
G1-16ethoxyPPh$_2$	2	2.0	> 99.9	8.3	78.1	6.4
G2-propyl-48ethylPPh$_2$	3	0.6	> 99.9	7.5	83.8	11.5

Reaction conditions: [Rh(acac)(CO)$_2$] = 2.0 × 10^{-5} mole, P/Rh =6/1, substrate 8.3 × 10^{-3} mole, toluene (4 cm^3), 120°C, CO/ H_2 10 bar.

[a]: Ar = 3,5-$C_6H_3(CF_3)_2$.

5.4.2.2 Hydroformylation reaction using G1-16ethylPAr$_2$.

The hydroformylation of oct-1-ene using the dendritic ligand G1-16ethylPAr$_2$ (Ar = 3,5-$C_6H_3(CF_3)_2$) (Figure 5.8) was also carried out under similar reaction conditions. Interestingly, the pre-formed catalytic mixture (solvent toluene) was heterogeneous at room temperature showing an extremely pale brown solution and a brown oily residue. This heterogeneity is amazing since both the rhodium-based catalyst, [Rh(acac)(CO)$_2$], and the dendrimer were independently soluble in toluene.

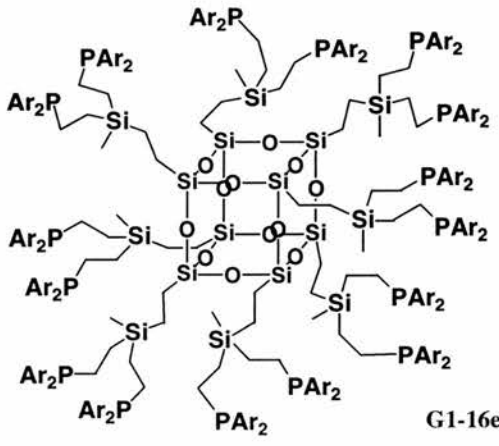

Figure 5.8 A phosphine-containing POSS dendrimer with electron withdrawing groups.

A homogeneous orange-brown solution was however obtained in warm toluene.

The hydroformylation of oct-1-ene catalysed by the dendritic rhodium complex led to the formation of 73.0 % of nonan-1-al (Table 5.6), a regioselectivity which was much lower than the one obtained using G1-16ethylPPh$_2$ (86.0 %). However the reaction led to a high linear to branched ratio of 15:1. This is due, in fact, to the high isomerisation process occurring during the reaction since as much as 20.0 % of the substrate was converted to oct-2-ene (19.7 %) and 3&4-octene (0.3 %). Nevertheless the dendritic complex did not hydroformylate the internal alkenes since only traces of 2-ethylheptan-1-al were found (see Appendix IV).

In previous studies, Casey *et al* reported that the introduction of electron withdrawing substituents on the aryl groups of the phosphine ligands gave only higher selectivity to the linear aldehyde when the bidendate phosphine ligand coordinated in an equatorial-equatorial (ee) position in the 5-coordinated rhodium complexes. In contrast, the equatorial-axial coordination of a electronically modified bis(diphenylphosphino)ethane ligand led to lower regioselectivity (see Chapter 2).[5, 6]

It is however important to note that van Leeuwen and co-workers showed that, using xantphos type ligands, the configuration of the bidendate ligands in the rhodium complexes (i.e. ee and ea coordination) and the substitution with electron withdrawing groups did not influence the regioselectivity to the linear aldehyde although an increase of the l:b ratios was obtained with more electron withdrawing ligands (see Chapter 2).[3, 7] It is therefore possible that the mode of coordination of the dendritic ligand to the rhodium species corresponds to an equatorial-axial configuration in a trigonal bipyramidal complex (see Section 5.5). However, the formation of poor selective rhodium complexes may also arise because of the low loading of phosphorus moieties onto the dendrimer (conversion of 75 %) or by the steric hindrance of such species (which explained the low loading). Nevertheless, the rate of reaction using G1-16ethylPAr$_2$ was similar to its non-substituted counterpart ligand, possibly suggesting that the first hypothesis for the low selectivity was indeed right.

The high isomerisation rate is easily explained by the high temperature, the low pressure and by the increase electrophicility of the rhodium centre, which favoured CO dissociation and β-hydrogen elimination on the rhodium (branched) alkyl species.[8]

The amount of octane (hydrogenation of the substrate) was slightly higher (1.84 %) than with the other dendrimers (see Appendix IV) but a similar amount of hydrogenated product, nonan-1-ol, was found (0.22 %).

5.4.2.3 Hydroformylation reaction using G1-16methoxyPPh$_2$.

Surprisingly the dendritic ligand G1-16methoxyPPh$_2$ (Figure 5.7), which has a similar structure that of G1-16ethylPPh$_2$, and so should form similar rhodium complexes, did not lead to high selectivity to nonan-1-al. Indeed, whilst 86.0 % of the products was the linear aldehyde using G1-16ethylPPh$_2$, only 76.2 % of nona-1-al was formed using the rhodium/G1-16methoxyPPh$_2$ species (see table 5.6). Therefore not only the length of the bridge between the P atoms is an important factor in determining the selectivity of the reaction (see above), but also the composition of this bridge influences the reactivity/selectivity of the catalytic species. It is important to note that the basicity of the phosphine species on the two different dendrimers differed since ^{31}P NMR resonances at δ_P -9.4 and δ_P -13.6 ppm for respectively G1-16ethylPPh$_2$ and G1-16methoxyPPh$_2$ were found. It should also

be noted that a small amount of precipitate (yellow solid) was found at the end of the reaction indicating that the dendritic ligand was not so stable under the reaction conditions (the pre-formed catalytic solution was a bright yellow solution). However, since the kinetics of the reaction were first order the hydroformylation reaction, it is unlikely that the differences observed in the distribution of the products arose from the decomposition of the catalyst. Another explanation considered is that there may be a different geometry of the two dendrimers due to the oxygen atom linker. Indeed if such a difference exists, it would modify the mode of coordination of the phosphine species in the rhodium complexes, possibly leading to different catalytic species and so different reactivity and selectivity. The lower rate of reaction obtained with this ligand (compared to the G1-16ethylPPh$_2$ system) supports such a hypothesis.

Isomerisation of the substrate was relatively high since 8.82 % and 0.22 % of the products were respectively oct-2-ene and oct-3-ene (see Appendix IV for full details). This high isomerisation rate led to a relative good l:b ratio of 5.7:1. However this isomerisation is not followed by hydroformylation of the internal alkenes since only traces of 2-ethylheptanal were found (0.17 %) (see Appendix IV).

As found previously, only low rates of hydrogenation of the substrate to octane and of the product nonan-1-al to nonan-1-ol occurred since only respectively 1.14 % and 0.18 % of these products were detected.

5.4.2.4 Hydroformylation reaction using G1-16ethoxyPPh$_2$ and G1-16propylPPh$_2$.

The use of the dendritic ligands G1-16ethoxyPPh$_2$ and G1-16propylPPh$_2$ (Figure 5.7) emphasises the importance of the chain length for this type of dendrimer. Indeed the regioselectivity to the linear aldehyde during the hydroformylation of oct-1-ene was lower with these two ligands (*ca* 78 % for both) than with the G1-16ethylPPh$_2$ dendritic ligand (86 %) (see Table 5.6) . Nevertheless, these selectivities are still higher than the small molecules (see Table 5.3). Interestingly, unlike for G1-16ethylPPh$_2$ and G1-16methoxyPPh$_2$, the different basicity of the phosphorus atoms of these two dendrimers, G1-16ethoxyPPh$_2$ and G1-16propylPPh$_2$, did not seem to influence the selectivity of the reaction. Indeed although different ^{31}P NMR chemical shifts were found respectively at δ_P –22.5 and –16.5 ppm for G1-16ethoxyPPh$_2$ and G1-16propylPPh$_2$, the selectivity to nonan-1-al

was respectively 78.1 % and 78.0 %. G1-16ethoxyPPh$_2$ led however to a higher linear to branched ratio than G1-16propylPPh$_2$ (l:b = 6.4:1 compared to 5.0:1) due to higher isomerisation of the substrate (amount of 2, 3 and 4-octene of 8.3 % for G1-16ethoxyPPh$_2$, 5.1 % for G1-16propylPPh$_2$). A slightly higher rate was also calculated for G1-16ethoxyPPh$_2$ (2.0×10^{-3} instead of 1.5×10^{-3} s^{-1}) (see Table 5.6). Nevertheless the rates of reaction using these two ligands were higher that obtained using the more selective G1-16ethylPPh$_2$ dendrimer, data which corroborate a weaker phosphine to rhodium interaction and so lower regioselectivity. It is thus believed that these dendrimers do not sufficiently constrain the phosphine end group species due to the longer chain length (spacer of 7 atoms).

Both dendritic ligands only slightly hydroformylate internal alkenes since no more than 0.22 % and 0.17 % of the products were found as 2-ethylheptan-1-al for respectively G1-16ethoxyPPh$_2$ and G1-16propylPPh$_2$. A low rate of hydrogenation of the substrate and of the linear aldehyde occurred since less than 1.2 % of octane (G1-16propylPPh$_2$) and 0.53 % of nonan-1-ol (G1-16ethoxyPPh$_2$) were detected (see full details in Appendix IV).

5.4.2.5 Hydroformylation reaction using G2-propyl-48ethylPPh$_2$.

Using identical conditions, hydroformylation of oct-1-ene catalysed by a rhodium complex formed with the dendritic ligand G2-propyl-48ethylPPh$_2$ (only functionalised at 85 %) (Figure 5.9) was carried out.

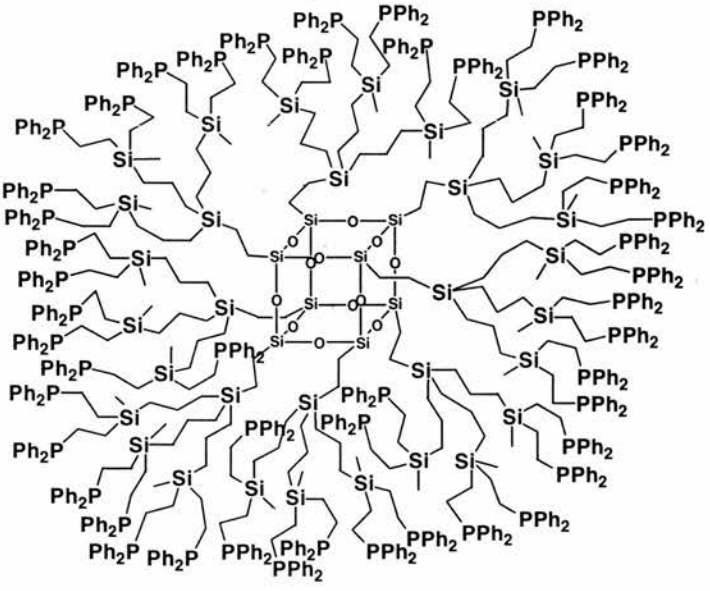

G2-propyl-48ethylPPh$_2$

Figure 5.9 A 2nd generation dendritic ligand.

It was found that the 2nd generation dendrimer acted similarly that of the G1-16ethylPPh$_2$ dendritic ligand since the rate and selectivity of the reaction were comparable. Indeed, using G2-propyl-48ethylPPh$_2$ as ligand, the regioselectivity to the linear aldehyde, nonan-1-al, was 83.8 % with a l:b ratio of 11.5:1 whilst the 16 arms ligand gave a selectivity of 86.0 % and a l:b ratio of 13.9:1. A drop in the rate of reaction by a factor *ca* 2 was nevertheless apparent (see Table 5.6), perhaps because of the steric hindrance of such bulky ligands or of the rate of diffusion of the large dendritic molecule. A slightly higher amount of isomerisation products (7.5 % instead of 6.6 % with G1-16ethylPPh$_2$ **B**) emphasises the probable bulkiness of this 2nd generation dendrimer since it was also found that the isomerisation process increased when passing from the partially functionalised G1-16ethylPPh$_2$ **A** to the bulkier G1-16ethylPPh$_2$ **B**. Although a high amount of oct-2-ene (7.3 %) was detected, the absence of 2-ethylheptan-1-al (0.07 %) in the reaction products (see Appendix IV for full details) showed that the dendritic complex did not favour the hydroformylation of the branched alkene.

Low rates of hydrogenation of the substrate to octane and of the linear aldehyde to nonan-1-ol occurred since only respectively 1.19 % and 0.24 % of these products were detected.

5.4.3 Summary.

It appears that only the POSS dendrimers built with a spacer of 5 atoms between the phosphorus moieties (G1-16ethylPPh$_2$ and G2-propyl-48ethylPPh$_2$) showed high selectivity to the linear aldehyde (*ca* 86 % and 84 %) for the hydroformylation of oct-1-ene leading to high linear to branched ratios (respectively 13.9: and 11.5:1) (Figure 5.10). In addition, the spacer atoms themselves seem to be important since the substitution of a carbon atom by an oxygen atom (respectively from G1-16ethylPPh$_2$ to G1-16methoxyPPh$_2$) led to low selectivity (76.2 %). It is thus hypothesised that these two dendritic ligands adopted different geometries during the hydroformylation reaction.

The substitution of the aryl groups by electron withdrawing species (G1-16ethylPAr$_2$) (Ar = 3,5-$C_6H_3(CF_3)_2$) led to low selectivity (73.0 %). The high linear to branched ratio (15:1) was due to the high isomerisation rate using such ligand (20.0 % of the substrate was isomerised). This lower selectivity could arise from the mode of coordination of the phosphorus atoms, i.e. equatorial-axial coordination in

the 5-coordinated rhodium complex (see above). Another possible explanation would be the steric hindrance of such dendritic species. The most compact ligand G1-methylPPh$_2$ was indeed the least selective species leading to low selectivity (68.5 %) and a high degree of isomerisation (12.1 % of 2, 3&4 octene). On the other hand the dendritic ligands with a spacer of 7 atoms (G1-16propylPPh$_2$ and G1-16ethoxyPPh$_2$) were probably not constraining enough since a lower selectivity to nonan-1-al (*ca* 78 %) was achieved using these ligands.

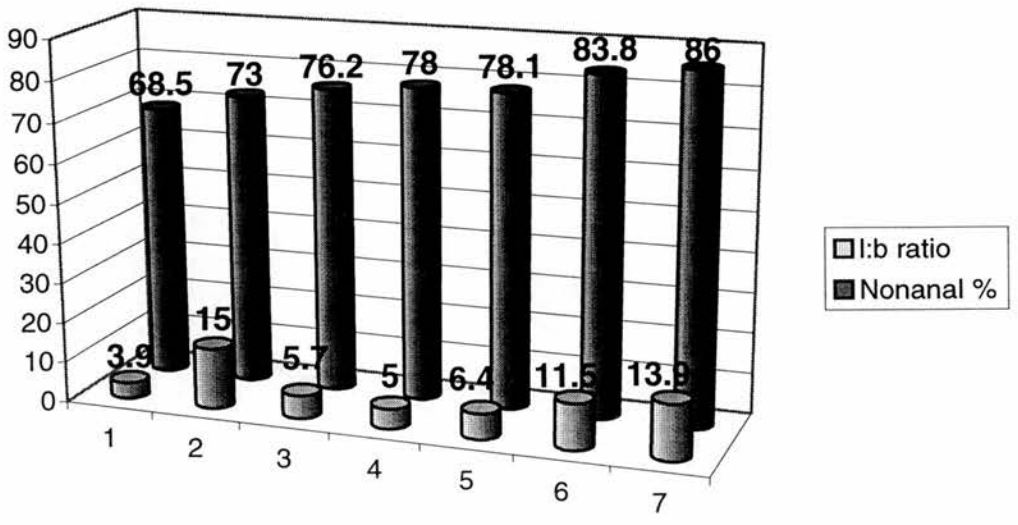

Figure 5.10 Selectivity to nonan-1-al using the different POSS dendritic ligands, 1 = *G1-16methylPPh$_2$,* 2 = *G1-16ethylPAr$_2$,* 3 = *G1-16methoxyPPh$_2$,* 4 = *G1-16propylPPh$_2$,* 5 = *G1-16ethoxyPPh$_2$,* 6 = *G2-propyl-48ethylPPh$_2$,* 7 = *G1-16ethylPPh$_2$..*

All dendritic complexes showed a first order dependence on substrate concentration (see Figure 5.11 and Chapter 6). The perfect straight line of the plots of *Ln[(P(t)-P(min)) / (P(0)-P(min))] versus Time* (see Chapter 6) of the different dendrimer clearly confirms that only hydroformylation of oct-1-ene occurred without other side reaction consuming H_2 or CO. It was also found that the rates of reaction depend on the structure of the dendrimers. The least regioselective and most compact ligand, G1-16methylPPh$_2$, led to the highest rate of reaction (*ca* 3 times the rate found with G1-16ethylPPh$_2$) while the less sterically hindered ligands G1-16ethoxyPPh$_2$ and G1-16propylPPh$_2$, showing intermediate selectivity, led to rate constants slightly higher than the G1-16ethyl PPh$_2$ catalytic system. However the

correlation between selectivity and rate of reaction, i.e. high selectivity coupled with low rate, is not straightforward. Indeed, although G1-16methoxyPPh$_2$ led to the lowest rate of reaction for the 1st generation dendrimers (k = 0.7 × 10^{-3} s^{-1}), a low regioselectivity to nonan-1-al was obtained (76.2 %). The rate constant using the 2nd generation dendrimer, G2-propyl-48ethylPPh$_2$, was *ca* half of the rate of the G1-16ethylPPh$_2$ system whilst G1-16ethylPAr$_2$ gave similar kinetics.

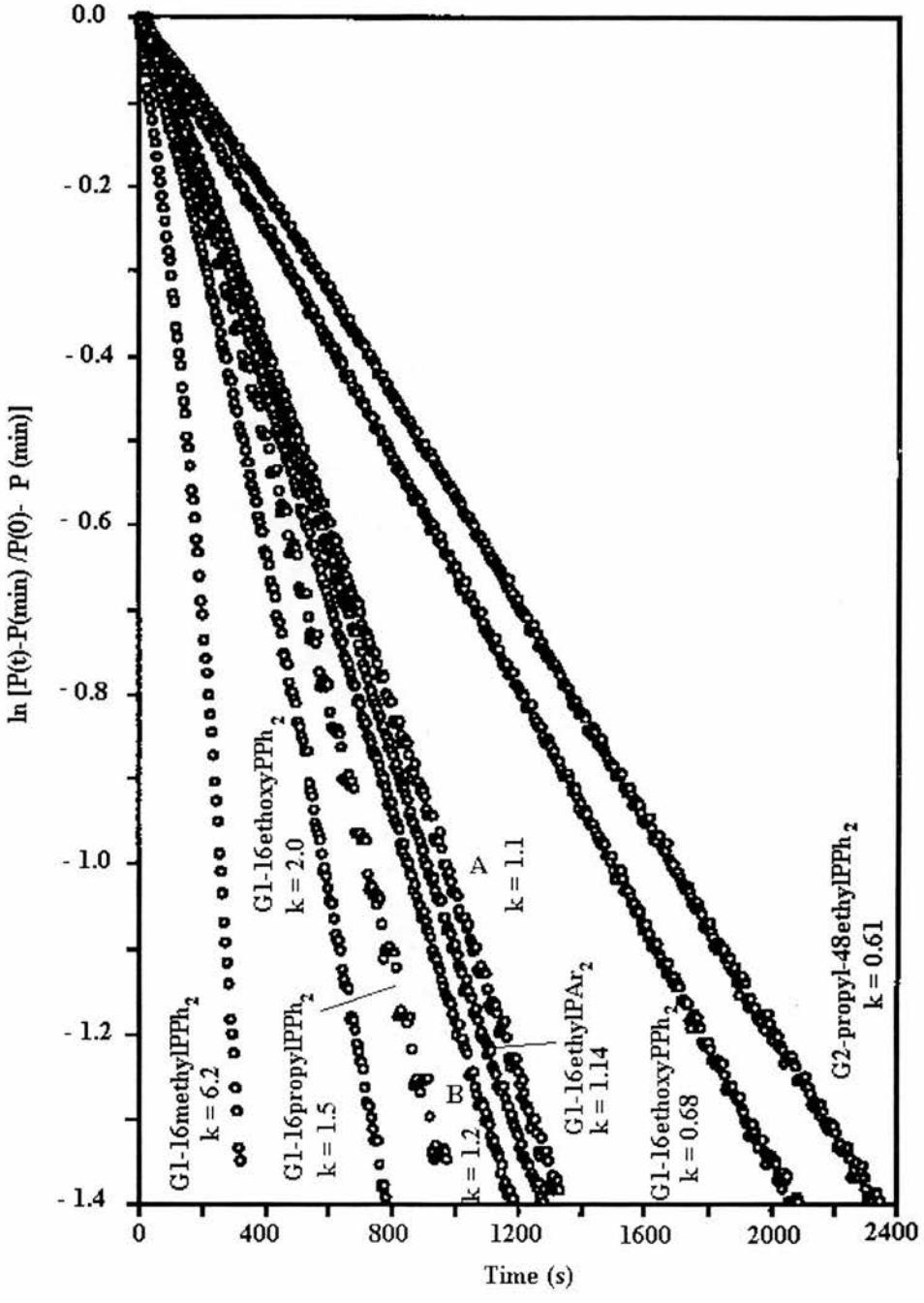

Figure 5.11 Effect of the dendrimer structure on the rate of hydroformylation of oct-1-ene (k in 10^{-3} s^{-1})([Rh] = 3.77 × 10^{-3} mol.dm^{-3}, P/Rh = 5.4/1, H$_2$/CO 10 bar, 120°C).

5.5 Mechanistic consideration.

The generally high l:b ratios obtained using G1-16ethylPPh$_2$ suggest that strong bidentate coordination occurred[1] or that the high local concentration of phosphorus atoms on the surface of the dendrimer increased the concentration of complexes containing three P donors.[9-11] The mechanism of reaction for these two hypothesises would be therefore similar to the one proposed by Wilkinson and co-workers[9, 10] (see Chapter 2 and Chapter 4). Another possibility for such selectivity could be the formation of bimetallic species as reported by Stanley and co-workers (see Chapter 2).[12, 13] We have attempted to obtain information on the species present in solution by using ^{31}P NMR and HP IR spectroscopy.

5.5.1 NMR spectra of the rhodium/G1-16ethylPPh$_2$ complexes.

As discussed previously the dendritic species G1-16ethylPPh$_2$ seems to chelate strongly to the rhodium since the selectivity was only slightly influenced by a phosphine/rhodium ratio varying from 3.6/1 to 12/1. Further confirmation that the metal was strongly bound to the dendrimer came from the ^{31}P NMR studies of solutions prepared from [Rh(acac)(CO)$_2$] and G1-16ethylPPh$_2$ (1:3) under CO and H_2.

Two resonances were observed at room temperature, one (δ 37 ppm) for phosphine species bound to rhodium complexes and the other from the free phosphorus atoms (G1-16ethylPPh$_2$ resonates at δ -9.5 ppm) (see Figure 5.12). Both resonances were very broad (width at half maximum = 470 Hz and 88 Hz respectively), possibly because of different binding environments for the rhodium since the spectrum is the same in different solvents (CH_2Cl_2, THF) and the linewidth at half maximum of the signal from the unbound P atoms only changes slightly between –40 (63 Hz) (Figure 5.13) and + 60°C (150 Hz) (Figure 5.14). This shows that the rhodium was not migrating rapidly around the surface of the dendrimer, nor dissociating on the NMR timescale.

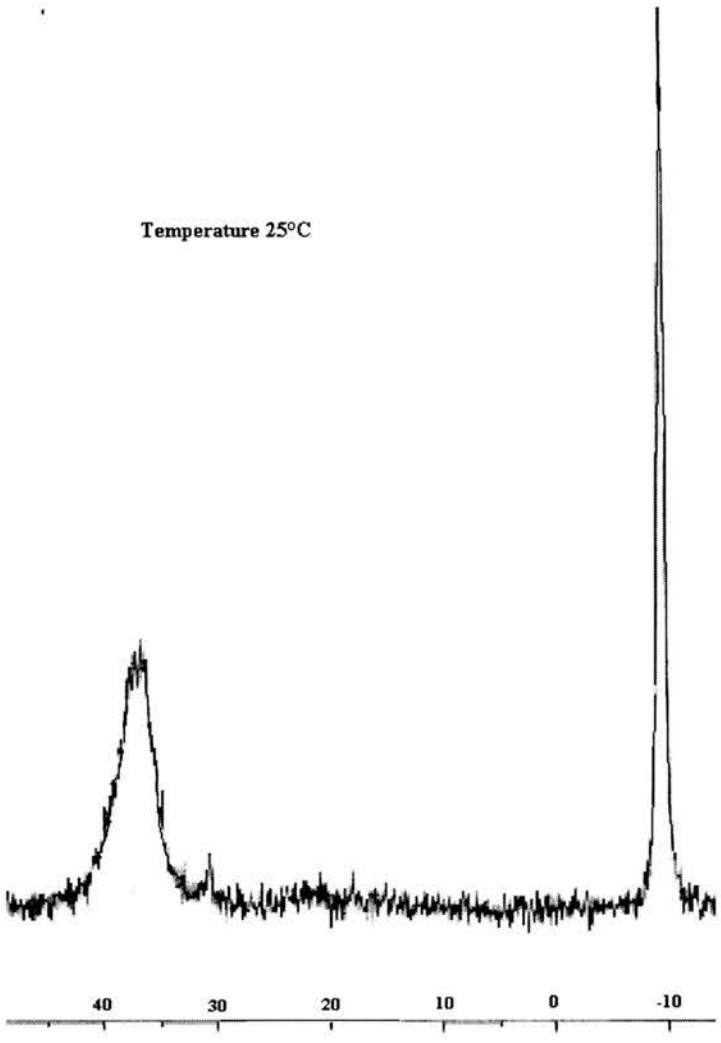

Figure 5.12 ^{31}P NMR spectrum of the rhodium-G1-16ethylPPh$_2$ complexes under an atmosphere of H_2/CO (1 bar) at 25°C.

The resonance from the Rh-bound phosphines appeared as two broad overlapping doublets (δ 37 and 36 ppm) at –40°C, but as a single broad doublet (δ 37 ppm, $J_{P\text{-}Rh} \approx 130$ Hz) at +60°C, suggesting fluxionability within the bound complex. A broad hydride signal was observed at δ -10.5 ppm (width at half maximum = 80 Hz) in the ^1H NMR spectrum at room temperature. It is difficult to assign such signal to any configuration of rhodium complexes since the broad signal could be the sum of different species.

Interestingly the ^{31}P and ^1H NMR resonances are close to the data collected during the HP NMR and HP IR studies of [Rh$_2$(μ-OMe)$_2$(cod)$_2$] and PEtPh$_2$ under CO and H_2 pressure.[14, 15]

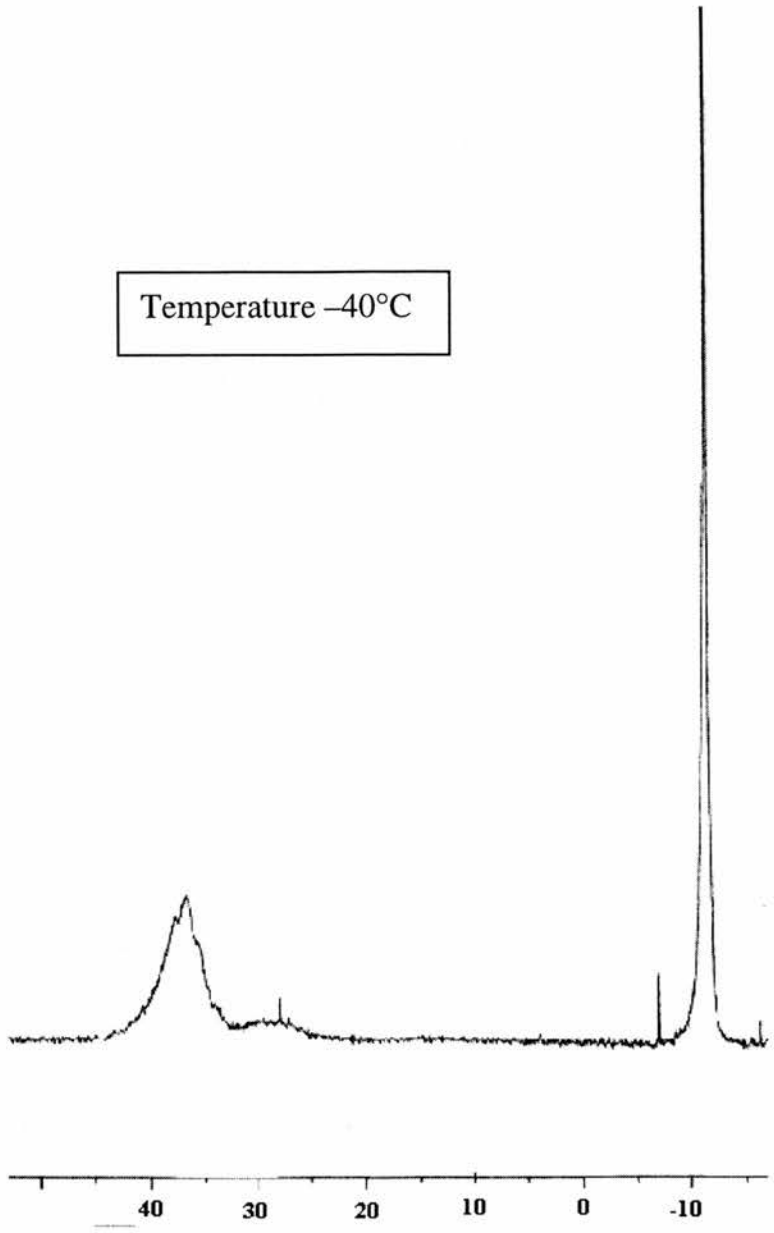

Figure 5.13 ^{31}P NMR spectrum of the rhodium-G1-16ethylPPh$_2$ complexes under an atmosphere of H_2/CO at -40°C.

Freixa *et al* assigned the ^{31}P NMR resonance at δ_P 31.2 ppm (doublet) to the diphosphine ligand in a trigonal bipyramidal geometry (equatorial-equatorial and equatorial-axial isomers) (Figure 5.16), while the hydride region of the ^{1}H NMR showed a signal (td) at δ_H -9.3 ppm (P/Rh = 2/1 to 4/1, 30 bar H_2/CO).[15] The phosphorus atoms of the dimeric rhodium species resonated (^{31}P NMR) between δ_P 20.3 ppm and 14.0 ppm.

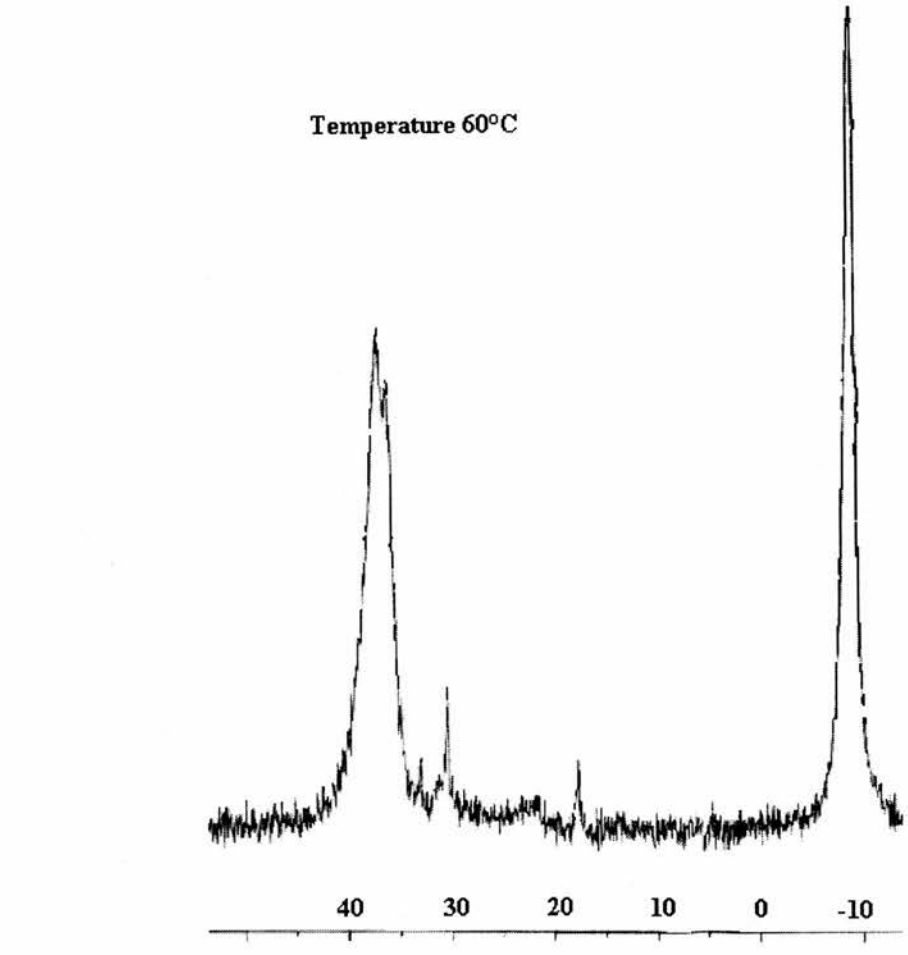

Figure 5.14 ^{31}P NMR spectrum of the rhodium-G1-16ethylPPh$_2$ complexes under an atmosphere of H_2/CO at 25°C.

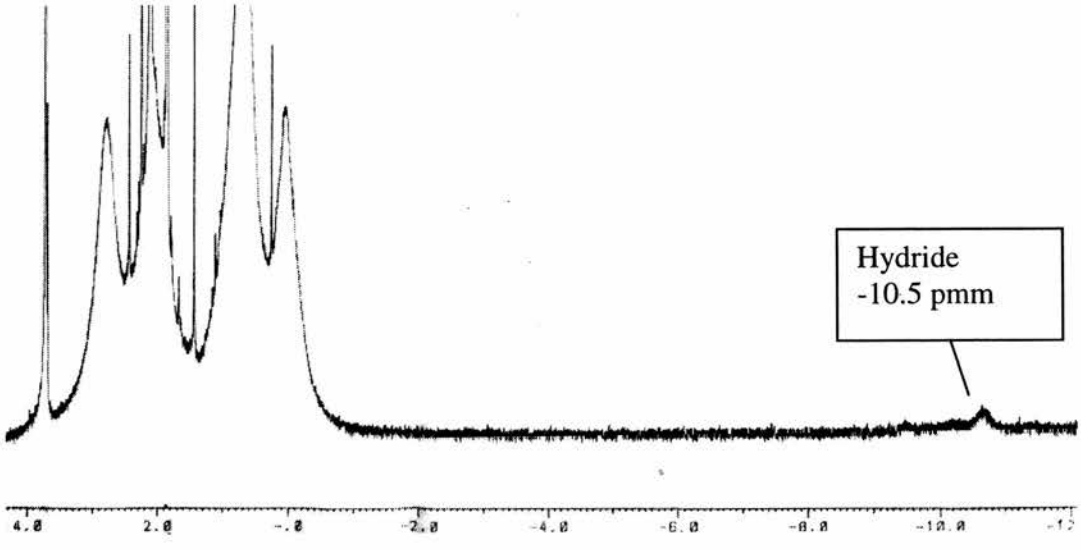

Figure 5.15 ^{1}H NMR spectrum of the rhodium-G1-16ethylPPh$_2$ complexes under an atmosphere of H_2/CO at 25°C.

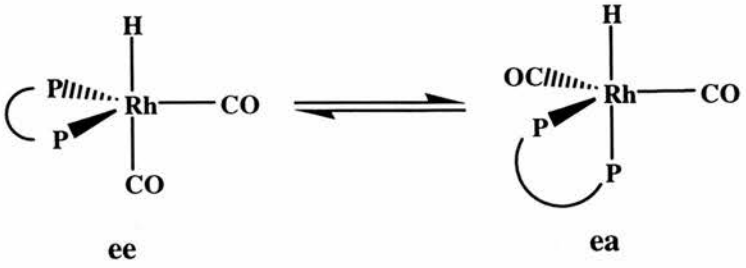

Figure 5.16 Diequatorial – equatorial/axial equilibrium.

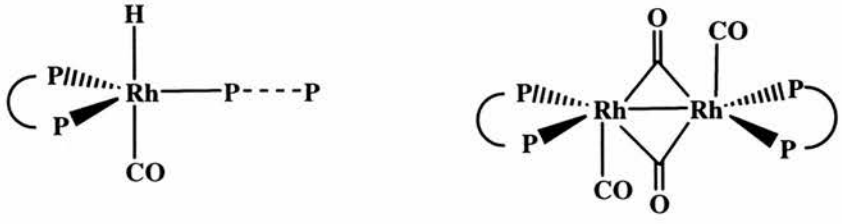

Figure 5.17 A tris(phosphine) rhodium complex (left) and a dimeric rhodium species (right).

In another study (P/Rh = 4/1, 20 bar H_2, 4 bar CO, [Rh] = 0.024 M), Claver and co-workers[14] assigned a new ^{31}P NMR resonance at δ_P 34.5 to the tris(phosphine) rhodium hydride (Figure 5.17, left) with a ^{1}H NMR resonance for the hydride at δ_H –10.1 ppm. The extrapolation of these previous studies to this dendritic system would suggest that the complex did not form a dinuclear species (Figure 5.17, right) under an atmosphere of H_2/CO, configuration expected under low pressure of H_2.[1] It would be also tempting to assign the broad ^{31}P and ^{1}H NMR signals to the tris(phosphine) rhodium complexes. Indeed, the different environment of the phosphorus atoms and the number of combinations (between arms) would give a multitude of disturbed geometries to the rhodium/phosphine complexes, leading to a broad resonance. However, since a low pressure of CO/H_2 (*ca* 1 atmosphere) and a different concentration of rhodium was used, it is difficult to extrapolate the results to the species present under catalytic conditions. In addition, the comparison of the integration of the ^{31}P NMR signal of the free phosphines and coordinated phosphines showed that only 2 phosphine species were coordinated to the metal centre (P/Rh = 4/1 in solution).

Two small resonances appeared in the ^{31}P NMR spectrum at δ_P 30.4 ppm and 17.8 ppm when the temperature was increased to 60°C showing the complexity of such dendritic species. It is thought that these resonances may indicate respectively

the formation of a more defined bidendate phosphine hydridorhodium species (Figure 5.16) and a dimeric rhodium complex (Figure 5.17, left).[14, 15]

5.5.2 Molecular modelling of G1-16ethylPPh$_2$.

In order to try to understand the higher l:b ratios observed with the dendrimer bound catalysts, we carried out some molecular modelling of the G1-16ethylPPh$_2$ dendrimer ($Si_8O_{12}[CH_2CH_2SiMe(CH_2CH_2PPh_2)]_8$) using the Discovery programme contained in the Insight (II) Molecular Modelling Suite of Molecular Simulations Inc.[16] A molecular model carried out by Katherine Haxton is shown in Figure 5.18. The P atoms are drawn in purple, while the Si atoms are represented in yellow (part of the branches) and green (cube) and the oxygen atoms are represented in blue. The molecular modelling showed that the diphenylphosphine moieties were mainly located on the outside of the dendrimer (see Figure 5.18) leading to a high concentration of phosphorus on the periphery with little space available for other substituents. This trend confirms the bulkiness of such species and explains the difficulties in achieving complete conversion for the 16-functionalised dendrimer and, of course for the 24-branched molecule.

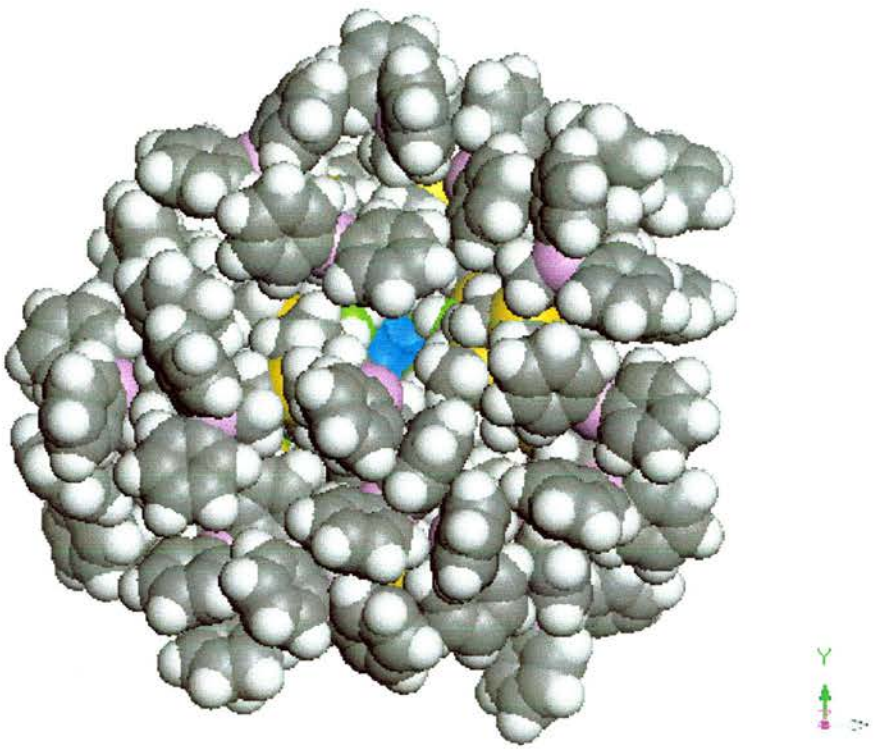

Figure 5.1 Molecular modelling of G1-16ethylPPh$_2$ dendrimer.

High selectivity to the linear aldehyde using ligands with a spacer of more than 5 atoms between the phosphorus atoms have been only achieved when the P atoms are constrained as in BISBI[2] and Xantphos[3] type ligands. The distribution of the P-P distances in BISBI, Xantphos and G0-8PPh_2 and G1-16ethylPPh_2 are shown in Figure 5.19. Whilst BISBI and Xantphos have P-P distances around 4.5 and 4.8 Å respectively, the molecular modelling of the dendrimer showed that within an arm, the P atoms were separated by 4-7 Å, whilst between arms there were always some distances in the 5-10 Å region. Rh-P distances are of the order of 2.5 Å, so very little disruption of the ground state structure of the dendrimer is required to facilitate bidentate binding.

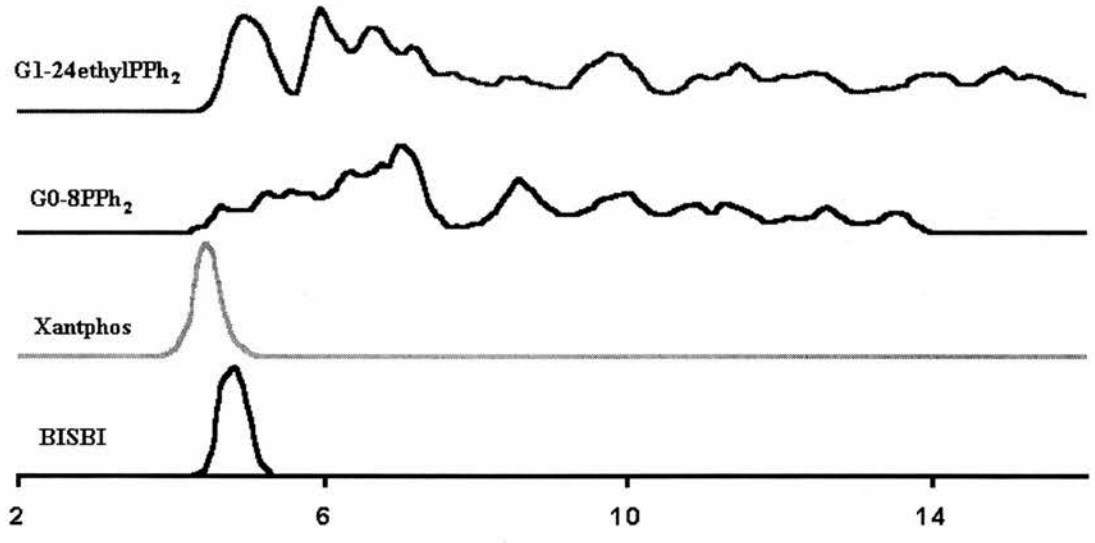

Figure 5.19 P-P distances in different bidendate phosphorus ligands.

Presumably the orientation of the PPh_2 groups relative to one another is determined by steric repulsion on the surface of the dendrimer whilst models of the small molecules showed the lowest energy structures had the phosphine groups far away from one another. If this is the case, one might expect that the compound tetra(diphenylphosphinoethyl)silane for which a X-ray crystal structure showed that the P atoms are 6.94 and 8.33 Å apart (see Figure 5.20 and Appendix II), might show intermediate behaviour between G1-16ethylPPh_2 and diphenylphosphine dimethylsilane. Indeed this was confirmed since a l:b ratio of 6:1 was found (see section 5.3). It is important to note that this model is of course very simplistic since no interactions with the metal are considered.

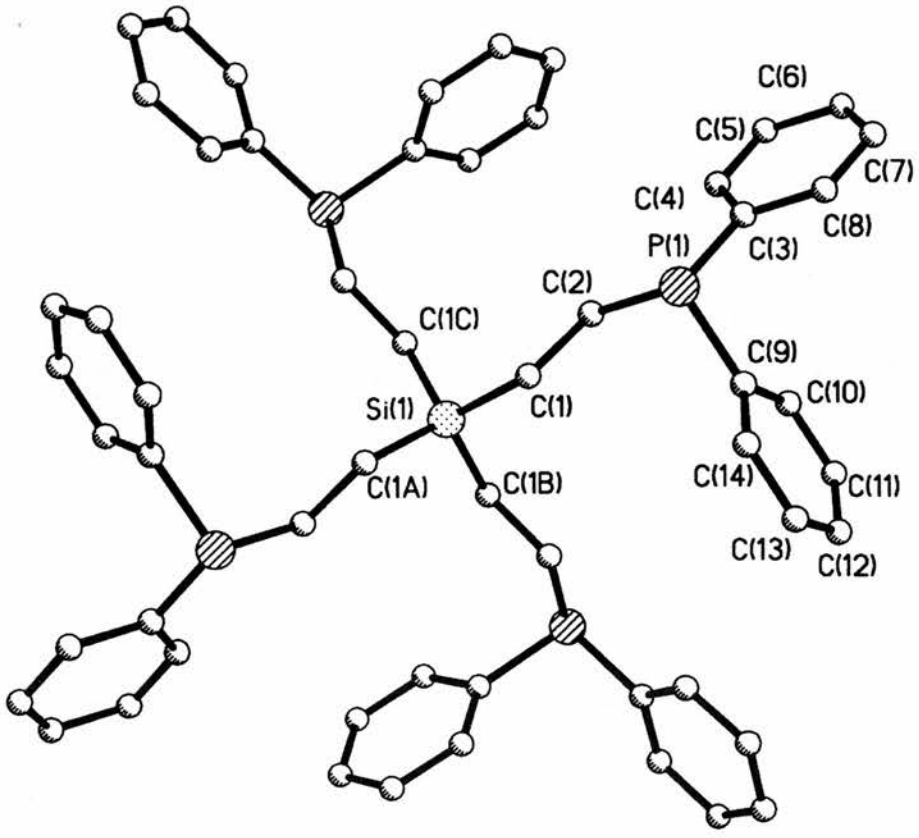

Figure 5.20 X-ray crystal structure of $Si(CH_2CH_2PPh_2)_4$.

5.5.3 High pressure Infrared study of rhodium/G1-16ethylPPh$_2$ complexes.

Since the NMR time scale is 1 to 10 seconds, this technique does not allow the distinction between the diequatorial (ee) and equatorial-axial (ea) geometric isomers of the hydridorhodium complex (fast equilibrium) (Figure 5.16). Averaged chemical shifts and coupling constants are thus observed. However the infrared time scale (10^{-8} s) is much faster than the NMR one, allowing the observation of the CO stretching symmetric and antisymmetric vibrations of the two isomers. The rhodium-hydride bands are usually weak and hidden behind the CO absorption bands.[1] Four absorption bands should therefore been observed if a 5-coordinated hydridorhodium complex is formed (two from each CO of $[RhH(CO)_2P_2]$). However if a tris(phosphine) rhodium complex is formed (Figure 5.17) only one or two bands are expected (see below).[14]

The HP IR spectrometry study was carried out using $[Rh(CO)_2(acac)]$ (0.02 mol dm^{-3}) and G1-16ethylPPh$_2$ (P/Rh = 4/1) in toluene (10 cm^3) at 20 bar of H_2/CO at various temperature (25 to 100°C). The infrared spectra are shown in Figure 5.20 and Figure 5.21.

Interestingly at 25°C (Figure 5.21) three absorption bands at 2030, 1979 and 1954 cm^{-1} and a shoulder around 1940 cm^{-1} were visible and indicating that the ee and ea configuration were already in equilibrium when one could mainly expect the formation of a dimeric species.[14, 15]

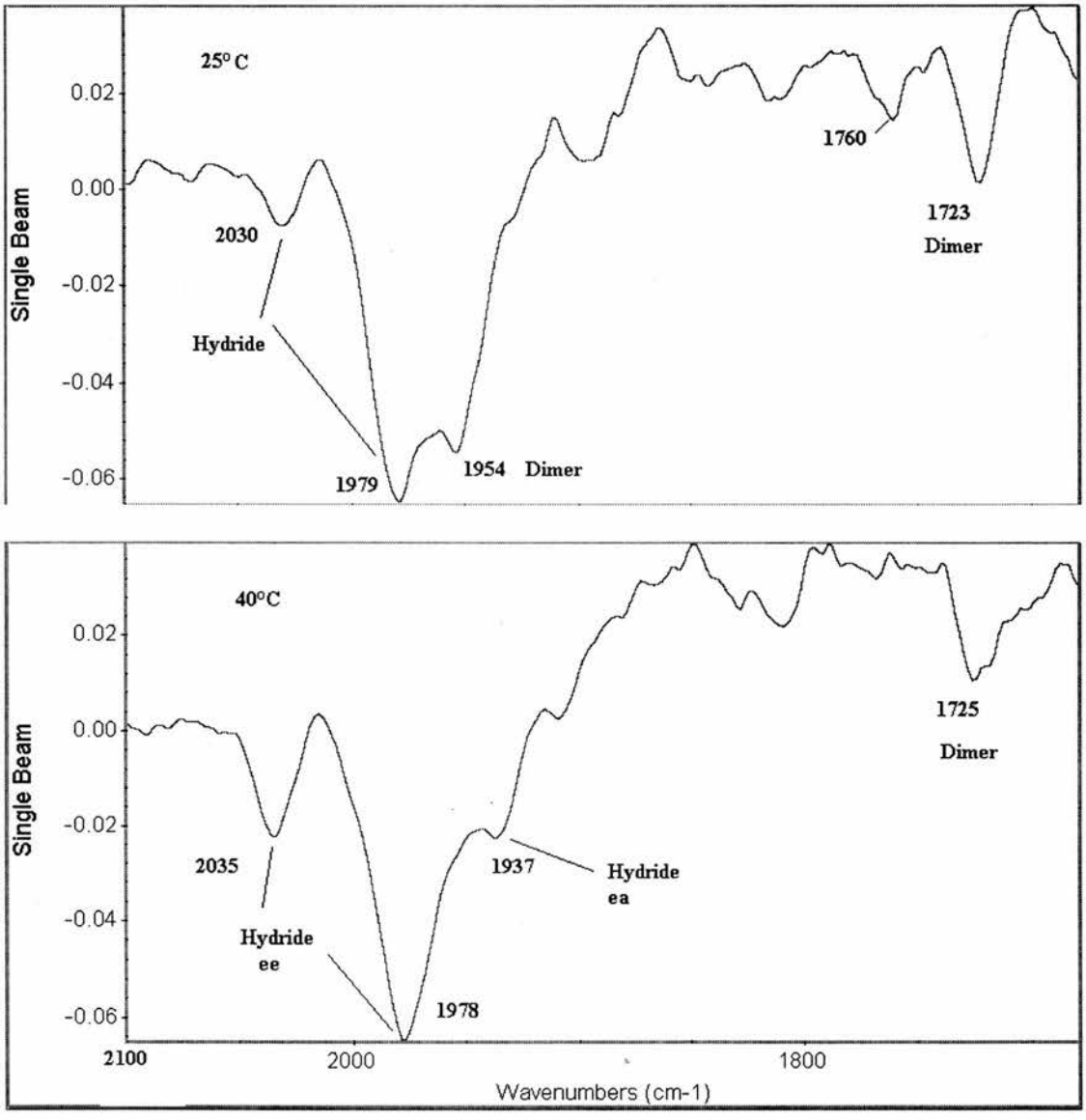

Figure 5.21 HP IR of the rhodium/G1-16ethylPPh$_2$ complexes under 20 bar of H_2/CO at 25°C and 40°C.

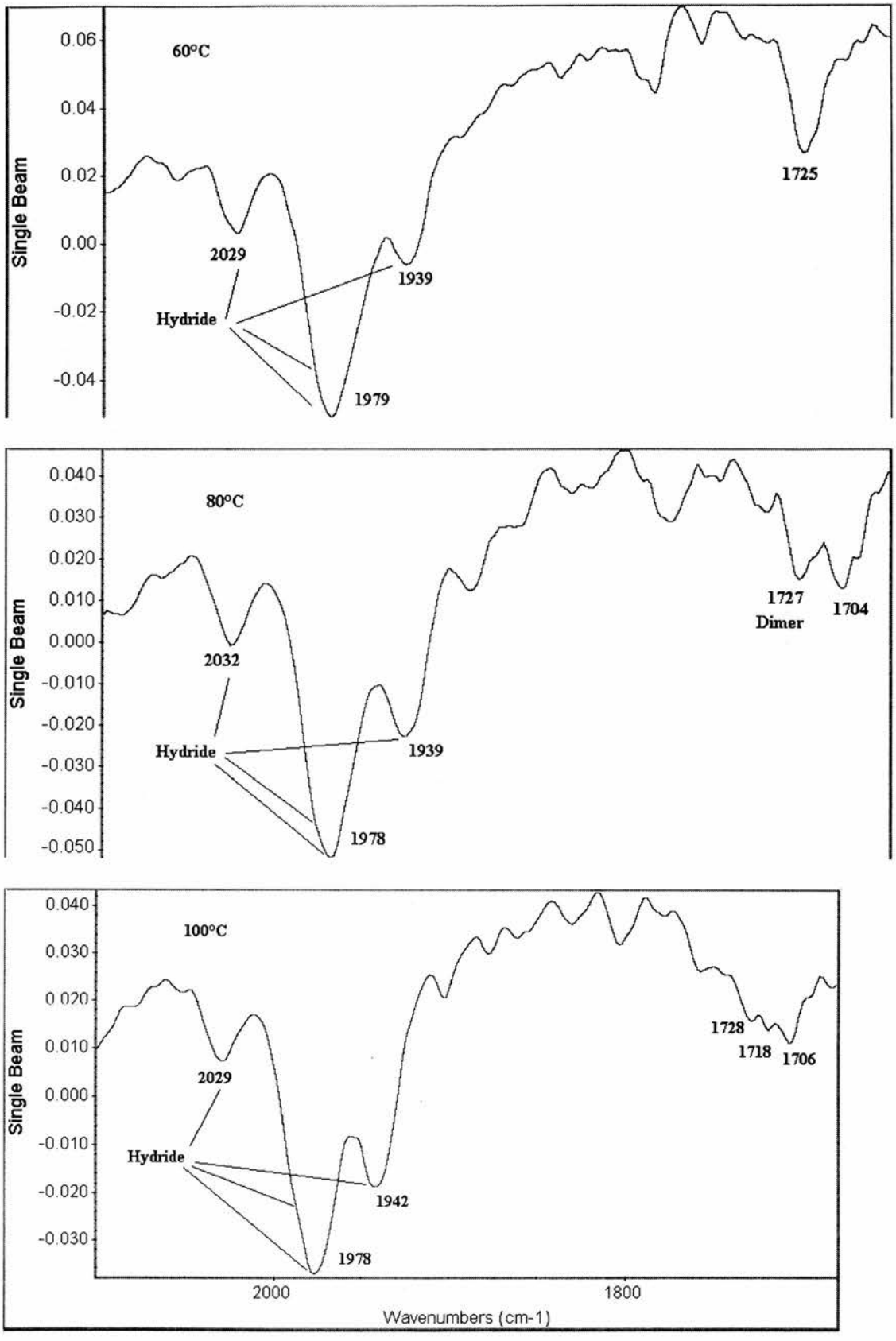

Figure 5.22 HP IR of the rhodium/G1-16ethylPPh$_2$ complexes under 20 bar of H$_2$/CO at 60°C, 80°C and 100°C.

The band at 2030 cm^{-1} (weak) was attributed to the symmetric CO stretching vibration (symmetric ν_{CO}) of the ee hydridorhodium complex.[14, 15, 17] This band emphasises the fact that the dendritic ligand is strongly bound to the metal complex and therefore limits the formation of the dimeric species. A ν_{CO} band from the hydride complex species (ea isomer) is thought to be partially hidden by the band at 1954 cm^{-1} since a shoulder is visible around 1940 cm^{-1} whilst the other band is probably hidden behind the strong CO absorption at 1978 cm^{-1}. Indeed at 40°C (Figure 5.21) the band at 1954 cm^{-1} disappeared and is to be replaced by a band at 1937 cm^{-1}, and then 1939 cm^{-1} at 60°C and 1942 cm^{-1} at 100°C (Figure 5.22), the intensity increasing with the temperature. The latter absorption band is believed to be the antisymmetric stretching vibration of the ea hydride complex.[14, 15, 17] The ν_{CO} band at 1954 cm^{-1} was thus attributed to the terminal ν_{CO} of a dimeric species similar to the one shown in Figure 5.17 while the weak absorption band at 1723 cm^{-1} was attributed to the bridging carbonyls of the dimeric rhodium complex.

The strongest absorption band present during all the experiment, i.e. at all temperatures between 25 to 100°C, was found at 1979-1978 cm^{-1}. This band is probably the band resulting from the antisymmetric CO stretching vibration of the ee hydride isomer. The relative intensity of the ν_{CO} band at 2030 cm^{-1} clearly increased with higher temperatures with little variation in the wave number (2034 cm^{-1}at 40°C, 2029 cm^{-1} at 60°C, 2032 cm^{-1} at 80°C, and 2029 cm^{-1} at 100°C). The missing ν_{CO} band for the ea hydridorhodium species (symmetric stretching vibration) is though to be hidden under the major absorption band at 1978 cm^{-1}since a shoulder is visible around 1990 cm^{-1} above 60°C. It is therefore clear that the dendritic rhodium complexes formed under catalytic conditions were mainly the ee and ea species as shown for the system $[Rh_2(\mu\text{-}OMe)_2(cod)_2]$ and $PEtPh_2$ (P/Rh =2/1, CO/H_2 8 bar, 80°C, [Rh] = 1.67×10^{-3} mol dm^{-3}).[14, 15] Indeed a similar HP IR spectrum was reported with carbonyl absorption at 2037, 1990, 1979 and 1947 cm^{-1}. The determination of the relative amount of the two isomers is however difficult to achieve.

Table 5.7 Selected IR absorption band of rhodium/G1-16ethylPPh$_2$ complexes under 20 bar of H_2/CO.

Temperature °C	ν_{CO} *ee* cm^{-1}	ν_{CO} *ea* cm^{-1}	ν_{CO} *dimer* cm^{-1}
25	2030, 1979	Hidden, 1940	1954, 1723
40	2035, 1978	1990, 1937	1725
60	2029, 1979	1990, 1939	1725
80	2032, 1978	1990, 1939	1727
100	2029, 1978	1990, 1942	1728

If a tris(phosphine) rhodium complex had been the major species one would have expected a single (major) absorption band around 1978 cm^{-1}.[14] However one cannot completely rule out the presence of this tris(phosphine) as a minor species in equilibrium with the ee and ea isomers.

The formation of a dicationic bimetallic Rh^{II} species as described by Stanley and co-workers can however be ruled out since higher energy absorption bands would be expected (2095 to 2058 cm^{-1}).[13] Nevertheless, when the temperature was brought to 80°C, a weak absorption band appeared at 1704-1706 cm^{-1}; absorption, which is in the IR vibration region expected for the bridging carbonyls of a dimeric complex indicating the presence of plausible dimeric species.

5.6 Hydroformylation reaction using phosphite-containing dendritic ligands.

Bulky phosphite ligands with a biphenol bridge have shown interesting properties in hydroformylation reactions since they allow high regioselectivity to the linear aldehyde and often higher rates than their phosphine counterparts (see Chapter 2). The functionalisation of the POSS dendrimer with such phosphite (see Chapter 3) and its use as ligand was therefore of great interest.

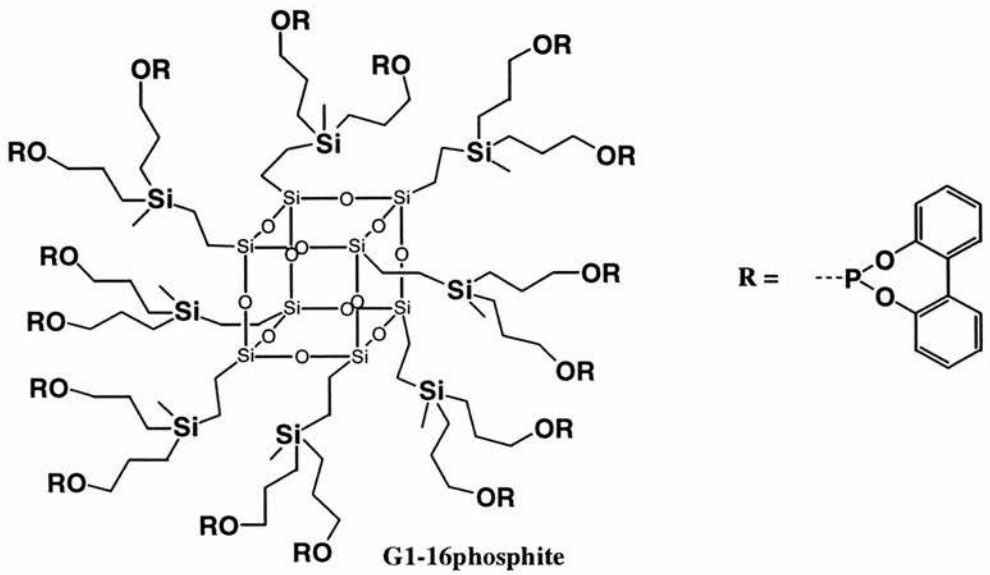

Figure 5.23 A phosphite-containing dendritic ligand.

The hydroformylation of oct-1-ene under CO/H_2 pressure catalysed by the complex formed by $[Rh(acac)(CO)_2]$ (2.0×10^{-5} mol) and G1-16phosphite dendritic ligand (Figure 5.23) was thus carried out in toluene (P/Rh = 6/1). However the results were disappointing. The complex only showed poor activity for hydroformylation reaction at 40 bar of CO/H_2 and at 110 or 120°C. The reaction conditions (pressure and temperature) were modified during the two experiments run since no hydroformylation reaction occurred (monitoring of the gas uptake) at 10 bar of CO/H_2 at the successive temperature 80, 100 and 120°C (first experiment) or at 40 bar at 100°C (second experiment). Both experiments showed long induction periods where the reaction gradually accelerated to actually stop before completion. Indeed total deactivation (monitored by gas uptake) of the 1st and 2nd catalytic solution occurred while conversion of oct-1-ene did not exceed *ca* 86 %. A maximum conversion of 21.1 % to the desired aldehyde, nonan-1-al, with poor linear to branched ratio of 1.1:1 was obtained for the second experiment. The first experiment, only led to formation of 13.3 % of nonan-1-al with a l:b ratio of 1.4:1.

In both experiments, a high proportion of isomerisation products was found with a maximum of 55.3 % for the first experiment. However the amount of oct-2-ene (27.8 %) and 3&4-octene (27.5 %) for this reaction does not necessarily correspond to the 'true' isomerisation process since the reaction solution was successively heated at 10 bar at the successive temperature 80, 100 and 120°C and

finally pressurised to 40 bar and heated to 120°C before showing any hydroformylation reactivity. Therefore it is probable that isomerisation occurred during these 'inactive' conditions. The 2nd experiment led to the isomerisation of 49.9 % of oct-1-ene with a distribution to oct-2-ene and 3&4-octene of respectively 22.6 and 17.3 %. Only the first catalytic solution showed traces of metallic deposit after reaction. High (relative) hydrogenation rate of the substrate and aldehydes occurred since 3.3 % of octane and a combined 1.6 % of nonan-1-ol and 2-methyloctanol were found as products of reaction.

Table 5.8 Hydroformylation of oct-1-ene catalysed by [Rh(acac)(CO)$_2$]/G1-16phosphite.

Reaction conditions[a]	*t* [a] *h*	*Conv.* %	*Oct-2-ene* %	*3&4 octene* %	*PrH & EtH* [b] %	*Nonan-1-al* %	*l:b ratio*
120°C, 40 b [c]	1	83.13	27.8	27.5	1.9	13.3	1.4
110°C, 40 b [d]	1.5	85.87	22.7	17.3	5.8	21.1	1.1

Reaction conditions: [Rh(acac)(CO)$_2$] (2.0×10^{-5} mol), H_2/CO, toluene 4 cm^3, P/Rh = 6/1.

[a] : time before deactivation, [b] : PrH = 2-propylhexanal, EtH = 2-ethylheptanal, [c] : reaction previously heated at 80, 100, 120°C and pressurized at 10 bar, [d] : reaction previously heated at 100°C and pressurized at 40 bar.

It is believed that the poor reactivity/selectivity for hydroformylation reaction of the dendritic rhodium complex was due to steric hindrance of such system. The initial catalytic solution was indeed found as a very pale yellow mixture with a small deposit at the bottom of the flask indicating the poor coordination of the phosphite ligand to the rhodium.

5.7 Conclusion.

It was shown that POSS dendritic ligands functionalised with diphenylphosphine (G1-16ethylPPh$_2$ and G2-propyl-48ethylPPh$_2$) could lead to high selectivity to the linear aldehyde (86 %, l:b ratios up to 14:1) during the hydroformylation of terminal alkenes. Interestingly analogue small molecules (**1**, **2**, and **3**) did not show such selectivity indicating that a 'positive dendritic effect' occurred (see Figure 5.24).

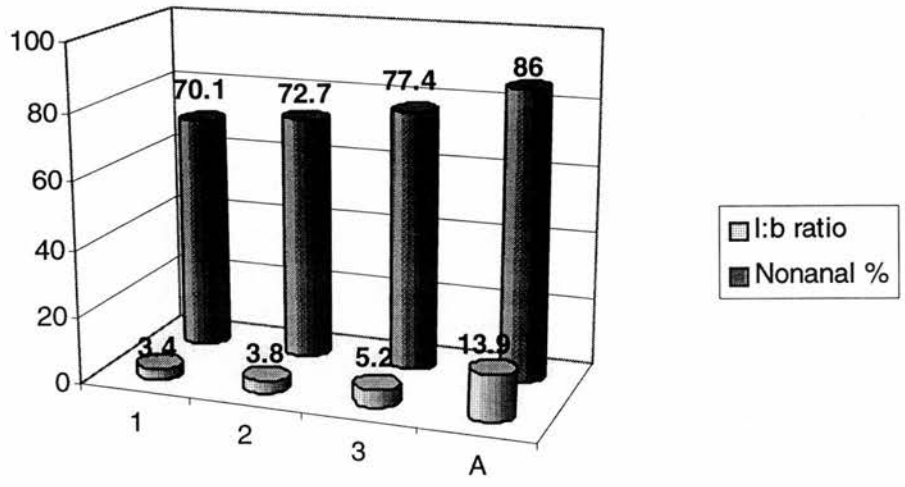

*Figure 5.24 Selectivity to nonan-1-al using the parent molecule ligands and G1-16ethylPPh$_2$ POSS, **1** = $H_2C(CH_2CH_2PPh_2)_2$, **2** = $Me_2Si(CH_2CH_2PPh_2)_2$, **3** = $Si(CH_2CH_2PPh_2)_4$..*

It also appeared that only one dendritic framework (spacer of 5 atoms between the phosphorus) led to high selectivity since other structures were either too compact (G1-16methylPPh$_2$, 3 atom spacers) or not enough constrained (G1-16ethoxyPPh$_2$ and G1-16propylPPh$_2$, 7 atom spacers) to give a high regioselectivity to the linear aldehyde (Figure 5.10). The 7 atom spacers gave better selectivity than the 3 atom spacers. Interestingly the 2nd generation dendrimer, G2-propyl-48ethylPPh$_2$, with a similar structure that of the G1-16ethylPPh$_2$ (5 atoms between the P atoms) maintained a high selectivity (83.8 %, l:b = 11.5) although leading to lower reactivity (rate *ca* half). The composition of the dendritic framework was also important since, when replacing a carbon atom by an oxygen atom β to the phosphorus atoms (from G1-16ethylPPh$_2$ to G1-16methoxyPPh$_2$) the selectivity dropped. It is believed that the low selectivity could arise from a different geometry of the rhodium/dendritic ligand. Indeed an electronic effect is unlikely in this case since no such effect was found in the dendrimers with a 7 atom spacer (G1-16ethoxyPPh$_2$ and G1-16propylPPh$_2$). The functionalisation of the dendritic ligand with electron withdrawing groups (G1-16ethylPAr$_2$, Ar = 3,5-($C_6H_3(CF_3)_2$) led to lower selectivity. Three hypotheses, an equatorial-axial coordination of the P atoms in the rhodium complex, a too sterically hindered ligand or actually lack of phosphorus species, were thus suggested to explain such an effect.

The use of a phosphite-functionalised dendritic ligand (G1-16phosphite) led to poor hydroformylation activity and selectivity possibly caused by a too sterically hindered molecule.

The characterisation of the rhodium complexes present in solution under H_2 and CO pressure was carried out using ^{1}H and ^{31}P NMR and HP IR techniques. It appeared that the species formed under H_2/CO was mainly the 5-coordinated hydridorhodium complex (trigonal bipyramidal structure) with the phosphorus species in equatorial-equatorial and equatorial-axial equilibrium. This result (presence of the ea coordination) may help to explain the low selectivity obtained when the POSS dendrimer was functionalised with more electron withdrawing arylphosphine species (G1-16ethylAr_2). The presence of a tris(phosphine) rhodium complex was not completely ruled out whilst no strong evidence of the formation of active dimeric species could be found at temperatures above 25°C. It is therefore believed that the high regioselectivity obtained with the G1-16ethylPPh_2 ligand is mainly due to the formation of a constrained bidentate ligand as in BISBI[2] or Xantphos[3] ligands. Molecular modelling studies tend to support this conclusion.

5.8 References for Chapter 5.

1 P. W. N. M. van Leeuwen and C. Claver, 'Rhodium Catalysed Hydroformylation', Kluwer Academic Publishers, Dordrecht, 2000.

2 C. P. Casey and L. M. Petrovich, *J. Am. Chem. Soc.*, 1995, **117**, 6007.

3 M. Kranenburg, Y. E. M. van der Burgt, P. C. J. Kamer, and P. W. N. M. van Leeuwen, *Organometallics*, 1995, **14**, 3081.

4 D. de Groot, P. G. Emmerink, C. Coucke, J. N. H. Reek, P. C. J. Kamer, and P. W. N. M. van Leeuwen, *Inorg. Chem. Commun.*, 2000, **3**, 711.

5 C. P. Casey, L. E. Paulsen, E. W. Beuttenmueller, B. R. Proft, L. M. Petrovich, and B. A. Matter, *J. Am. Chem. Soc.*, 1997, **119**, 11817.

6 C. P. Casey, E. L. Paulsen, E. W. Beuttenmueller, B. R. Proft, B. A. Matter, and D. R. Powell, *J. Am. Chem. Soc.*, 1999, **121**, 63.

7 L. A. van der Veen, P. H. Keeven, G. C. Schoemaker, J. N. H. Reek, P. C. J. Kamer, P. W. N. M. van Leeuwen, M. Lutz, and A. L. Spek, *Organometallics*, 2000, **19**, 872.

8 J. D. Unruh and J. R. Christenson, *J. Mol. Cata.*, 1982, **14**, 19.

9 D. Evans, J. A. Osborn, and G. Wilkinson, *J. Chem. Soc. A.*, 1968, 3133.

10 D. Evans, G. Yagupsky, and G. Wilkinson, *J. Chem. Soc. A*, 1968, 2660.

11 G. Gregorio, G. Montrasi, M. Tampieri, P. Cavalieri d'Oro, G. Pagani, and A. Andreetta, *Chim. Ind. (Milan)*, 1980, **62**, 389.

12 M. E. Broussard, B. Juma, S. G. Train, W.-J. Peng, S. A. Laneman, and G. G. Stanley, *Science*, 1993, **260**, 1784.

13 R. C. Matthews, D. K. Howell, W.-J. Peng, S. G. Train, W. D. Treleavan, and G. G. Stanley, *Angew. Chem. Int. Ed.*, 1996, **35**, 2253.

14 del Río, W. G. J. de Lange, P. W. N. M. van Leeuwen, and C. Claver, *J. Chem. Soc., Dalton Trans.*, 2001, 1293.

15 Z. Freixa, M. Pereira, A. A. C. C. Pais, and J. C. Bayón, *J. Chem. Soc., Dalton Trans.*, 1999, 3245.

16 Materials Studio, , San Diego 2000.

17 M. Diéguez, C. Claver, A. M. Masdeu-Bultó, A. Ruiz, P. W. N. M. van Leeuwen, and G. C. Schoemaker, *Organometallics*, 1999, **18**, 2107.

Chapter Six: Experimental

6 Experimental.

All experiments were carried out under inert atmosphere (argon) using standard Schlenk techniques. Argon was dried through a Cr (II) / silica packed glass column.

Compounds were purchased from Aldrich, Acros or Strem and were used without further purification unless otherwise mentioned. Chlorosilane products were distilled under inert atmosphere before used. All gases were purchased from BOC gases. The solvents were distilled and kept under argon. Ethanol and methanol were distilled over magnesium ethoxide under argon and stored under argon over molecular sieves. Cyclohexane and hexane were distilled over sodium under inert atmosphere. Water was distilled and stored under nitrogen/argon. Petroleum ether (boiling range 40-60°C) and diethyl ether were distilled over sodium diphenylketyl. Dichloromethane was distilled over calcium hydride. Toluene was distilled over sodium. Deuteriated solvents were purchased from Cambridge Isotope Laboratories, degassed by repeated freeze-pump-thaw cycles under high vacuum and stored under argon over molecular sieves.

Infrared spectra were obtained using a Nicolet Protege 460 with CsI optics. The infrared spectrometer was interfaced to a personal computer via the OMNIC operating system. Carbon, proton and phosphorous NMR spectra were recorded on a Bruker AM 300 NMR spectrometer or a Varian 300 NMR spectrometer. Broad band decoupling was used for ^{13}C spectra and ^{31}P spectra. ^{1}H and ^{13}C NMR spectra were referenced internally to deuterated solvents: CD_2Cl_2: ^{1}H, δ, 5.35 ppm, ^{13}C, δ, 53.8 ppm; CD_3OD: ^{1}H, δ, 3.35 ppm, ^{13}C, δ, 49.0 ppm; C_6D_6: ^{1}H, δ, 7.16 ppm, ^{13}C, δ, 128.39 ppm; C_7H_8: ^{1}H, δ, 2.09 ppm, ^{13}C, δ, 20.4 ppm; $CDCl_3$: ^{1}H, δ, 7.27 ppm, ^{13}C, δ, 77.23 ppm. ^{31}P NMR were referenced externally to phosphoric 85 % H_3PO_4.

Chemical analysis was performed by the University of St. Andrews Microanalysis service on a Carlo Erba model 1106 elemental analyser. Matrix assisted laser desorption/ionisation (MALDI) mass spectrometry measurements were performed on a Micromass Tof Spec 2E mass spectrometer system (Manchester, UK) equipped with a 337 nm N_2 laser and operating in positive ion reflectron mode. Samples were prepared by addition of the matrix (α-cyano-4-hydroxycinnamic acid, 2,6-dihydroxyacatophenone (good resolution spectra) or 2,5-dihydroxybenzoic acid) and were then dissolved in a suitable solvent (THF, acetonitrile or dichloromethane).

All mass measurements stated refer to observed peaks for the most common isotopes (^{12}C, ^{1}H, ^{28}Si and ^{16}O) and so are not necessarily the most abundant species.

6.1 Synthesis of dendritic molecules built on a polyhedral oligo-silsesquioxane core.

6.1.1 Synthesis of successive generation dendrimers.

6.1.1.1 First generation dendrimer.

1, 3, 5, 7, 11, 13, 15-Octavinylpentacylclo-[9.5.1.1^{3,9}.1^{5,15}.1^{7,13}] octasiloxane (G0-8vinyl).[1, 2]

The compound vinyltrichlorosilane (24 cm^3) was added dropwise to a solution of water (270 cm^3) and acetone (900 cm^3) cooled in an ice bath. The ice bath was removed and the solution stirred at room temperature for 1 month. The solution was filtered to give 3.5 g of a white solid (23 %).

^{1}H NMR ($CDCl_3$):δ_H 5.5- 6.6 ppm (m, 24 H, $CH=CH_2$).

^{13}C -{^{1}H} NMR ($CDCl_3$):δ_C (ppm) 137.31 (**C**H=CH_2), 129.02 (CH=**C**H_2).

1,3,5,7,11,13,15-Octakis[2-dichloromethylsilyl)ethyl]pentacyclo-[9.5.1.1^{3,9}.1^{5,15}.1^{7,13}]octasiloxane (G1-16Cl).[3]

The compounds $HSiMeCl_2$ (6.7 cm^3, 59.3 mmol) and $H_2[PtCl_6]$ (0.1 mol dm^{-3} in $^{i}PrOH$, 10 drops) were added to a solution of **G0-8vinyl** (1.0 g, 1.58 mmol) in diethyl ether (50 cm^3). The resulting mixture was heated under reflux for 8 h and stirred at 20°C for 15 h. The solvent was removed *in vacuo* to give 2.40 g (98 %) of **G1-16Cl** as a white solid.

^{1}H NMR ($CDCl_3$):δ_H (ppm) 1.52 (m, 16 H, CH_2), 0.83 (m, 16 H, CH_2), 0.80 (s, 24 H, CH_3).

^{13}C -{^{1}H} NMR ($CDCl_3$):δ_C (ppm) 16.77 (**C**H_2SiCl_3), 3.41 (O_3SiCH_2),

IR/cm^{-1} (KBr disc): 2920m, 1409s, 1274s, 1156vs ($SiCH_2CH_2Si$), 1116vs (SiOSi), 757s, 665s ($OSiCH_2$), 587s and 565s (SiCl), 453s.

Vinyl magnesium bromide.

Vinyl bromide (gas) was carefully bubbled through a slurry of magnesium turnings (12.12 g, 0.50 mol) in THF (500 cm^3). Once the reaction had started, the gas flow was monitored to maintain a gentle reflux. After reaction (no Mg left), the

reaction was refluxed 30 min. Argon was then bubbled through at room temperature for 10 min. The brown mixture was filtered and kept under argon at –6°C (precipitation of white crystals). The solution was titrated by an aqueous HCl solution (0.1 mol dm^{-3}) to determine the concentration (1.0 mol dm^{-3}). The mixture was allowed to reach room temperature (homogeneous solution) before used.

1,3,5,7,11,13,15-Octakis[2-divinylmethylsilyl)ethyl]pentacyclo-[9.5.1.1^{3,9}.1^{5,15}.1^{7,13}]octasiloxane (G1-16vinyl).[3]

Vinylmagnesium bromide (1.0 mol dm^{-3} in THF, 35 cm^3) was added to a solution of **G1-16Cl** (2.65 g, 1.71 mmol) in THF (40 cm^3). The resulting solution was stirred at room temperature for 17 h. The mixture was slowly added to a cooled (ice bath) aqueous solution of ammonium chloride (1.0 mol dm^{-3} in water, 50 cm^3). The aqueous solution was extracted with petroleum (2 × 80 cm^3). The combined organic layers were washed with a saturated aqueous solution of NaCl (20 cm^3), dried over Na_2SO_4 and concentrated *in vacuo*. The residue was loaded onto a column of silica gel and eluted with petroleum to afford compound **G1-16vinyl** (2.06 g, 85 %).

Microanalysis found C, 47.1; H, 7.3; $Si_{16}O_{12}C_{56}H_{104}$ requires C, 47.0; H, 7.3.

^{1}H NMR ($CDCl_3$): δ_H (ppm) 6.13 (dd, $^3J_{HH}$ = 19.5 Hz, $^2J_{HH}$ = 14.2 Hz, 24 H, CH_2=), 6.02(dd, $^3J_{HH}$ = 14.2 Hz, $^3J_{HH}$ = 4.4 Hz, 24 H, =CH_2), 5.71 (dd, $^3J_{HH}$ = 19.5 Hz, $^3J_{HH}$ = 4.4 Hz, 24 H, SiCH=), 0.62 (m, 16 H, $SiCH_2$), 0.76 (m, $SiCH_2$, 16H),

^{13}C -{^{1}H} NMR ($CDCl_3$):δ_C (ppm) 136.65 (**C**H=CH_2), 133.14 (CH=**C**H_2), 5.35 ($O_3SiCH_2CH_2$), 4.27 ($O_3SiCH_2CH_2$), -5.90 ($SiCH_3$).

IR/cm^{-1} (KBr disc): 3048m (Si-vinyl), 2923m, 1592m (C=C), 1404s (C=C), 1263m, 1143vs ($SiCH_2CH_2Si$), 1116vs (SiOSi), 1006s (C=C), 952s, 707s, 531m

1,3,5,7,11,13,15-Octakis[2-diallylmethylsilyl)ethyl]pentacyclo-[9.5.1.1^{3,9}.1^{5,15}.1^{7,13}] octasiloxane (G1-16allyl).

Allylmagnesium bromide (1.0 mol dm^{-3} in THF, 35 cm^3) was added to a solution of **G1-16Cl** (2.65 g, 1.71 mmol) in THF (40 cm^3). The resulting solution was stirred at room temperature for 17 h. The mixture was slowly added to a cooled (ice bath) aqueous solution of ammonium chloride (1.0 mol dm^{-3} in water, 50 cm^3). The aqueous solution was extracted with petroleum (2 × 80 cm^3). The combined

organic layers were washed with saturated aqueous solution of NaCl (20 cm^3), dried over Na_2SO_4 and concentrated *in vacuo*. The residue was loaded onto a column of silica gel and eluted with petroleum to afford 2.5 g (90 % yield) of the oily **G1-16allyl**.

Microanalysis found C, 52.3; H: 8.3; $Si_{16}O_{12}C_{72}H_{136}$ requires C, 52.6; H, 8.3.

^{1}H NMR ($CDCl_3$): δ_H (ppm) 5.77 (m, 16 H, C**H**=CH_2), 4.86 (m, 32 H, CH=C**H**$_2$), 1.57 (d, $^3J_{HH}$ = 7.1 Hz, 32 H, SiC**H**$_2$CH=CH_2), 0.59 (m, 32 H, $SiCH_2CH_2Si$), 0.00 ($SiCH_3$).

^{13}C -{^{1}H} NMR ($CDCl_3$):δ_C (ppm) 134.26 (**C**H=CH_2), 113.86 (CH=**C**H$_2$), 19.32 (**C**H$_2$CH=CH_2), 4.27 (O_3Si**C**H$_2$CH$_2$), 2.75 (O_3CH_2**C**H$_2$), -5.40 ($SiCH_3$).

1,3,5,7,11,13,15-Octakis[2-trichlorosilyl)ethyl]pentacyclo-[9.5.1.1^{3,9}.1^{5,15}.1^{7,13}] octasiloxane (G1-24Cl).[3]

The compounds $HSiCl_3$ (6 cm^3, 59.3 mmol) and $H_2[PtCl_6]$ (0.1 $mol.dm^{-3}$ in ^{i}PrOH, 10 drops) were added to a solution of **G0-8vinyl** (1.0 g, 1.58 mmol) in diethyl ether (50 cm^3). The resulting mixture was heated under reflux for 8 h and stirred at 20°C for 15 h. The solvent was removed *in vacuo* to give 2.65g (97.8 %) of **G1-24Cl** as a white solid.

^{1}H NMR ($CDCl_3$):δ_H (ppm) 1.45 (m, CH_2, 16H), 0.95 (m, 16 H, CH_2).

^{13}C -{^{1}H} NMR ($CDCl_3$):δ_C (ppm) 16.81 (CH_2SiCl_3), 3.43 (O_3Si**C**H$_2$).

IR/cm^{-1} (KBr disc): 2920m, 1409s, 1274s, 1156vs ($SiCH_2CH_2Si$), 1116vs (SiOSi), 757s, 665s ($OSiCH_2$), 587s and 565s (SiCl), 453s.

1,3,5,7,11,13,15-Octakis[2-trivinylsilyl)ethyl]pentacyclo-[9.5.1.1^{3,9}.1^{5,15}.1^{7,13}] octasiloxane (G1-24vinyl).[3]

Vinylmagnesium bromide (1.0 $mol.dm^{-3}$ in THF, 45 cm^3) was added to a solution of **G1-24Cl** (2.65 g, 1.54 mmol) in THF (40 cm^3). The resulting solution was stirred at room temperature for 17 h. The mixture was slowly added to a cooled (ice bath) aqueous solution of ammonium chloride (1.0 $mol.dm^{-3}$ in water, 50 cm^3). The aqueous solution was extracted with petroleum (2 × 80 cm^3). The combined organic layers were washed with saturated aqueous solution of NaCl (20 cm^3), dried over Na_2SO_4 and concentrated *in vacuo*. The residue (2.33 g) was loaded onto a

column of silica gel and eluted with petroleum to afford the compound **G1-24vinyl** (1.90 g, 81 %).

Microanalysis found C, 50.8; H: 7.3; $Si_{16}O_{12}C_{64}H_{104}$ requires C, 50.8; H, 7.1.

^{1}H NMR ($CDCl_3$): δ_H (ppm) 6.08-6.21 (m, 48 H, $=CH_2$), 5.78 (dd, $^3J_{HH}$ = 16.8 Hz, 24 H, SiCH=), 0.76 (m, 16 H, CH_2), 0.62 (m, 16 H, CH_2).

^{13}C -{^{1}H} NMR ($CDCl_3$):δ_C (ppm) 134.74 ($CH=CH_2$), 134.44 ($CH=CH_2$), 4.22 ($O_3SiCH_2CH_2$), 4.02 ($O_3SiCH_2CH_2$).

IR/cm^{-1} (KBr disc): 3048m (Si-vinyl), 2923m, 1592m (C=C), 1404s (C=C), 1263m, 1143vs ($SiCH_2CH_2Si$), 1116vs (SiOSi), 1006s (C=C), 952s, 707s, 531m.

1,3,5,7,11,13,15-Octakis[2-triallylsilyl)ethyl]pentacyclo-[9.5.1.1^{3,9}.1^{5,15}.1^{7,13}] octasiloxane (G1-24allyl).[3]

Allylmagnesium bromide (1.0 mol dm^{-3} in THF, 45 cm^3) was added to a solution of **G1-24Cl** (2.65 g, 1.54 mmol) in THF (40 cm^3). The resulting solution was stirred at room temperature for 17 h. The mixture was slowly added to a cooled (ice bath) aqueous solution of ammonium chloride (1.0 mol dm^{-3} in water, 50 cm^3). The aqueous solution was extracted with petroleum (2 × 80 cm^3). The combined organic layers were washed with saturated aqueous solution of NaCl (20 cm^3), dried over Na_2SO_4 and concentrated *in vacuo*. The residue was loaded onto a column of silica gel and eluted with petroleum to afford the desired compound **G1-24allyl** (1.90 g, 81 %) as an oil.

Microanalysis found C, 56.6; H: 8.8; $Si_{16}O_{12}C_{88}H_{152}$ requires C, 57.1; H, 8.3.

^{1}H NMR ($CDCl_3$): δ_H (ppm) 5.79 (m, 24 H, C**H**=CH_2), 4.90 (m, 48 H, CH=C**H**$_2$), 1.61 (d, $^3J_{HH}$ = 8.0 Hz, 48 H, SiC**H**$_2$CH=CH_2), 0.63 (m, 32 H, $SiCH_2CH_2Si$).

^{13}C -{^{1}H} NMR ($CDCl_3$):δ_C (ppm) 134.28 (**C**H=CH_2), 113.83 (CH=**C**H$_2$), 19.06 (**C**H$_2$CH=CH_2), 4.28 ($O_3SiCH_2CH_2$), 2.76 ($O_3CH_2CH_2$).

6.1.1.2 Second generation dendrimers.

1,3,5,7,11,13,15-Octakis{2-{tris[2-(trichlorosilyl)ethyl]sily}ethyl}pentacyclo-[9.5.1.1^{3,9}.1^{5,15}.1^{7,13}]octasiloxane (G2-ethyl-72Cl).[3]

The compounds $HSiCl_3$ (13 cm^3, 0.128 mol) and $H_2[PtCl_6]$ (0.1 mol.dm^{-3} in ^{i}PrOH, 15 drops) were added to a solution of **G1-24vinyl** (1.8 g, 1.19 mmol) in diethyl ether (50 cm^3). The resulting mixture was heated at reflux for 27 h. The solvent was removed *in vacuo* to give **G2-ethyl-72Cl** as a white solid (4.97 g, 88 %).

^{1}H NMR ($CDCl_3$):δ_H (ppm) 1.31 (m, 48 H, CH_2SiCl_3), 0.87 (m, 48 H, $CH_2CH_2SiCl_3$), 0.68 (m, 16 H, $SiCH_2CH_2Si$), 0.63 (m, 16 H, $SiCH_2CH_2Si$).

^{13}C -{^{1}H} NMR ($CDCl_3$):δ_C (ppm) 17.22 (CH_2SiCl_3), 4.27 (br, $O_3SiCH_2CH_2Si$), 1.95 ($CH_2CH_2SiCl_3$).

^{29}Si NMR ($CDCl_3$): δ (ppm) 12.31 ($SiCl_3$), 11.02 ($SiCH_2$), -67.02 (O_3SiC).

1,3,5,7,11,13,15-Octakis{2-{tris[2-(trivinylsilyl)ethyl]silyl}ethyl}pentacyclo-[9.5.1.1^{3,9}.1^{5,15}.1^{7,13}]octasiloxane (G2-ethyl-72vinyl).[3]

Vinylmagnesium bromide (1.0 mol dm^{-3} in THF, 80 cm^3) was added to a solution of **G2-ethyl-72Cl** (2.65 g, 1.54 mmol) in THF (50 cm^3). The resulting solution was stirred at room temperature for 16 h and refluxed for 2 h. The mixture was slowly added to a cooled (ice bath) aqueous solution of ammonium chloride (1.0 mol dm^{-3} in water, 50 cm^3). The aqueous solution was extracted with petroleum (2 × 80 cm^3). The combined organic layers were washed with saturated aqueous solution of NaCl (20 cm^3), dried over Na_2SO_4 and concentrated *in vacuo*. The residue (4.63 g) was loaded onto a column of silica gel and eluted with petroleum to afford compound **G2-ethyl-72vinyl** (1.97 g, 45 %).

^{1}H NMR ($CDCl_3$):δ_H (ppm) 6.21-6.08 (m, 144 H, $=CH_2$), 5.78 (dd, $^3J_{HH}$ = 16.8 Hz, $^2J_{HH}$ = 6.3 Hz, 72 H, $SiCH=CH_2$), 0.54 (m, 128 H, $SiCH_2$).

^{13}C -{^{1}H} NMR ($CDCl_3$): δ_C (ppm) 134.55 (br, $CH=CH_2$), 4.86 (br, CH_2CH_2), 2.55 (br, CH_2CH_2).

1,3,5,7,11,13,15-Octakis{2-{tris[2-(dichloromethylsilyl)propyl]sily} ethyl}pentacyclo-[9.5.1.1^{3,9}.1^{5,15}.1^{7,13}]octasiloxane (G2-propyl-48Cl).

The compounds $HSiMeCl_2$ (15 cm^3, 0.15 mol) and $H_2[PtCl_6]$ (0.1 mol.dm^{-3} in ^{i}PrOH, 15 drops) were added to a solution of **G1-24allyl** (2.0 g, 1.08 mmol) in toluene (50 cm^3). The resulting mixture was heated at reflux for 96 h. The solvent was removed *in vacuo* to give **G2-propyl-48Cl** as a white solid (4.7 g, 95 %).

^{1}H NMR ($CDCl_3$):δ_H (ppm) 1.84 (β hydrosilylation, $MeCl_2SiCH(CH_3)CH_2$-), 1.55 (m, $CH_2CHMeSiCl_3$, $CH_2CH_2SiCl_3$), 1.20 (m, 48 H, $CH_2CH_2SiCl_3$), 0.78 (s, 72 H, $SiCH_3$), 0.76-0.55 (m, 80 H, $SiCH_2$).

^{13}C -{^{1}H} NMR ($CDCl_3$):δ_C (ppm) 28.36 (27.65), 17.37 (16.64), 14.71, 4.41 (br, $O_3SiCH_2CH_2Si$).

1,3,5,7,11,13,15-Octakis{2-{tris[2-(trichlorosilyl)propyl]sily}ethyl}pentacyclo-[9.5.1.1^{3,9}.1^{5,15}.1^{7,13}]octasiloxane (G2-propyl-72Cl).

The compounds $HSiCl_3$ (13 cm^3, 0.128 mol) and $H_2[PtCl_6]$ (0.1 $mol.dm^{-3}$ in ^iPrOH, 15 drops) were added to a solution of **G1-24allyl** (2.20 g, 1.19 mmol) in toluene (50 cm^3). The resulting mixture was heated at reflux for 96 h. The solvent was removed *in vacuo* to give **G2-propyl-72Cl** as a white solid (5.05 g, 92 %).

^{1}H NMR ($CDCl_3$):δ_H (ppm) 1.64 (br, 48 H, $CH_2CH_2SiCl_3$), 1.51 (m, 48 H, $CH_2CH_2SiCl_3$), 1.30- 0.45 (m, 80 H, CH_2Si).

^{13}C -{^{1}H} NMR ($CDCl_3$):δ_C (ppm) 28.37 (CH_2SiCl_3), 17.37 ($CH_2CH_2SiCl_3$), 14.71 $SiCH_2CH_2CH_2$), 4.41 (br, $SiCH_2$)

1,3,5,7,11,13,15-Octakis{2-{tris[2-(divinylmethylsilyl)propyl]silyl}ethyl} pentacyclo-[9.5.1.1^{3,9}.1^{5,15}.1^{7,13}]octasiloxane (G2-propyl-48vinyl).

Vinylmagnesium bromide (1.0 mol dm^{-3} in THF, 60 cm^3) was added to a solution of **G2-propyl-48Cl** (4.52 g, 0.98 mmol) in THF (50 cm^3). The resulting solution was stirred at room temperature for 48 h. The mixture was slowly added to a cooled (ice bath) aqueous solution of ammonium chloride (1.0 mol dm^{-3} in water, 50 cm^3). The aqueous solution was extracted with petroleum (2 × 80 cm^3). The combined organic layers were washed with saturated aqueous solution of NaCl (20 cm^3), dried over Na_2SO_4 and concentrated *in vacuo*. The residue was loaded onto a column of silica gel and eluted with petroleum to afford compound **G2-propyl-48vinyl** as a colourless oil (3.83 g, 70 %).

Microanalysis found C, 59.3; H, 10.1; $Si_{40}O_{12}C_{208}H_{392}$ requires C, 59.4; H, 9.3.

^{1}H NMR ($CDCl_3$):δ_H (ppm) 6.20-5.94 (m, 96 H, $=CH_2$), 5.73 (dd, $^3J_{HH}$ = 19.8 Hz, $^2J_{HH}$ = 4.3 Hz, 48 H, $SiCH=CH_2$), 1.80 (br, SiCH), 1.36 (m br, CH_2), 0.78-0.40 (m, $SiCH_2$), 0.12 (br, 72 H, CH_3Si).

^{13}C -{^{1}H} NMR ($CDCl_3$): δ_C (ppm) 137.23 ($CH=CH_2$), 132.78 ($CH=CH_2$), 18.92, 18.47, 16.76, 4.57 (br, $O_3SiCH_2CH_2$), -5.08 (CH_3Si).

1,3,5,7,11,13,15-Octakis{2-{tris[2-(trivinylsilyl)propyl]silyl}ethyl}pentacyclo-[9.5.1.1^{3,9}.1^{5,15}.1^{7,13}]octasiloxane (G2-propyl-72vinyl).

Vinylmagnesium bromide (1.0 mol dm^{-3} in THF, 80 cm^3) was added to a solution of **G2-propyl-72Cl** (4.9 g, 0.96 mmol) in THF (50 cm^3). The resulting

solution was stirred at room temperature for 72 h. The mixture was slowly added to a cooled (ice bath) aqueous solution of ammonium chloride (1.0 mol dm^{-3} in water, 50 cm^3). The aqueous solution was extracted with petroleum (2 × 80 cm^3). The combined organic layers were washed with saturated aqueous solution of NaCl (20 cm^3), dried over Na_2SO_4 and concentrated *in vacuo*. The residue was loaded onto a column of silica gel and eluted with petroleum to afford the compound **G2-propyl-72vinyl** as a heavy colourless oil (2.5 g, 58 %).

^{1}H NMR ($CDCl_3$):δ_H (ppm) 6.2-6.0 (m, $=CH_2$), 5.73 (dd, $^3J_{HH}$ = 18.2 Hz, $^2J_{HH}$ = 5.6 Hz, Si**C**H=CH_2), 1.8-1.2 (m, CH_2), 1.0-0.4 (m, $SiCH_2$).

^{13}C -{^{1}H} NMR ($CDCl_3$): δ_C (ppm) 135.00 ($CH=CH_2$), 134.36 ($CH=CH_2$), 18.43, 17.16, 16.60, 4.50 (br, $O_3SiCH_2CH_2Si$).

6.1.2 Functionalisation of dendrimers with phosphorus species.

6.1.2.1 Radical addition onto the alkenyl groups.

6.1.2.1.1 Functionalisation with alkylphosphines.

6.1.2.1.1.1 Addition of $HPEt_2$.

1,3,5,7,11,13,15-Octakis[2-di{diethylphosphinoethyl}methylsilyl)ethyl] pentacyclo-[9.5.1.1^{3,9}.1^{5,15}.1^{7,13}]octasiloxane (G1-16ethylPEt$_2$).

G1-16vinyl (0.25 g, 0.176 mmol) was added to a dry 20 cm^3 round bottomed Schlenk flask. AIBN (0.0078 g) was added and the flask was charged with cyclohexane (5 cm^3) and diethylphosphine (1.0 g, 11.3 mmol). The flask was sealed and heated to 60°C for 8 days. The resulting solution was allowed to cool and taken to dryness *in vacuo*. The resulting crude product was a colourless oil (0.497 g, 99 % yield for a conversion > 96 %).

MALDI-TOF: m/z 2923 (M expected 2860) (M + 3 oxide)$^+$, small peak at 2645.

NMR Data:

^{31}P -{^{1}H} NMR ($CDCl_3$) δ_P -15.2 ppm (br)

^{1}H NMR ($CDCl_3$) δ_H (ppm) 1.44 (m, $^3J_{H-H}$ = 7.7 Hz, 96 H, PC**H$_2$**-); 1.15 (dt, $^3J_{H-H}$ = 7.7 Hz, J_{P-H} = 13.5 Hz, 96 H, PCH_2CH_3); 0.66 (br, 64 H, Si-C**H$_2$**), 0.10 (s, 24 H, Si-C**H$_3$**).

^{13}C -{^{1}H} NMR ($CDCl_3$): δ_C (ppm) 19.45 (d, J_{C-P} = 15.0 Hz, $SiCH_2CH_2P$), 18.66 (d, J_{C-P} = 12.7 Hz, PCH_2CH_3), 9.95 (d, J_{C-P} = 12.7 Hz, PCH_2CH_3), 7.91 (d, J_{C-P} = 6.0 Hz, PCH_2CH_2Si), 5.16 ($SiCH_2CH_2Si$), 4.82 ($SiCH_2CH_2Si$), -5.52 ($SiCH_3$).

IR/cm^{-1} (KBr disc): 2956s, 2919s, 2873s, 1455vs, 1409vs (PCH_2), 1260vs ($SiCH_2$), 1120vs ($SiCH_2CH_2Si$), 1040vs (SiOSi), 952s, 800m, 750vs, 707vs.

1,3,5,7,11,13,15-Octakis[2-tri{diethylphosphinoethyl}silyl)ethyl]pentacyclo-[9.5.1.1^{3,9}.1^{5,15}.1^{7,13}]octasiloxane (G1-24ethylPEt$_2$).

G1-24vinyl (0.245 g, 0.162 mmol) was added to a dry 20 cm^3 round bottomed Schlenk flask. AIBN (0.0078 g) was added and the flask was charged with cyclohexane (7 cm^3) and diethylphosphine (1.40 g, 15.6 mmol). The flask was sealed and heated to 60°C for 10 days. The resulting solution was allowed to cool and taken to dryness *in vacuo*. The resulting crude product was a colourless oil (0.573 g, 97 % yield for a conversion >96 %).

MALDI-TOF: m/z 3676.3 (M expected 3677.4), other peaks at m/z 3803 (M + matrix), 3582.0 (M – PEt_2), 3497.9 (M – {2 × PEt_2}), 3406.2 (M – {3 × PEt_2}), 3315.7 (M – {4 × PEt_2}).

Microanalysis found C, 51.7, H, 10.5, $C_{160}H_{368}O_{12}P_{24}Si_{16}$ requires C, 52.3, H, 10.9.

NMR Data:

^{31}P -{^{1}H} NMR ($CDCl_3$) δ_P -15.9, -16.0 ppm

^{1}H NMR ($CDCl_3$) δ_H (ppm) 1.34 (m, 122 H, PC**H$_2$**-); 1.04 (dt, $^3J_{PH}$ = 14.0 Hz, $^3J_{H-H}$ = 7.7 Hz, 122 H, PCH_2CH_3); 0.66 (br, 80 H, Si-C**H$_2$**).

^{13}C -{^{1}H} NMR ($CDCl_3$): δ_C (ppm) 19.21 (d, J_{C-P} = 14.7 Hz, $SiCH_2CH_2P$), 18.66 (d, J_{C-P} = 14.7 Hz, PCH_2CH_3), 9.95 (d, J_{C-P} = 12.1 Hz, PCH_2CH_3), 5.95 (d, J_{C-P} = 6.0 Hz , PCH_2CH_2Si), 4.44 ($SiCH_2CH_2Si$), 3.07 ($SiCH_2CH_2Si$), -5.52 ($SiCH_3$).

IR/cm^{-1} (KBr disc): 2957s, 2919s, 2874s, 1458vs, 1409vs (PCH_2), 1259vs ($SiCH_2$), 1120vs ($SiCH_2CH_2Si$), 1040vs (SiOSi), 952s, 800m, 750vs, 706vs.

1,3,5,7,11,13,15-Octakis[2-tri{diethylphosphinopropyl}silyl)ethyl]pentacyclo-[9.5.1.1^{3,9}.1^{5,15}.1^{7,13}]octasiloxane (G1-24propylPEt$_2$).

G1-24allyl (0.30 g, 0.162 mmol) was added to a dry 20 cm^3 round bottomed Schlenk flask. AIBN (0.0078 g) was added and the flask was charged with cyclohexane (7 cm^3) and diethylphosphine (1.40 g, 15.6 mmol). The flask was sealed and heated to 60°C for 10 days. The resulting solution was allowed to cool and taken to dryness *in vacuo*. The resulting crude product was a colourless oil (0.592 g, 98 % yield for a conversion > 87 %).

MALDI-TOF: m/z 4012 (small) (M expected 4014.2), other major peaks at m/z 3921 (M –{PEt_2}); 3839 (M – 2 × {PEt_2}); 3789; 3750 (M – 3 × {PEt_2}) (major); 3660 (M – 4 × {PEt_2}); 3632; 3569 (M – 5 × {PEt_2}).

NMR Data:

^{31}P -{^{1}H} NMR ($CDCl_3$) δ_P –23.6, -23.9, -24.3 ppm

^{1}H NMR ($CDCl_3$) δ_H (ppm) 1.37 (m, 170 H, $CH_2CH_2CH_2$, PCH_2-); 1.04 (dt, $^3J_{PH}$ = 14.6 Hz, $^3J_{H-H}$ = 7.7 Hz, 122 H, PCH_2CH_3); 0.69 (br, 48 H, $SiCH_2$), 0.53 (br, 32 H, $SiCH_2CH_2Si$).

^{13}C -{^{1}H} NMR ($CDCl_3$): δ_C (ppm) 31.10 (br, CH_2), 20.64 (d, $^1J_{C-P}$ = 13.4 Hz, CH_2CH_2P), 18.95 (d, J_{C-P} = 10.7 Hz, PCH_2CH_3), 14.39 (d, $^2J_{C-P}$ = 10.7 Hz, PCH_2CH_2), 9.68 (d, $^1J_{C-P}$ = 12.1 Hz, PCH_2CH_3), 4.58 ($SiCH_2CH_2Si$), 4.05 ($SiCH_2CH_2Si$).

1,3,5,7,11,13,15-Octakis[2-tris[2-{di(diethylphosphinoethyl)methylsilyl}allyl} silyl]-ethyl]pentacyclo-[9.5.1.1^{3,9}.1^{5,15}.1^{7,13}]octasiloxane (G2-propyl-48ethylPEt$_2$).

G2-propyl-48vinyl (0.22 g, 5.2×10^{-5} mol) was added to a dry 20 cm^3 round bottomed Schlenk flask. AIBN (0.008 g) was added and the flask was charged with cyclohexane (5 cm^3) and diethylphosphine (0.9 g, 0.01 mol). The reaction mixture was heated to 50°C for 12 days. The resulting solution was allowed to cool and taken to dryness *in vacuo*. The resulting crude product was a colourless oil (0.411 g, 96 % yield for a conversion > 90 %).

MALDI-TOF: m/z 3693 (br) (M expected 8502)

Microanalysis found C, 54.0, H, 12.2, $C_{400}H_{920}O_{12}P_{48}Si_{40}$ requires C, 56.3, H, 10.9.

^{31}P -{^{1}H} NMR ($CDCl_3$) δ_P -15.8, -16.1 ppm

^{1}H NMR ($CDCl_3$)δ_H (ppm) 1.30 (m, $^3J_{H-H}$ = 7.7 Hz, 96 H, PCH_2-); 1.03 (dt, $^3J_{H-H}$ = 7.7 Hz, J_{P-H} = 13.7 Hz, 96 H, PCH_2CH_3); 0.66 (br, 68 H, Si-CH_2), 0.10 (s, 24 H, Si-CH_3).

^{13}C -{^{1}H} NMR ($CDCl_3$): δ_C (ppm) 19.55 (d, J_{C-P} = 15.0 Hz, CH_2CH_2P), 18.73 (d, J_{C-P} = 12.7 Hz, PCH_2CH_3), 10.08 (d, J_{C-P} = 11.5 Hz, PCH_2CH_3), 8.75 ($CH_2CH_2CH_2$), 6.38 (d, J_{C-P} = 7.0 Hz, CH_2CH_2P), 5.5 (br, $SiCH_2$), 4.90 (br, $SiCH_2$), 1.34, -5.34 9 (br, $SiCH_3$)

1,3,5,7,11,13,15-Octakis[2-tris[2-{tri(diethylphosphineethyl)silyl}ethyl}silyl]-ethyl]pentacyclo-[9.5.1.1^{3,9}.1^{5,15}.1^{7,13}]octasiloxane (G2-ethyl-72ethylPEt$_2$).

G2-ethyl-72vinyl (0.424 g, 0.102 mmol) was added to a dry 2-necked 50 cm^3 round bottomed Schlenk flask. AIBN (0.0066 g) was added and the flask was charged with cyclohexane (7 cm^3) and diethylphosphine (0.314 g, 2.94 mmol). The reaction mixture was heated to 70°C for 10 days. The resulting solution was allowed to cool and taken to dryness *in vacuo*. The resulting crude product was a white amorphous solid with low solubility (0.71 g, conversion 65 %).

^{31}P -{^{1}H} NMR ($CDCl_3$) δ_P -15.6 ppm (br)

^{1}H NMR ($CDCl_3$)δ_H (ppm) 5.78 (m, 25 H, SiC**H**=CH_2), 6.08-6.21 (m, 50 H, CH=C**H$_2$**), 1.40 (m, 280 H, P-C**H$_2$**CH_3); 0.99 (m, 280 H, P-CH_2C**H$_3$**), 0.66 (br, 128 H, Si-C**H$_2$**).

6.1.2.1.1.2 Addition of $HPCy_2$.

1,3,5,7,11,13,15-Octakis[2-{dicyclohexylphosphinoethyl}{diethylphosphinoethyl} methylsilyl)ethyl] pentacyclo-[9.5.1.1^{3,9}.1^{5,15}.1^{7,13}]octasiloxane (G1-16ethylPCy$_{1.36}$Et$_{0.64}$).

G1-16vinyl (0.133 g, 0.0939 mmol) was added to a dry 20 cm^3 round bottomed Schlenk flask. AIBN (0.007 g) was added and the flask was charged with cyclohexane (5 cm^3) and dicyclohexylphosphine (0.446 g, 2.25 mmol). The flask was sealed and heated to 60°C for 3 days. Diethylphosphine (0.270 g, 3.0 mmol) was then added. The flask heated to 60°C for 5 further days. The resulting solution was allowed to cool and the excess phosphine was removed by vacuum distillation (100°C, 0.1 mm Hg). The resulting crude product was a colourless solid (0.360 g, 95 % yield for a conversion > 98 %).

NMR Data:

^{31}P -{^{1}H} NMR ($CDCl_3$) δ_P 4.8, -14.9 ppm

^{1}H NMR ($CDCl_3$) δ_H (ppm) 1.86 (br, 96 H, C**H$_2$**); 1.70-1.20 (br m, CH_3 and CH_2), 1.15 (dt, $^3J_{H-H}$ = 7.7 Hz, J_{P-H} = 13.7 Hz, 30 H, PCH_2C**H$_3$**); 0.90-0.55 (br, 64 H, Si-C**H$_2$**), 0.20-0.02 (br, 24 H, Si-C**H$_3$**).

^{13}C -{^{1}H} NMR ($CDCl_3$): δ_C (ppm) 33.48 (d, J_{C-P} = 13.4 Hz, CH_2P), 30.47 (d, J_{C-P} = 12.1 Hz, CH_2P), 29.38, 27.04, 26.66, 19.50 (d, J_{C-P} = 15.0 Hz, $SiCH_2$CH_2P), 18.66

(d, $J_{C\text{-}P}$ = 12.6 Hz, PCH_2CH_3), 9.95 (d, $J_{C\text{-}P}$ = 12.5 Hz, PCH_2CH_3), 7.80 (d, $J_{C\text{-}P}$ = 6.0 Hz, PCH_2CH_2Si), 5.5-4.8 (br, $SiCH_2CH_2Si$), -5.45 ($SiCH_3$).

1,3,5,7,11,13,15-Octakis[2-{dicyclohexylphosphinoethyl}methylsilyl)ethyl] pentacyclo-[9.5.1.1^{3,9}.1^{5,15}.1^{7,13}]octasiloxane (G1-16ethylPCy$_2$).

G1-16vinyl (0.133 g, 0.0939 mmol) was added to a dry 20 cm^3 round bottomed Schlenk flask. AIBN (0.007 g) was added and the flask was charged with cyclohexane (5 cm^3) and dicyclohexylphosphine (0.446 g, 2.25 mmol). The flask was sealed and heated to 60°C for 10 days. The resulting solution was allowed to cool and the excess phosphine was removed by vacuum distillation (100°C, 0.1 mm Hg). The resulting crude product was a colourless solid (0.356 g, 98 % yield for a conversion > 75 %).

MALDI-TOF: m/z 3746 (very broad) (*ca* 12 arms substituted due to poor quality G1-16vinyl), M expected 4591.5.

NMR Data:

^{31}P -{^{1}H} NMR ($CDCl_3$) δ_P 4.8, -14.9 ppm

^{1}H NMR ($CDCl_3$) δ_H (ppm) 1.75 (br, 120 H, CH_2); 1.53 (br, 32 H, CH_2), 1.26 (br, 158 H, CH_2 and CH_3); 0.75-0.45 (br, 64 H, Si-CH_2), 0.20-0.02 (br, 24 H, Si-CH_3).

^{13}C -{^{1}H} NMR ($CDCl_3$): δ_C (ppm) 33.45 (d, $J_{C\text{-}P}$ = 13.4 Hz, CH_2P), 30.47 (d, $J_{C\text{-}P}$ = 12.1 Hz, CH_2P), 29.38, 27.04, 26.66, 4.44 (br, $SiCH_2CH_2Si$), -5.40 (br, $SiCH_3$).

1,3,5,7,11,13,15-Octakis[2-tri{dicyclohexylphosphinoethyl}silyl)ethyl] pentacyclo-[9.5.1.1^{3,9}.1^{5,15}.1^{7,13}]octasiloxane (G1-24ethylPCy$_2$).

G1-24vinyl (0.245 g, 0.162 mmol) was added to a dry 20 cm^3 round bottomed Schlenk flask. AIBN (0.0078 g) was added and the flask was charged with cyclohexane (7 cm^3) and dicyclohexylphosphine (3.08g, 15.5 mmol). The flask was sealed and heated to 60°C for 10 days. The resulting solution was allowed to cool and the excess phosphine was removed by vacuum distillation (100°C, 0.1 mm Hg). The resulting crude product was a colourless solid (0.621 g, 95 % yield for a conversion 55 %).

NMR Data:

^{31}P -{^{1}H} NMR ($CDCl_3$) δ_P 4.04 ppm

^{1}H NMR ($CDCl_3$) δ_H (ppm) 6.10 (m, 22 H, $=CH_2$), 5.45 (m, 11 H, SiCH=), 1.70 (br, H, CH_2); 1.52 (br, CH_2), 1.26 (br, CH_2 and CH_3); 0.75-0.45 (br, 58 H, Si-CH_2).

^{13}C -{^{1}H} NMR ($CDCl_3$): δ_C (ppm) 33.45 (d, J_{C-P} = 13.4 Hz, CH_2P), 30.47 (d, J_{C-P} = 12.1 Hz, CH_2P), 29.38, 27.04, 26.66, 4.44 (br, $SiCH_2CH_2Si$).

6.1.2.1.2 Functionalisation with arylphosphines.

6.1.2.1.2.1 Addition of $HPPh_2$.

1,3,5,7,11,13,15-Octakis[2-di{diphenylphosphinoethyl}methylsilyl)ethyl] pentacyclo-[9.5.1.1^{3,9}.1^{5,15}.1^{7,13}]octasiloxane (G1-16ethylPPh$_2$).

G1-16vinyl (0.25 g, 0.176 mmol) was added to a dry 20 cm^3 round bottomed Schlenk flask. AIBN (0.0078 g) was added and the flask was charged with cyclohexane (5 cm^3) and diphenylphosphine (2.1 g, 11.3 mmol). The flask was sealed and heated to 60°C for 10 days. The resulting solution was allowed to cool and concentrated *in vacuo*. The excess phosphine was removed by vacuum distillation (120°C, 0.1 mm Hg) (0.730 g, yield 95 %) or the product was loaded into a silica gel column (eluent: gradient of petroleum/diethyl ether) (0.657 g, yield 85 %). The resulting crude product was a colourless low melting point solid (conversion > 99 %, compound B).

MALDI-TOF: m/z: multiplets (mass increment of 16, oxidation) centered at 4582 (large multiplet); 4299 (major multiplet); 4113 (medium multiplet); 3830 (br, small); 3628 (br, very small) corresponding respectively to 16, 15, 14, 13, 12 substituted arms ([M – n × {PPh_2}], n = 0, 1, 2, 3, 4) (m/z expected 4397.9). The peaks at m/z 4582, 4299 and 4113 corresponded to the molecule with 11, 5 and 5 phosphine species oxidised respectively.

The MALDI-TOF spectrum of the partially substituted compound A gave a broad signal centered at m/z 3680 (*ca* 12 arms substituted).

Microanalysis found for compound **B**: C, 67.9, H, 6.4, $C_{248}H_{280}O_{12}P_{16}Si_{16}$ requires C, 67.7, H, 6.4.

NMR Data:

^{31}P -{^{1}H} NMR ($CDCl_3$) δ_P –9.4, -9.5 ppm.

^{1}H NMR ($CDCl_3$) δ_H (ppm) 7.40-7.20 (br m, 160 H, P(C_6H_5)$_2$); 1.86 (br m, 32 H, PCH_2); 0.64-0.32 (m, 64 H, Si-CH_2), -0.16 (br, 24 H, Si-CH_3).

^{13}C -{^{1}H} NMR ($CDCl_3$): δ_C (ppm) 139.27 (d, J_{C-P} = 14.7 Hz, P(C_6H_5), C-P), 139.18 (d, J_{C-P} = 14.7 Hz, C-P), 132.80 (d, J_{C-P} = 18.8 Hz, C ortho), 132.70 (d, J_{C-P} = 17.4 Hz, C ortho), 128.55 (s, C para), 128.45 (d, $^{1}J_{C-P}$ = 6.71 Hz, C meta), 21.40 (d, $^{1}J_{C-P}$ = 14.8 Hz, **C**H_2P), 8.30 (d, $^{2}J_{C-P}$ = 12.1 Hz, Si**C**H_2CH_2P), 4.78 (O_3Si**C**H_2CH_2), 4.24 (O_3SiCH_2**C**H_2), -6.08 (Si**C**H_3).

1,3,5,7,11,13,15-Octakis[2-di{diphenylphosphinoethyl}methylsilyl)ethyl] pentacyclo-[9.5.1.1^{3,9}.1^{5,15}.1^{7,13}]octasiloxane (G1-16propylPPh$_2$).

G1-16allyl (0.133 g, 0.081 mmol) was added to a dry 20 cm^3 round bottomed Schlenk flask. AIBN (0.0078 g) was added and the flask was charged with cyclohexane (5 cm^3) and diphenylphosphine (0.965 g, 5.20 mmol). The flask was sealed and heated to 60°C for 20 days. The resulting solution was allowed to cool and concentrated *in vacuo*. The excess phosphine was removed by vacuum distillation (120°C, 0.1 mm Hg). The resulting crude product was a colourless oil (0.25 g, yield 92 % for a conversion of 56 %).

NMR Data:

^{31}P -{^{1}H} NMR ($CDCl_3$) δ_P –17.2, -17.3 ppm.

^{1}H NMR ($CDCl_3$) δ_H (ppm) 7.60-7.20 (br m, 90 H, P(C_6**H**$_5$)$_2$); 5.75 (br, 7 H, SiCH=), 4.89 (br, 14 H, CH_2=), 2.08 (br, CH_2), 1.86 (br m, 32 H, P**C**H_2); 0.90-0.40 (m, 48 H, Si-**C**H_2), 0.00 (br m, 24 H, Si-**C**H_3).

1,3,5,7,11,13,15-Octakis[2-tri{diphenylphosphinoethyl}silyl)ethyl]pentacyclo-[9.5.1.1^{3,9}.1^{5,15}.1^{7,13}]octasiloxane (G1-24ethylPPh$_2$).

G1-24vinyl (0.245 g, 0.162 mmol) was added to a dry 20 cm^3 round bottomed Schlenk flask. AIBN (0.0078 g) was added and the flask was charged with cyclohexane (7 cm^3) and diphenylphosphine (2.90 g, 0.0156 mol). The flask was sealed and heated to 60°C for 10 days. The resulting solution was allowed to cool and the excess phosphine was removed by vacuum distillation (120°C, 0.1 mm Hg). The resulting crude product was a white solid (0.65g, yield 95 % for a conversion of 60 %).

NMR Data:

^{31}P -{^{1}H} NMR (CD_2Cl_2) δ_P -9.5 ppm (br).

^{1}H NMR ($CDCl_3$) δ_H (ppm) 7.7-7.2 (br m, 140 H, $P(C_6\mathbf{H}_5)_2$); 6.1-5.8 (br, 20 H, $CH=C\mathbf{H}_2$), 5.7-5.5 (br, 10 H, $C\mathbf{H}=CH_2$), 2.2-1.8 (br, 28 H, $PC\mathbf{H}_2$), 0.90-0.25 (br, 60 H, $SiC\mathbf{H}_2$).

IR/cm^{-1} (KBr disc): 2956s, 2919s, 2873s, 1455vs, 1409vs (PCH_2), 1260vs ($SiCH_2$), 1120vs ($SiCH_2CH_2Si$), 1040vs (SiOSi), 952s, 800m, 750vs, 707vs.

1,3,5,7,11,13,15-Octakis[2-tris[2-{di(diphenylphosphinoethyl)methylsilyl}allyl} silyl]-ethyl]pentacyclo-[9.5.1.1^{3,9}.1^{5,15}.1^{7,13}]octasiloxane (G2-propyl-48ethylPPh$_2$).

G2-propyl-48vinyl (0.22 g, 5.2×10^{-5} mol) was added to a dry 20 cm^3 round bottomed Schlenk flask. AIBN (0.008 g) was added and the flask was charged with cyclohexane (5 cm^3) and diphenylphosphine (1.86 g, 0.01 mol). The reaction mixture was heated to 50°C for 12 days. The resulting solution was allowed to cool and taken to dryness *in vacuo*. The product was loaded into a silica gel column (eluent: gradient of petroleum/diethyl ether). The isolated product was a colourless low melting point solid (0.443 g, yield 75 % for a conversion of 84 %).

^{31}P -{^{1}H} NMR ($CDCl_3$) δ_P –9.9 ppm (br).

^{1}H NMR ($CDCl_3$) δ_H (ppm) 7.6-7.0 (br m, 408 H, $P(C_6\mathbf{H}_5)_2$); 6.2-5.8 (br, 14 H, $CH=C\mathbf{H}_2$), 5.65-5.45 (br, 7 H, $C\mathbf{H}=CH_2$), 1.86 (br, 82 H, $PC\mathbf{H}_2$); 1.62 (br, $C\mathbf{H}_2$), 1.45-1.00 (br, $C\mathbf{H}_2$), 1.00-0.20 (br, $SiC\mathbf{H}_2$), 0.20 to -0.20 (br, 72 H, Si-$C\mathbf{H}_3$).

^{13}C -{^{1}H} NMR ($CDCl_3$): δ_C (ppm) 139.27 (d, $J_{C\text{-}P}$ = 14.7 Hz, $P(C_6H_5)$, C-P), 139.18 (d, $J_{C\text{-}P}$ = 14.7 Hz, $P(C_6H_5)$, C-P), 137.0 (CH_2, Si-vinyl), 132.8 (d, $J_{C\text{-}P}$ = 18.8 Hz, C ortho), 132.70 (d, $J_{C\text{-}P}$ = 18.0 Hz, C ortho), 128.50 (s, C para), 128.45 (d, $J_{C\text{-}P}$ = 6.7 Hz, C meta), 21.50 (d, $^1J_{C\text{-}P}$ = 14.2 Hz, $C\mathbf{H}_2P$), 18.52, 16.89, 9.07 (d, $^2J_{C\text{-}P}$ = 12.0 Hz, $Si\mathbf{C}H_2CH_2P$), 4.57 (br, $O_3Si\mathbf{C}H_2\mathbf{C}H_2$), -5.38 ($Si\mathbf{C}H_3$).

6.1.2.1.2.2 Addition of $HP(3,5\text{-}C_6H_3(CF_3)_2)_2$.

Bis[3,5-bis(trifluoromethyl)]phenylchlorophosphine.[4]

A 1.0 mol dm^{-3} solution of [3,5-bis(trifluoromethyl)phenyl]magnesium bromide was prepared by slow addition of 3,5-bis-(trifluoromethyl) bromobenzene (18.5 g, 60 mmol) in THF (40 cm^3) to a slurry of Mg turnings (1.5 g, 62 mmol) in THF (20 cm^3). After 1 h, this solution was added slowly to a solution of $(Et_2N)PCl_2$ (5.0 g, 29 mmol) in THF (30 cm^3) at 0°C. After 2 h, the mixture was concentrated in

vacuo. Cyclohexane (100 cm^3) was added and the mixture was filtered through celite to provide a solution of bis[3,5-bis(trifluoromethyl)phenyl] (diethylamino)phosphine. Dry HCl was passed through this solution for 1 h. After filtration under a nitrogen atmosphere (it was necessary to degas by bubbling with argon the solution to precipitate the amine hydrochloride) and concentration, the chlorophosphine was collected as a white solid (12.1 g, 86 %).

^{1}H NMR ($CDCl_3$) δ_H 8.14 (dd, J_{H-H} = 2, J_{P-H} = 7.2 Hz, 4 H), 8.10 (t, J_{H-H} = 2 Hz, 2 H, ortho).

^{31}P NMR ($CDCl_3$) δ_P (ppm) 71.5.

Bis[3,5-bis(trifluoromethyl)]phenylphosphine.[5]

A solution of $[3,5\text{-}(CF_3)_2C_6H_3]_2PCl$ (17.5 g, 0.036 mol) in diethyl ether (200 cm^3) was slowly added to a suspension of $LiAlH_4$ (1.35 g, 0.036 mol) in diethyl ether at –78°C. The pale brown solid slurry was refluxed for 2 hours, cooled to 0°C, and hydrolysed with a 10 % aqueous NH_4Cl solution. The fluorescent yellow-green organic layer was separated, and the remaining white precipitate was extracted 5 times with diethyl ether. The combined ether extracts were washed with water, dried over Na_2SO_4, and evaporated to give the product as a pale yellow air-sensitive solid. Sublimation at 60°C under vacuum gave $[3,5\text{-}(CF_3)_2C_6H_3]_2PH$ as a white crystalline solid (12.6 g, 77 %).

^{31}P – {^{1}H} NMR ($CDCl_3$) δ_P (ppm) –39.8.

^{1}H NMR ($CDCl_3$) δ_H (ppm) 8.04 (s, 2 H, para), 8.02 (d, J_{HP} = 6.4 Hz, 4 H, ortho), 5.60 (d, J_{HP} = 223 Hz, PH),

^{13}C NMR – {^{1}H} ($CDCl_3$) δ_C (ppm) 136.55 (d, J_{CP} = 16.1 Hz, C-P), 133.88 (d, J_{CP} = 18.4 Hz, C ortho) 132.67 (qd, J_{CF} =30.3 Hz, J_{CP} = 5.7 Hz, C meta), 123.70 (br, d, J_{CP} = 3.8 Hz), 123.65 (q, J_{CF} = 273 Hz, CF_3)

1,3,5,7,11,13,15-Octakis[2-di{di{bis(3,5-difluoromethyl)phenyl}phosphino ethyl}methylsilyl)ethyl] pentacyclo-[9.5.1.1^{3,9}.1^{5,15}.1^{7,13}]octasiloxane (G1-16ethylPAr$_2$).

G1-16vinyl (0.25 g, 0.176 mmol) was added to a dry 20 cm^3 round bottomed Schlenk flask. AIBN (0.0078 g) was added and the flask was charged with cyclohexane (5 cm^3) and $[3,5\text{-}(CF_3)_2C_6H_3]_2PH$ (3.87 g, 8.45 mmol). The flask was

sealed and heated to 60°C for 30 days. The resulting solution was allowed to cool and the excess phosphine was removed by vacuum distillation (140°C, 0.02 mm Hg) to give a colourless solid (1.17 g, yield 96 % for a conversion of 75 %).

MALDI-TOF: m/z: 6919, 6459, 6001 (major), 5543 (major), 4988 (respectively 12, 11, 10, 9, 8 arms substituted). Other peaks at 6365, 5905, 5446, 4891 (fragmentation)

NMR Data:

^{31}P -{^{1}H} NMR ($CDCl_3$) δ_P (ppm) -6.6, -6.9, -7.0, -12.9.

^{1}H NMR ($CDCl_3$) δ_H (ppm) 8.2-7.8 (m, 72 H, $P(C_6\mathbf{H}_3(CF_3)_2)_2$); 6.0 (br, 24 H, $CH=C\mathbf{H}_2$), 5.7 (br, 12 H, $C\mathbf{H}=CH_2$), 2.1 (br, 24 H, $PC\mathbf{H}_2$); 1.0-0.4 (br m, 56 H, $Si-C\mathbf{H}_2$), 0.6 (br, 24 H, $Si-C\mathbf{H}_3$).

^{13}C -{^{1}H} NMR ($CDCl_3$): δ_C (ppm) 140.60 (m, C quaternary), 135.75, 133.80, 132.73, 132.50, 125.00, 124.66, 123.63, 121.39, 110.16, 21.34 ($SiCH_2\mathbf{C}H_2P$), 8.30 ($Si\mathbf{C}H_2CH_2P$), 5.20 ($O_3Si\mathbf{C}H_2CH_2$), 4.33 ($O_3SiCH_2\mathbf{C}H_2$), -6.08 ($Si\mathbf{C}H_3$).

6.1.2.2 Synthesis of diphenylphosphinoethyl silane compounds.

Bis(diphenylphosphinoethyl)dimethylsilane.

Divinyldimethylsilane (0.267 g, 2.39 mmol) was added to a dry 20 cm^3 round bottomed Schlenk flask. AIBN (0.0078 g) was added and the flask was charged with toluene (5 cm^3) and diphenylphosphine (2.675 g, 14.3 mmol). The flask was sealed and heated to 60°C for 4 hours. The resulting solution was allowed to cool and taken to dryness *in vacuo*. The excess phosphine was removed by vacuum distillation (120°C, 1.0 mm Hg). The product was recrystallised from petroleum to give a white crystalline solid (1.06 g, 92 %).

Microanalysis found C, 73.95, H, 7.02; $C_{30}H_{34}P_2Si$ requires C, 74.35, H, 7.07.

NMR Data:

^{31}P -{^{1}H} NMR ($CDCl_3$) δ_P –9.4 ppm.

^{1}H NMR ($CDCl_3$) δ_H (ppm) 7.42-7.30 (m, 20 H, $P(C_6\mathbf{H}_5)_2$); 1.94 (m, 4 H, $PC\mathbf{H}_2$); 0.60 (m, 4 H, $Si-C\mathbf{H}_2$), -0.16 (br, 6 H, $Si-C\mathbf{H}_3$).

^{13}C -{^{1}H} NMR ($CDCl_3$): δ_C (ppm) 138.95 (d, J_{C-P} = 17.6 Hz, C-P), 132.90 (d, J_{C-P} = 17.5 Hz, C ortho), 128.70 (d, $^{1}J_{C-P}$ = 6.71 Hz, C meta), 128.46 (C para), 21.62 (d, $^{1}J_{C-P}$ = 13.4 Hz, $\mathbf{C}H_2P$), 10.40 (d, $^{2}J_{C-P}$ = 9.40 Hz, $Si\mathbf{C}H_2CH_2P$), -3.78 ($Si\mathbf{C}H_3$).

Tetra(diphenylphosphinoethyl)dimethylsilane.[6]

Tetravinylsilane (0.20 g, 1.47 mmol) was added to a dry 20 cm^3 round bottomed Schlenk flask. AIBN (0.0078 g) was added and the flask was charged with toluene (5 cm^3) and diphenylphosphine (2.73 g, 14.7 mmol). The flask was sealed and heated to 60°C for 4 hours. The resulting solution was allowed to cool and taken to dryness *in vacuo*. The excess phosphine was removed by vacuum distillation (120°C, 1.0 mm Hg). The product was recrystallised from hot dichloromethane to give a white crystalline solid (1.20 g, 93 %).

Microanalysis found C, 76.03, H, 6.10, $C_{56}H_{56}P_4Si$ requires C, 76.34, H, 6.40.

NMR Data:

^{31}P -{^1H} NMR ($CDCl_3$) δ_P (ppm) –9.48 ppm.

^1H NMR ($CDCl_3$) δ_H (ppm) 7.33 (br m, 40 H, $P(C_6\mathbf{H}_5)_2$); 1.79 (br m, 8l H, $PC\mathbf{H}_2$); 0.61 (br m, 8 H, Si-$C\mathbf{H}_2$).

^{13}C -{^1H} NMR ($CDCl_3$): δ_C (ppm) 138.95 (d, $J_{C\text{-}P}$ = 17.6 Hz, $P(C_6H_5)$, C-P), 132.90 (d, $J_{C\text{-}P}$ = 17.5 Hz, C ortho), 128.70 (d, $^1J_{C\text{-}P}$ = 6.71 Hz, C meta), 128.46 (s, C para), 21.62 (d, $^1J_{C\text{-}P}$ = 13.4 Hz, $\mathbf{C}H_2P$), 10.40 (d, $^2J_{C\text{-}P}$ = 9.40 Hz, $Si\mathbf{C}H_2CH_2P$).

6.1.2.3 Nucleophilic substitution on the dendrimers.

6.1.2.3.1.1 Addition of -CH_2PMe_2 groups.

Synthesis of dimethylphosphino methyl lithium.

Bu^{t}Li (50 cm^3, 0.085 mole) (1.7 M in pentane) was added via a cannula to Schlenk flask containing PMe_3 (9 cm^3, 0.087 mole). The reaction was stirred for 72h. The unreacted PMe_3 and the solvent were removed *in vacuo* to give a white solid (6.96 g, 99%).

^{31}P-{^1H} NMR (C_6D_6) δ_P (ppm) –42.

1,3,5,7,11,13,15-Octakis[2-tri{dimethylphosphino methyl}silyl)ethyl]pentacyclo-[9.5.1.$1^{3,9}$.$1^{5,15}$.$1^{7,13}$]octasiloxane (G1-24methylPMe_2).

$LiCH_2PMe_2$ (0.272 g, 3.32 mmol) was dissolved at –78°C in a flask containing THF (20 cm^3). The solution was transferred via cannula to a Schlenk flask containing **G1-24Cl** (0.218 g, 0.127 mmol) in THF (10 cm^3). The mixture was stirred for 60 hours. The solvent was removed *in vacuo*. Dichloromethane was added (40 cm^3). After LiCl had settled, the liquid was transferred via cannula to another flask

and taken to dryness *in vacuo*. The solid was washed twice with hexane. The resulting product was a white solid (0.329 g, 97 %).

MALDI-TOF m/z 2677 (very broad)(m/z expected 2667.5). Other peak at m/z 2603 (M- $\{CH_2PMe_2\}$).

Microanalysis found C, 32.7, H, 7.5, $C_{88}H_{224}O_{24}P_{16}Si_{16}$ requires C, 36.9, H, 8.5.

$^{31}P-\{^1H\}$ NMR (CD_2Cl_2) δ_P (ppm) –54.5

^1H NMR (CD_2Cl_2) δ_H (ppm) 1.0 (br, 144 H, $P(CH_3)_2$); 0.78 (br, 48 H,-$CH_2P(CH_3)_2$); 0.66 (m, 32 H,Si-CH_2CH_2-Si).

$^{13}C-\{^1H\}$ NMR (CD_2Cl_2) δ_C (ppm) 18.5 (br, P-CH_3), 13.8 (br, P-CH_2), 5.0 (br, $SiCH_2CH_2Si$).

IR/cm^{-1} (KBr disc): 2951m, 2892m, 1428m ($SiCH_2P$), 1417m (PCH_3), 1292m (PCH_3), 1274m-1262m ($SiCH_2P$), 1143vs ($SiCH_2CH_2Si$), 1097vs (SiOSi), 938m (PCH_3), 895m (PCH_3), 761s (PCH_3), 707m, 665m.

1,3,5,7,11,13,15-Octakis{2-{tris[2-(tri(dimethylphosphinomethyl)silyl)ethyl]sily}-ethyl}pentacyclo-[9.5.1.1^{3,9}.1^{5,15}.1^{7,13}]octasiloxane (G2-ethyl-72methylPMe$_2$).

$LiCH_2P(Me)_2$ (0.202 g, 2.47 mmol) was dissolved at –78°C in a flask containing THF (20 cm^3). The solution (room temperature) was transferred via cannula to a Schlenk flask containing POSS **G2-ethyl-72Cl** (0.25 g, 0.0052 mmol) in THF (10 cm^3). The mixture was stirred for 60 h (a precipitate appeared). The solid (precipitate) was removed and washed twice with THF. The resulting product was a white solid (80 %) with poor solubility.

IR/cm^{-1} (KBr disc): 2952m, 2893m, 1416s ($SiCH_2P$ and PCH_3), 1289w (PCH_3), 1260m ($SiCH_2P$), 1140vs ($SiCH_2CH_2Si$), 1097vs (SiOSi), 1027m, 946w (PCH_3), 894m (PCH_3), 758s -743s (PCH_3), 712s, 465m.

6.1.2.3.1.2 Addition of –$CH_2P(C_6H_{13})$ groups.

di-n-hexyl methylphosphine.

Magnesium turnings (3.5 g, 0.144 mole) were charged into a three neck Schlenk flask fitted with a reflux condenser and a gas bubbler. Diethyl ether (250 cm^3) was added, followed by the addition dropwise of 1-bromohexane (17 cm^3, 0.121 mole) causing an exothermic reaction (reflux). After completion of the addition, the grey reaction mixture was stirred at room temperature for 1 hour, and

then the unreacted magnesium was allowed to settle. The solution was filtered to give a Grignard solution of $C_6H_{13}MgBr$. Dichloromethylphosphine (5 cm^3, 55.7 mmol) was added to a Schlenk flask containing diethyl ether. The flask was then cooled (ice bath) and $C_6H_{13}MgBr$ was added slowly (1 hour) to the well-stirred solution. A white precipitate of MgBrCl was formed. The solution mixture was stirred overnight. The liquid was filtered into another flask. The precipitate was twice washed with petroleum (20 cm^3) and the washings added to the second flask. The liquid was distilled under vacuum (10^{-2} mm Hg, 120°C) to give a colourless liquid (3.3 g, 26 %).

^{31}P-{^{1}H} NMR ($CDCl_3$)δ_P -41.4 ppm

^{1}H NMR ($CDCl_3$) δ_H (ppm) 1.46-1.20 (m, 26 H, hexyl CH_2); 0.95 (d, $^2J_{PH}$= 1.8 Hz, 3 H, PCH_3); 0.74 (m, 4 H, CH_2P).

^{13}C -{^{1}H} NMR ($CDCl_3$) δ_C (ppm) 31.67, 31.15 (d, J_{PC} = 11.6 Hz), 29.87 (d, J_{PC} = 9.7 Hz), 25.79 (d, J_{PC} = 12.6 Hz), 22.59, 14.08, 11.65 (d, J_{PC} = 14.5 Hz, PCH_3).

Synthesis of dihexylphosphino methyllithium

$PMe(C_6H_{13})_2$ (3.23 g, 14.9 mmol) was dissolved in petroleum (40 cm^3). Bu^tLi (8.8 cm^3, 14.9 mmol) (1.7 M in pentane) was added at room temperature and the reaction mixture was stirred for 5 days. The solvent was removed *in vacuo* to give a pale yellow heavy liquid. The conversion was only 78 % (determined by ^{31}P NMR).

^{31}P-{^{1}H} NMR (C_6D_6)δ_P -24.9 ppm ($LiCH_2P$), -43.2 ppm (CH_3P)

^{1}H NMR (C_6D_6) δ_H (ppm) 1.8-1.10 (m, 26 H, CH_2); 0.95 (m, PCH_3); 0.82 (br, 6 H, CH_2CH_3); -0.35 (br, PCH_2Li)

1,3,5,7,11,13,15-Octakis[2-tri{dihexylphosphine methyl}silyl)ethyl]pentacyclo-[9.5.1.1^{3,9}.1^{5,15}.1^{7,13}]octasiloxane (G1-24methylP(Hex)$_2$).

$LiCH_2P(C_6H_{13})_2$ (0.3236 g, 1.09 mmol) was dissolved at –78°C in a Schlenk flask containing THF (20 cm^3). The solution (room temperature) was transferred via cannula to a Schlenk flask containing **G1-24Cl** (0.0778 g, 0.0453 mmol) in THF (10 cm^3). The mixture was stirred for 60 h. The solvent was removed *in vacuo*. Dichloromethane was added (20 cm^3). After settling overnight, the liquid was transferred via cannula and taken to dryness *in vacuo*. The product was washed by

diethyl ether (3 × 5 cm^3) and dried *in vacuo*. The resulting product was a white solid (yield 40 %).

$^{31}P-\{^1H\}$ NMR ($CDCl_3$)δ_P -36.3 ppm

^1H NMR ($CDCl_3$) δ_H (ppm) 1.64-1.20 (m, 384 H, hexyl CH_2); 0.95 (br, 115 H, CH_3); 0.74 (br, SiCH_2P); 0.7-0.45 (m, 32 H, Si-CH_2CH_2-Si)

$^{13}C-\{^1H\}$ NMR ($CDCl_3$) δ_C (ppm) 31.7, 31.2 (d, J_{PC} = 11.5 Hz), 29.8 (d, J_{PC} = 10 Hz), 25.79 (d, J_{PC} = 12.3 Hz), 22.6, 14.1, 10.3 (d, J_{PC} = 14.5 Hz, PCH_2Si).

6.1.2.3.1.3 Addition of CH_2PPh_2 groups.

Synthesis of (diphenylphospino)methyllithium-TMEDA complex. [7]

A solution n-butyllithium (20 cm^3, 2.5 mol dm^{-3}, 50 mmol) in petroleum (35 cm^3) was treated dropwise with TMEDA (5.8 g , 50 mmol) at room temperature. Then $MePPh_2$ (10.0 g, 50 mmol) was added and the mixture stirred for 72 h. A precipitated yellow product was isolated by filtration (cannula) followed by washing with 3 × 20 cm^3 of petroleum and drying *in vacuo* to give the pyrophoric complex (10.8 g, 67 %).

$^{31}P-\{^1H\}$ NMR (C_6D_6) δ_P 1.86 ppm

^1H NMR (C_6D_6) δ_H (ppm) 7.89 (m, 4 H, phenyl), 7.23 (m, 2 H, phenyl), 6.98-7.1 (m, 4 H, phenyl), 1.89 (s, 16 H, TMEDA), 0,2 (br, 2 H, PCH_2).

1,3,5,7,11,13,15-Octakis[2-tri{diphenylphosphino methyl}silyl)ethyl]pentacyclo-[9.5.1.$1^{3,9}$.$1^{5,15}$.$1^{7,13}$]octasiloxane (G1-24methylPPh$_2$).

$LiCH_2PPh_2$ /TMEDA (0.741 g, 2.22 mmol) was dissolved at –78°C in a Schlenk flask containing THF (20 cm^3). The solution was transferred via cannula to a Schlenk flask containing G1-24Cl (0.15 g, 0.0874 mmol) in THF (10 cm^3). The mixture was stirred for 60 h. The solvent was removed *in vacuo*. Dichloromethane was added (20 cm^3). After settling overnight, the liquid was transferred via cannula and taken to dryness *in vacuo*. The product was washed with diethyl ether (3 × 10 cm^3) and dried *in vacuo*. The resulting product was a white solid (0.44 g, conversion 70 %, yield 93 %).

MALDI-TOF: broad peak centered at m/z 4678 (*ca* 17 arms substituted) (M expected 5646.8)

NMR Data:

^{31}P-{^{1}H} NMR (CD_2Cl_2)δ_P -23.9 ppm

^{1}H NMR (CD_2Cl_2) δ_H (ppm) 7.5-6.6 (m, 240 H, $C_6\mathbf{H}_5$), 1.03 (s, 48 H, -$\mathbf{CH_2}$P); 0.9-0.4 (m, 32 H, Si-$\mathbf{CH_2CH_2}$-Si)

^{13}C -{^{1}H} NMR (CD_2Cl_2) δ_C (ppm) 141.3 (br, P-**C**), 132.7 (br, C ortho), 128.4 (br, C para, C meta), 11.6 (br, Si**C**H_2P), 5.0 (br, Si$\mathbf{CH_2}$$\mathbf{CH_2}$Si).

IR/cm^{-1} (KBr disc): 3049vs (C=C), 2908m, 1584w (C=C), 1479s (C=C, PPh), 1433s ($SiCH_2P$), 1088vs ($SiCH_2CH_2Si$), 1025vs (SiOSi), 999s (PPh), 740s, 695s, 471m

1,3,5,7,11,13,15-Octakis[2-di{diphenylphosphinomethyl}methylsilyl)ethyl] pentacyclo-[9.5.1.1^{3,9}.1^{5,15}.1^{7,13}]octasiloxane (G1-16methylPPh$_2$).

$LiCH_2PPh_2$ /TMEDA (0.741 g, 2.22 mmol) (50 % excess) was dissolved at –78°C in Schlenk flask containing THF (20 cm^3). The solution was transferred via cannula to a Schlenk flask containing G1-16Cl (0.145 g, 0.0925 mmol) in THF (10 cm^3). The mixture was stirred for 4 days. The solvent was removed *in vacuo* and the solid mixture was loaded onto silica gel and eluted with a gradient of petroleum and diethyl ether. After evaporation under vacuum of the solvent, the product was obtained as a white solid (0. 262 g, conversion > 95 %, yield 70 %).

MALDI-TOF: m/z 4176 (M expected 4173.5), other peak at 4194 (1 oxide), 4036.5, 3992.3 (M– CH_2PPh_2), 3736.0.

Microanalysis found C, 58.9, H, 6.3, $C_{232}H_{248}O_{12}P_{16}Si_{16}$ requires C, 66.8, H, 6.3.

NMR Data:

^{31}P-{^{1}H} NMR ($CDCl_3$)δ_P -22.6, –22.7 ppm

^{13}C -{^{1}H} NMR ($CDCl_3$) δ_C (ppm) 141.50 (d, $J_{C\text{-}P}$ = 12.7 Hz, **C**-P), 141.33 (d, $J_{C\text{-}P}$ = 12.7 Hz, **C**-P), 133.03 (d, $J_{C\text{-}P}$ = 19.6 Hz, C ortho), 132.78 (d, $J_{C\text{-}P}$ = 17.2 Hz, C ortho), 128.56 (s, C meta, C para), 12.80 (d, $J_{C\text{-}P}$ = 28 Hz, Si**C**H_2P), 7.97 (br, $SiCH_2\mathbf{C}H_2SiO_{3/2}$), 5.00 (br, $CH_3Si\mathbf{C}H_2$), –2.67 (br, $SiCH_3$).

^{1}H NMR ($CDCl_3$) δ_H (ppm) 7.4-7.0 (m, 160 H, $C_6\mathbf{H}_5$), 1.21 (br, 32 H, -$\mathbf{CH_2}$P); 0.75-0.45 (m, 32 H, Si-$\mathbf{CH_2CH_2}$-Si), -0.36 (br, 24 H, Si$\mathbf{CH_3}$)

IR/cm^{-1} (KBr disc): 3049vs (C=C), 2908m, 1584w (C=C), 1479s (C=C, PPh), 1433s ($SiCH_2P$), 1088vs ($SiCH_2CH_2Si$), 1025vs (SiOSi), 999s (PPh), 740s, 695s, 471m

6.1.2.3.1.4 Addition of alkoxyPPh_2 groups

1,3,5,7,11,13,15-Octakis[2-di{diphenylphosphinomethoxy}methylsilyl)ethyl] pentacyclo-[9.5.1.1^{3,9}.1^{5,15}.1^{7,13}]octasiloxane (G1-16methoxyPPh_2).

$HPPh_2$ (1.2 cm^3, 9.96 mmol) and paraformaldehyde (0.2088 g) were heated in a Schlenk tube for 90 min at 120°C to afford Ph_2PCH_2OH.[8] The compound formed *in situ* and NEt_3 (1.4 cm^3) in THF (20 cm^3) were added to a Schlenk flask containing G1-16Cl (0.3223 g, 0.207 mmol) in THF (10 cm^3). The mixture was stirred for 4 days. The solvent was removed *in vacuo* and the solid mixture was loaded onto a silica gel and eluted with a gradient of petroleum and diethyl ether. After evaporation under vacuum of the solvent, the product was obtained as a white solid (0.604 g, conversion > 86 %, yield 76 %).

MALDI-TOF: m/z 4432.3 (M expected 4429.8), other major peaks at 4448 (oxide), 4248 (M – {PPh_2}), 4234 (M - {CH_2PPh_2}), 4051 (M – 2 × {PPh_2}), 4037 (M – 2 × {CH_2PPh_2}), 3836(M – 3×{PPh_2}), 3819(M – 3 ×{CH_2PPh_2}), 3636 (M – 4 × {PPh_2}), 3622 (M - 4×{CH_2PPh_2}).

Microanalysis found C, 66.1, H, 6.3, $C_{232}H_{248}O_{28}P_{16}Si_{16}$ requires C, 62.9, H, 5.6.

NMR Data:

^{31}P-{^{1}H} NMR ($CDCl_3$) δ_P (ppm) –13.6 (br).

^{1}H NMR ($CDCl_3$) δ_H (ppm) 7.8-7.1 (m, 160 H, $C_6\mathbf{H_5}$); 4.35 (br, O**CH_2**, 32 H); 0.80-0.35 (m br, 32 H, Si-**CH_2CH_2**-Si), -0.05 (br, 24 H, Si**CH_3**).

^{13}C -{^{1}H} NMR ($CDCl_3$) δ_C (ppm) 143.30 (br, phenyl P-**C**), 133.24 (d, $J_{C\text{-}P}$ = 26.5 Hz, C ortho), 128.87 (s, C para), 128.64 (d, $J_{C\text{-}P}$ = 6.71 Hz, C meta), 63.17 (br, O**CH_2**), 4.74 (br, $SiCH_2\mathbf{CH_2}SiO_{3/2}$), 3.14 (br, $Si\mathbf{CH_2}CH_2SiO_{3/2}$), –6.15 (br, $SiCH_3$).

2-(diphenylphosphino)ethanol.[9]

THF (250 cm^3) was slowly added to a stirred mixture of triphenylphosphine (26.6 g, 0.1 mol) and finely cut lithium wire (3.5 g, 0.5 mol) kept at -10°C. Stirring was maintained for 2 h at room temperature. After filtration of the excess lithium (via cannula), 2-chloroethanol (0.1 mole) was slowly added to the cooled solution (-10°C). The mixture was then allowed to reach room temperature and stirring was maintained for a further 3 h. The solution was then hydrolysed, the organic layer separated and the aqueous layer extracted with THF. The combined organic layers

were dried over Na_2SO_4 and concentrated under vacuum. The product was purified by silica gel chromatography (eluent gradient of petroleum and diethyl ether) to give 16.79 g (73 %) of the desired compound as an oily colourless product.

^{31}P-{^{1}H} NMR ($CDCl_3$) δ_P (ppm) –23.6.

^{1}H NMR ($CDCl_3$) δ_H (ppm) 7.50-7.28 (m, 10 H, $C_6\mathbf{H_5}$); 3.80 (dt, $^3J_{H-H}$ = 7.14 Hz, $^3J_{P-H}$ = 9.3 Hz, 2 H, $OC\mathbf{H_2}$); 2.4 (dt, J_{H-H} = 7.14 Hz, $^3J_{P-H}$ = 1.37 Hz, 2 H, $PC\mathbf{H_2}$), 1.63 (br s, 1 H, OH).

^{13}C -{^{1}H} NMR ($CDCl_3$) δ_C (ppm) 138.08 (d, J_{C-P} = 12.9 Hz, phenyl P-**C**), 132.83 (d, J_{C-P} = 18.80 Hz, phenyl meta), 128.87 (s, C para), 128.64 (d, J_{C-P} = 6.71 Hz, C meta), 60.25 (d, J_{C-P} = 22.8 Hz, OCH_2), 32.25 (d, J_{C-P} = 13.4 Hz, PCH_2).

1,3,5,7,11,13,15-Octakis[2-di{diphenylphosphinoethoxy}methylsilyl)ethyl] pentacyclo-[9.5.1.1^{3,9}.1^{5,15}.1^{7,13}]octasiloxane (G1-16ethoxyPPh$_2$).

$Ph_2PCH_2CH_2OH$ (1.12 g, 4.9 mmol, 2.5 fold excess) and NEt_3 (0.75 cm^3) in THF (20 cm^3) were added to a Schlenk flask containing G1-16Cl (0.198 g, 0.128 mmol) in THF (10 cm^3). The mixture was stirred 5 days. The solvent was removed *in vacuo* and the solid mixture was loaded onto a silica gel and eluted with a gradient of petroleum and diethyl ether. After evaporation of the solvent under vacuum, the product was obtained as a white solid (0.48 g, conversion > 92 %, yield 85 %).

MALDI-TOF: m/z 4657.6 (M expected 4653.8), other major peaks at 4505; 4445.2 (M – {CH=CHPPh$_2$}); 4233.7 (M – 2× {CH=CHPPh$_2$}); 4156; 4047; 3943.

NMR Data:

^{31}P-{^{1}H} NMR ($CDCl_3$) δ_P (ppm) -22.3, –22.5.

^{1}H NMR ($CDCl_3$) δ_H (ppm) 7.6-7.3 (m, 160 H, $C_6\mathbf{H_5}$); 3.84 (br d, $^3J_{P-H}$ = 7.6 Hz, $OC\mathbf{H_2}$, 32 H); 2.4 (br d, $^2J_{P-H}$ = 7.7 Hz, 32 H, $PC\mathbf{H_2}$); 0.75-0.55 (m, 32 H, Si-$C\mathbf{H_2}C\mathbf{H_2}$-Si), 0.02 (br, 24 H, $SiC\mathbf{H_3}$).

^{13}C -{^{1}H} NMR ($CDCl_3$) δ_C (ppm) 141.4 (br,C-P), 132.90 (br, C ortho), 128.56 (s, C meta, C para), 60.54 (d, J_{C-P} = 26.5 Hz, $\mathbf{C}H_2P$), 32.33 (d, J_{C-P} = 12.6 Hz, OCH_2), 7.97 (br, $SiCH_2\mathbf{C}H_2SiO_{3/2}$), 5.00 (br, $CH_3Si\mathbf{C}H_2$), –5.37 (br, $SiCH_3$).

6.1.2.3.1.5 Addition of -$(CH_2)_3PPh_2$ groups.

3-chloropropyldiphenylphosphine $Ph_2P(CH_2)_3Cl$.[10]

n-BuLi (17.95 cm^3, 1.6 mol dm^{-3} in hexane) was added dropwise to a Schlenk flask containing $HPPh_2$ (5.35 g, 28.7 mmol) in THF (25 cm^3). The orange mixture was stirred at room temperature for 1 h and slowly added to a solution of 1,3-dichloropropane (15.95 g, 141 mmol) in toluene (30 cm^3) cooled at –78°C. The mixture was allowed to reach room temperature. The solution was concentrated *in vacuo* and water was added (30 cm^3). The organic phase was dried over Na_2SO_4, and the solvent removed in vacuo. The oily residue was loaded onto a silica gel column and the product eluted with a gradient of petroleum and diethyl ether to yield the desired product as a colourless oil (6.41 g, 85 %).

^{31}P-{^1H} NMR ($CDCl_3$) δ_P (ppm) -15.9.

^1H NMR ($CDCl_3$) δ_H (ppm) 7.58-7.37 (m, 10 H, $C_6\mathbf{H_5}$); 3.73 (t, $^3J_{H\text{-}H}$ = 6.5 Hz, 2 H, $ClC\mathbf{H_2}$); 2.30 (m, 2 H, $C\mathbf{H_2}$), 2.02 (m, 2 H, $C\mathbf{H_2}$).

^{13}C -{^1H} NMR ($CDCl_3$) δ_C (ppm) 138.45 (d, $J_{C\text{-}P}$ = 14.0 Hz, phenyl P-**C**), 133.20 (d, $J_{C\text{-}P}$ = 18.4 Hz, C ortho), 129.07 (s, C para), 128.83 (d, $J_{C\text{-}P}$ = 6.9 Hz, C meta), 46.16 (d, $J_{C\text{-}P}$ = 15.0 Hz, $Cl\mathbf{C}H_2$), 29.51 (d, $J_{C\text{-}P}$ = 17.3 Hz, $P\mathbf{C}H_2$), 25.79 (d, $J_{C\text{-}P}$ = 12.7 Hz, $C\mathbf{C}H_2C$).

1,3,5,7,11,13,15-Octakis[2-di{diphenylphosphinopropyl}methylsilyl)ethyl] pentacyclo-[9.5.1.1^{3,9}.1^{5,15}.1^{7,13}]octasiloxane (G1-16propylPPh$_2$).

Magnesium turnings (0.50 g, 20.7 mmol) and $Ph_2PCH_2CH_2CH_2Cl$ (4.982 g, 18.96 mmol) were mixed in THF (20 cm^3). The mixture was heated to reflux and initiated with a small amount of reacting $BrCH_2CH_2Br$/Mg.[11] Heating and stirring were continued for 1 h. The mixture was added (filtered) to a Schlenk flask containing G1-16Cl (0.615 g, 0.396 mmol) in THF (20 cm^3). The mixture was stirred for 4 days. The mixture was added to an aqueous solution of NH_4Cl (0.1 mol dm^{-3}). The organic phase was concentrated *in vacuo* and the residue was loaded onto silica gel and eluted with a gradient of petroleum and diethyl ether. After evaporation of the solvent under vacuum, the product was obtained as a non-crystalline solid (1.30 g, conversion > 85 % (^1H NMR), yield 75 %).

MALDI-TOF: m/z 3574.9 (unknown, fragmentation)(M expected 4623), other major peaks (unknown fragmentation) at 3426, 3365, 3153.

Microanalysis found C, 63.3, H, 7.2, $C_{264}H_{312}O_{12}P_{16}Si_{16}$ requires C, 68.6, H, 6.8.

NMR Data:

^{31}P-{^{1}H} NMR ($CDCl_3$) δ_P (ppm) –16.1, –16.2, -16.4.

^{1}H NMR ($CDCl_3$) δ_H (ppm) 7.6-7.3 (m, 160 H, $C_6\mathbf{H_5}$); 3.84 (br d, $^{3}J_{P-H}$ = 7.6 Hz, $OC\mathbf{H_2}$, 32 H); 2.4 (br d, $^{2}J_{P-H}$ = 7.7 Hz, 32 H, $PC\mathbf{H_2}$); 0.75-0.55 (m, 32 H, Si-$C\mathbf{H_2}C\mathbf{H_2}$-Si), 0.02 (br, 24 H, $SiC\mathbf{H_3}$).

^{1}H NMR ($CDCl_3$) δ_H (ppm) 7.55-7.30 (m, 160 H, $C_6\mathbf{H_5}$); 2.18 (br, 32 H, $PC\mathbf{H_2}$), 1.60-1.40 (br, 32 H, $C\mathbf{H_2}$), 0.88 (br, 32 H, $SiC\mathbf{H_2}$), 0.80-0.55 (br, 32 H, $SiC\mathbf{H_2}$), 0.15 (br, $SiCH_3$)

^{13}C -{^{1}H} NMR ($CDCl_3$) δ_C (ppm) 139.0 (br, P-**C**), 133.00 (d, J_{C-P} = 18.4 Hz, C ortho), 128.75 (s, C para), 128.70 (d, J_{C-P} = 5.8 Hz, C meta), 32.29 (br), 20.31 (d, J_{C-P} = 17.2 Hz, $P\mathbf{C}H_2$), 18.16, 4.00 (br, $SiCH_2$), -2.10 (s, $SiCH_3$).

6.1.2.4 Synthesis of phosphite-containing POSS dendrimer.

2,2'-bisphenoxyphosphorus chloride.[12]

A 250 cm^3 three-necked, round bottomed flask equipped with a 100 cm^3 dropping funnel was filled with pyridine (11.9 g, 125 mmol) and PCl_3 (4.1g, 30 mmol). 2-2'-bisphenol (2.32 g, 12.5 mmol) was azeotropically dried with toluene (3 × 15 cm^3), dissolved in 90 cm^3 of toluene and added dropwise to the PCl_3/pyridine solution at 0°C. When the addition was completed the reaction was refluxed overnight. The formed pyridine salts were removed by filtration. The reaction mixture was concentrated at reduced pressure. The product was purified by distillation at reduced pressure (bp 140°C, 1.0 mm Hg) to give 2.485 g (79 %) of a heavy colourless oil. The compound was stored in a toluene solution (1.652 mol.dm^{-3}) at –20°C in the dark.

NMR Data:

^{31}P-{^{1}H} NMR ($CDCl_3$) δ_P (ppm) 180.1.

^{1}H NMR ($CDCl_3$) δ_H (ppm) 7.56-7.31 (m, H, aromatic).

1,3,5,7,11,13,15-Octakis[2-bis{3-hydroxypropyl}methylsilyl)ethyl]pentacyclo-[9.5.1.$1^{3,9}$.$1^{5,15}$.$1^{7,13}$]octasiloxane (G1-16hydroxy).

The procedure used was directly adapted from a previous report on hydroxy-containing dendrimers.[13]

G1-16allyl (2.60g, 1.21 mmol) in THF (150 cm^3) was added to a 500 cm^3 flask. The solution was cooled to -10°C and a 9-BBN solution (100 cm^3 of 0.5 mol dm^{-3} solution in THF, 50 mmol) was added slowly to the cooled solution at this temperature. The solution was stirred for 3 hours at -10°C and at room temperature overnight. ^1H NMR showed that no double bonds were left. Subsequently, the reaction mixture was cooled to -10°C again and an aqueous solution of NaOH (2.6 g in 7.5 cm^3) was added. Immediately, H_2O_2 (15.5 cm^3, 30 % aqueous solution) was added slowly. The reaction mixture was stirred for an additional 1 hour at -10°C, and warmed to room temperature. The THF solution was decanted from the precipitated boric acid and the aqueous medium and washed three times with a saturated solution of NaCl. The product solution was dried over $MgSO_4$. The reaction mixture was concentrated at reduced pressure. The product and by-product (1,5-cyclooctanediol) were separated by column chromatography (silica gel), eluent ethyl acetate (by product) followed by pyridine to obtained a colourless low melting point solid (1.40 g, 60 %). The solid was azeotropically dried with toluene (3 × 30 cm^3) and stocked under argon for further used.

MALDI-TOF: m/z: 1955.5 $(M + Na)^+$ (M expected 1931.4), other peak at 1939.0 $(M + Na - OH)^+$

NMR Data:

^1H NMR (DMSO d^6) δ_H (ppm) 4.49 (br m, 16 H, OH); 3.41 (dt, $^3J_{H-H}$ = 6.75 Hz, $^3J_{H-H}$ = 5.0 Hz, 32 H, C**H_2**OH), 1.48 (br m, 32 H, C**H_2**CH_2OH); 0.65-0.40 (br m, 64 H, Si-C**H_2**), 0.02 (br, 24 H, Si-C**H_3**).

^{13}C -{^1H} NMR (DMSO d^6): δ_C (ppm) 63.39 (**C**H_2OH), 27.39 (**C**H_2CH_2O), 9.16 (Si**C**$H_2CH_2CH_2$), 5.21 (O_3Si**C**H_2CH_2), 4.48 (O_3SiCH_2**C**H_2), -5.29 (Si**C**H_3).

1,3,5,7,11,13,15-Octakis[2-bis{(3-(2,2'-bisphenoxyphosphin)oxy)propyl} methylsilyl)ethyl]pentacyclo-[9.5.1.$1^{3,9}$.$1^{5,15}$.$1^{7,13}$]octasiloxane (G1-16phosphite).

G1-16hydroxy (0.193 g, 0.10 mmol) in pyridine (20 cm^3) was added dropwise to a solution of 2,2'-bisphenoxyphosphorus chloride (1.5 cm^3, 1.652 $mol.dm^{-3}$, 2.478 mmol), in toluene (15 cm^3) and pyridine (2 cm^3). The reaction was stirred overnight. The reaction mixture was filtered and concentrated *in vacuo*. The residue was loaded onto a (short) silica gel column and eluted with toluene/CH_2Cl_2 to give a white solid (0.243 g, 45 %).

MALDI-TOF: m/z: 722 (M expected 5357.96).

Microanalysis found C, 60.0, H, 5.1, $C_{264}H_{280}O_{60}P_{16}Si_{16}$ requires C, 59.2, H, 5.3.

NMR Data:

^{31}P-{^{1}H} NMR (toluene d^8) δ_P (ppm) 137.75.

^{1}H NMR (toluene d^8) δ_H (ppm) 7.30-6.90 (m, 128 H, aromatic H), 3.78 (br m, 32 H, CH_2O); 1.46 (br m, 32 H, C**H$_2$**CH_2O), 0.82 (br m, 32 H, Si**H$_2$**CH_2CH_2O); 0.38 (br m, 32 H, Si**H$_2$C H$_2$**Si), -0.13 (br, 24 H, Si-**H$_3$**).

^{13}C -{^{1}H} NMR (toluene d^8): δ_C (ppm) 150.53 (**C**O aromatic), 131.23 (C aromatic), 130.00 (CH aromatic), 129.20 (CH aromatic), 124.84 (CH aromatic), 122.01 (CH aromatic), 67.15 (**C**H_2O), 25.52 (CH_2**C**H_2CH_2O), 8.61 (Si**C**$H_2CH_2CH_2$), 5.35 (br, O_3Si**C**H_2**C**H_2), -6.06 (Si**C**H_3).

6.1.3 Synthesis of chiral SEMI-ESPHOS type compounds.

(S)-5-Oxopyrrolidine-2-carboxanilide. [14]

In a 500 cm^3 round-bottomed flask fitted with a dean-Stark apparatus, a mixture of L-glutamic acid (60 g, 0.4 mol) and aniline (350 cm^3) was stirred at 195-200°C. After 30 min, the mixture became clear, and the water formed was removed by azeotropic distillation. Stirring was maintained for 4h. Excess aniline was then recovered at 60-70°C under reduced pressure distillation. The hot oily residue was swirled with acetone (250 cm^3) to lead to the formation of a brown solid, which was collected by filtration and dissolved in hot methanol (200 cm^3). The solution was slowly cooled to room temperature to afford crystalline optically pure (S)-5-oxopyrrolidine-2-carboxanilide as white needles in 85 % yield (69 g).

^{1}H NMR (DMSO-d^6) δ_C (ppm) 10.11 (s, 1 H, NH), 7.97 (s, 1 H, NH), 7.71 (d, J_{H-H} = 7.5 Hz, 2 H, CH aromatic), 7.41 (t, J_{H-H} = 7.5 Hz, 2 H, CH aromatic), 7.13 (t, 1 H, J =7.5 Hz, CH aromatic), 4.28 (dd, J_{H-H} = 8.5 Hz, J_{H-H} = 4.3 Hz, 1 H, C**H**N), 2.42 (tdd, J_{H-H} = 9.7, 12.3, 8.5 Hz, 1 H), 2.26 (td, J = 9.7, 14.4 Hz, 2 H), 2.08 (tddd, J_{H-H} = 9.7, 12.3, 4.3 Hz, 1 H).

^{13}C -{^{1}H} NMR (DMSO-d^6): δ_H (ppm) 178.20, 172, 05, 139.60, 129.54, 124.28, 120.14, 57.21, 30.06, 26.16.

(S)-2-Anilinomethyl pyrrolidine.[14]

Lithium aluminium hydride (10.0 g, 0.2501 mole) was slowly added at –10°C to dry THF (100 cm^3) in a 250 cm^3 three-necked round bottomed flask with a condenser. This suspension was allowed to warm to 0°C and (S)-5-oxopyrrolidine-2-carboxanilide (17.85 g, 0.0875 mol) was slowly added in portions to maintain a gentle bubbling. After stirring overnight at room temperature, the suspension was heated for 1h under reflux. After that the mixture was cooled to 0°C, the excess lithium aluminium hydride was decomposed by careful addition of 30 % KOH solution (19 cm^3). This solution was then stirred overnight at room temperature. The inorganic salts were removed by filtration and washed with dichloromethane (2 × 20 cm^3). The solvents were removed under vacuum, and the oily residue was purified by distillation to afford the desired (S)-2-Anilinomethyl pyrrolidine in 89% yield (14.0 g) (bp 92°C at 0.1 mm Hg).

Microanalysis found C, 73.7, H, 9.7, N, 15.9, $C_{11}H_{16}N_2$ requires C, 74.9, H, 9.2, N, 15.9.

^{1}H NMR ($CDCl_3$) δ_C (ppm) 7.29 (dt, J_{H-H} = 7.5 Hz, J_{H-H} = 1.9 Hz, 2 H, CH aromatic), 6.81 (t, J_{H-H} = 7.5 Hz, 2 H, CH aromatic), 6.75 (dd, J_{H-H} =7.5 Hz, J_{H-H} = 1 Hz, 1 H, CH aromatic), 4.25 (br, s, NH), 3.49 (dddd, J_{H-H} = 7.7 Hz, J_{H-H} = 6.7 Hz, J_{H-H} = 5.3 Hz, J_{H-H} = 4.5 Hz, 1 H, C**H**N), 3.29 (dd, J_{H-H} = 12.0, J_{H-H} = 4.5 Hz, 1 H), 3.08 (dd, J_{H-H} = 11.9, J_{H-H} = 7.7 Hz, 1 H), 3.05 (td, J_{H-H} = 9.7, J_{H-H} = 14.4 Hz, 2 H), 2.18 (br, 1 H, NH), 2.30 (dddd, J_{H-H} = 12.0 Hz, J_{H-H} = 8.9 Hz, J_{H-H} = 6.7 Hz, J_{H-H} = 5.3 Hz, 1 H), 1.86 (dddd, J_{H-H} = 6.5 Hz, J_{H-H} = 1.9 Hz, J_{H-H} = 6.7 Hz, J_{H-H} = 8.9 Hz, 2 H), 1.57 (tdd, J_{H-H} = 8.9, Hz, J_{H-H} = 12.3 Hz, J_{H-H} = 6.7 Hz, 1 H)

^{13}C -{^{1}H} NMR ($CDCl_3$): δ_H (ppm) 148.90, 129.54, 117.59, 113.33, 58.06, 49.03, 46.89, 29.94, 26.17.

(5S)-3-phenyl-2-chloro-1,3-diaza-2-phosphabicyclo[3.3.0]octane (8).

A 250 cm^3 three-necked, round bottomed flask equipped with a 100 cm^3 dropping funnel was filled with pyridine (24 cm^3, 0.3 mol) and PCl_3 (58.8 mmol, 8.1 g). (S)-2-Anilinomethyl pyrrolidine (4.146 g, 23.54 mmol) was dissolved in toluene (90 cm^3) and added dropwise to the PCl_3/pyridine solution at 0°C. When the addition was complete the reaction was refluxed overnight. The formed pyridine salts were removed by filtration. The reaction mixture was concentrated at reduced pressure.

The product was purified by vacuum distillation (180°C, 0.2 mm Hg) to give 4.85 g (85 %) of a white crystalline solid.

Microanalysis C, 54.5, H, 6.7, N, 11.4, $C_{11}H_{14}ClN_2P$ requires C, 54.9, H, 5.9, N, 11.6.

^{13}P -{^1H} NMR (C_6D_6) δ_P (ppm) 150.34, 142.33

^1H NMR (C_6D_6) δ_H (ppm) 7.30-7.10 (m, 5 H), 3.80-3.50 (br m, 1 H), 3.24 (br, 2 H), 3.00-2.86 (br, 2 H), 1.90 (br, 0.75 H), 1.46 (br, 3 H), 0.94 (br, 0.25 H)).

^{13}C -{^1H} NMR (C_6D_6): δ_C (ppm) 143.80 (br), 129.60, 122.15 (small peak 121.1), 118.17 (small peak 116.7), 66.73 (small peak 65.1), 52.81 (br) (small peak 52.1), 44.33 (br), 31.54 (small peak 30.2), 28.15 (small peak 27.5).

Reaction of $LiAlH_4$ with (5S)-3-phenyl-2-chloro-1,3-diaza-2-phosphabicyclo [3.3.0] octane (8).

This reaction was carried out following related work found in the litterature.[15]

A solution of **8** (4.85 g, 20.15 mmol) in THF (15 cm^3) was slowly added dropwise to a cooled (0°C) solution of $LiAlH_4$ (0.7647 g, 20.15 mmol) in diethyl ether (200 cm^3). The mixture was stirred at room temperature for 72 h. The solvent was removed *in vacuo*. Extraction with pentane failed. Extraction of the residue with toluene led to a polymeric-like material (^{31}P NMR showed 3 weak peaks δp 106, 100, 54 ppm). Recrystallisation of the mixture failed since the only product isolated was **8** (no ^{31}P resonance). Distillation under reduced pressure also failed as decomposition occurred (black material).

Reaction of tri-n-butylstannane with (5S)-3-phenyl-2-chloro-1,3-diaza-2-phospha bicyclo[3.3.0]octane (8).

This reaction was carried out following related work found in the litterature.[16]

Compound **8** (12.970 g, 53.9 mmol) and tri-n-butylstannane (15.684, 53.9 mmol) were added to a round bottomed flask and the mixture was heated for 30 min at 50-60°C. The solution was distilled under vacuum. The only product of distillation was $ClSn(C_4H_9)_3$ (^1H NMR). The residue was not characterised.

6.2 Catalytic experiments.

The metal complexes $[Rh(CO)_2(acac)]$ and $[Rh_2(O_2CMe)_4]$ were purchased from Strem or from Aldrich. The substrates prop-2-en-1-ol, hex-1-ene, oct-1-ene and non-1-ene were purchased from Aldrich. Prop-2-en-1-ol was dried with $CaSO_4$, refluxed with magnesium, fractionally distilled, and it was stored under argon over molecular sieves in the dark.

G.C. analyses were carried out using a Phillips PU 4000 fitted with a capillary column with nitrogen as the carrier gas and a flame ionisation detector. G.C. M.S. analysis were carried out using a Hewlett Packard 5890 G.C. with an Incos quadrupole mass spectrometer fitted with a SGE BP1 column and a Hewlett Packard HP6890 G.C. with a 5973 mass selective detector fitted with a 5 % phenyl methyl siloxane capillary column.

6.2.1 Catalytic solutions.

6.2.1.1 Hydrocarbonylation reactions.

6.2.1.1.1 $Rh_2(O_2CMe)_4$ as metal-based complex.

Solution of $Rh_2(O_2CMe)_4$ and PMe_3.

$[Rh_2(O_2CMe)_4]$ (0.0084 g, 2.0×10^{-5} mol) was charged into a Schlenk tube and degassed. Ethanol (4 cm^3) was added (green solution) followed by addition of PMe_3 (0.012 cm^3, 12.0 10^{-5} mol). The solution instantly turned red-brown.

Solutions of $Rh_2(O_2CMe)_4$ and dendritic ligands.

The functionalised POSS dendrimer, $[Rh_2(O_2CMe)_4]$ and ethanol or THF (4 cm^3) were charged into a Schlenk tube and stirred until complexation of the rhodium dimer with the phosphine species, the solution becoming red-brown from green. The phosphine/ rhodium ratio used was 3/1. The amounts of dendritic ligands and metal-based complex and some observations are summarised in Table 6.1.

Table 6.1 Solutions of $[Rh_2(O_2CMe)_4]$ and dendritic ligands.

Ligand	*Amount of ligand*	*$[Rh_2(O_2CMe)_4]$*	*Solvent*	*Complex formation*	*Observ.*
G1-24methylPMe$_2$	0.0133 g 5.0×10^{-6} mol	0.0084 g 2.0×10^{-5} mol	Ethanol	4 h	Red-brown
G1-24methylPMe$_2$	0.0073 g 2.75×10^{-6} mol	0.0045 g 1.1×10^{-5} mol	Ethanol	3 h	Red-brown
G1-ethyl-72methylPMe$_2$	0.0127 g 1.67×10^{-6} mol	0.0084 g 2.0×10^{-5} mol	Ethanol	-	Red-brown, hetero-geneous
G1-24methylP(Hex)$_2$	0.0301 g 5.0×10^{-6} mol	0.0084 g 2.0×10^{-5} mol	Ethanol	3 h	Red-brown
G1-24ethylPEt$_2$	0.0368 g 5.0×10^{-6} mol	0.0084 g 2.0×10^{-5} mol	Ethanol	2-3 h	Red-brown
G1-24ethylPEt$_2$	0.0368 g 5.0×10^{-6} mol	0.0084 g 2.0×10^{-5} mol	THF	< 5 min	Red-brown

6.2.1.1.2 [Rh(CO)$_2$(acac)] as metal-based complex.

Solutions of [Rh(CO)$_2$(acac)] and dendritic ligands.

The functionalised POSS dendrimer, [Rh(CO)$_2$(acac)] (0.0103 g, 4.0×10^{-5} mol) and ethanol or THF (4 cm^3) were charged into a Schlenk tube and stirred until complexation of the rhodium complex with the phosphine species (total dissolution). The phosphine/rhodium ratio used was 6/1. The amounts of dendritic ligands and some observations are summarised in Table 6.2.

Table 6.2 Solutions of [$Rh(CO)_2(acac)$] and dendritic ligands.

Ligand	*Amount of ligand*	*Solvent*	*Complexation*	*Obervation*
G1-16ethylPEt$_2$	0.0430g, 1.5 $\times 10^{-5}$ mol	Ethanol	< 10 min	Yellow
G1-24ethylPEt$_2$	0.0368 g, 1.0×10^{-5} mol	Ethanol	< 1 h	Yellow
G1-24ethylPEt$_2$	0.0368 g, 1.00×10^{-5} mol	THF	< 1 min	Yellow
G1-24propylPEt$_2$	0.0400 g, 1.00×10^{-5} mol	Ethanol	< 5 min	Yellow
G2-propyl-48ethyl PEt$_2$	0.0427 g, 0.50×10^{-5} mol	Ethanol	16 h	Slightly cloudy, yellow
G1-16ethylPCy$_{1.34}$Et$_{0.36}$	0.0609 g, 1.5×10^{-5} mol	Ethanol	1 h	Slightly cloudy, yellow

6.2.1.2 Hydroformylation reaction.

6.2.1.2.1 $Rh_2(O_2CMe)_4$ as metal-based complex.

Solution of $Rh_2(O_2CMe)_4$ and dendritic ligands.

The functionalised POSS dendrimer, [$Rh_2(O_2CMe)_4$] and ethanol or toluene (4 cm^3) were charged into a Schlenk tube and stirred until complexation of the rhodium complex with the phosphine species (total dissolution). The phosphine/rhodium ratio used was 3/1. The amounts of dendritic ligands and rhodium-based complex and some observations are summarised in Table 6.3.

Table 6.3 Solution of $[Rh_2(O_2CMe)_4]$ and dendritic ligands (P/Rh = 4/1).

Ligand	*ligand*	*$[Rh_2(O_2CMe)_4]$*	*Solvent*	*Complex formation*	*Observ.*
G1-24methylPPh$_2$	0.0282 g 0.5×10^{-5} mol	0.0084 g 2.0×10^{-5} mol	Ethanol	4 h	Red-brown
G1-24methylPPh$_2$	0.0141 g 0.25×10^{-5} mol	0.0045 g 1.1×10^{-5} mol	Toluene	1 h	Red-brown
G1-24methylPPh$_2$	0.0282 g 0.5×10^{-5} mol	0.0084 g 2.0×10^{-5} mol	Toluene	1.5 h	Red-brown

6.2.1.2.2 [Rh(CO)$_2$(acac)] as metal-based complex.

Solution of 1,5-bis(diphenylphosphino)pentane and [Rh(CO)$_2$(acac)].

1,5-bis(diphenylphosphino)pentane (0.0264 g, 6.0×10^{-5} mol), [Rh(CO)$_2$(acac)] (0.0052 g, 2.0×10^{-5} mol) (phosphine/rhodium = 6/1) and toluene (4 cm^3) were charged into a Schlenk tube and stirred until complexation of the rhodium complex with the phosphine species (total dissolution < 1 min) to form a bright yellow solution.

Solutions of bis(diphenylphosphinoethyl)dimethyl silane and [Rh(CO)$_2$(acac)].

Bis(diphenylphosphinoethyl)dimethyl silane (0.0049 g, 2.0×10^{-5} mol, P/Rh = 1/1) (0.0097 g, 4.0×10^{-5} mol, P/Rh = 2/1) (0.0290 g, 6.0×10^{-5} mol, P/Rh = 6/1) (0.0581 g, 12.0×10^{-5} mol, P/Rh = 12/1) and [Rh(CO)$_2$(acac)] (0.0052 g, 2.0×10^{-5} mol) and toluene (4 cm^3) were charged into a Schlenk tube and stirred until complexation of the rhodium complex with the phosphine species (< 1 min) to form bright yellow solutions.

Solutions of tetra(diphenylphosphinoethyl) silane and [$Rh(CO)_2(acac)$].

Tetra(diphenylphosphinoethyl)silane (0.0088 g, 1.0×10^{-5} mol) and [$Rh(CO)_2(acac)$] (0.0052 g, 2.0×10^{-5} mol) (phosphine/rhodium = 2/1) and toluene (4 cm^3) were charged into a Schlenk tube and stirred until complexation of the rhodium complex with the phosphine species (total dissolution < 5 min) to form a bright yellow solution.

Tetra(diphenylphosphinoethyl)silane (0.0265 g, 3.0×10^{-5} mol) and [$Rh(CO)_2(acac)$] (0.0052 g, 2.0×10^{-5} mol) (phosphine/rhodium = 6/1) and toluene (4 cm^3) were charged into a Schlenk tube and stirred. Complete solubility of the mixture was obtained by warming the bright yellow solution.

Tetra(diphenylphosphinoethyl)silane (0.0530 g, 6.0×10^{-5} mol) and [$Rh(CO)_2(acac)$] (0.0052 g, 2.0×10^{-5} mol) (phosphine/rhodium = 12/1) and toluene (4 cm^3) were charged directly into the autoclave since the ligand could not be fully dissolved in solution.

Solutions of dendritic ligand and [$Rh(CO)_2(acac)$].

The functionalised POSS dendrimer, [$Rh(CO)_2(acac)$] (0.0052 g, 2.0×10^{-5} mol) and toluene (4 cm^3) were charged into a Schlenk tube and stirred until complexation of the rhodium complex with the phosphine species (total dissolution). The phosphine/rhodium ratio used was 6/1. The amounts of dendritic ligands and rhodium-based complex and some observations are summarised in Table 6.4.

Table 6.4 Solutions of dendritic ligand and [$Rh(CO)_2(acac)$] in toluene.

Ligand	*Amount of ligand*	*complexation*	*Observation*
G1-16ethylPCy$_2$	0.0347 g 0.76×10^{-5} mol	< 5 min	Yellow solution
G1-16methylPPh$_2$	0.0313 g 0.75×10^{-5} mol	< 10 min	Yellow solution
G1-16ethylPPh$_2$	0.0330 g 0.75×10^{-5} mol	< 5 min	Orange solution
G1-16ethylPAr$_2$	0.0691 g 1.0×10^{-5} mol	-	Insoluble at room temp., oily residue, orange solution if warmed.
G1-16propylPPh$_2$	0.0367 g 0.86×10^{-5} mol	< 1 min	Pale yellow solution
G2-propyl-48ethylPPh$_2$	0.0353g 0.32×10^{-5} mol	-	Poor solubility at r.t., brown red when heated
G1-16methoxylPPh$_2$	0.0332 g 0.75×10^{-5} mol	< 5 min	Bright yellow solution
G1-16ethoxylPPh$_2$	0.0349 g 0.75×10^{-5} mol	< 5 min	Pale yellow solution
G1-16phosphite	0.040 g 0.75×10^{-5} mol	< 5 min	Very pale yellow solution, precipitate solid

6.2.2 Batch autoclave reactions.

Steel autoclaves of internal capacity 225 cm^3 fitted with a head such that the autoclave could also be used like a Schlenk tube were employed. A glass liner was inserted into the autoclave. The autoclave was closed apart from the valve to the pressurising gas cylinder and was flushed by pressurising to 20 bars with CO-H_2 and venting. This process was repeated three times. The cap was then removed from the autoclave and CO-H_2 allowed to pass through the open top. The catalyst solution (4 cm^3, varied concentration) and the substrate, either prop-2-en-1-ol (1 cm^3, 14.7×10^{-3} mol), hex-1-ene (1 cm^3, 8.0×10^{-3} mol), non-1-ene (1 cm^3, 5.8×10^{-3} mol), or oct-1-ene (1.3 cm^3, 8.3×10^{-3} mol), were injected into the open port and the cap replaced. The autoclave was pressurised to 40 bar (H_2/CO), sealed heated into a heating band

to the required operating temperature (120°C) for the appropriate reaction time. During the reaction, the mixture was stirred magnetically at 700 rpm. At the end of the reaction the autoclave was removed from the oven and placed in a cold water-bath for 20 min. Once the autoclave was cool the gases were slowly vented and the solutions poured out from inside and outside the autoclave liner. Some observations are summarised in Table 6.5. All the results are discussed in Chapter 4 and Chapter 5.

Table 6.5 Hydrocarbonylation and hydroformylation reactions at 120°C in a batch autoclave.

Complex	*Substrate*	*Conditions*	*Products (major)*	*Observation after reaction*
G1-24methylPMe$_2$ / Rh$_2$(O$_2$CMe)$_4$	Hex-1-ene	Ethanol, P/Rh = 3, 16 h	Heptan-1-ol and 2-methylhexan-1-ol, l:b = 2.1	Yellow-brown solution, a yellow precipitate found in some cases.[a]
G2-ethyl-72methylPMe$_2$ / Rh$_2$(O$_2$CMe)$_4$	Hex-1-ene	Ethanol, P/Rh = 4/1, 16 h	Heptan-1-ol and 2-methylhexan-1-ol, l:b = 2.4	Heterogeneous solution (yellow precipitate).
G1-24ethylPEt$_2$ / [Rh(CO)$_2$(acac)] or Rh$_2$(O$_2$CMe)$_4$	Hex-1-ene	Ethanol, P/Rh = 4/1, 16 h	Heptan-1-ol and 2-methylhexan-1-ol, l:b = 3.1	Yellow-brown solution, a yellow precipitate found in some cases.[a]
G1-24methylP(Hex)$_2$ / Rh$_2$(O$_2$CMe)$_4$	Hex-1-ene	Ethanol, P/Rh = 4/1, 16 h	Heptan-1-ol and 2-methylhexan-1-ol, l:b = 2.4	Yellow-brown solution, a yellow precipitate found in some cases.[a]
G1-24methylPPh$_2$ / Rh$_2$(O$_2$CMe)$_4$	Hex-1-ene	Toluene, P/Rh = 4/1, 16 h	Heptan-1-al and 2-methylhexan-1-al, l:b = 2.3	Yellow-brown solution, a yellow precipitate found in some cases.
G1-16ethylPPh$_2$ / [Rh(CO)$_2$(acac)]	Oct-1-ene	Toluene, P/Rh = 4/1, 16 h	nonan-1-al and 2-methyloctan-1-al, l:b = 6.6	Yellow-brown solution, a yellow precipitate found in some cases.[a]

[a]: this precipitate was probably due to the lack of solvent contained in the glass liner since the solution was mainly recovered between the autoclave wall and the glass liner.

Complex	*Substrate*	*Conditions*	*Products (major)*	*Observation after reaction*
G1-24ethylPEt$_2$ / Rh$_2$(O$_2$CMe)$_4$	prop-2-en-1-ol	Ethanol, P/Rh = 3, 16 h	Butane-1,4-diol (60 %), 2-methylpropan-1-ol (26 %).	Yellow-brown solution, a yellow precipitate found in some cases. [a].

The products were analysed by GLC as follows. An aliquot of the solution (100 μl) was diluted with ethanol (80 μl) containing octan-1-ol (20 μl) as an internal standard. A sample (0.3 μl) was then injected into a gas chromatograph. The temperature was held at 75 °C for 1 min then raised at 16°C min^{-1} to 150°C where it was held for a few minutes (around 5 min). The chromatograph was calibrated using standard solutions of the analyte with octanol (10% by volume) as an internal standard. The amount of butane-1,4-diol was determined by ^{13}C NMR by allowing long relaxation time or addition of chromium acetyl acetate since no reproductible results could be obtained by GC technique.

6.2.3 Hydroformylation with the CATS Catalyst Testing Unit.

The kinetic measurement for hydroformylation and hydrocarbonylation reactions were carried out with a specially designed autoclave owned and operated by the CATS (Catalytic Evaluation and Optimisation Services) service.

A schematic of the CATS kinetic autoclave is shown in Figure 6.1. The set-up includes an autoclave (A), an injection arm (B), a pressure controller and transducer (C), a ballast vessel (D), and a control panel (E). Each section can be isolated from each other with valves. The autoclave parts were supplied by Baskerville and assembled by the University of St. Andrews, School of Chemistry Workshop.

The catalytic solution was first injected into the autoclave under atmosphere of CO/H$_2$. The autoclave was then pressurised to below reaction pressure and heated to reaction temperature. These conditions were maintained for 0.5-1 h to form the active rhodium complexes. The substrate, either 2-propen-1-ol (1 cm^3, 14.7 × 10^{-3} mol), hex-1-ene (1 cm^3, 8.0 × 10^{-3} mol) or oct-1-ene (1.3 cm^3, 8.3 × 10^{-3} mol), was

then injected with a stream of synthesis gas, which brought the autoclave to reaction pressure. The reaction mixture was stirred at 1000 rpm. As the reaction proceeded the consummation of synthesis gas was monitored. The pressure in the autoclave was, however, kept constant by the pressure controller. The gas stream was fed by the ballast vessel, which was pressurised all along the reaction to higher pressure than the autoclave. The autoclave and ballast vessel could be filled with gas independently of each other using different gas inlets. The pressures of the autoclave, ballast vessel, and injection port were all monitored by pressure transducers, which were in turn controlled from the control panel.

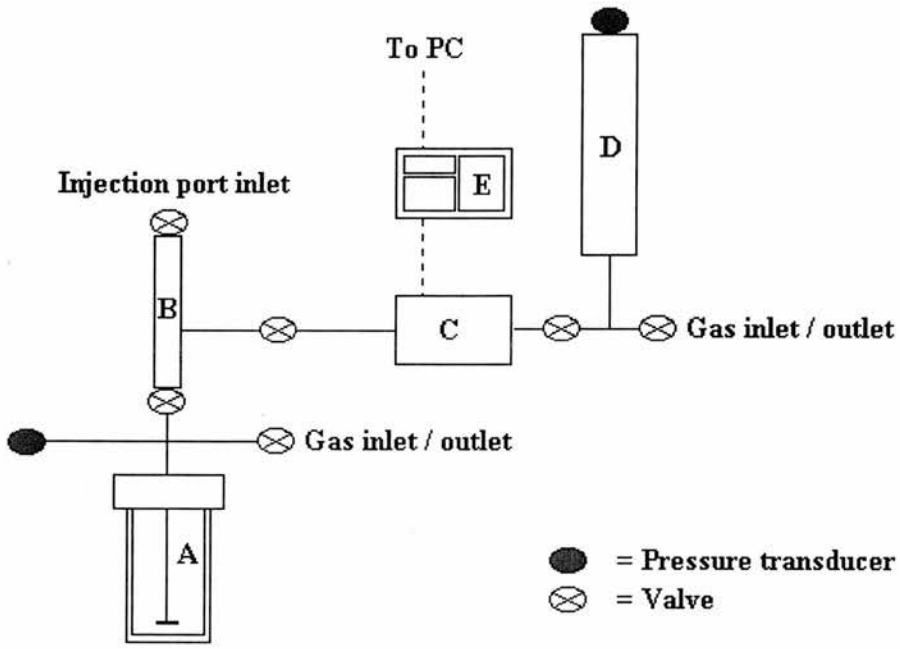

Scheme 6.1 Schematic of the CATS kinetic autoclave.

The gas consumed by the reaction was monitored by recording the drop in pressure in the ballast vessel during the reaction period. Data were collected via a link from a data logging hardware (Pico Monitor, model ADC16) which was fitted to a PC though a COM port. The computer used data logging software (PicoLog for Windows, version 5.04.2) to monitor and record the pressures. The data collected were then used for the calculation of the rates of reaction. For a first order reaction the plot of [ln(1-conversion/100)] versus time is linear over two or more half lives of the reaction. The gradient of that line represents the rate constant of the reaction (s^{-1}).

In practice this value is the logarithm of the total amount of gas in bar consumed by the reaction, minus the amount of gas in bar consumed at time t, divided by the total amount of gas in bar consumed by the reaction (see Equation 6.1).

Equation 6.1

$$k = \ln (P_t/P_{t=0})$$

P_t = Ballast vessel pressure, assuming $P_{final} = 0$.

$P_{t=0}$ = Total pressure of gas consumed by the reaction.

The initial rate (s^{-1} mol dm^{-3}) of reaction is calculated by multiplying the rate constant by the concentration of substrate at the start of the reaction. The initial rate is dependant upon the concentration of rhodium and the initial concentration of substrate. The initial rate of reaction can therefore be expressed as the initial turn over frequency (TOF_{init}), which represents the number of moles of substrate per one mole of catalyst reacting in a second (or an hour).

Equation 6.2

$$TOF = k \times [substrate] / [Rh]$$

TOF_{init} is defined as the rate constant multiplied by the initial substrate concentration, divided by the rhodium conncentration (in s^{-1} or h^{-1}).

The solution was analysed by G.C. and G.C. M.S.

All the catalytic results are discussed in Chapter 4 and Chapter 5. Tables presenting the detailed results are also shown in Annexe III and IV. Some observations are summarized in Table 6.6 (hydrocarbonylation) and Table 6.7 (hydroformylation).

Table 6.6 Hydrocarbonylation reaction catalysed by complex [$Rh(CO)_2(acac)$] and dendritic ligands (P/Rh = 6/1) at 120°C.

Ligand	*Substrate*	*Conditions*	*Products (major)*	*Observation after reaction*
G1-24ethylPEt$_2$	Hex-1-ene	Ethanol, 8 h	Heptan-1-ol and 2-methylhexan-1-ol, l:b = 3.0	Yellow-orange solution with yellow (crystalline) suspended solid
G1-24ethylPEt$_2$	Prop-2-en-1-ol	Ethanol, 2 h	1,4-butanediol 60.8 %, 2-methylpropan-1-ol 26.1 %	Yellow solution
G1-24ethylPEt$_2$	Prop-2-en-1-ol	THF, 3 h	1,4-butanediol 59.3 %, 2-methylpropan-1-ol 17.1 %	Yellow solution
G1-24ethylPEt$_2$	Oct-1-ene	Ethanol, 8 h	Heptan-1-ol and 2-methylhexan-1-ol, l:b = 3.1	Yellow-orange solution with yellow (crystalline) suspended solid
G1-16ethylPEt$_2$	Oct-1-ene	Ethanol, 8 h	nonan-1-ol and 2-methyloctan-1-ol, l:b = 3.1	Yellow-orange solution with yellow (crystalline) suspended solid
G2-propyl-48ethylPEt$_2$	Oct-1-ene	Ethanol, 8 h	nonan-1-ol and 2-methyloctan-1-ol, l:b = 3.0	Yellow-orange solution with yellow (crystalline) suspended solid
G1-24propylPPh$_2$	Oct-1-ene	Ethanol, 4 h	nonan-1-ol and 2-methyloctan-1-ol, l:b = 2.9	Yellow-orange solution with yellow (crystalline) suspended solid
G1-16ethylPCyEt	Oct-1-ene	Ethanol, 8 h	nonan-1-ol and 2-methyloctan-1-ol, l:b = 1.8	Yellow solution

Table 6.7 Hydroformylation of oct-1-ene in toluene catalysed by complex of [$Rh(CO)_2(acac)$] and dendritic ligands[a] at 120°C and 10 bar H_2/CO.

Ligand	*time h*	*l:b ratio[b]*	*Observation after reaction*
G1-16ethylPCy$_2$	5	1.4	Yellow solution
G1-16ethylPPh$_2$	2	13.9	Yellow solution
G1-16ethylPAr$_2$	2	15.0[c]	Yellow/brown solution
G1-16methylPPh$_2$	0.3	3.9	Yellow solution
G2-propyl-48ethylPPh$_2$	3	11.5	Yellow solution with yellow orange crystals
G1-16propylPPh$_2$	2	5.0	Yellow solution
G1-16methoxyPPh$_2$	2	5.7	Yellow solution with yellow orange crystals
G1-16ethoxyPPh$_2$	1	6.4	Yellow solution
G1-16phosphite	< 1.5	< 1.4[d]	Dark brown solution

[a]: P/Rh = 6/1, [b] : the main products are the aldehydes nonan-1-al and 2-methyloctan-1-al, c : 20 % of isomerised substrate, [d] : 40 to 55 % of isomerised substrate.

6.3 NMR spectra of the catalytic solutions.

6.3.1 G1-24ethylPEt$_2$ /[$Rh(CO)_2(acac)$] solution.

A solution of G1-24ethylPEt$_2$ (0.040 g, 1.087 x 10^{-5} mol) in dry/degassed deuteriated toluene (4 cm^3) under argon was added to [$Rh(CO)_2(acac)$] (0.0168 g, 6.52 x 10^{-5} mol) (P/Rh = 4/1) and stirred to form a yellow homogeneous solution. CO/H_2 was then bubbled through the resulting solution for 0.5-1 h. The solution was transferred to a NMR tube under CO/H_2 pressure and analysed.

Slow evaporation of the solvent by bubbling the syngas through the solution led to the formation of crystalline fine particles, which were isolated for X-ray analysis. No diffraction of the crystalscould however be obtained.

6.3.2 G1-16ethylPPh$_2$/[$Rh(CO)_2(acac)$] solution.

A solution of G1-16ethylPPh$_2$ (0.047 g, 1.068 x 10^{-5} mol) in dry/degassed deuterated toluene (4 cm^3) under argon was added to [$Rh(CO)_2(acac)$] (0.0147 g,

5.70 x 10^{-5} mol) (P/Rh = 4/1) and stirred to form a yellow homogeneous solution.. CO/H_2 was then bubbled through the resulting solution for 0.5-1 h. The solution was transferred to a NMR tube under CO/H_2 pressure and analysed.

A lower P/Rh ratio (< 2) or slow evaporation of the solvent led to precipitation of a yellow solid, which was insoluble in other solvents.

6.4 High Pressure IR Experiments.

The high pressure infrared studies were carried out in a cylindrical internal reflectance Fourrier transform infrared high pressure (HP CIR FTIR) autoclave. The autoclave had an internal volume of 35 cm^3 and was fitted with an injection port for the substrate, a gas inlet/outlet for pressurising/depressurising, a pressure gauge, a thermocouple located in the reaction medium, and a cylindrical internal reflectance (CIR) crystal bathing in the reaction solution. Heating was effected by heating rods, which passed into holes in the base of the Parr vessel. The autoclave was stirred mechanically from above. The CIR crystal was a polished cylinder with 45° conical ends and was made of either silicon or zinc selenide (obtained from Spectra-Tech.). The HP CIR FTIR autoclave was placed on the optical bench of an FTIR spectrometer where the infrared beam was directed into a set of convex cone mirrors and a toroidal mirror with the energy beam focused onto the 45° angle of the CIR crystal. As the beam passed through the crystal, it underwent internal reflections at the sample surface (approximately ten times). At each point of reflection the IR beam penetrated into the surrounding solution by about 1.0 to 1.5 μm giving a total path length of about 10-15 μm. The resultant beam which emerged would be then deficient in the specific frequencies absorbed by the species in solution. After the IR beam had reflected along the inside of the CIR crystal, it was directed to another set of toroidal and convex cone mirrors finally to reach the detector of the FTIR spectrometer. The optics were optimised by making small adjustments to the autoclave position relative to the beam. The infrared spectrometer was set for ATR correction.

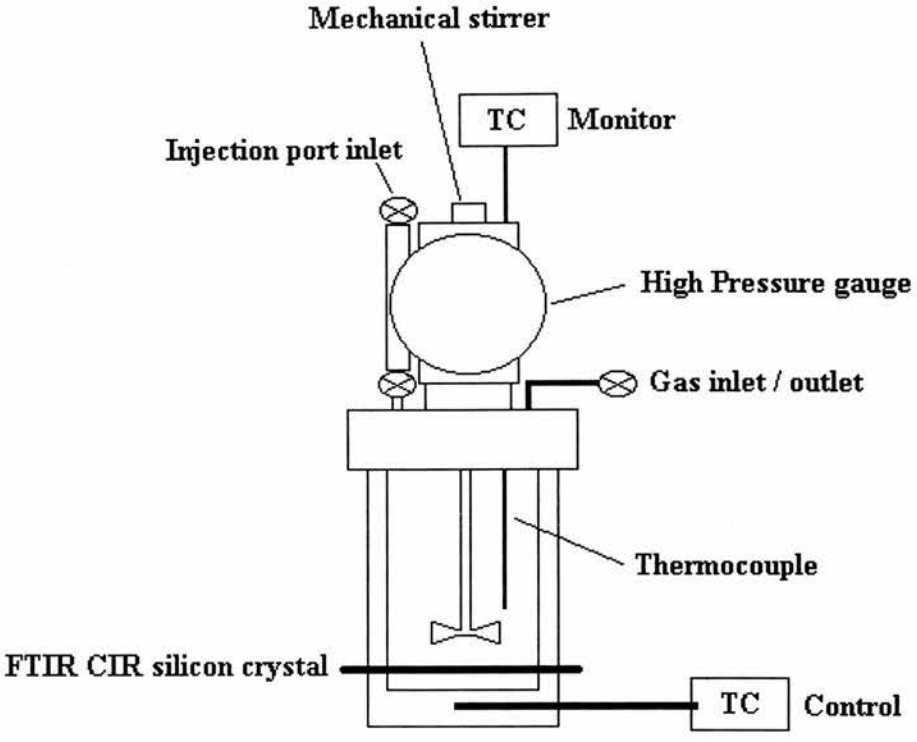

Scheme 6.2 Schematic of the HP CIR FTIR reactor cell.

The rhodium complex solutions were prepared under argon atmosphere using Schlenk techniques. The dendritic ligand and the rhodium precursor [$Rh(CO)_2(acac)$] were dissolved in toluene (10 cm^3). The autoclave was degassed by subsequent pressurisation/depressurisation with argon (three times). Argon was then passed into the gassing/degassing side arm and out of the open injection port. The reaction solution was injected into the vessel through the injection port. The autoclave was then sealed and pressurised with H_2/CO to 20 bar. The autoclave was placed on the optical bench of a Nicolet Protege 460 infrared spectrometer, where the heating elements and mechanical stirrer were fitted, and the CIR crystal aligned. The autoclave was then heated to the desired temperature and the FTIR spectrum recorded on an interfaced PC via the OMNIC operating system. The background spectra of the catalytic solution under identical pressure and temperatures were previously recorded. The spectra were corrected manually using the OMNIC package.

6.5 Molecular modelling.

Molecular modelling was carried out by Kate Haxton using the Discover programme contained in the Insight (II) Molecular Modelling suite of Molecular Simulations Inc.[17]

Molecular dynamics were performed using the consistent valence force field (CVFF), which was altered to represent the cases of a good and poor solvent. CVFF (good) represented the cases of a good solvent by only considering the repulsive van der Waals forces between non-bonded atoms. CVFF (poor) was used to represent a poor solvent by considering both Coulombic and van der Waals forces between non-bonded atoms.

The dendrimers were drawn using the draw facility on the Materials Studio viewer and minimized using steepest descent/conjugate gradient methods to a maximum energy derivative of less than RMS 0.001 kcal $mol^{-1}Å^{-1}$, relaxing bond lengths to their equilibrium distances. The models were then subjected to the heating and annealing process designed to reach a global minimum of energy for the structure. The structures were first heated to 1000 K to facilitate full expansion of the branches with a time step of 1 fs, and then annealed by reducing the temperature in 50 K steps for 5 ps dynamics down to 50 K. At 50 K the structures were again minimized to a maximum energy derivative of less than 0.001 kcal $mol^{-1}Å^{-1}$and allowed to equilibrate at 273 K for 600 ps. Every 1000^{th} configuration of the structure was saved in full for analysis. The final 500 ps (500 frames) of the equilibration trajectory was used for analysis.

6.6 References for Chapter 6.

1 M. G. Voronkov and V. L. Lavrent'yev, *Top. Curr. Chem.*, 1982, **102**, 199.

2 T. N. Martynova and V. P. Korchkov, *Zh. Obshch. kim.*, 1982, **52**, 1522.

3 P.-A. Jaffrès and R. E. Morris, *J. Chem. Soc., Dalton Trans.*, 1998, 2767.

4 A. L. Casalnuovo, T. V. RajanBabu, T. A. Ayers, and T. H. Warren, *J. Am. Chem. Soc.*, 1994, **116**, 9869.

5 C. P. Casey, L. E. Paulsen, E. W. Beuttenmueller, B. R. Proft, L. M. Petrovich, and B. A. Matter, *J. Am. Chem. Soc.*, 1997, **119**, 11817.

6 W. Schalk, P. Wirth, G. E. M. Dannenberg, and V. Schmied-Kowarzik, Deutsches Pat., DE 1118781, 1959, Koppers Co.

7 D. J. Peterson, *J. Organometal. Chem*, 1967, **8**, 199.

8 M. Slany, M. Bardaji, A.-M. Caminade, B. Chaudret, and J.-P. Majoral, *Inorg. Chem.*, 1997, **36**, 1939.

9 D. Chantreux, J.-P. Gamet, R. Jacquier, and J. Verducci, *Tetrahedron*, 1984, **40**, 3087.

10 E. Arpac and L. Dahlenburg, *Z. Naturforsch.*, 1980, **35b**, 146.

11 S. O. Grim and R. C. Barth, *J. Organomet. Chem.*, 1975, **94**, 327.

12 G. J. H. Buisman, P. C. J. Kamer, and v. L. P. W. N. M., *Tetrahedron: Asymmetry*, 1993, **4**, 1625.

13 C. Kim, S. Son, and B. Kim, *J. Organometal. Chem.*, 1999, **588**, 1.

14 J. M. Brunel, T. Constancieux, and G. Buono, *J. Org. Chem.*, 1999, **64**, 8940.

15 R. B. King and P. M. Sundaram, *J. Org. Chem.*, 1984, **49**, 1784.

16 E. E. Nifantiev, S. F. Sorokina, A. A. Borisenko, A. A. Zavalishina, and L. A. Vorobjeva, *Tetrahedron*, 1981, **37**, 3183.

17 Materials Studio, Molecular Simulations Inc., San Diego 2000.

Chapter Seven: Conclusions and Future work.

7 Conclusions and Future work.

7.1 Conclusions.

The synthesis of 1st and 2nd generation POSS dendrimers with up to 72 arms (vinyl, allyl, hydroxy or chloro endgroups) was achieved leading to highly functionalisable macromolecules. Various structure patterns (ends groups, chain length, number of ends groups) were used to build these dendritic compounds leading to different physical and chemical properties. These dendrimers were functionalised in high yield by some phosphine species either by radical addition of diphosphine compounds (HPR_2) onto the vinyl/allyl groups or by nucleophilic substitution of the chloro atoms in the chlorosilane type POSS by a nucleophile bearing the phosphorus species. Alkyl and arylphosphine dendrimers (respectively containing methyl, ethyl, cyclohexyl, n-hexyl groups and phenyl, as well as 3,5-$C_6H_3(CF_3)_2$ substituents) were prepared in this way with 16, 24, 48 or 72 endgroups. Various diphenylphosphine-functionalised dendrimers (16 endgroups) were synthesised by varying the chain length between the P (grafted) and Si (dendrimer) atoms and the composition of this chain. A phosphite-containing dendrimer was also synthesised by addition of the corresponding chlorophosphite to a hydroxy-substituted POSS.

These potentially dendritic ligands were then used in catalytic reactions. Hydroformylation and hydrocarbonylation reactions of alkenes (prop-2-en-1-ol, hex-1-ene, oct-1-ene and non-1-ene) were carried out using rhodium ($[Rh(acac)(CO)_2]$ or $[Rh_2(OCMe_2)_4]$) as metal-based catalyst under pressure of H_2/CO. Aldehydes (hydroformylation) and alcohols (hydrocarbonylation) were produced by the intermediate of these dendritic complexes with generally high activity and good selectivity (comparable to the small molecules) to the desired linear products.

The reactivity and/or selectivity of the different dendritic complexes were found to be dependent upon the structure pattern of the dendrimer. The rate of reaction was very often affected by the bulkiness of the ligand leading to lower rate for large dendrimers. Higher selectivity to the linear aldehyde (l:b = 14:1) compared to the small molecule analogues was found using a specific dendritic structure with diphenylphosphine groups on the periphery of the dendrimer (16 or 48 endgroups, spacer of 5 atoms between the P atoms). It is believed that other structures were

either too compact or not enough constrained to form regioselective catalyst species. This increased selectivity showed that a 'dendritic effect' occurred. The characterisation of the active rhodium species by NMR and HP IR techniques showed that this selectivity was probably due to a bidentate chelation of the phosphorus atoms in an equatorial-equatorial or equatorial-axial geometry in the trigonal bipyramidal configuration.

The hydrocarbonylation reactions proceeded mainly in a two step process, i.e. hydroformylation and subsequent hydrogenation. Plausible evidences for a competing one step process were, however, found.

7.2 Future work.

The mechanism of the hydrocarbonylation process remained unclear since possibly two mechanisms (one and two step mechanisms) were competing. Further studies, e.g. a labelling study, could certainly clarify this catalytic process.

The dendritic ligands only hydroformylated the terminal alkenes leaving the isomerised substrate unreacted. Therefore, it would be of great interest to use this property by performing the hydroformylation of internal alkenes albeit very low rates are expected since the dendrimers have been shown to give relatively slow hydroformylation of terminal alkenes.

Unfortunately it has been impossible for us to conduct the recycling of these dendritic ligands using ultrafiltration membranes. The lack of technology and appropriate membrane did not allow us to carry out such task. The development of a suitable membrane and its application in a hydroformylation recycling process should be the major target for further research.

Finally, hydroformylation and hydrocarbonylation were the only catalytic reactions performed with these dendritic ligands. It would be interesting to widen the scope of catalytic reactions for this type of ligands to other reactions where phosphine ligands have been shown to be successful (e.g. the carbonylation of ethylene, the Heck reaction, etc.). The large range of dendritic structures available could indeed lead to different reactivity/selectivity as we have observed for the hydroformylation reaction.

Appendix.

Appendix I : X-Ray Crystallography Data for $Si_8O_{12}[CH_2CH_2SiMe(CH=CH_2)_2]_8$.

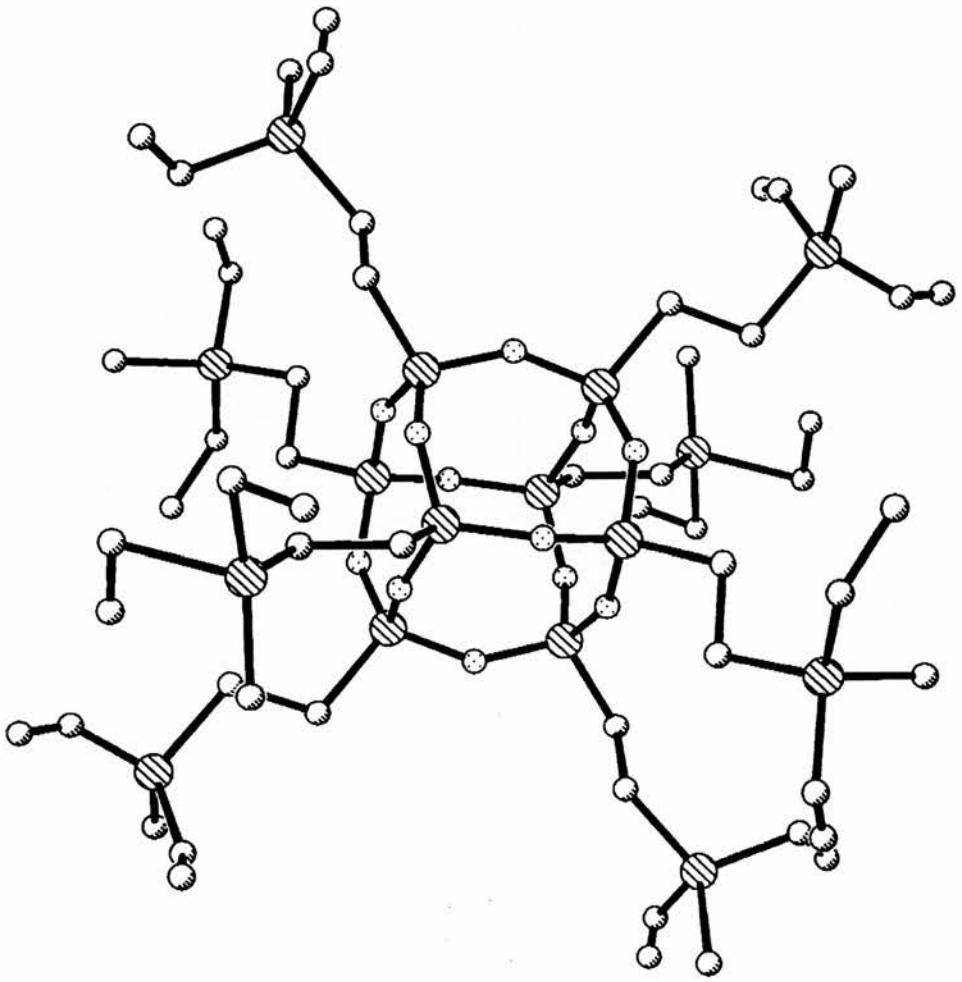

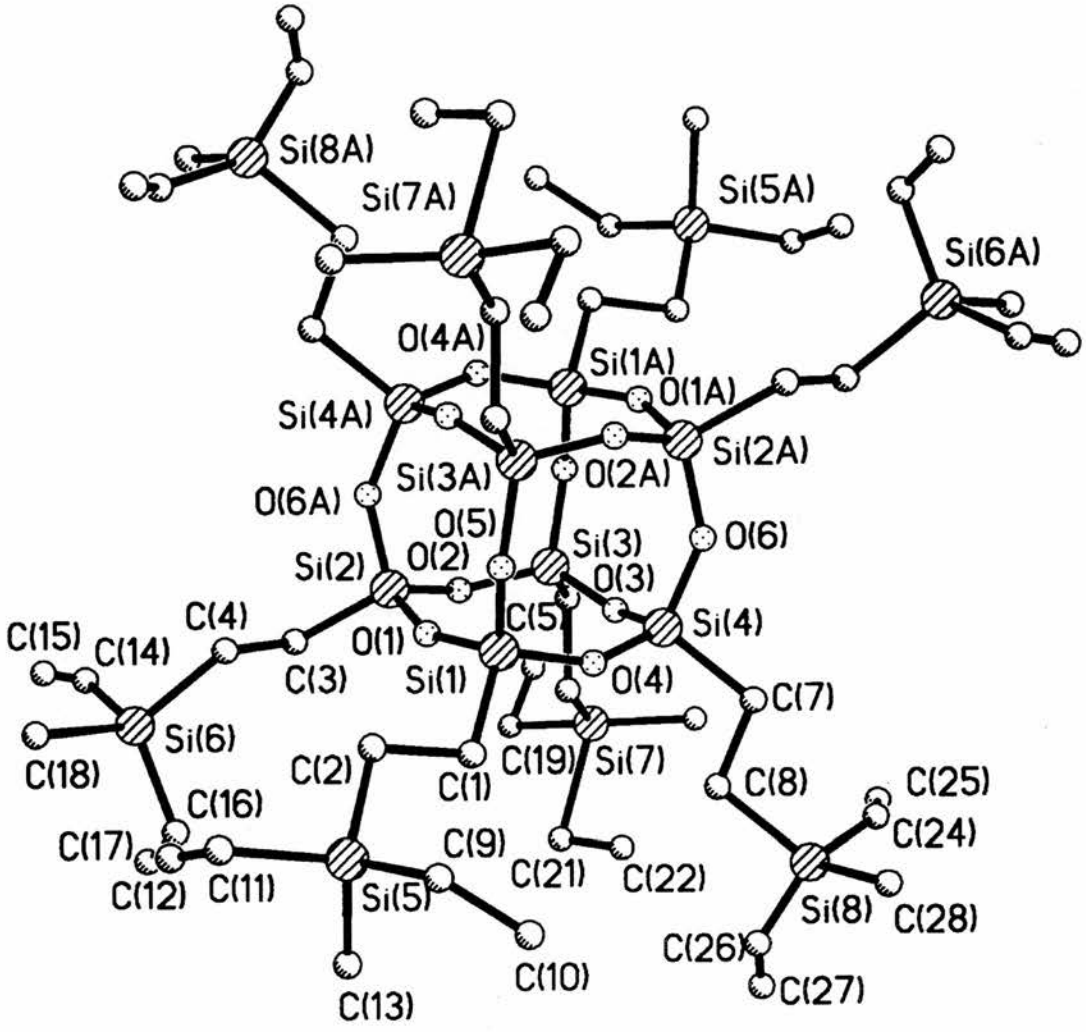
Si(8A)
Si(7A)
Si(5A)
Si(6A)
O(4A)
Si(1A)
O(1A)
Si(4A)
Si(2A)
Si(3A)
O(2A)
O(6A)
O(5)
Si(3)
O(6)
Si(2)
O(2)
O(3)
C(4)
C(5)
Si(4)
C(15)
C(14)
O(1)
C(3)
Si(1)
O(4)
C(7)
Si(6)
C(18)
C(2)
C(1)
C(19)
Si(7)
C(8)
C(25)
C(16)
C(24)
C(17)
C(9)
C(21)
C(22)
C(12)
C(11)
Si(5)
Si(8)
C(28)
C(26)
C(10)
C(27)
C(13)

Table 1. Crystal data and structure refinement for $C_{56}H_{104}O_{12}Si_{16}$.

Identification code	*lrdchl*
Empirical formula	$C_{56}H_{104}O_{12}Si_{16}$
Formula weight	*1418.83*
Temperature	*293 (2) K*
Wavelength	*0.71073 Å*
Crystal system	*Monoclinic*
Space group	$P2_1/c$
Unit cell dimensions	*a = 13.6425(7) Å alpha = 90°*
	b = 13.8802(6) Å beta = 96.445(3)°
	c = 23.2237(8) Å gamma = 90°
Volume, Z	*4369.9 (3) Å^3, 2*
Density (calculated)	*1.078 Mg/m^3*
Absorption coefficient	*0.277 mm^{-1}*
F(000)	*1520*
Crystal size	*.12 x .1 x .1 mm*
8 range for data collection	*1.71 to 23.23°*
Limiting indices	*$-13 \leq h \leq 15$, $-15 \leq k \leq 14$, $-20 \leq 1 \leq 25$*
Reflections collected	*18587*
Independent reflections	*6252 (R_{int} = 0.1085)*
Absorption correction	*SADABS*
Max. and mm. transmission	*1.00000 and 0.448671*
Refinement method	*Full-matrix least-squares on F^2*
Data I restraints I parameters	*6251 / 0 / 240*
Goodness-of-fit on F^2	*0.985*
Final R indices [I>2σ(I)]	*R1 = 0.1342, wR2 = 0.3853*
R indices (all data)	*R1 = 0.2868, wR2 = 0.5100*
Extinction coefficient	*0.0009 (12)*
Largest diff. peak and hole	*0.583 and -0.408 eÅ^{-3}*

Table 2. Atomic coordinates [10^4] and equivalent isotropic displacement parameters [Å x 10^{-3}] for $C_{56}H_{104}O_{12}Si_{16}$. U(eq) is defined as one third of the trace of the orthogonalized U_{ij} tensor.

	x	*y*	*z*	*U(eq)*
Si (1)	-1034(3)	8888(3)	663(2)	112(2)
O(1)	-1558(6)	9000(7)	3(4)	124(3)
Si (2)	-1647(3)	9386(3)	-648(2)	112(2)
O(2)	-691(7)	9010(6)	-951(4)	126(3)
Si (3)	493(3)	8989(3)	-912(2)	115(2)
O(3)	893(7)	8529(6)	-301(4)	122(3)
Si (4)	1102(3)	8484(3)	398(2)	110(2)
O(4)	41(6)	8428(6)	646(4)	116(3)
O(5)	-920(7)	9927(7)	949(4)	124(3)
Si(5)	-3520(5)	7636(5)	1556(3)	201(3)
O(6)	1668(6)	9460(7)	636(4)	117(3)
Si (6)	-4825(4)	8449(5)	-1098(3)	178(2)
Si (7)	1095(6)	6404(5)	-2014(3)	214(3)
Si (8)	2211(5)	5421(4)	651(4)	200(3)
C(1)	-1740(13)	8098(13)	1096(7)	158(6)
C(2)	-2822(15)	8433(15)	1086(9)	183(7)
C(3)	-2760(11)	8911(11)	-1075(7)	135(5)
C(4)	-3659(14)	9157(14)	-771(8)	168(6)
C(5)	951(13)	8279(13)	-1534(7)	158(6)
C(6)	643 (19)	7225(18)	-1465(11)	220(9)
C(7)	1902(11)	7472 (11)	628(7)	137(5)
C(8)	1361(14)	6481(13)	468(8)	160(6)
C(9)	-2828(30)	7703(27)	2401(17)	310(16)
C(10)	-2094(52)	6953(46)	2563 (26)	447(32)
C(11)	-4997(53)	8240(54)	1587(33)	433 (45)
C(12)	-5106(49)	8074(49)	1274(32)	386(38)
C(13)	-3728(28)	6354(27)	1234(17)	320(16)
C(14)	-5088(23)	8729(23)	-1905(13)	225(11)
C(15)	-5375(61)	9183(55)	-1991(36)	504(48)
C(16)	-4660(27)	7144(26)	-966(17)	281(14)
C(17)	-5122(57)	6848(57)	-1350(35)	524(42)
C(18)	-6015(21)	8928(22)	-590(13)	260(12)
C(19)	360(43)	6476(39)	-2645(24)	372 (26)
C(20)	1205(65)	6892(64)	-2874(36)	722(53)
C(21)	325 (59)	4787(48)	-1879(33)	508(39)
C(22)	1115(55)	4996(44)	-1542(31)	462(33)
C(23)	2415(25)	6176(22)	-1979(13)	345(13)
C(24)	3406(31)	5540(26)	269(16)	299(15)
C(25)	4248(87)	5131(91)	-159(64)	783(88)
C(26)	1397(22)	4445(25)	523(13)	286(12)
C(27)	1408(27)	3838(28)	318(16)	307(16)
C(28)	2612(23)	5420(22)	1511(14)	279(12)

Table 3. Bond lengths [Å] and angles [°] for $C_{56}H_{104}O_{12}Si_{16}$.

atoms	length	atoms	length
Si (1)-O(5)	1.588(10)	Si (1)-O(4)	1.604(10)
Si (1)-O(1)	1.625(9)	Si (1)-C(1)	1.83(2)
O(1)-Si (2)	1.595(10)	Si (2)-O(6)#1	1.602(10)
Si (2)-O(2)	1.636(10)	Si (2)-C(3)	1.84(2)
O(2)-Si (3)	1.607(10)	Si (3)-O(3)	1.596(10)
Si (3)-O(5)#1	1.620(10)	Si (3)-C(5)	1.91(2)
O(3)-Si (4)	1.617(9)	Si (4)-O(4)	1.617(9)
Si (4)-O(6)	1.626(10)	Si (4)-C(7)	1.82(2)
O(5)-Si (3)#1	1.620(10)	Si (5)-C(2)	1.88(2)
Si (5)-C(13)	1.94(4)	Si (5)-C(11)	2.19(7)
Si (5)-C(9)	2.08(4)	O(6)-Si (2)#1	1.602(10)
Si (6)-C(16)	1.85(3)	Si(6)-C(4)	1.95(2)
Si (6)-C(14)	1.91(3)	Si(6)-C(18)	2.21(3)
Si (6)-C(17)	2.32(8)	Si (7)-C(19)	1.68(5)
Si (7)-C(23)	1.82(3)	Si (7)-C(6)	1.87(3)
Si (7)-C(20)	2.13 (8)	Si (7)-C(21)	2.51(7)
Si (7)-C(22)	2.24(6)	Si (8)-C(26)	1.76(3)
Si (8)-C(8)	1.89(2)	Si(5)-C(28)	2.01(3)
Si (8)-C(24)	1.95(4)	Si(8)-C(27)	2.54(4)
C(1)-C(2)	1.55(2)	C(3)-C(4)	1.52(2)
C(5)-C(6)	1.53(3)	C(7)-C(5)	1.59(2)
C(9)-C(10)	1.46(6)	C(11)-C(12)	0.76(11)
C(14)-C(15)	0.76(8)	C(16)-C(17)	1.11(8)
C(19)-C(20)	1.44(9)	C(21)-C(22)	1.29(8)
C(24)-C(25)	1.70(13)	C(26)-C(27)	0.97(4)

atoms	angle	atoms	angle
O(5)- Si(1) -O(4)	109.0(5)	O(5)-Si(1)-O(1)	108.6(5)
O(4)- Si (1)- O(1)	108.7(5)	O(5)-Si (1)- C(1)	110.3(7)
O(4)- Si (1)- C(1)	108.3(7)	O(1) -Si (1)-C(1)	111.9(7)
Si (2)- O(1)- Si (1)	154.8(6)	O(l)- Si (2)- O(6)#1	105.6(5)
O(1)- Si (2)- O(2)	108.7(5)	O(6)#1- Si(2)- O(2)	110.0(5)
O(1)- Si (2)- C(3)	111.2(6)	O(6)#1- Si(2)- C(3)	110.6(6)
O(2)- Si (2)- O(3)	107.7(6)	Si (3) - O(2)- Si (2)	145.8(6)
O(2)- Si (3)- O(3)	107.4(5)	O(2)- Si (3)- O(5)#1	110.2(5)
O(3)- Si (3)- O(5)#1	109.2(5)	O(2) - Si(3) - C(5)	112.3(6)
O(3)- Si (3)- C(5)	111.0(7)	O(5)#1- Si (3)- C(5)	106.8(7)
Si (4)- O(3)- Si (3)	155.8(6)	O(4)- Si (4) - O(3)	107.1(5)
O(4)- Si (4)-O(6)	109.2(5)	O(3)-Si (4)-O(6)	109.4(5)
O(4)- Si (4)- C(7)	112.9(6)	O(3)-Si (4)-C(7)	110.9(6)
O(6)- Si (4)- C(7)	107.3(6)	Si (4)- O(4)-Si (1)	147.8(6)
Si (1)- O(5)-Si (3)#1	147.2(6)	C(2)- Si(5)-C(13)	112.2(14)
C(2)- Si(5)- C(11)	109(2)	C(13)- Si (5)- C(11)	106(2)
C(2)- Si(5)- C(9)	108.3(13)	C(13)- Si (5)- C(9)	116(2)
C(11)- Si(5)- C(9)	106(2)	Si (2)#1- O(6)- Si (4)	146.1(6)
C(16)- Si (6)- C(4)	110.5(14)	C(16)- Si (6) - C(14)	112(2)
C(4)- Si (6) - C(14)	109.6(11)	C(16) - Si(6)- C(18)	106.8(14)
C(4)- Si (6)- C(18)	104.8(10)	C(14)- Si(6) - C(18)	113.2(13)
C(16)- Si (6)- C(17)	28(2)	C(4)- Si(6)- C(17)	134(2)
C(14) - Si(6) - C(17)	86(2)	C(18)- Si (6)- C(17)	108(2)
C(19)- Si (7) - C(23)	123(2)	C(19)- Si (7) - C(6)	110(2)
C(23)- Si (7) - C(6)	118.4(13)	C(19)- Si (7)- C(20)	42(3)
C(23)- Si (7)- C(20)	86(3)	C(6)- Si (7)- C(20)	121(3)
C(19)- Si (7) - C(21)	87(3)	C(23) -Si (7)- C(21)	105(2)
C(6)- Si (7) - C(21)	107(2)	C(20) -Si (7)- C(21)	118(3)
C(19)- Si (7) - C(22)	117(3)	C(23)- Si (7) -C(22)	82(2)
C(6)- Si (7) - C(22)	101(2)	C(20)-Si (7) -C(22)	138(3)

atoms	angle	atoms	angle
C(21)- Si (7)- C(22)	31(2)	C(26) -Si(8) -C(8)	101.7(12)
C(26)- Si(5)- C(28)	105.3(13)	C(8)- Si(8)- C(28)	108.4(11)
C(26)- Si (8)- C(24)	122(2)	C(8)- Si(8)-C(24)	110.7(13)
C(28)-Si (8) -C(24)	108(2)	C(26)-Si (8) -C(27)	15.6(14)
C(8) -Si (8) -C(27)	111.9(10)	C(28) -Si(8) -C(27)	111.3(12)
C(24)-Si(8) -C(27)	106.8(14)	C(2) -C(1)-Si (1)	111.8(13)
C(1) -C(2)-Si (5)	110.9(14)	C(4) -C(3)-Si (2)	109.2(11)
C(3) -C(4)-Si (6)	111.8(12)	C(6)-C(5) -Si(3)	107.2(14)
C(5) -C(6)-Si (7)	113(2)	C(8) -C(7)-Si (4)	110.6(11)
C(7)-C(8) -Si(8)	111.4(12)	C(10) -C(9)-Si(5)	116(4)
C(12) -C(11) -Si (5)	86(10)	C(15) -C(14)-Si (6)	117 (8)
C(17) -C(16) -Si(6)	100(5)	C(16) -C(17)-Si (6)	52(4)
C(20) -C(19)-Si (7)	56(5)	C(19) -C(20)-Si (7)	52(4)
C(22) -C(21)-Si (7)	63(5)	C(21) -C(22)-Si (7)	86 (5)
C(25) -C(24)-Si (8)	153(6)	C(27) -C(26)-Si(8)	135(4)
C(26) -C(27)-Si (8)	29(3)		

Symmetry transformations used to generate equivalent atoms:

#1 -x, -y+2, -z

Table 4. Anisotropic displacement parameters [$Å^2$ x 10^3] for $C_{56}H_{104}O_{12}Si_{16}$. The anisotropic displacement factor exponent takes the form:

$-2\pi^2 [(ha^*)^2 U_{11} + ... + 2hka^* b^* U_{12}]$

	U11	*U22*	*U33*	*U23*	*U13*	*U12*
Si(1)	110(3)	121(4)	108(3)	14(3)	20(2)	-12(3)
O(1)	111(7)	145(8)	113(8)	11(6)	0(5)	2(6)
Si(2)	106(3)	115(4)	111(3)	1(2)	-5(2)	-14(2)
O(2)	125(8)	137(7)	115(7)	-32(6)	12(5)	5(6)
Si(3)	124(3)	123(4)	99(3)	-14(3)	16(2)	13(3)
O(3)	128(7)	125(7)	112(8)	-9(6)	8(5)	24(5)
Si(4)	121(3)	107(3)	102(3)	6(2)	9(2)	14(2)
O(4)	118(7)	124(7)	106(7)	15(5)	11(5)	-3(6)
O(5)	134(7)	128(8)	113(7)	-4(6)	33(5)	15(6)
Si(5)	172(5)	218(7)	227(7)	37(5)	80(5)	-28(5)
O(6)	121(7)	122(8)	106(7)	-13(5)	6(5)	-2(6)
Si(6)	98(3)	214(6)	218(6)	-23(5)	1(3)	5(3)
Si(7)	213(7)	208(7)	217(7)	-101(6)	6(5)	27(5)
Si(8)	203(6)	105(4)	283(9)	10(4)	-17(6)	24(4)

No data for hydrogen coordinates and isotropic displacement parameters.

Appendix II: X-ray Crystallography data of $Si(CH_2CH_2PPh_2)_4$.

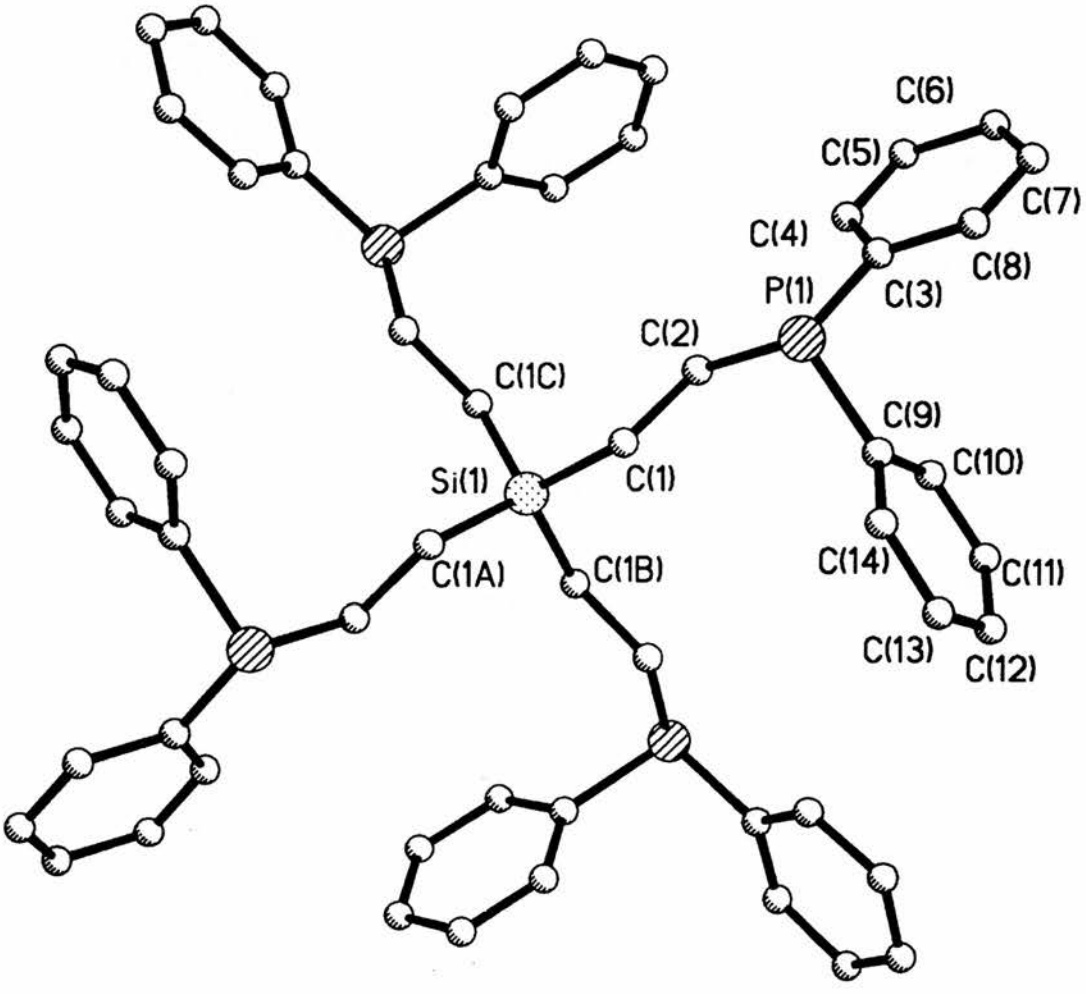

Table 1. *Crystal* data and structure refinement for $C_{56}H_{56}P_4Si$ **(3)**.

Identification code	lrdch2
Empirical formula	$C_{56}H_{56}P_4Si$
Formula weight	880.98
Temperature	293 (2) K
Wavelength	0.71073 Å
Crystal system	Tetragonal
Space group	I4
Unit cell dimensions	a = 20.4806(14) Å alpha = 90°
	b = 20.4806(14) Å beta = 90°
	c = 5.7429(6) Å gamma = 90°
volume, z	2408.9(3) $Å^3$, 2
Density (calculated)	1.215 Mg/m^3
Absorption coefficient	0.218 mm^{-1}
F(000)	932
Crystal size	.18 x .1 x .1 mm
θ range for data collection	1.41 to 23.31°
Limiting indices	$-22 \leq h \leq 22, -22 \leq k \leq 22, -6 \leq l \leq 6$
Reflections collected	6198
Independent reflections	1758 (R_{int} = 0.1033)
Absorption correction	Sadabs
Max. and mm. transmission	1.00000 and 0.761556
Refinement method	Full-matrix least-squares on F^2
Data I restraints I parameters	1725 / 0 / 139
Goodness-of-fit on F^2	0.823
Final R indices [$I>2\sigma(I)$]	R1 = 0.0453, wR2 = 0.0512
R indices (all data)	R1 = 0.0956, wR2 = 0.0671
Absolute structure parameter	0.01(13)
Extinction coefficient	0.0006(2)
Largest diff. peak and hole	0.162 and -0.172 $eÅ^{-3}$

Table 2. Atomic coordinates [x 10^4] and equivalent isotropic displacement parameters [$Å^2$ x 10^3] for $C_{56}H_{56}P_4Si$. U(eq) is defined as one third of the trace of the orthogonalized U_{ij} tensor.

	x	*y*	*z*	*U(eq)*
Si(1)	0	0	0	40(1)
C(1)	-689(1)	208(2)	1994(6)	43(1)
C(2)	-1391(2)	212(2)	993(6)	44(1)
P(1)	-1962(1)	532(1)	3197(2)	47(1)
C(3)	-2749(2)	496(2)	1699(7)	45(1)
C(4)	-2862(2)	192(2)	-383(8)	61(1)
C(S)	-3479(2)	156(2)	-1327(8)	75(1)
C(6)	-3998(2)	450(2)	-192(11)	83(2)
C(7)	-3897(2)	765(2)	1855(11)	79(2)
C(8)	-3279(2)	788(2)	2803(8)	70(1)
C(9)	-1783(2)	1405(2)	3003(7)	42(1)
C(10)	-1972(2)	1797(2)	1144(7)	59(1)
C(11)	-1832(2)	2452(2)	1091(7)	67(1)
C(12)	-1490(2)	2737(2)	2846(11)	74(2)
C(13)	-1287(2)	2363(2)	4671(9)	75(1)
C(14)	-1433(2)	1704(2)	4783(8)	59(1)

Table 3. Bond lengths [Å] and angles [°] for $C_{56}H_{56}P_4Si$.

atoms	length	atoms	length
Si(1)- C(1)	1.867(3)	Si (1) -C(1)#l	1.867(3)
Si(1)- C(1)#2	1.867(3)	Si (1) -C(1)#3	1.867(3)
C(1)- C(2)	1.547(4)	C(2) -P(1)	1.844(3)
P(1)- C(9)	1.829(3)	P(1) -C(3)	1.829(3)
C(3)- C(4)	1.368(5)	C(3) -C(8)	1.393(4)
C(4)- C(S)	1.377(5)	C(5) -C(6)	1.384(5)
C(6)- C (7)	1.357(6)	C(7) -C(5)	1.379(5)
C(9)- C(10)	1.390(5)	C(9) -C(14)	1.390(5)
C(10)- C(11)	1.372(4)	C(11) -C(12)	1.359(5)
C(12) -C(13)	1.363(6)	C(13) -C(14)	1.385(4)

atoms	angle	atoms	angle
C(1) -Si (1) -C(1)#1	104.4(2)	C(1) -Si (1) -C(1)#2	112.09(11)
C(1)#1-Si(1) -C(1)#2	112.09(11)	C(1) -Si (1) -C(1)#3	112.09(11)
C(1)#1-Si(1)-C(1)#3	112.09(11)	C(1)#2-Si(1)-C(1)#3	104.4(2)
C(2) -C(1) -Si (1)	118.4(2)	C(1) -C(2) -P(1)	109.6(2)
C(9) -P (1) -C(3)	100.8(2)	C(9) -P(1) -C(2)	100.3(2)
C(3) -P(1) -C(2)	102.8(2)	C(4) -C(3) -C(5)	117.5(3)
C(4) -C(3) -P(1)	125.4(3)	C(5) -C(3) -P(1)	117.1(3)
C(3) -C(4) -C(5)	121.6(4)	C(4) -C(5) -C(6)	119.7(4)
C(7) -C(6) -C(5)	119.9(4)	C(6) -C(7) -C(5)	119.9(4)
C(7) -C(5) -C(3)	121.4(4)	C(10) -C(9) -C(14)	117.0(3)
C(10) -C(9) -P(1)	123.7(3)	C(14) -C(9) -P(1)	119.2(3)
C(11) -C(10) -C(9)	121.5(4)	C(12) -C(11) -C(10)	120.7(4)
C(11) -C(12) -C(13)	119.1(4)	C(12) -C(13) -C(14)	121.2(4)
C(13) -C(14) -C(9)	120.4(4)		

Symmetry transformations used to generate equivalent atoms:

#1 -x, -y, z #2 y, -x, -z #3 -y, x,-z

Table 4. Anisotropic displacement parameters [$Å^2$ x 10^3] for $C_{56}H_{56}P_4Si$. The anisotropic displacement factor exponent takes the form: $-2\pi^2$ [$(ha^*)^2 U_{11}$ + ... + 2hka* b* U_{12}].

	U11	*U22*	*U33*	*U23*	*U13*	*U12*
Si(1)	37(1)	37(1)	48(2)	0	0	0
C(1)	35(2)	46(2)	49(2)	7(2)	1(2)	4(2)
C(2)	48(3)	37(2)	46(3)	-1(2)	0(2)	-1(2)
P(1)	40(1)	49(1)	50(1)	2(1)	6(1)	4(1)
C(3)	36(2)	44(2)	56(3)	6(2)	14(3)	-3(2)
C(4)	40(3)	71(3)	72(3)	-5(3)	4(2)	2(2)
C(S)	59(3)	71(3)	95(4)	-1(3)	-19(3)	-10(3)
C(S)	47(3)	59(4)	141(6)	21(4)	-32(4)	-7(3)
C(7)	41(3)	56(3)	139(5)	3(4)	20(4)	-1(2)
C(8)	47(3)	64(3)	99(4)	2(3)	10(3)	5(2)
C(9)	41(2)	47(3)	38(2)	-5(2)	4(2)	7(2)
0(10)	58(3)	54(3)	66(4)	-3(2)	-1(2)	-8(2)
C(11)	76(3)	53(3)	71(4)	11(2)	0(3)	-3(2)
C(12)	69(3)	48(3)	105(5)	-7(3)	0(3)	-3(3)
C(13)	63(3)	70(4)	92(4)	-33(3)	-10(3)	-5(3)
C(14)	56(3)	53(3)	67(3)	-8(3)	-13(3)	13(2)

Table 5. Hydrogen coordinates (10^4) and isotropic displacement parameters ($Å^2$ x 10^3) for $C_{56}H_{56}P_4Si$.

	x	*y*	*z*	*U(eq)*
H(1A)	-680(1)	-98(2)	3280(6)	52
H(1B)	-604(1)	638(2)	2637(6)	52
H(2A)	-1517(2)	-228(2)	559(6)	53
H(2B)	-1407(2)	483(2)	-391(6)	53
H(4A)	-2514(2)	5(2)	-1181(8)	73
H(5A)	-3547(2)	-64(2)	-2722(8)	90
H(6A)	-4415(2)	432(2)	-831(11)	99
H(7A)	-4244(2)	965(2)	2616(11)	95
H(8A)	-3215(2)	1003(2)	4211(8)	84
H(1OA)	-2199(2)	1611(2)	-91(7)	71
H(I1A)	-1973(2)	2704(2)	-160(7)	80
H(12A)	-1396(2)	3181(2)	2802(11)	89
H(13A)	-1047(2)	2555(2)	5864(9)	90
H(14A)	-1295(2)	1459(2)	6055(8)	71

Appendix III.

Hydrocarbonylation of prop-2-en-1-ol by rhodium/G1-24ethylPEt$_2$ complexes.

Solvent	*t*	K_1 10^{-3} s^{-1}	K_2 10^{-3} s^{-1}	*Conv.* %	*BDO* %	*MPO* %	*MPD* %	*MPA* %	*MAA* %	*PO* %	*PA* %	*MPEA* %	*HBA* %	*MHPA* %	*DHF* %	*γBA* %	*unknown* %
Ethanol	2	1.2	0.8-1.1	99.9	60.8	26.1	4.4	2.5	0.3	1.4	t	0.2	0.5	t	t	0.4	3.4
Ethanol	0.25	-	-	67.5	14.1	3.6	1.8	15.6	0.3	0.9	0.9	1.3	25.0	0.9	0.9	0.4	1.6
Ethanol	-	-	-	100	20.9	5.4	2.7	23.2	0.4	1.3	1.4	2.0	37.1	1.3	1.4	0.6	2.4
THF	3	1.2	2.3	99.8	59.3	17.1	5.5	8.0	0.2	1.1	0.1	nd	4.1	0.2	0.2	0.4	3.6
THF	9	-	-	99.9	64.9	21.9	6.9	1.1	0.1	1.1	0.0	nd	0.2	0.1	0.0	0.5	3.1

Reaction conditions [Rh(acac)(CO)$_2$] (4.0×10^{-5} mole, 8.0×10^{-3} mol dm^{-3}), G1-24ethylPEt$_2$ (1.0×10^{-5} mol) , solvent 4 cm^3, substrate 1 cm^3 (14.7×10^{-3} mol), 120°C, 40 bar H_2/CO.

K_1 = rate constant for the hydroformylation step, K_2 = rate constant for the hydrogenation step

BDO = 1,4-butanediol, PO = propan-1-ol, MPO = 2-methylpropan-1-ol, MPA = 2-methylpropan-1-al, MPD = 2-methylpropane-1,3-diol, PA = propan-1-al, MAA = methyl allyl alcohol, MPEA = 2-methylprop-2-en-1-al, HBA= 4-hydroxybutan-1-al, MHPA = 2-methyl-3-hydroxypropan-1-al, DHF = 2,3-dihydrofuran, γBA = γ-butyrolactone.

Nd non determined since only small amounts and partially hidden by THF.

Hydrocarbonylation of oct-1-ene catalysed by rhodium dendritic complexes.

Ligand	*t*	*Rate const.*	*Initial rate*	*TOF*	*Conv.*	*1-O*	*2-O*	*3&4-O*	*O*	*MeO*	*N*	*PrHol*	*EtHol*	*MeOol*	*Nol*	*Sel*	*n:i ratio*
	h	10^{-4} s^{-1}	10^{-4} *mol* dm^{-3} s^{-1}	s^{-1}	*%*	*%*	*%*	*%*	*%*	*%*	*%*	*%*	*%*	*%*	*%*	*%*	
G1-16ethylPEt$_2$	8	1.5	2.3	0.031	>99.9	0	0.37	2.26	0.49	t	t	0.04	0.11	23.25	73.49	74	3.1
G1-propyl-48ethylPEt$_2$	8	2.1	3.3	0.044	>99.9	0	0.44	1.67	0.49	t	t	t	0.09	24.46	72.84	73	3.0
G1-24ethylPEt$_2$	8	1.7	2.7	0.036	>99.9	0	0.77	1.28	0.54	0.27	0.10	t	0.06	23.82	73.15	73	3.1
G1-24propylPEt$_2$	4	3.7	5.8	0.077	>99.9	0	0.45	0.92	0.41	0.06	0.04	t	0.05	25.24	72.83	73	2.9
G1-24propylPEt$_2$	1	-	-	-	57.92	42.08	0.33	0.29	0.32	4.08	2.07	0	0	10.50	40.34	-	3.8
G1-ethylPEtCy	8	2.4	3.7	0.049	>99.9	0	0.57	1.98	0.42	4.63	0.08	t	0.05	32.40	59.85	60	1.8

O = n-Octane, 1-O = oct-1-ene, 2-O = oct-2-ene, 3,4-O= 3&4-Octene, MeO = 2-Methyloctan-1-al, N = nonan-1-al, PrHol = 2-propylhexan-1-ol, EtHol = 2-Ethylheptan-1-ol, MeOol = 2-Methyloctan-1-ol, Nol= Nonan-1-ol.

[a] Rate constant and initial rates refer to Hydrocarbonylation of oct-1-ene only, [b] TOF(I)=Initial turnover frequency (moles of oct-1-ene consumed per mole of rhodium per second), [c] Sel.= Selectivity to nonan-1-ol, [d] n:i = Ratio of straight to branched alcohol.

All the final reaction solutions were bright yellow in colour, all except the last also containing yellow (crystalline) suspended solid.

Typical Conditions: solution of $[Rh(acac)(CO)_2]$ (4.0×10^{-5} mole) and D-$[SiMe(CH_2CH_2PEt_2)_2]_8$ (1.5×10^{-5} mole) (total P/Rh = 6/1) in ethanol (4 cm^3) heated at 120°C under 30 bar of CO/H_2 (1:1) for 1 h. Oct-1-ene (1.3 cm^3, 8.3×10^{-5} mol) (Rh/substrate = 1/207) was injected with simultaneous increase in autoclave pressure up to 40 bar. The reaction was run for the stated time before the reaction was quenched by cooling the autoclave with water. Overall: [Rh] = 7.55×10^{-3} mol dm^{-3} and [oct-1-ene] = 1.56 mol dm^{-3}.

Appendix IV.

Hydroformylation of oct-1-ene catalysed by rhodium/dendritic ligands.

Ligand	*(P_2): Rh*	*T °C*	*P bar*	*T h*	*Rate[a] 10^{-3}*	*Initial rate[b,a]*	*TOF[c] s^{-1}*	*Conv. %.*	*1-O %*	*2-O %*	*3-O %*	*4-O %*	*O %*	*PrH %*	*EtH %*	*MeO*	*N %*	*Nol %*	*Sel[d] %*	*l:b[e] ratio*
G1-16ethylPPh$_2$	2.7	80	20	24	0.052	0.081	0.02	>99.9	0	2.25	0.18	0.08	0.49	0.00	0.02	12.65	83.93	0.40	84	6.6
G1-16ethylPPh$_2$	2.7	100	20	6	0.33	0.52	0.14	>99.9	0	2.99	0.15	0.07	0.57	0.00	0.05	11.21	84.66	0.31	85	7.5
G1-16ethylPPh$_2$	2.7	80	10	19	0.081	0.13	0.03	>99.9	0	5.26	0.57	0.13	0.76	0.00	0.02	9.50	83.46	0.31	84	8.8
G1-16ethylPPh$_2$	2.7	100	10	4	0.42	0.66	0.18	>99.9	0	4.66	0.23	0.08	0.69	0.00	0.03	7.93	86.17	0.21	86	10.8
G1-16ethylPPh$_2$	1.8	120	10	2	0.95	1.5	0.40	>99.9	0	6.18	0.75	0.12	1.34	0.00	0.06	7.02	84.30	0.23	84	11.9
G1-16ethylPPh$_2$	2.7	120	10	2	1.1	1.7	0.45	>99.9	0	6.07	0.19	0.07	0.84	0.00	0.06	7.04	85.55	0.19	86	12.0
G1-16ethylPPh$_2$	5.4	120	10	2	1.5	2.3	0.61	>99.9	0	6.30	0.21	0.06	0.99	0.00	0~10	6.90	85.16	0.29	85	12.2
G1-16ethylPPh$_2$	2.7	120	10	0.2	1.1	1.7	0.45	56.72	43.28	4.18	0.14	0.07	0.70	0.00	0.00	3.15	48.50	0.00	86[f]	15.4
G1-16ethylPPh$_2$	3.0	120	10	2	1.2	1.9	0.50	>99.9	0	6.35	0.20	0.06	1.01	0.00	0.07	6.14	86.02	0.16	86	13.9
G1-16ethylPPh$_2$	1.0	120	10	2	0.52	0.81	0.22	>99.9	0	30.75	4.27	0.45	0.94	0.07	0.62	13.61	48.40	0.89	48	3.4
G1-16ethylPAr$_2$	3.0	120	10	2	1.1	1.7	0.45	>99.9	0	19.71	0.32	t	1.84	0.00	0.14	4.73	73.04	0.22	73	15.0
G1-propyl-48ethylPPh$_2$	3.0	120	10	3	0.61	0.95	0.25	>99.9	0	7.30	0.18	t	1.19	0.00	0.07	7.24	83.78	0.24	84	11.5
G1-16ethylPCy$_2$	3.0	120	10	5	0.19	0.3	0.08	>99.9	0	0.77	0.12	t	0.36	0.00	0.05	40.28	57.17	1.26	57	1.4
G1-16methylPPh$_2$	3.0	120	10	0.3	6.2	9.7	2.57	>99.9	0	11.72	0.39	t	1.63	0.09	1.19	16.31	68.51	0.17	69	3.9
G1-16methoxyPPh$_2$	3.0	120	10	2	0.68	1.1	0.28	>99.9	0	8.82	0.22	t	1.14	0.00	0.16	13.30	76.17	0.18	76	5.7
G1-16propylPPh$_2$	3.0	120	10	2	1.5	2.3	0.61	>99.9	0	4.94	0.16	t	0.75	0.00	0.17	15.40	78.05	0.53	78	5.0
G1-16ethoxylPPh$_2$	3.0	120	10	1	2.0	3.1	0.83	>99.9	0	8.11	0.22	t	1.18	0.00	0.22	12.02	78.05	0.20	78	6.4

Ligand	*(P_2): Rh*	*T*	*p*	*t*	*Rate[a] 10^{-3}*	*Initial rate[b,a]*	*TOF[c] s^{-1}*	*Conv. %.*	*1-O %*	*2-O %*	*3-O %*	*4-O %*	*O %*	*PrH %*	*EtH %*	*MeO*	*N %*	*Nol %*	*Sel[d] %*	*l:b[e] ratio*
3	1.0	120	10	2	2.1	3.3	0.87	>99.9	0	12.22	4.91	1.18	1.50	0.46	2.05	21.66	55.91	0.11	56	2.3
3	3.0	120	10	2	2.1	3.3	0.87	>99.9	0	6.24	0.34	0.06	1.05	0.03	0.37	14.50	77.39	0.02	77	5.2
3	6.0	120	10	2	2.4	3.7	0.99	>99.9	0	5.71	0.33	0.06	1.12	0.04	0.52	12.10	79.90	0.22	80	6.3
2	0.5	120	10	2	1.6	2.5	0.66	>99.9	0	15.93	2.95	0.42	0.96	0.10	0.68	17.24	61.68	0.05	62	3.4
2	1.0	120	10	2	2.8	4.4	1.16	>99.9	0	8.83	1.29	0.19	1.14	0.12	1.06	18.34	68.90	0.14	69	3.5
2	3.0	120	10	2	3.0	4.7	1.24	>99.9	0	5.79	0.79	0.11	1.17	0.13	1.19	18.00	72.73	0.09	73	3.8
2	6.0	120	10	2	3.1	4.8	1.28	>99.9	0	7.02	0.87	0.16	3.78	0.12	1.06	16.33	70.18	0.48	70	4.0
1	1.5	120	10	2	3.0	4.7	1.24	>99.9	0	10.62	7.33	2.68	1.16	1.16	3.13	21.86	51.86	0.22	52	1.9
1	3.0	120	10	2	3.6	5.6	1.49	>99.9	0	5.84	0.72	0.11	2.36	0.14	1.28	19.36	70.12	0.08	70	3.4
G1-16phosphite	3.0	120	40	1	-	-	-	83.13	16.87	27.79	27.49		3.27	0.68	1.24	7.52	13.32	1.52	13	1.4
G1-16phosphite	3.0	110	40	1.5	-	-	-	85.87	14.23	22.65	17.28		3.25	2.54	3.49	14.01	21.09	1.28	21	1.1

O = octane, 1-O = oct-1-ene, 2-O = oct-2-ene, 2-O = oct-2-ene, 2-O = oct-2-ene, PrH = 2-propylhexanal, EtH = 2-Ethylheptanal, MeO = 2-Methyloctanal, N = n-nonanal, Nol = n-nonanol.

1 = $CH_2Si(CH_2CH_2PPh_2)_2$, 2 = $(CH_3)_2Si(CH_2CH_2PPh_2)_2$, 3 = $Si(CH_2CH_2PPh_2)_4$

[a] : Rate constant and initial rates refer to hydroformylation of oct-1-ene only, [b] : initial rate (10^{-3} mol dm^{-3} s^{-1}), [c] : initial turn over frequency (moles of oct-1-ene consumed per mole of rhodium per second), [d] : selectivity to octan-1-al, [e] : linear to branched ratio of aldehyde, [f] : based on the amount of oct-1-ene consumed.

Typical conditions: solution of $[Rh(acac)(CO)_2]$ (2.0×10^{-5} mole) and dendritic ligand in toluene (4 cm^3) heated at stated reaction temperature under 6 bar of CO/H_2 for 1 hour. Oct-1-ene (1.3 cm^3, 8.3×10^{-3} mole) (Rh/substrate = 1/414) was injected with simultaneous increase in autoclave pressure up to stated reaction pressure. The reaction was run for the stated time before the reaction was quenched by cooling the autoclave with water.